ISSN 0366-5542
CODEN:CCHHAQ

REPORT No. 279
GEOLOGICAL SURVEY OF JAPAN

MAGMATIC CONTRIBUTIONS TO HYDROTHERMAL SYSTEMS

Extended Abstracts of the Japan - U.S. Seminar on
"Magmatic Contributions to Hydrothermal Systems",
held at Kagoshima and Ebino, November, 1991.

-and-

THE BEHAVIOR OF VOLATILES IN MAGMA

Abstracts of the 4th Symposium on Deep-crustal Fluids
"The Behavior of Volatiles in Magma",
held at Tsukuba, November, 1991.

Edited by

Jeffrey W. HEDENQUIST

GEOLOGICAL SURVEY OF JAPAN

Higashi 1-1-3, Tsukuba-shi, Ibaraki-ken, 305 Japan

1992

REPORT No. 279
GEOLOGICAL SURVEY OF JAPAN

Katsuro OGAWA, Director

MAGMATIC CONTRIBUTIONS TO HYDROTHERMAL SYSTEMS

Extended Abstracts of the Japan - U.S. Seminar on
"Magmatic Contributions to Hydrothermal Systems",
held at Kagoshima and Ebino, November, 1991.

-and-

THE BEHAVIOR OF VOLATILES IN MAGMA

Abstracts of the 4th Symposium on Deep-crustal Fluids
"The Behavior of Volatiles in Magma",
held at Tsukuba, November, 1991.

Edited by
Jeffrey W. HEDENQUIST

August 1992
Geological Survey of Japan

CONTENTS

PART II 4th Symposium on Deep-crustal Fluids: The Behavior of Volatiles in Magma

Preface and Acknowledgements

Hydrothermal systems form wherever water becomes heated in the upper crust, and magmas are the most common source of heat. These systems are exploited in the near-surface for their goethermal heat, whereas extinct equivalents formed many of the ore deposits mined today. Although there is wide agreement on the importance of magmas as a heat source, there is much less agreement about whether magmas contribute water and other constituents to hydrothermal systems, and if so, to what degree and importance. As research on volcanoes and their parent magmas, ore deposits and geothermal systems progresses, we recognize a complex environment from the magma to the most distal extent of hydrothermal activity. In order to better understand this continuum, several fields of study must be integrated. Thus the purpose of this seminar, held in Kyushu in November 1991, was to bring together individuals from varied disciplines to consider the general topic of Magmatic Contributions to Hydrothermal Systems.

At the IAVCEI General Assembly in 1989, Patrick Muffler and Jeffrey Hedenquist convened a half-day symposium focussed on aqueous magmatic fluids, ore deposits and geothermal systems, at which Stephen Kesler and Eiji Izawa made keynote presentations. There was a large amount of enthusiastic discussion among people of various disciplines, although the lack of time and the rather broad topic prevented any satisfactory conclusions to be drawn, except that there should be a future multidisciplinary meeting of specialists, preferably close to a magmatic hydrothermal system.

Therefore, we four committed ourselves to organizing a small seminar in southern Kyushu, site of several volcanoes, geothermal systems and related ore deposits. Because of the number of specialists gathered in one place, we took the opportunity to arrange a variety of related symposia both before and after the Kyushu seminar. The first two were held in Tsukuba at the Geological Survey of Japan. One focussed on the Behavior of Volatiles in Magma, held as the 4th Symposium on Deep-crustal Fluids, sponsored by the Tsukuba EXPO '85 Memorial Foundation and the Geological Survey of Japan, organized by Tetsuro Urabe and Akira Takada. The abstracts of this symposium are also presented here in Part II. The other one-day symposium was on Deep Geothermal Systems, sponsored by the Geothermal Research Department of the Geological Survey of Japan, organized by Shiro Tamanyu. After the Kyushu seminar, a one-day Kagoshima Volcanoes Forum was held in Kagoshima city, sponsored by the Kagoshima Prefectural Government. Following a post-seminar field trip, the Metal Mining Agency of Japan sponsored a field conference on Gold Mineralization and Exploration in Island Arcs, held in northern Kyushu.

The week-long seminar in Kagoshima and Ebino provided the 38 invited participants a tremendous opportunity for interaction among disciplines related to Magmatic Contributions to Hydrothermal Systems. These participants also variously joined in some of the related symposia, promoting interaction of members of this gathering with others, largely from Japan. However, it was our desire to share some of our discussions with a much wider audience, hence the compilation of the extended abstracts into this Report of the Geological Survey of Japan. The introductory summary article on the outcome of the seminar was prepared by the organizers, based on final reports of five Discussion Groups which met several times during the

week. A shortened version of this article has also been published recently in Eos (1992, vol. 73, no. 21, p. 233-234). One of the clearest outcomes of the seminar, outlined in these summaries, is the need for such interdisciplinary meetings to share information; large advances can be made in understanding hydrothermal systems simply by integrating existing knowledge from a variety of fields and specialties.

It would have been impossible to organize this seminar without a broad base of support and sponsorship. The initial and principal sponsors of the Japan - U.S. Seminar on Magmatic Contributions to Hydrothermal Systems were the Japan Society for the Promotion of Science and the U.S. National Science Foundation, under the aegis of the Japan - U.S. Cooperative Science Program. Associate sponsors included the Kagoshima and Miyazaki Prefectural Goverments, the Kagoshima University Research Center for the South Pacific, the Metal Mining Agency of Japan, the Tsukuba EXPO '85 Memorial Foundation, the U.S. Geological Survey, and the Geological Survey of Japan. Additional travel support was suplied by the Science and Technology Agency of Japan, the Japan New Energy Development Organization, the Geological Survey of Canada, the Natural Sciences and Engineering Research Council of Canada, and several universities in the United States.

Many individuals made essential contributions to the organization of the seminar and related symposia, and the organizers wish to thank scientists of the Geological Survey of Japan, particularly those in the International Geology Office and the Mineral Resources and Geothermal Resources Departments, plus Ms. Hiroyama, Ms. Nagayoshi and Ms. Tomishima. Logistics in Kyushu were greatly supported by the efforts of Prof. Nedachi, Drs. Taguchi and Watanabe, and Mr. Kuroki. We also appreciate the assistance and cooperation from the Kagoshima Bank, Ltd., Kasuga Mining Company, Mitsui Mining and Smelting Company, Sumitomo Metal Mining Company, the MMAJ Nansatsu office and Kyoto University Sakurajima Volcano Observatory.

Jeffrey W. Hedenquist
Tsukuba, August 1992

Participants, Japan - U.S. Seminar

Organizers of the seminar were:

Eiji IZAWA	Kyushu University
Stephen E. KESLER	University of Michigan
L. J. Patrick MUFFLER	U. S. Geological Survey
Jeffrey W. HEDENQUIST	Geological Survey of Japan

Additional participants were:

Alfred T. ANDERSON, Jr	University of Chicago
Masahiro AOKI	Geological Survey of Japan
Richard E. BEANE	Consultant, Tucson, Arizona
Robert J. BODNAR	Virginia Polytechnic University
Philip A. CANDELA	University of Maryland
Thomas J. CASADEVALL	U. S. Geological Survey

Lawrence M. CATHLES	Cornell University
Hitoshi CHIBA	Okayama University, Misasa (presently Kyushu University)
Bruce W. CHRISTENSON	DSIR Chemistry, New Zealand
Sachio EHARA	Kyushu University
Robert O. FOURNIER	U. S. Geological Survey
Toshitsugu FUJII	University of Tokyo
Bruce F. HOUGHTON	DSIR Geology and Geophysics, New Zealand
Tsuneomi KAGIYAMA	University of Tokyo, Kirishima Volcano Observatory
Tetsuo KOBAYASHI	Kagoshima University
Minoru KUSAKABE	Okayama University, Misasa
Jacob B. LOWENSTERN	Stanford University (presently Geological Survey of Japan)
Michael A. McKIBBEN	University of California at Riverside
Yukihiro MATSUHISA	Geological Survey of Japan
Takanori NAKANO	University of Tsukuba
Munetomo NEDACHI	Kagoshima University
Bruce E. NESBITT	University of Alberta, Canada
Mark H. REED	University of Oregon
Joselito R. RUAYA	PNOC-EDC Geothermal Division, Philippines
Hiroshi SHINOHARA	Geological Survey of Japan
Richard H. SILLITOE	Consultant, London, England
Edward M. STOLPER	California Institute of Technology
Robert B. Symonds	Geological Survey of Japan (presently U. S. Geological Survey)
Sachihiro TAGUCHI	Fukuoka University
Shiro TAMANYU	Geological Survey of Japan
Yuri A. TARAN	Institute of Volcanic Geology & Geochemistry, Kamchatka, Russia
Bruce E. TAYLOR	Geological Survey of Canada
Tetsuro URABE	Geological Survey of Japan
Koichiro WATANABE	Kyushu University

PART I

MAGMATIC CONTRIBUTIONS TO HYDROTHERMAL SYSTEMS

Extended Abstracts of the Japan - U.S. Seminar on "Magmatic Contributions to Hydrothermal Systems", held at Kagoshima and Ebino, November, 1991.

Rept. Geol. Surv. Japan, No. 279, p. 1-6, 1992

Japan-U.S. Seminar on Magmatic Contributions to Hydrothermal Systems

L. J. Patrick MUFFLER[1], Jeffrey W. HEDENQUIST[2], Stephen E. KESLER[3], and Eiji Izawa[4]

[1] *U. S. Geological Survey*
MS 910, 345 Middlefield Road, Menlo Park, CA 94025, U.S.A.
[2] *Mineral Resources Dept., Geological Survey of Japan*
Higashi 1-1-3, Tsukuba, Ibaraki 305, Japan
[3] *Department of Geological Sciences, University of Michigan*
Ann Arbor, MI 48109, U.S.A.
[4] *Faculty of Engineering, Kyushu University*
Hakozaki 6-10-1, Higashiku, Fukuoka 812, Japan

Introduction

Although there is agreement that many hydrothermal systems found in the upper crust derive their thermal energy from magmas, there is considerable debate about the extent to which magmas contribute H_2O, metals, and sulfur to such hydrothermal systems. European geologists in the 19th century had already debated the relative importance of magmatic and meteoric water in hot springs, and, as the study of ore deposits matured, the controversy grew to include deeper hydrothermal systems. By the early 1900s, the views of the magmatists had largely prevailed with publication of Waldemar Lindgren's classification of ore deposits, which claimed that even epithermal vein systems formed by emanations from deep magma chambers. Since then, however, the pendulum of opinion has swung back toward the role of meteoric water, propelled by studies of hot springs and by stable-isotope studies of active and extinct hydrothermal systems. By the 1970s, magmatic water was widely thought to have little influence outside intrusion-hosted hydrothermal systems such as porphyry-copper deposits, and even here its influence was not unanimously accepted.

In recent years, however, the pendulum has once again begun to swing back toward acceptance of magmatic contributions to hydrothermal systems, with field and laboratory studies in the western Pacific island arcs leading the way. In this context, a multidisciplinary Seminar on Magmatic Contributions to Hydrothermal Systems was held at Ebino and Kagoshima on the island of Kyushu, Japan, 10-16 November, 1991. We sought to establish what is understood about this topic, what are the major unanswered questions, and what is the most promising research to answer these questions. Some of the obvious applications of this research include understanding the source of metals and sulfur in hydrothermal deposits related to porphyritic intrusions, determining the potential for movement of deep acid fluids into the shallow levels of exploited geothermal systems (and thus hindering exploitation), and understanding the degree to which hydrothermal systems interact with magma bodies in influencing volcanic eruptions.

Keywords: hydrothermal system, magmatic fluid, epithermal ore deposit, porphyry deposit, volcanic gas, geothermal system

The principal purpose of the Ebino/Kagoshima Seminar was to bring together a small group of individuals whose active research bears on magmatic contributions to hydrothermal systems. The Seminar focussed on the porphyry and epithermal ore environments because of the potential to relate these environments to active volcanic and geothermal systems. Disciplines represented included volcanology, volcanic gas geochemistry, water geochemistry, isotope geochemistry, geochemical modeling, experimental geochemistry, igneous petrology, geothermal geology, economic geology, fluid-inclusion study, geophysics, and physical modeling. Participants included 18 from Japan, 13 from the United States, 2 each from Canada and New Zealand, and 1 each from England, the Philippines, and Russia. The Seminar was conducted in English.

Organization of the Seminar

The Ebino/Kagoshima Seminar was organized around 5 major topics:

- Composition of fluids in equilibrium with magma,
- Processes of fluid separation from magma and the nature of hydrothermal systems enveloping magmas,
- Geometry and dynamics of fluid flow in magma/hydrothermal systems,
- Signatures and importance of magmatic fluids in active hydrothermal and volcanic systems,
- Signatures and importance of magmatic fluids in extinct hydrothermal systems.

Each topic was introduced by three oral presentations followed by poster presentations. All sessions were designed to move away from restrictive disciplines and toward a multi-disciplinary approach. Formal discussion groups for each of the five topics met several times and prepared detailed reports that were presented and discussed in a final session. These reports and the extended abstracts prepared by each participant served as the basis of this summary (also published in greatly condensed form in Eos, vol. 73, no. 21, p. 233-234). The extended abstracts of each presentation follow in this volume. Further copies of this volume are available to those in North America from L.J. Patrick Muffler, U.S. Geological Survey, MS 910, Menlo Park, CA 94205, Fax (415) 329-5203. Those outside North America can obtain copies for the cost of postage from Jeffrey W. Hedenquist, Mineral Resources Department, Geological Survey of Japan, Higashi 1-1-3, Tsukuba, 305, Japan, Fax 81-298-54-3533.

What do we know?

Substantial consensus was reached on the following points:

- By definition, magmatic fluids are aqueous fluids in chemical, isotopic, and thermal equilibrium with an igneous melt, regardless of the ultimate origin of the components. At depths up to a few km, H_2O is usually the major constituent of such fluids, although they can contain important amounts of CO_2 and S (as SO_2 and H_2S), NaCl, KCl, FeClx, $CaCl_2$, HCl, HF, and metals.
- The salinity of fluids separating from a magma is controlled by initial water and Cl content of the melt, pressure, and degree of crystallization. Chemical modeling indicates that saline fluids can be produced in three ways: (1) early, moderately saline fluids from high-pressure melts of low water content, (2) late, extremely saline fluids from low-pressure melts, and (3) (most commonly) ex-

tremely saline fluids and a separate gas phase, usually rich in CO_2, SO_2, and HCl, produced by immiscibility at pressures less than a few hundred MPa. Partitioning of metals between melt and aqueous fluid is more strongly affected by pressure than by temperature, with low pressure favoring concentration of metals (such as Zn and Pb) in the aqueous phase. Initial H_2O, ratios of Cl and F to H_2O, and fugacities of oxygen and sulfur also affect the partitioning of metals between melt and the fluid phase(s).

- Fluid movement adjacent to a magmatic intrusion is strongly affected by the brittle-plastic transition that occurs in most rocks at about 350°-400°C. This transition appears to separate regions of hydrostatic pressure (with brittle failure) from regions of lithostatic pressure (with plastic failure) and is the zone of greatest interaction between magmatic and meteoric fluids. Numerical modeling suggests that this zone is only a few meters wide in some systems.
- The movement of fluid phases exsolved from a magma is controlled by pressure gradients, fluid densities, and the temperature and porosity of the local environment. Under some conditions, a gas phase will rise and separate completely from its parent magma. Experimental data suggest that NaCl is dominant over HCl in magmatic fluids at depth and that the NaCl/HCl ratio of these fluids decreases with decreasing pressure, as during ascent in a volcano.
- Magmatic contributions to active volcanoes and geothermal systems are indicated by their stable isotopic and gas compositions. High-temperature, active fumaroles in island-arc volcanic areas have $\delta^{18}O$ and δD compositions of $+7\pm2$ per mil and -25 ± 10 per mil, respectively, and are thought to represent the isotopic composition of water vapor of direct magmatic origin. Isotopic compositions for some other active systems fall on mixing lines between this vapor and local meteoric water. The δD characteristic range cited above is distinct from the commonly accepted "magmatic water box" (δD = -40 per mil to -80 per mil) and requires reinterpretation of some existing ore-deposit data. Magmatic gases can also be recognized in many active geothermal systems, particularly in acid systems associated with active or dormant volcanoes in island-arc settings, but also in some neutral-pH, meteoric-water-dominated systems, based on signatures of non-reactive gases.
- Magmatic contributions to extinct systems are more difficult to recognize. Acid-sulfate (high-sulfidation) deposits contain minerals (e.g., alunite and phyllosilicates) that exhibit a range of $\delta^{18}O$ and δD compositions that converge on the composition of high-temperature fumarole steam, suggesting that the water in many deposits had a significant magmatic component, particularly in the early stages. Coexisting alunite and pyrite has also been interpreted to indicate a magmatic source of SO_2 and H_2S, but paragenetic relations in other deposits suggest that alunite and pyrite can form by other mechanisms. Early alteration minerals in porphyry-copper deposits have $\delta^{18}O$ and δD compositions diagnostic of magmatic water and contain cogenetic highly saline fluid inclusions considered to be of magmatic origin. Although Cu was deposited by these fluids in some deposits, Cu mineralization and phyllic alteration in several well studied North American deposits indicate significant contribution from meteoric waters.
- Porphyry-copper deposits may pass upward into acid-sulfate (high-sulfidation) epithermal deposits, but documentation of the transition remains scarce because few systems expose both deposit types. There appears to be little gradation between adularia-sericite (low-sulfidation) epithermal deposits and either high-

sulfidation epithermal deposits or porphyry deposits, although all three types may be present in a given mineralized system.

- The pressure-temperature history of hydrothermal systems within or beneath volcanoes is greatly influenced by processes such as caldera subsidence, sector collapse, and hydrothermal eruptions, which can cause decreases in pressure at rates that are fast compared to the lifetime of hydrothermal systems.

Major unanswered questions

- *What are the solubilities of volatiles in magmas?* Solubility data for H_2O and CO_2 in magmas are available at pressures of interest, primarily for rhyolitic and basaltic compositions. The solubility and behavior of sulfur-bearing phases (vapors, crystals, and immiscible melts) in silicate melts are less well understood and need to be determined systematically as a function of melt composition, vapor composition, temperature, pressure, oxygen fugacity, and sulfur fugacity. Information on mixed volatile solubilities is very limited, but is necessary for realistic modeling of melt systems.
- *How do metals partition between melts and the magmatic fluids?* Only a few components have been investigated systematically over a range of pressure, temperature, melt composition, and composition of the aqueous fluids. Most data are limited to rhyolitic melts, and aqueous fluids are usually limited to Cl-bearing, CO_2-poor compositions. A comprehensive experimental program is needed, especially emphasizing the role of sulfur and its speciation. Also, studies of metals in natural melt inclusions show great promise and need to be augmented.
- *What are the thermodynamic properties of saline solutions over a wide spectrum of temperatures, pressures, and CO_2 concentrations?* Data are currently restricted primarily to the NaCl-H_2O system and are incomplete, especially at high temperatures and low pressures. Interpretation of fluid inclusions is critically dependent on PVTX data at appropriate temperatures (200°-900°C), pressures (10-200 MPa), and fluid compositions (including effects of KCl, $CaCl_2$, FeClx, NaCl, CO_2, H_2S, SO_2, CH_4, and N_2).
- *What are the compositions of magmatic fluids in crustal environments?* An intensified effort needs to be made to identify, characterize and analyze fluid inclusions of suspected magmatic origin in extinct hydrothermal systems. Of particular importance are efforts to characterize the stable-isotope compositions of water in highly saline fluids and to analyze gases in a range of systems. In these studies, an emphasis needs to be placed on micro-sampling methods that permit accurate analysis of individual inclusions.
- *What are properties, conditions and timing for escape of volatile-rich bubbles from magma?* The processes of fracture of magma and bubble migration need attention. Related studies in the materials-science literature should be scrutinized for possible applicability to magmatic conditions where shear stress may be important.
- *What is the nature of permeability in the marginal zones of magmas and immediately adjacent to magmas, and how is it produced?* Additional work is necessary to determine the relevant rheological properties of magma, igneous rocks, and wall rocks that govern flow and fracture of magma and rocks at temperatures of 200°-900°C and pressures of 50-300 MPa. Field studies are also needed to determine the nature and origin of porosity and permeability in these marginal zones.

- *What is the physical and chemical transition from the high-temperature near-magmatic environment to the lower-temperature hydrothermal systems?* An initial approach to this question can be made by direct examination through relatively shallow drilling in a confined volcano-hydrothermal system, such as White Island, New Zealand, as well as by detailed mass-budget studies of other active and eroded volcano-hydrothermal systems.
- *What similarities or differences are there in the composition and volatile evolution between ore-forming and barren magmas?* Needed are comprehensive comparative studies of the magmatic and hydrothermal evolution of ore-bearing and barren porphyry intrusions, emphasizing fluid inclusions, glass inclusions, isotopes, and paragenesis of both primary and hydrothermal phases.
- *What are the mechanics, dynamics, and rates of formation of porphyry intrusions?* The primary need is for geologically constrained numerical modeling involving the (non-linear?) interactions of magma composition and properties, pressure (lithostatic vs. hydrostatic), stress, strain release, and hydraulic fracturing.
- *Does focussing of magmatic fluids from batholiths play a fundamental role in the size and style of ore and geothermal systems at higher levels?* This question should be addressed by regional geological and geophysical studies of the igneous and tectonic environments of large porphyry deposits.
- *What do the edges of hydrothermal systems look like and how do they merge with adjacent systems?* Most studies of hydrothermal systems, particularly those of ore deposits, focus on the central, strongly affected parts of the systems. The edges of these systems are also of scientific importance. What are the characteristics of the deeper parts of acid-sulfate (high-sulfidation) systems? What is the nature of the rocks and fluid inclusions around and above porphyry-copper deposits? What is the relationship between porphyry systems and adularia-sericite (low-sulfidation) epithermal systems? Can high-sulfidation systems evolve into or from low-sulfidation systems? These studies should focus on recognition and delineation of specific fluid reservoirs by integrated field, mineralogic, fluid-inclusion and isotopic studies, in some cases returning to otherwise well studied deposits with new outlooks and advanced techniques (particularly for micro-analysis).
- *What is the duration of the mineralizing process?* As isotopic age measurements become more precise, it is possible to distinguish events that differ little in age and thus address the question of the active life of hydrothermal systems. Do porphyry systems operate for thousands or millions of years? If millions, then are the heat and fluid contents of the pluton sufficient to supply the systems, or are deeper sources required? Do epithermal systems operate for similar lengths of time? Recent successes in dating individual fluid inclusions from various paragenetic stages may help to answer some of these questions.
- *Do magmatic waters or gases flow into epithermal and other shallow hydrothermal systems episodically?* Paragenetic and geochemical data show that high-level hydrothermal systems have discrete zones that mark major pulses of ore deposition. Careful field and laboratory studies are needed to identify these zones, to determine whether their chemical and thermal characteristics represent magmatic fluids, and to determine their chronology.
- *What are the geologic factors that produce "telescoping" of ore deposits?* There is a need for integrated studies of the effects that essentially instantaneous near-

surface events in volcanic and geothermal systems (e.g., sector collapse of a volcano) have on pressure at depth, with resultant changes in the exsolution of volatiles from magma and the distribution of metals between the melt and the aqueous phase?

- *Do the high-temperature and high-pressure environments that occur at depth in some active geothermal systems represent a transition to a potentially mineralized porphyry environment?* Although these environments have been encountered at depths of ~3 km in four geothermal areas in Italy, Iceland, and California, almost no quantitative information is available other than approximate temperatures (>400°C) and pressures (>24 MPa in excess of hydrostatic). A focussed program is needed to determine temperatures, fluid compositions, and nature of the rock in the pressure-transition zone.
- *How does the interaction of magma with hydrothermal systems influence or trigger volcanic eruptions?* Additional studies are needed to evaluate and amplify the suggestion that the high SO_2 and the anhydrite in the products of Nevado del Ruiz and Pinatubo volcanoes are related to vaporization of a hydrothermal system by magmatic intrusions.

Conclusions

Investigations to date have produced a general framework for the interaction of magma and hydrothermal systems, and much of the information needed to understand magmatic contributions to hydrothermal systems now exists, but in isolated specialties. Some important advances can be made simply by broadening the communication and cooperation among disciplines and viewing this complex topic from a variety of perspectives, as at the Ebino/Kagoshima Seminar. Fundamentally, however, understanding magmatic contributions to hydrothermal systems will require augmented experimental investigations, numerical modeling, field studies, and drilling. Crosscutting many of the scientific questions listed above are several generic threads required for significant progress:

- A need for systematic data on the PVT properties of Na-(K-,Ca-)Cl-H_2O-CO_2-S fluids below 200 MPa.
- Expanded study of melt and fluid inclusions, both within and outside of mineralized zones, as a means of tracing the path of magmatic and hydrothermal evolution.
- Development of microanalytical techniques for fluids, gases, melt, and daughter minerals in inclusions.
- Integrated field, laboratory, and numerical modeling studies of magma/hydrothermal systems, both mineralized and barren and both extinct and active, acquiring and utilizing new drillhole date as appropriate, particularly in the active systems.

Rept. Geol. Surv. Japan, No. 279, p. 7-11, 1992

Diffuse Degassing of Carbon Dioxide Through Volcanic Systems: Observed Facts and Implications

Patrick ALLARD

Centre des Faibles Radioactivites
CNRS-CEA, 91190 Gif/Yvette, France

Carbon dioxide, after water, is the main component of volcanic fluids and thus a main contributor to global emissions of volcanic volatiles. Its mantle-magmatic derivation is generally supported by ^{13}C data (e.g., Allard, 1983; Javoy *et al.*, 1986; Taylor, 1986) and by mass balance considerations. Erupting volcanoes indeed emit much (10 to 100 times) more CO_2 than can be supplied by the volumes of extruded lava, i.e., the CO_2 essentially escapes from intruded magma (e.g., Gerlach and Graeber, 1985). This results from the low solubility (early saturation) of CO_2 in silicate melts at moderate to shallow pressure (Stolper and Holloway, 1987), a property which allows it a) to be the dominant compound of deep magmatic fluids, b) to accumulate in and/or bubble through shallow portions of magma reservoirs, c) to act as a carrier phase for other volatile species (rare gases, sulfur, etc.), and d) to supply surface emissions even during quiescent fumarolic activity. As such, carbon dioxide is a major component of magmatic contributions to volcanic hydrothermal systems. Assessing the emission rate of volcanic carbon dioxide is thus important to constrain the size of underlying magma bodies, their degassing stage, and their volatile contribution to the host environment. After considering the global release of carbon dioxide from volcanic craters, I outline here recent evidence of diffuse degassing of magmatic CO_2 through volcanic piles and the potential implications of this process for magmatic/hydrothermal systems.

Emissions of carbon dioxide from volcanic craters

Volcanic release of carbon dioxide commonly occurs in 'visible' manifestations such as plumes, fumaroles, and bubbling thermal waters. The integrated flux of carbon dioxide at a single volcano can be evaluated by scaling the CO_2/SO_2 ratio of the volcanic plume or hot volcanic gases to the SO_2 plume flux, as measured by remote correlation spectrometry (COSPEC). This procedure applies only to volcanoes which are active enough to generate a plume, but these are major gas contributors. Global emission rates can then be estimated by extrapolating to such data and/or by using the concentration ratio of CO_2 to other volatile species whose global volcanic fluxes have been evaluated independently (e.g., from atmospheric balancing). From such an approach, the global release of carbon dioxide by steady subaerial volcanism was recently re-estimated to be around 100 Tg (Tg = 10^{12} g) per year (Gerlach, 1991; Allard and Sigurdsson, in prep.). This figure largely exceeds the potential supply from annually extruded lavas and supports the idea that most emitted CO_2 is derived from non-erupted magma and, occasionally, from crustal sources (especially in arcs, according to isotopic data). Moreover, it is comparable to or higher than current estimates of mantle CO_2 degassing from mid-ocean ridges

Keywords: volcanic emanations, carbon dioxide, magma degassing, contributions, impact.

(MOR, 30-110 Tg/yr; see the reviews by Gerlach, 1989, 1991). Because subaerial volcanism produces only about one quarter as much magma as MOR, this implies either that the MOR CO_2 flux is underestimated or that, compared to MOR, intrusive magma degassing at subaerial volcanoes produces proportionally more carbon dioxide, as a consequence of both higher average magma CO_2 content (reflecting the major contribution by CO_2-rich alkaline volcanoes) and a greater decoupling between gas release and lava extrusion (favoured by longer crustal residence time, higher crystal content and higher average viscosity of the magmas).

Diffuse CO_2 degassing through volcanic flanks

In addition to visible emissions, diffuse soil release of carbon dioxide occurs from the flanks of active volcanoes. This phenomenon, which had been foreshadowed by Sulerzhitsky (1970), was first recognized on Mt. Etna, Sicily, an erupting alkali-basaltic volcano (Carbonnelle and Zettwoog, 1982; Allard *et al.*, 1991). It has since been documented at other volcanoes in the fumarolic stage and fed by different magma types: Vulcano, Vesuvius, Phlegrean Fields and Stromboli, in Italy; Lamongan and Dieng, Indonesia; Soufriere, Guadeloupe (e.g., Allard *et al.*, 1988; Baubron, 1989; Baubron *et al.*, 1990, 1991; Allard and Baubron, 1991). Hence, such a degassing process may be widespread in volcanically active regions. Its main characteristics and main implications are summarized below:

a) At first, this degassing has been termed 'diffuse', because it is completely invisible (no associated vapour plume) and can take place over wide areas. However, confusion with the term 'diffusive' must be avoided, since the emanations are frequently associated with sub-surface thermal anomalies and convective fluid circulation in the ground.

b) Volcanic diffuse emanations consist essentially of carbon dioxide, associated with rare gases (He, Ar and Rn) and traces of H_2, and variably diluted by air. Other volcanic species, such as sulfur and halogen acid compounds, are absent. Depending on sites and air dilution (itself controlled by parameters such as the gas flux, the soil porosity, etc.), the CO_2 concentrations measured at one meter depth in volcanic ground can vary from a few percent up to 100% by volume (e.g., at Vulcano). They are usually much higher than local biogenic CO_2 background, even when measured on vegetated volcanic flanks.

c) The magmatic derivation of diffuse emanations and/or their genetic link with crater emissions can be verified from their chemical (He/CO_2) and isotopic ($^3He/^4He$, $^{13}C/^{12}C$) ratios. For example, the CO_2 emanating from the upper flanks of Etna is isotopically identical to the magmatic gas sampled at $T \geq 1{,}000°C$ from molten lava or vents in the summit craters, while the soil helium is typically of mantle derivation (Allard *et al.*, 1991). At Vulcano, diffuse soil emanations at the base of the active cone display chemical and isotopic proportions of He and C which are similar to those of the crater fumaroles (400°-650°C; Baubron *et al.*, 1990). At some sites, however, more distal emanations exhibit different chemical and isotopic compositions, due to either fractionation during gas ascent or local contributions of non-magmatic sources.

d) Measurements of diffuse gas fluxes (by either dynamic or static methods) provide important information. Available data (e.g., at Etna, Vulcano, or Campi Flegrei) show that comparable amounts of CO_2 can be released by diffuse flank degassing as by crater (plume or fumarolic) degassing. At dormant volcanoes (e.g.,

Vesuvius) diffuse degassing can even be the dominant process of gas release. Diffuse gas fluxes at some volcanoes are high enough to generate a CO_2 anomaly in the ambient atmosphere, as revealed by field and airborne measurements (the existence of flank degassing at Etna was originally detected from such a signal).

Several implications result from these observations:

1) Diffuse release of magma-derived carbon dioxide through volcanic piles must be taken into account in the evaluation of local and global volcanic ouput of CO_2 (the global values estimated from only crater plume emissions may be conservative by a factor of 2 at least), as well as in the evaluation of intruded volumes of degassing magma.

2) The spatial distribution and the temporal change of diffuse volcanic degassing provide interesting indications for volcano monitoring. Detailed prospecting for soil gas emanations allows geochemical maps of volcanoes to be drawn and used for both structural studies (discrimination between active, gas-leaking faults and inactive ones) and forecasting purposes (detection of intrusions). Once the relationship between the emanations and deep magma degassing has been verified, soil gas leaks are appropriate tracers for continuous geochemical monitoring, since they are much more accessible than crater emissions, are closer to electrical power when necessary, and do not expose monitoring equipment to corrosion by acid gases.

3) The potential bearing of ^{14}C-devoid CO_2 emanations from volcanic slopes upon the ^{14}C content of local vegetation should be considered in radiocarbon dating of recent eruptions. Preliminary results on Vulcano show a correlation between the soil gas flux (and related air anomaly) and apparent aging of local living vegetation, whose "age" ranges up to 2,500 years!

4) Finally, diffuse degassing of magma-derived carbon dioxide through volcanoes may have relevant implications to volcanic/hydrothermal systems. Two cases can be considered:

- *High-temperature volcanic systems.*

Widespread emanation of CO_2 through active volcanoes, at distances from central craters and conduits, provides measurable evidence of extensive transfer of magmatic gas through the host rocks. In high-temperature systems, intrusive degassing of CO_2 from magma bodies is likely to be followed by gas migration through fractures and porous layers of volcanic edifices. At the surface, the emanations contain only CO_2 and inert gases but, depending on their depth of generation, could originally contain other magmatic species (e.g., SO_2, H_2S, HCl, metals, etc.) whose entrainment is favoured by the effervescence of less soluble CO2. These more reactive species should be lost at depth, during water-gas-rock interactions upon ascent. So, diffuse release of CO_2 from such systems may be associated with and indicative of extensive precipitation of magma-derived components within volcanic piles, including the formation of ore deposits.

- *Low-temperature systems.*

In low-temperature systems, magma-derived CO_2 is more likely to be absorbed in deeply circulating groundwater, rather than being able to rise 'directly' toward the surface. Subsequent boiling of the resulting solutions should generate CO_2-rich vapours which, given favourable conditions (impermeable barriers), may accumulate as gas-pockets (Allard *et al.*, 1989; Giggenbach *et al.*, 1991). Partial

leakage of the gas could account for low-temperature CO_2-rich surface discharges, such as mofettes, soda springs, and fault-related soil emanations (e.g., at Dieng, Indonesia). It also is a potential process for CO_2 accumulation in deep crater lakes (e.g., at Nyos, Cameroon). Hence, diffuse soil degassing in such systems may be one typical indication of CO_2 storage at depth and, then, should be carefully considered, since sudden expansion and effusion of CO_2-rich gas pockets beneath volcanoes may contribute to and be a major hazard from hydrothermal eruptions (Chivas *et al.*, 1987; Allard *et al.*, 1989).

Further study of diffuse volcanic degassing is sorely needed to better assess its overall extent and implications for magmatic/volcanic systems.

References

Allard, P. (1983) The origin of water, carbon, sulfur, nitrogen and rare gases in volcanic exhalations: evidence from isotope geochemistry. In Tazieff, H. and Sabroux, J. C., eds., *Forecasting Volcanic Events*, Elsevier, Amsterdam, p. 337-386.

———, Baubron J. C., Luongo, G. and Pece R. (1988) Geochemical survey of volcanic soil gas emanations and eruption forecasting: the Vesuvius case, Italy. *Proc. Int. Conf. on Volcanoes, Kagoshima, Japan*, p. 212.

———, Carbonnelle, J., Dajlevic, D., Le Bronec, J., Morel, P., Robe, M. C., Maurenas, J. M., Faivre-Pierret, R., Martin, D., Sabroux, J. C. and Zettwoog, P. (1991) Eruptive and diffuse emissions of CO_2 from Mount Etna. *Nature*, vol. 351, p. 387-391.

———, Dajlevic, D. and Delarue, C. (1989) Origin of carbon dioxide emanation from the 1979 Dieng eruption, Indonesia: implications for the origin of the 1986 Lake Nyos catastrophe. *Jour. Volcanol. Geotherm. Res.*, vol. 39, p. 195-206.

——— and Sigurdsson, H. (in preparation) Global release of carbon dioxide from subaerial volcanism.

Baubron, J. C. (1989) Geochemical surveillance of some Italian volcanoes: Vulcano, Vesuvius and Solfatara. *BRGM Report*, 30110 ANA DT 89, Orleans, 34 p.

———, Allard, P. and Toutain, J. P. (1990) Diffuse emissions of carbon dioxide from Vulcano island, Italy. *Nature*, vol. 344, p. 51-53.

———, ———, Sabroux, J. C., Tedesco, D. and Toutain, J. P. (1991) Soil gas emanations as precursory indicators of volcanic eruptions. *Jour. Geol. Soc. London*, vol. 148, p. 571-576.

Carbonnelle, J. and Zettwoog, P. (1982) Local and scattered gas emissions at Etna volcano. Bull. PIRPSEV-CNRS, Paris, no. 55, 25 p.

Chivas, A. R., Barnes, I., Evans, W. C., Lupton, J. E. and Stone, J. O. (1987) Liquid carbon dioxide and its role in volcanic eruptions. *Nature*, vol. 326, p. 587-589.

Gerlach, T. M. J. (1989) Degassing of carbon dioxide from basaltic magma at spreading centers: II. Mid-oceanic ridge basalts. *Jour. Volcanol. Geotherm. Res.*, vol. 39, p. 221-232.

———(1991) Present-day CO_2 emissions from volcanoes. *EOS*, vol. 249, p. 249-255 (June 4).

——— and Graeber, E. J. (1985) Volatile budget of Kilauea volcano. *Nature*, vol.

313, p. 273-277.

Giggenbach, W. F., Sano, Y. and Schmincke, H. U. (1991) CO_2-rich gases from Lake Nyos and Monoun, Cameroon; Laacher See, Germany; Dieng, Indonesia, and Mt. Gambier, Australia: variations on a common theme. *Jour. Volcanol. Geotherm. Res.*, vol. 45, p. 311-323.

Javoy, M., Pineau, F. and Delorme, H. (1986) Carbon and nitrogen isotopes in the mantle. *Chem. Geology*, vol. 57, p. 41-62.

Stolper, E. and Holloway, J. R. (1988) Experimental determinations of the solubility of carbon dioxide in molten basalt at low pressure. *Earth Plan. Sci. Lett.*, vol. 87, p. 397-408.

Sulerzhitsky, C. D. (1970) Radiocarbon dating of volcanoes. *Bull. Volcanol.*, vol. 35, p. 85-94.

Taylor, B. E. (1986) Magmatic volatiles: isotopic variations of C, H and S. In Valley, J. W., Taylor, H. P., and O'Neil, J. R., eds., Stable Isotopes in High Temperature Geological Processes, *Mineral. Soc. America, Reviews in Mineralogy*, vol. 16, p. 185-220.

Rept. Geol. Surv. Japan, No. 279, p. 12-15, 1992

Subvolcanic Degassing of Magma

Alfred T. ANDERSON, Jr.

Department of the Geophysical Sciences, The University of Chicago
5734 S. Ellis Ave, Chicago, Illinois 60637, U.S.A.

The amount of gas that can exsolve from melt during eruption may be estimated based on volatiles dissolved in melt inclusions in phenocrysts (Devine *et al.*, 1984). The amount of gas actually released during some eruptions has been independently determined from gas monitoring studies (e.g., Rose *et al.*, 1981; Andres *et al.*, 1991). It is common that the latter figure exceeds the former, signifying that the pre-eruptive magma contained excess gas. The excess may be very large, and in some cases the dominant mass of erupted material is gas (Chouet *et al.*, 1974). Isotopic studies indicate that at least in some cases the erupted gas is not of superficial, meteoric origin (Gerlach and Taylor, 1990). It is difficult to escape the generalization that pre-eruptive subvolcanic magmas contain an accumulation of gas that plausibly is derived from a large body of subjacent magma. This appears to be so for basaltic (Hawaiian, e.g., Wilson and Head; 1981, Bottinga and Javoy, 1991) as well as andesitic and rhyolitic systems (Anderson *et al.*, 1989). Volcanoes thus provide an escape route for gas of subsurface orgin.

Paradoxically, although accumulation of gas in magma seems necessary, escape of gas from unvented bodies must also occur, because volcanoes are observed to emit abundant gas even when they are not erupting (Allard, this volume). Does such non-eruptive gas come from magma or only from subsolidus rock? At least at Kilauea, the decrease in CO_2 in eruptive gas away from the summit (Gerlach and Graeber, 1985) and the near synchronaeity between changes in rates of both flank eruption and summit degassing (Greenland *et al.*, 1985; Greenland, 1987) suggests that CO_2-rich gas is released from magma before the magma crystallizes or erupts. A primary CO_2 content of at least 0.3 wt. percent in magma (Greenland *et al.*, 1985) and a pressure of about 1.5 Kb near the base of Kilauea's summit magma storage reservoir (Thurber, 1987) are such that new magma (even if relatively MgO-rich) entering the base of the reservoir would be buoyant (because of CO_2 bubbles) and tend to rise to the top of the magma reservoir. Turbulent mixing (Huppert *et al.*, 1988) between newly input magma (arriving at the rate of about $2*10^7$ m^3/yr [Dzurisin *et. al.*, 1984]) and resident magma might be limited by wall shape. If it reaches the top of the reservoir, buoyant, bubbly magma may spread out and form a cap in which bubbles rise and coalesce. If a bubble-rich foam develops (Jaupart and Vergniolle, 1989), it may form a stably stratified, conductively cooling layer, the cool and brittle upper part of which may collapse (Vergniolle and Jaupart, 1990) and allow gas to escape into cracks. Because the cap may be extensive and thin, the time between influx of new magma and release of gas by foam formation and collapse may be as short as a few weeks. The paradox arises, therefore, as to how gas both accumulates in and escapes from subsurface magmas.

In view of the probable competition between accumulation and escape, the extent of accumulation will depend in part on factors that control the rate at which gas can escape from magma. These factors plausibly include the rise rate of

Keywords: magma, volatile, H_2O, CO_2, SO_2

bubbles, their coalescence rate (Sahagian *et al.*, 1989), collapse of foam (Jaupart and Vergniolle, 1989), spacing and behavior of cracks (Hibbard and Watters, 1985) in subsolidus rock encasing the magma. In general, gas escape may be more difficult at greater depths because higher pressure keeps more of the volatiles dissolved (less gas), bubbles are generally smaller and consequently rise and coalesce more slowly, and cracks in surrounding rocks are more tightly closed. Thus we may expect magmas that stagnate at greater depths to accumulate more and lose less gas. At least for the extremes this seems to agree with observations: Kilauean basalts lose much of their gas at pressures less than about 1 Kb whereas the Bishop rhyolitic ash flow tuff-producing magma accumulated several weight percent of gas at more than 2 Kb before eruption (Anderson *et al.*, 1989). In addition, the variable solubilities of H_2O and CO_2 are important, because the amount of dissolved volatiles can contribute, as crystallization proceeds, to the amount of gas available for both accumulation and loss. Thus granitic magmas, which typically contain substantial dissolved H_2O, have a greater potential to accumulate and lose gas than do basaltic magmas which typically are poor in dissolved H_2O.

High pressure increases the density of newly added magma mainly by compressing and dissolving its bubbles. Consequently, primitive magma that enters a high-pressure magma body from below will likely be dense and pond at the bottom of it rather than rise buoyantly to the top. Input gas would then only arrive at the top of the magma by rising through the bulk of the body of magma over a long time. If the rise rate of bubbles is comparable with the rate of thickening of solidifying roof, it can be expected that the gas will be rather uniformly distributed throughout the roof rock and will escape mainly after the material cools below the solidus and develops brittle fractures and melt-free cracks. It seems possible that as the summit storage reservoir of Kilauea migrates upward (Ryan, 1987), there may be intervals of time during which the lower part of the magma reservoir is quite deep and under such a great pressure that new, MgO-rich magma might pond at depth rather than rise to the top. Such behavior would be consistent with the delayed arrival at the summit of new compositional batches of magma, as documented by Wright *et al.* (1975) for Kilauean lava between 1968 and 1971. Shallowing of the reservoir (or increased primary CO_2) could lead to different behavior with newly added primitive magma rising promptly to the top and being immediately available for summit eruption.

Eruption forecasting based on gas emission rates, gas compositions and inflation rates should be approached with thoughts of gas in mind. Given the competition between deep accumulation and loss of gas, inflation could be due to gas accumulation and clogging of escape paths as well as new magma input. Gas emission rate might increase with increased permeability or with increased rate of magma input.

Emitted gas might become richer in CO_2 due to new magma input or due to increased depth of outgassing. In particular, inflation accompanied by a growing mass deficit indicated by monitoring gravity as well as elevation would be an ominous sign of potential energy accumulation as compressed gas.

Broadly conceived, the level of magma stagnation will primarily control the amount and composition of accumulated gas. At the most shallow levels (e.g., Kilauea), gas escapes readily, with or without volcanism, and little accumulation occurs. At intermediate levels, shallower than the depth where hydrous minerals are stable at igneous temperatures, crystallization causes abundant effervescence (second boiling) of gas rich in H_2O, much of which may accumulate in pockets until subsolidus cracks open and allow escape. At deeper levels, hydrous minerals soak

up much of the available magmatic H_2O at near-solidus temperatures. Consequently, the mass fraction of gas available to accumulate in magma is less. It is generally thought that rocks rich in hydrous minerals derive from magmas relatively rich in volatiles, but this may be mainly a result of pressure.

Gas composition will generally depend on depth. Because pressure stabilizes hydrous minerals, it is expected that gas escaping from crystallizing magma will become poor in H_2O (and presumably rich in CO_2) at greater depths. Consequently, a crystallizing pluton would tend to simultaneously release a spectrum of gas compositions. The spectrum would broaden for plutons with the largest vertical dimensions. CO_2 is so insoluble that it would tend to escape from the magma at the earliest stages of crystallization. In most cases, we would expect the bulk gas to become increasingly rich in H_2O as the body crystallized. On the other hand, experimental work by Peterson and Newton (1989) suggests that some CO_2-bearing silicic magmas may evolve a residual CO_2-rich melt. Caution is indicated in relating the magmatic trends mentioned here to the trends observed in fluid inclusions from hydrothermal minerals that likely formed from extraneous fluids.

Finally, the reverse of subsurface degassing occurs when extraneous volatile material enters the magma from the surroundings (Friedman *et al.*, 1974, Hildreth *et al.*, 1984). The ways that this occurs are not known. Whatever the mechanism, it is to be expected that volatiles added to magma in one place can be lost or accumulated in other parts. In general this may provide a kind of rinse for the magma, depleting it in substances that readily enter the gas. Because of its low solubility in silicate melts, externally-derived CO_2 would be likely to be more effective than H_2O at purging the magma of volatiles because addition of CO_2 would cause comparatively early gas saturation. In extreme cases, flushing abundant CO_2 through a magma may dehydrate the magma and cause crystallization with increasing temperature (retention of latent heat).

References

Allard, P. (1992) Diffuse degassing of carbon dioxide through volcanic systems: observed facts and implications. *Geol. Surv. Japan Rept.* no. 279, p. 7-11 (this volume).

Anderson, A. T., Jr., Skirius, C. M., Lu, F. and Davis, A. M. (1989) Preeruption gas content of Bishop Plinian rhyolitic magma. *Geol. Soci. Amer., Abstracts with Programs*, 21, no. 6, p. A270.

Andres, R. J., Rose, W. I., Kyle, P. R., deSilva, S., Francis, P., Gardeweg, M. and Moreno Roa, H. (1991) Excessive sulfur dioxide emissions from Chilean volcanoes. *Jour. Volcanol. Geotherm. Res.*, vol. 46, p. 323-329.

Bottinga, Y. and Javoy, M. (1991) The degassing of Hawaiian tholeiite. *Bull. Volcanol.*, vol. 53, p. 73-85.

Chouet, B., Hamisevicz, N. T. and McGetchin, T. R. (1974) Photoballistics of volcanic jet activity at Stromboli, Italy. *Jour. Geophys. Res.*, vol. 79, p. 4961-4976.

Devine, J. D., Sigurdsson, H., Davis, A. N. and Self, S. (1984) Estimates of sulfur and chlorine yield to the atmosphere from volcanic eruptions and potential climatic effects. *Jour. Geophys. Res.*, vol. 89, p. 6309-6325.

Dzurisin, D., Koyanagi, R. Y. and English, T. T. (1984) Magma supply and storage at Kilauea Volcano, Hawaii, 1956-1983. *Jour. Volcanol. Geotherm. Res.*,

vol. 21, p. 177-206.

Friedman, I., Lipman, P. W., Obradovich, J. D., Gleason, J. D. and Christiansen, R. L. (1974) Meteoric water in magmas. *Science*, vol. 184, p. 1069-1072.

Gerlach, T. M. and Graeber, E. J., (1985) Volatile budget of Kilauea Volcano, Hawaii. *Nature*, vol. 313, p. 273-277.

——— and Taylor, B. E. (1990) Carbon isotope constraints on degassing of carbon dioxide from Kilauea Volcano. *Geochim. Cosmochim. Acta*, vol. 54, p. 2051-2058.

Greenland, L. P. (1987) Hawaiian eruptive gases. *U.S. Geol. Surv. Prof. Paper*, no. 1350, p. 759-770.

———, Rose, W. I. and Stokes, J. B. (1985) An estimate of gas emissions and magmatic gas content from Kilauea Volcano. *Geochim. Cosmochim. Acta*, vol. 49, p. 125-129.

Hibbard, M. J. and Watters, R. J. (1985) Fracturing and diking in incompletely crystallized granitic plutons. *Lithos*, vol. 18, p. 1-12.

Hildreth, W., Christiansen, R. L. and O'Neil, J. R. (1984) Catastrophic isotopic modification of rhyolitic magma at times of caldera subsidence, Yellowstone Plateau volcanic field. *Jour. Geophys. Res.*, vol. 89, p. 8339-8369.

Huppert, H. E., Sparks, R. S. J., Whitehead, J. A. and Hallworth, M. A. (1986) Replenishment of magma chambers by light inputs. *Jour. Geophys. Res.*, vol. 91, p. 6113-6122.

Jaupart, C., and Vergniolle, S. (1989) The generation and collapse of a foam layer at the roof of a basaltic magma chamber. *Jour. Fluid Mech.*, vol. 203, p. 347-380.

Peterson, J.W. and Newton, R.C. (1989) CO_2-enhanced melting of biotite-bearing rocks at deep crustal pressure-temperature conditions. *Nature*, vol. 340, no. 6232, p. 378-380.

Rose, W. I., Jr., Stoiber, R. E. and Malinconico, L. L. (1981) Eruptive gas compositions and fluxes of explosive volcanoes: budget of S and Cl emitted from Fuego volcano, Guatemala. In R. S. Thorpe, ed., *Orogenic Andesite and Related Rocks*, J. Wiley, New York, p. 669-676.

Ryan, M. P. (1987) Elasticity and contractancy of Hawaiian olivine tholeiite and its role in the stability and structural evolution of subcaldera magma reservoirs and rift systems. *U.S. Geol. Surv. Prof. Paper*, no. 1350, p. 1395-1447.

Sahagian, D., Anderson, A. T. and Ward, B. (1989) Bubble coalescence in basalt flows: comparison of a numerical model with natural examples. *Bull. Volcanol.*, vol. 52, p. 49-56.

Thurber, C. H. (1987) Seismic structure and tectonics of Kilauea volcano. *U.S. Geol. Surv., Prof. Paper*, no. 1350, p. 919-934.

Vergniolle, S. and Jaupart, C. (1990) The dynamics of degassing at Kilauea Volcano (Hawaii). *Jour. Geophys. Res.*, vol. 95, p. 2793-2809.

Wilson, L. and Head, J. W. III (1981) Ascent and eruption of basaltic magma on the earth and moon. *Jour. Geophys. Res.*, vol. 86, p. 2971-3001.

Wright, T. L., Swanson, D. and Duffield, W. A. (1975) Chemical composition of Kilauea East Rift lava, 1968-1971. *Jour. Petrol.*, vol. 16, p. 110-133.

Rept. Geol. Surv. Japan, No. 279, p. 16-21, 1992

Magmatic Fluid Discharging to the Surface from the Osorezan Geothermal System, Northern Honshu, Japan

Masahiro AOKI

Mineral Resources Department, Geological Survey of Japan
Higashi 1-1-3, Tsukuba, Ibaraki 305, Japan

The Osorezan geothermal system is located on the Shimokita Peninsula in northern-most Honshu (Fig. 1, inset). Neutral pH hot springs are actively precipitating gold and mercury tellurides as well as arsenic and antimony sulfides at the surface. Of greatest interest and relevance to this seminar is the evidence for magmatic fluids reaching the surface after acid components have been neutralized, but before much dilution by meteoric waters. The presence of magmatic-dominant but neutralized waters in hot springs is unique to Osorezan. In other volcanic-associated hydrothermal systems where the isotopic composition indicates a large magmatic component (e.g., at Tamagawa, Esan, Satsuma Iwojima and Kuju, Japan, plus other systems around the Pacific), the fluids discharging at the surface preserve their

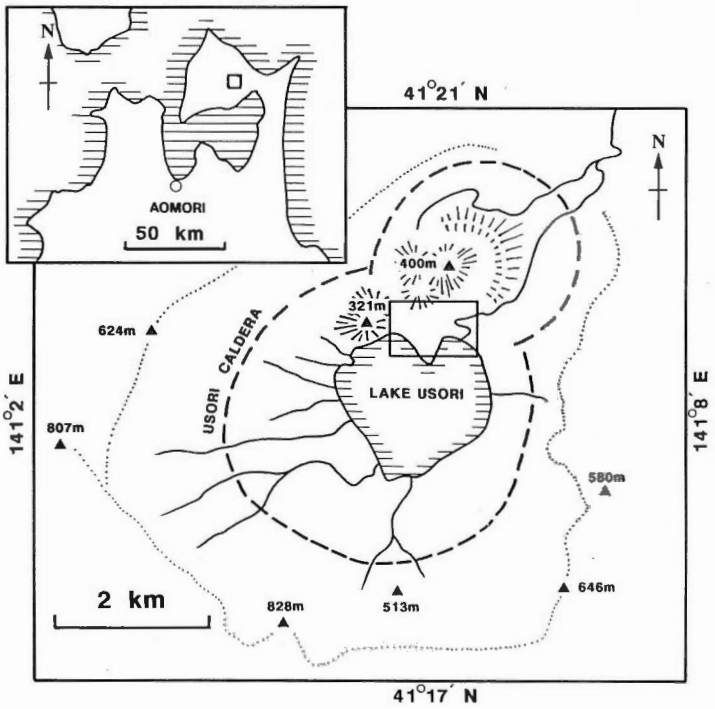

Fig. 1 Location of Osorezan in northern Honshu (inset), and the position of the geothermal system on the north shore of the Lake Usori in Usori caldera.

Keywords: Osorezan, caldera, dacite dome, hot spring, magmatic fluid, gold mineralization, arsenic sulfide, hydrothermal eruption crater

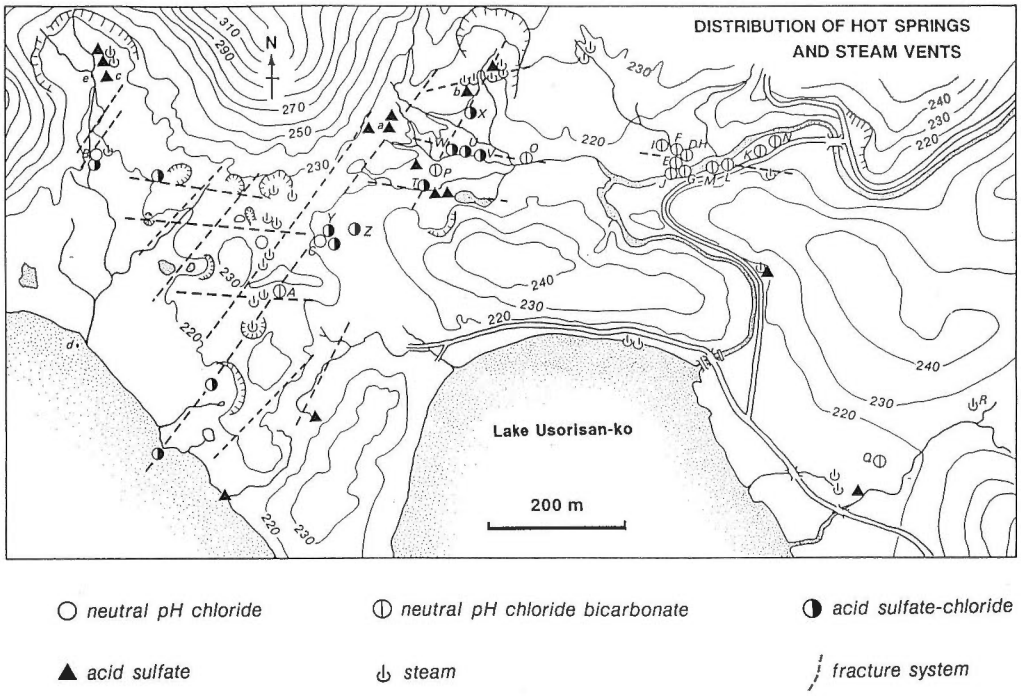

Fig.2 Distribution of thermal features; area of figure from box in Fig. 1.

highly acid character (pH 0.5-1.5) due to the presence of magmatic HCl and other acids.

Present activity at Osorezan is located along the northern shore of Lake Usori, which partially fills a depression formed by caldera collapse. A basaltic andesite stratovolcano first erupted about 1.0 Ma, followed by andesite to dacite volcanism at 0.6 Ma; hypogene acid sulfate alteration of these volcanic rocks indicates an early period of hydrothermal activity dominated by the discharge of volcanic gases. Subsequent caldera collapse was then followed at about 0.2 Ma by emplacement of hornblende dacite domes, with the most recent domes located just north of Lake Usori, associated with present geothermal activity (Figs. 1 and 2).

Hot spring discharges are largely distinguished by their chloride, sulfate and bicarbonate contents, and pH, with three endmembers present. 1) Neutral pH, chloride-rich boiling waters discharge near the base of a dacite dome in the northwestern portion of the system (Fig. 2). These waters are gas-poor, and reflect the surface discharge of the deep fluid from the system. 2) Acid sulfate springs are scattered around the area, most notably in the central and eastern areas. They are formed by steam heating of groundwater, with the steam derived from boiling of the ascending chloride fluid. H_2S is transported with the steam and other gases, to be oxidized to sulfate in the vadose zone, giving the steam-heated water its acid nature. 3) Condensation of steam and gases (mainly CO_2 and H_2S) into groundwaters on the margins of the system, below the vadose zone (thus restricting oxidation of H_2S), results in the formation of CO_2-rich, steam-heated water. This endmember is not present at the surface, except after mixing with other waters, with its presence indicated by high

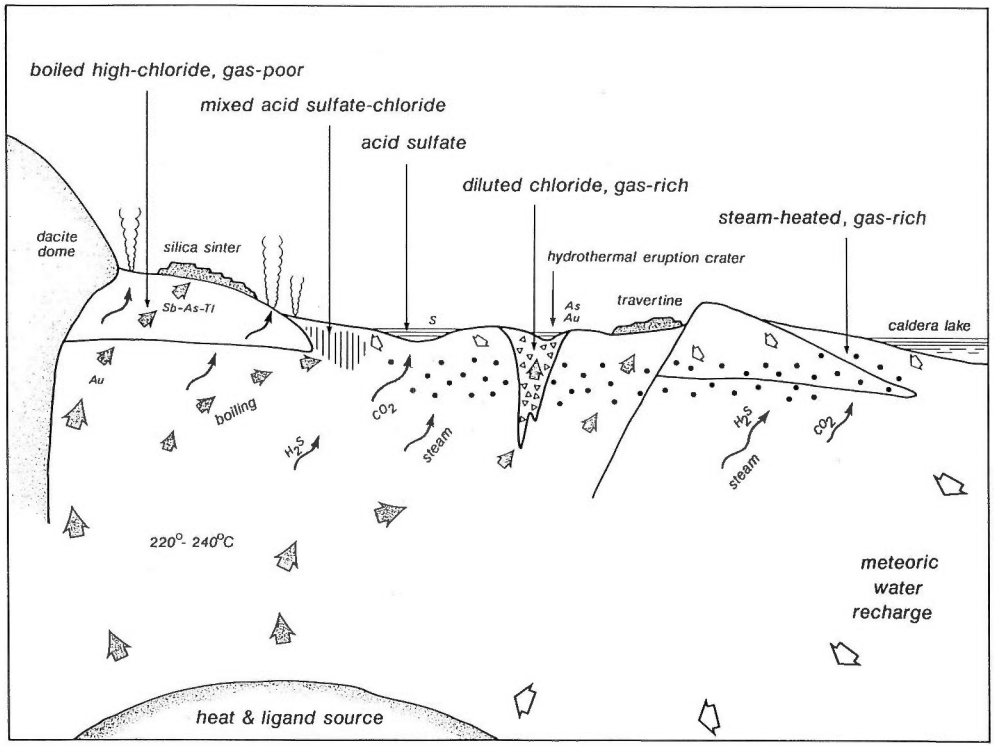

Fig.3 Schematic cross section from the dacite dome in the NW (left), to the lake in the SE, showing the inferred distribution of fluid end members in the system.

bicarbonate contents.

Mixing of the three endmember fluids (neutral pH chloride, steam-heated acid sulfate and steam-heated CO_2-rich) and cold groundwater at shallow depths can explain the observed variations in surface composition of hot springs. As the chloride fluid rises, boiling will be quenched if it mixes with any of the non-boiling waters at depth (acid sulfate, CO_2-rich or cold groundwater). Mixing with the first two accounts for the acid sulfate-chloride and neutral pH chloride-bicarbonate waters, respectively. Dilution by cold groundwater accounts for the dilute chloride, gas-rich waters of some springs (since boiling is quenched, the gases that otherwise would have been lost with steam are kept in solution, sometimes effervescing once the water reaches the surface).

These endmember fluids and zones of mixing are shown schematically in a cross section (Fig. 3) from the dacite dome in the northwest to the lake in the southeast (Fig. 2). Steam-heated waters are restricted to the near-surface zone, particularly on the margin of the system. Surface precipitates, including silica sinter, associated with the highest chloride waters contain arsenic and antimony sulfides, but are poor in gold.

This is most likely due to subsurface boiling and loss of H_2S, the principal ligand for transport of gold. If true, the fluids beneath this area should be actively precipitating gold. In contrast, the diluted chloride waters discharging at lower

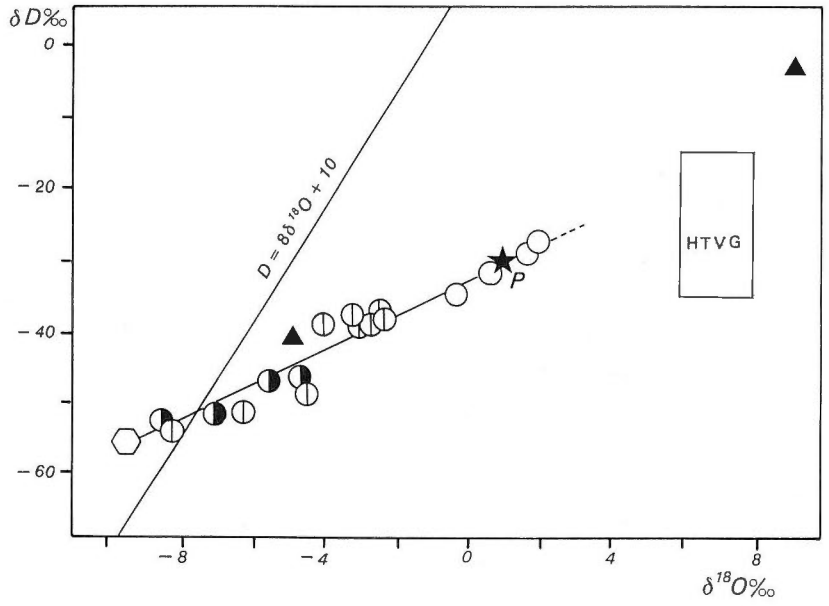

Fig.4 $\delta^{18}O$-δD plot of Osorezan hot spring waters, showing the mixing trend between local groundwater and high temperature volcanic fluids (HTVG).

elevations from a hydrothermal eruption crater are H_2S-rich (dilution having quenched subsurface boiling, thus maintaining H_2S and gold in solution until the surface). The precipitates actively forming in this crater contain up to 6500 ppm gold with percentage concentrations of arsenic, antimony and metals commonly associated in the epithermal ore environment.

The least-diluted neutral pH chloride fluid reaching the surface has a composition which indicates a shallow reservoir temperature of about 220 to 240°C (based on alkali and silica geothermometers). Assuming this fluid is boiling, the depth to this shallow reservoir is about 300 to 400 m. The isotopic composition of this least-diluted chloride fluid is about +2 and -28 per mil in $\delta^{18}O$ and δD, respectively, much heavier than local meteoric water (about -9 and -55 per mil, respectively)(Fig. 4). A simple trend from this isotopically-heavy chloride water to local groundwater is evident from analyses of hot springs at Osorezan (Fig. 4). A plot of δD versus Cl confirms this simple dilution model (Fig. 5). Deviations from this simple trend are due to the variable isotopic enrichment of steam-heated waters, and their subsequent mixing with the chloride fluid or its groundwater-diluted daughter.

Extrapolation of this mixing trend from local meteoric water through the composition of the deep chloride fluid projects to the range of isotopic values identified for high temperature volcanic gases from dacite to andesite volcanoes in Japan and elsewhere (Fig. 4; see Matsuhisa, this volume); this composition is greatly different from seawater, indicating that the Osorezan deep fluids are not diluted seawater. The composition of the relatively non-reactive gases (N_2, Ar and He) show a magmatic signature (Fig. 6), similar to the composition of gases in 225°C fumaroles from the recently active Esan andesite volcano, in Hokkaido just across the straits from Osorezan. These compositions also suggest that the gases have a magmatic source,

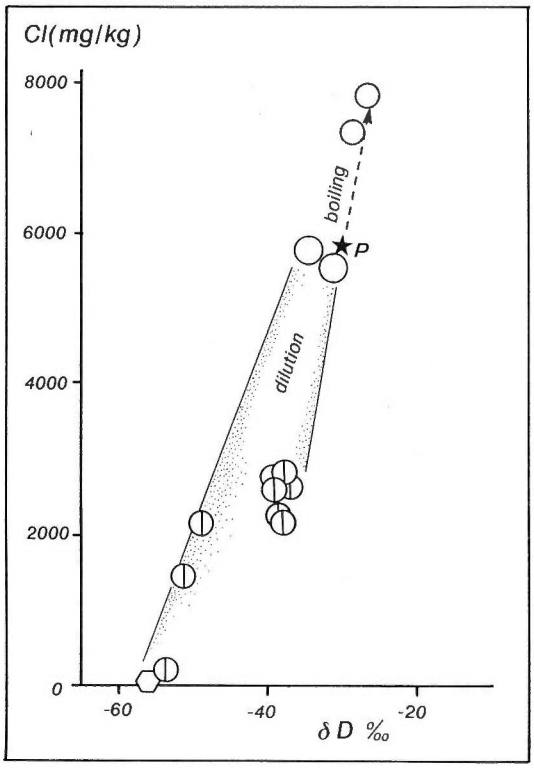

Fig.5 δD-Cl plot showing high chloride waters being diluted by groundwater.

with little effect from mixing with meteoric gases.

Therefore, the least-diluted chloride fluid which discharges at the surface of Osorezan is a mixture of about two parts high-temperature magmatic water and one part local meteoric water. Given the available information from surface springs only, it is not possible to determine whether this ratio is the result of shallow mixing (at a few hundred meters), or whether the mixing occurs closer to the source of magmatic fluid. The neutral pH (and relatively reduced redox state) of the chloride-rich endmember is surprising, given the isotopic evidence for magmatic dominance to the water. Although the partial dilution by meteoric water may partially account for the neutralization, water-rock interaction at depths below the 300-400 m deep reservoir must occur.

In summary, magmatic fluids discharge to the surface at Osorezan close to the margins of young dacite domes. The fluid reaching the surface has been neutralized through water-rock interaction at depth, though mixing with meteoric water is minimal until very shallow depths. The chloride water may be depositing gold and other metals of the epithermal suite where boiling is occurring at shallow depths. Where boiling is quenched due to dilution with groundwater, gold and its principal ligand, H_2S, remains in solution until the surface, where spectacular metal-rich precipitates are now forming. Given the relatively short path length between the source of the magmatic fluid and the surface, as indicated by the minor extent of meteoric water dilution, the volume of rock leached by the ascending fluids must be minimal. This

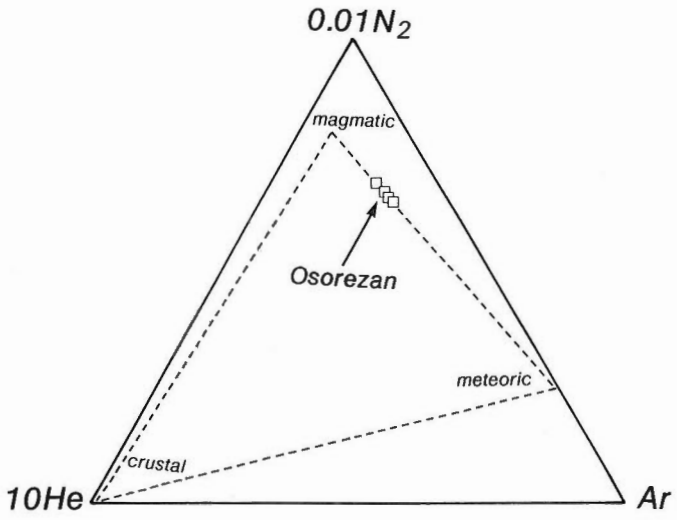

Fig.6 N2-Ar-He composition of Osorezan gases lie on a mixing trend between magmatic (andesitic) and air saturated ground water. This composition is identical to that of gases from fumaroles of near by Esan volcano.

reasoning suggests that in addition to the water and gases, the principal source of the metals in this metal-rich system may also be magmatic.

If these conclusions are correct, then an oxidizing, high sulfidation environment underlies the relatively reducing, low sulfidation hydrothermal system discharging to the surface at Osorezan. Highly leached and alunite-altered rock fragments (with heavy sulfur isotopic composition) have been derived from a preexisting hydrothermal alteration halo, indicating that at one time the high sulfidation (acid and oxidizing magmatic fluid) environment was closer to the surface. The present system may be distinct from this earlier activity, or it could be an evolved state, related to an increased degree of magmatic fluid-rock interaction (and thus neutralization) with time.

Rept. Geol. Surv. Japan, No. 279, p. 22-25, 1992

Magmatic and Meteoric Fluids in Porphyry Copper Deposits

Richard E. BEANE

1761 E. Deer Hollow Loop, Tucson, AZ 85737, U.S.A.

Porphyry copper deposits of southwestern North America provide a natural laboratory to study features of hydrothermal fluids temporally related to crystallization of epizonal plutons. These mineralized intrusive systems are a source of several types of data which define thermal and chemical characteristics of fluids of magmatic and meteoric origin, and the transition between them.

Most porphyry copper deposits in southwestern North America are associated with sub-volcanic intrusions of quartz monzonitic composition which were emplaced in an extensional tectonic regime. In some cases, the plutons intrude coeval volcanic rocks. In this geologic terrain, alteration silicates are zoned relative to the quartz monzonite intrusion (Lowell and Guilbert, 1970), with central K-feldspar plus biotite (potassic) and intermediate quartz plus sericite (phyllic) in the intrusion, and peripheral albite, chlorite, and epidote (propylitic) in granitic wall rocks. The ore zone, containing chalcopyrite and pyrite, lies at the outer margin of a barren core, straddling the boundary between the potassic and phyllic zones. The phyllic zone itself has relatively high sulfide contents, consisting almost entirely of pyrite, and it is located near the outer margins of the central porphyritic intrusion. Farther out in silicate wall rocks, the propylitic zone contains only minor amounts of pyrite. Numerous paragenetic studies indicate that both the central-potassic and marginal-propylitic assemblages are overprinted by phyllic alteration which lies spatially between them.

The characteristics of different fluids in the porphyry copper hydrothermal systems can be determined by studying changes related to the transition from early potassic to later phyllic alteration within the central quartz monzonitic pluton. Based on hydrogen and oxygen isotope ratios, Sheppard *et al.* (1969, 1971) defined two kinds of hydrothermal fluids in porphyry copper deposits of southwestern North America. Stable isotope ratios of biotites from potassic alteration in several deposits are essentially the same regardless of geographic location, and are in the range of igneous biotite. Thus the waters responsible for formation of alteration biotite are from a deep-seated or magmatic source. Hypogene sericite, on the other hand, shows systematic variation in hydrogen isotope ratios with geographic latitude. These variations were interpreted to be a result of formation of sericites from waters of dominantly meteoric origin.

Fluid inclusions in veins associated with hydrothermal biotite and sericite can be used to define some thermal and chemical characteristics of the two types of waters responsible for their formation. Detailed fluid inclusion and mineral paragenetic data have been reported by Reynolds and Beane (1985) for the Santa Rita, New Mexico porphyry copper deposit. The Santa Rita deposit was one of those used by Sheppard *et al.* (1969, 1971) to isotopically identify the presence of magmatic and meteoric fluids.

Keywords: magmatic/meteoric fluids, porphyry copper

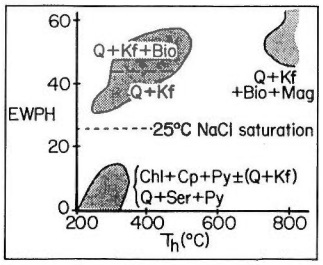

Fig. 1 Homogenization temperatures and salinities of fluid inclusions, and related minerals from the Santa Rita, New Mexico, USA porphyry copper deposit (Reynolds and Beane, 1985).

Early veins at Santa Rita, containing quartz, orthoclase, and biotite, are commonly discontinuous and ptygmatically folded. This suggests formation while the intrusion was in a quasiplastic state. Oxygen isotope ratios have been determined for quartz (ca. 8.2 per mil) and orthoclase (avg. 7.4 per mil) (Sheppard *et al.*, 1971; Reynolds and Beane, 1985). There are two types of hypersaline fluid inclusions in these early quartz veins. One of these has salinities in the range 45 to 70 equivalent weight percent NaCl (EWP NaCl) and homogenization temperatures in excess of 775°C. The second group, which is later, has homogenization temperatures from 260° to 520°C and salinities from 35 to 55 EWP NaCl. When homogenization temperatures of hypersaline fluid inclusions fall below 400°C, related quartz veins contain only K-feldspar, and biotite is no longer present. Vapor-rich fluid inclusions containing CO_2 + H_2O occur with liquid-rich inclusions homogenizing near 500°C. The saline fluids are complex brines containing significant concentrations of Cl, Na, K, Fe, Cu, Ca and S (Anthony *et al.*, 1984). Chalcopyrite occurs as a daughter mineral in some of the hypersaline inclusions, but this phase was not found as a deposited mineral in the quartz veins of magmatic origin.

Mineralized veins and breccia cement from Santa Rita contain chlorite, chalcopyrite, and pyrite with or without K-feldspar and quartz. Fluid inclusions related to this copper mineralization have homogenization temperatures in the range 260° to 360°C, and salinities lower than 10 EWP NaCl. Paragenetic studies indicate that hypogene copper mineralization follows the change from biotite- to chlorite-stable alteration, and is accompanied by a significant decrease in fluid inclusion salinity. Quartz from this stage has oxygen isotope ratios near 9 per mil, and the quartz-chlorite partitioning temperature determined for the mineralization assemblage (300°C) is concordant with fluid inclusion homogenization temperatures.

Veins of quartz plus pyrite transect the two types of veinlets described earlier containing either the potassic assemblage or copper mineralization. Quartz-pyrite veins have well-developed alteration haloes of sericite and pyrite, developed at the expense of pre-existing mafic minerals and feldspars. Fluid inclusions in these veins have salinities from 1 to 10 EWP NaCl and homogenization temperatures from 200° to 350°C, with a major population in the range 250°-325°C. Thus the fluids forming the quartz-sericite event at Santa Rita, which Sheppard *et al.* (1969, 1971) defined as being of meteoric origin, have the same homogenization temperatures and salinities as those responsible for hypogene copper mineralization. Both of these later sets of dilute fluid inclusions also have the same homogenization temperatures as older hypersaline fluid inclusions related to the development of quartz plus ortho-

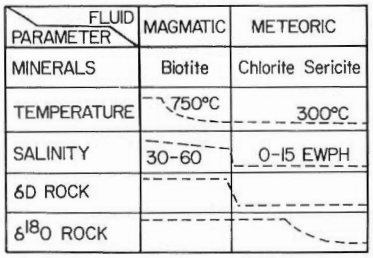

Fig. 2 Changes in several hydrothermal parameters with time in intrusion-centered porphyry copper deposits from southwestern North America. Decreases in D and ^{18}O are schematic because absolute values are a function of geographic location.

clase. The three different mineral assemblages formed at similar temperatures at Santa Rita, so the change in mineralogy must be a result of chemical rather than thermal effects.

Changes in fluid inclusion characteristics during development of evolving hydrothermal assemblages at Santa Rita are shown in Figure 1. Proposed qualitative and quantitative variations in several hydrothermal parameters during extended development of porphyry copper mineralization, as determined from Santa Rita and other similar studies, are shown in Figure 2. One conclusion which may be drawn is that minerals in veins formed from magmatic fluids can be recognized not only by isotopic criteria, but also by their physical characteristics, by their similarity to phases in the parent intrusion, and by the high homogenization temperatures and salinities of related fluid inclusions. The incursion of meteoric water, originally identified isotopically, corresponds with a sharp decrease in fluid salinity. This influx of meteoric fluids is marked, mineralogically, by chloritization of biotite formed from earlier magmatic fluids, and by deposition of chalcopyrite and pyrite. The minerals composing hypogene copper mineralization precede development of the "meteoric" quartz-sericite-pyrite assemblage, but are apparently formed by fluids of similar temperature, salinity, and oxygen isotope composition.

The fluid inclusion data derived from the study of Santa Rita and other porphyry copper deposits in southwestern North America, combined with stable isotope data reported previously, indicate that potassic alteration is caused by hypersaline magmatic fluids, and that mineralization and later phyllic alteration are formed by waters with a significant meteoric component. The salinity of fluids related to hypogene mineralization and to phyllic alteration are in the range 0 to 10 EWP NaCl. These late fluids could be derived by mixing of a hypersaline magmatic fluid (up to 75 EWP NaCl) with a very dilute hydrothermal fluid of meteoric origin in mass ratios on the order of 1:10. Fluid inclusion data indicate that magmatic fluids had cooled to temperatures of 300° to 400°C by the time heated meteoric fluids from the wall rock were introduced. Thus the magmatic-meteoric transition is not accompanied by a dramatic decrease in fluid temperature. The major effects are reflected in the chemical characteristics of the dominantly meteoric fluid: relatively-low salinity, decreased cation to hydrogen ratios, and a hydrogen isotope ratio which is related to geographic location.

Additional studies have shown that: 1) alteration zoning in southwestern North American porphyry copper deposits is a function of changing fracture permea-

bility in the porphyry systems as fluid compositions evolve (Haynes and Titley, 1980), 2) that the pattern of changes in fluid inclusion salinities varies systematically with position in the porphyry systems (Beane, 1983), and 3) that alteration mineralogy is influenced significantly by wall rock composition (Preece and Beane, 1983).

References

Anthony, E. Y., Reynolds, T. J. and Beane, R. E. (1984) Identification of daughter minerals in fluid inclusions using scanning electron microscopy and energy dispersive analysis. *Amer. Mineralogist*, vol. 69, p. 1053-1057.

Beane, R. E. (1983) The magmatic-meteoric transition. *Geotherm. Resources Council, Spec. Report*, no. 13, p. 245-253.

Haynes, F. M. and Titley, S. R. (1980) The evolution of fracture-related permeability within the Ruby Star granodiorite, Sierrita porphyry copper deposit, Pima County Arizona. *Econ. Geol.*, vol. 75, p. 673-683.

Lowell, J. D. and Guilbert, J. M. (1970) Lateral and vertical alteration-mineralization zoning in porphyry ore deposits. *Econ. Geol.*, vol. 65, p. 373-408.

Preece, R. K. III and Beane, R. E. (1982) Contrasting evolutions of hydrothermal alteration in quartz monzonite and quartz diorite wall rocks at the Sierrita porphyry copper deposit, Arizona. *Econ. Geol*, vol. 77, p. 1621-1641.

Reynolds, T. J. and Beane, R. E. (1985) Evolution of hydrothermal fluid characteristics at the Santa Rita, New Mexico, porphyry copper deposit. *Econ. Geol.*, vol. 80, p. 1328-1347.

Sheppard, S. M. F., Nielsen, R. L. and Taylor, H. P., Jr. (1969) Oxygen and hydrogen isotope ratios of clay minerals from porphyry copper deposits. *Econ. Geol.*, vol. 64, p. 755-777.

———, ——— and ——— (1971) Hydrogen and oxygen isotope ratios in minerals from porphyry copper deposits. *Econ. Geol.*, vol. 64, p. 515-542.

Rept. Geol. Surv. Japan, No. 279, p. 26-30, 1992

Can We Recognize Magmatic Fluid Inclusions in Fossil Systems Based on Room-temperature Phase Relations and Microthermometric Behavior?

Robert J. BODNAR

Fluids Research Laboratory, Department of Geological Sciences,
Virginia Polytechnic Institute & State University
Blacksburg, VA 24061, U.S.A.

In order to evaluate possible magmatic contributions to fossil hydrothermal systems, it is necessary to first identify and characterize the magmatic fluids that were present when the system formed. In active magmatic/hydrothermal systems, the magmatic fluids may often be sampled directly. In younger and/or more shallow magmatic/hydrothermal systems the nature of the magmatic fluid may be obtained through spectroscopic studies of melt (glass) inclusions or through heating experiments on the glasses to melt and release the volatile components for analysis. Additionally, fluid (non-silicate melt) inclusions of unarguably primary origin in magmatically-derived minerals are common in these rocks and provide samples of the magmatic fluids for direct analysis. In older and/or deeper magmatic/hydrothermal systems, glass inclusions are rare or absent and fluid inclusions which can be proven to be primary are the exception. Moreover, numerous generations of later fluid inclusions containing hydrothermal fluids or heated groundwaters often occur in the same samples with the magmatic fluid inclusions, and these later inclusions often display microthermometric behavior similar to inclusions of presumed early and possibly magmatic origin. The problem we are then confronted with in studies of these deeper and/or older systems is: "How do we recognize those inclusions which trapped the magmatic fluids?".

The room temperature phase relations and microthermometric behavior of fluid inclusions are dependent on the density and composition of the bulk fluid originally trapped in the inclusion. Thus, if we know the density and composition of magmatic fluids and how these properties vary as the system evolves, we can also predict the room temperature phase relations and microthermometric behavior of fluid inclusions which have trapped these magmatic fluids. Using available experimental and theoretical data for the model system albite-H_2O-NaCl, the salinity of the aqueous phase exsolving from melts crystallizing at various depths (pressures) in the crust have been calculated. Then, the densities of these fluids were calculated using an equation of state for H_2O-NaCl, and the room temperature phase relations and homogenization temperatures of the inclusions were predicted using PVTX data for the system H_2O-NaCl. The results describe salinity trends predicted for magmatic fluids exsolving from silicic magmas, as well as the expected behavior of inclusions which trap these magmatic fluids.

The salinity of the magmatic fluid exsolving from a crystallizing melt varies in a systematic manner as a function of pressure (Fig. 1). For pressures greater than 1.3 kbar, the initial fluid to separate from the melt has a low to moderate salinity. The salinity continues to decrease during crystallization and the final fluid to

Keywords: fluid inclusion, magmatic fluid, H_2O-NaCl-albite, fluid immiscibility, halite, porphyry copper deposit

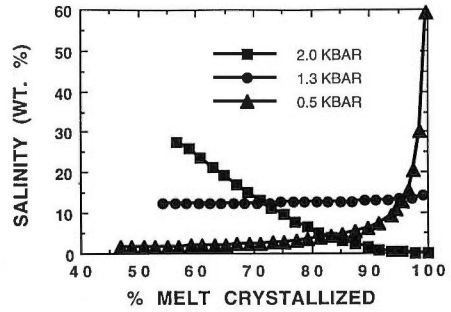

Fig. 1 Trends in salinity of the magmatic fluid exsolved from a crystallizing granitic melt as a function of pressure. The actual salinities will vary as the initial water and chlorine contents of the melt vary, but the trends remain constant.

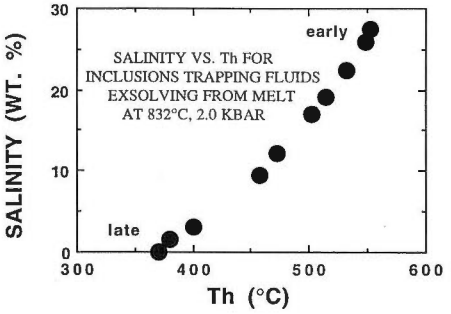

Fig. 2 Variation in the salinity and homogenization temperatures of fluid inclusions which trap the magmatic fluid exsolving from a crystallizing melt at 832°C and 2 kbar.

exsolve is nearly pure water. At pressures below 1.3 kbar, the initial fluid has a low salinity. The salinity continues to increase during crystallization and the last aqueous solution to exsolve from the melt may have very high salinities (>50 wt.%). At a pressure of 1.3 kbar, the initial fluid to separate from the melt is low to moderate salinity, and the salinity of the magmatic aqueous phase remains constant during the entire crystallization history.

Homogenization temperature trends of fluid inclusions trapping these magmatic fluids at various pressure conditions also vary in a systematic manner. For example, an albite melt containing 30 mole percent (2.9 wt.%) H_2O and crystallizing at 832°C and 2 kbar, corresponding to the water-saturated liquidus in the H_2O-albite system, would reach water saturation after 57% of the melt had crystallized. The first magmatic aqueous fluid to separate from the melt would have a salinity of 27.4 wt.% NaCl and a density of 0.704 g/cm^3, corresponding to a homogenization temperature to the liquid phase at 552°C (Fig. 2). With continued crystallization the salinity of the exsolving aqueous phase steadily decreases. The magmatic fluid associated with the very last melt has a salinity of less than 1 wt.%, and inclusions which trap this fluid would homogenize at ~365°C (Fig. 2). In this example, all of the magmatic fluid inclusions would contain two phases at room temperature (liquid + vapor) and all would homogenize to the liquid phase, although the vapor/(vapor +

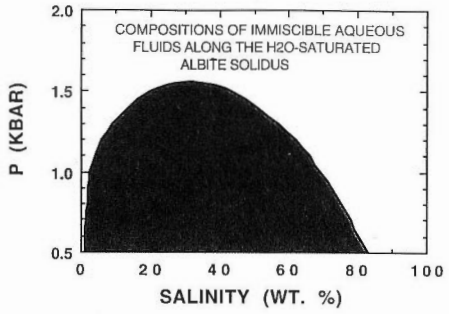

Fig. 3 Range in salinities over which immiscibility may occur in the H2O-NaCl system as a function of pressure for temperatures along the H2O-albite vapor-saturated solidus.

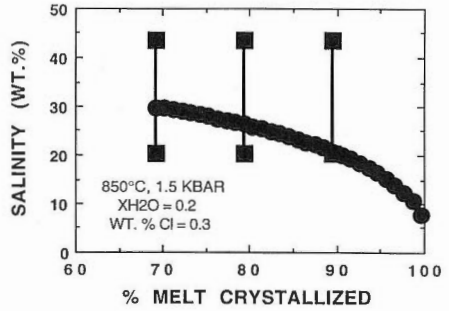

Fig. 4 Variation in salinity of the magmatic fluid exsolving from a crystallizing melt at 850°C and 1.5 kbar. The continuous line formed by the dots represents the bulk composition of the exsolving fluid. The boxes connected by tie-lines represent the compositions of the coexisting liquid and vapor for PTX conditions within the two-phase field in the H2O-NaCl system.

liquid) volume fraction of the inclusions at room temperature would increase from the early to late stages.

Inclusions containing halite daughter phases at room temperature are common in silicic magmatic systems. The presence of halite daughter minerals indicates that the fluid has a salinity in excess of the room temperature saturation value, which is approximately 26.4 wt.%. The origin of this inclusion type is not always obvious, as these inclusions may be produced by several different mechanisms, depending on the pressure and initial water content of the melt. As noted above and shown in Figure 1, at low pressures the salinity of the latest fluids to exsolve from the melt can be very high. Inclusions trapping these late-stage, high-salinity fluids would contain halite daughter minerals. At high pressures, the earliest fluids to exsolve from the melt have the highest salinities, and the salinity decreases as crystallization proceeds (Fig. 1). If the initial water content of the melt is sufficiently low that the melt does not become saturated until relatively late in the crystallization history, these early fluids may have salinities of 30-50 wt.% NaCl, and would produce halite-bearing fluid inclusions. Perhaps the most common origin of halite-bearing fluid inclusions in silicic magmatic rocks is as a result of aqueous fluid immiscibility. If

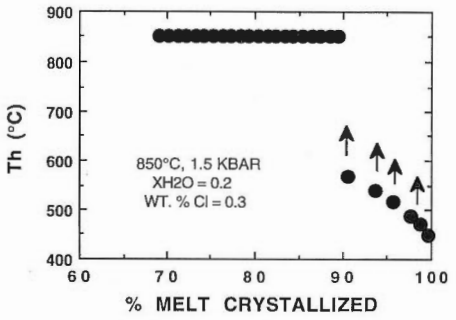

Fig. 5 Homogenization temperatures of fluid inclusions which have trapped the magmatic fluid exsolving from a crystallizing melt at 850°C and 1.5 kbar and shown in Figure 4. Data points (dots) corresponding to the later fluids represent minimum Th's, as PVT data at higher temperatures are not available. Actual Th must be between the trapping temperature (850°C) and the temperature represented by the dots.

the PTX conditions of the exsolving aqueous fluid are within the two-phase (liquid + vapor) field in the H_2O-NaCl system, the original magmatic fluid will separate into a high-salinity liquid coexisting with a low-salinity vapor. Inclusions which trap the high-salinity liquid would become saturated in halite during cooling, to produce halite-bearing inclusions at room temperature.

The range of pressure-salinity conditions along the H_2O-albite solidus over which fluid immiscibility occurs in the H_2O-NaCl system is shown in Figure 3. At pressures below about 1.6 kbar, immiscibility is possible for a wide range of salinities, and this range expands as pressure decreases. For example, at 1.5 kbar any fluid with a salinity between about 20 and 44 wt.% NaCl is within the two-phase field and will split into liquid and vapor. Thus, a fluid exsolving from a melt at 850°C and 1.5 kbar would have an initial salinity of ~30 wt.% (Fig. 4). This fluid would immediately split into liquid and vapor with compositions of 44 and 20 wt.% NaCl, respectively. With continued crystallization the bulk salinity of the exsolving fluid would decrease, but the salinities of the coexisting phases (and resulting fluid inclusions) would remain constant. Only after about 90% of the melt has crystallized and the salinity has dropped below 20 wt.% would the composition exit the two-phase region. During the last 10 % of crystallization the exsolving fluid would be trapped as inclusions within the one-phase field to produce simple two-phase, liquid plus vapor inclusions at room temperature. The homogenization temperatures of the early inclusions trapped within the two-phase field would be identical to the formation temperatures (850°C); later inclusions trapped in the single-fluid-phase field would have considerably lower homogenization temperatures (Fig. 5). At pressures above 1.6 kbar, immiscibility does not occur at any salinity. Thus, the presence of primary halite-bearing fluid inclusions in magmatic minerals in granitic rocks which are known from geologic relationships to have formed at relatively great depths (batholithic rocks) must represent early magmatic fluids.

The results of the analysis of the characteristics of fluid inclusions trapped during crystallization of a silicic melt indicate that great care must be exercised in the selection of fluid inclusions to study magmatic fluids. Halite-bearing inclusions

may be produced early in the crystallization history in deep systems or late in the crystallization history in shallow systems by direct exsolution of high-salinity fluids from the melt. In intermediate to shallow systems, halite-bearing inclusions may also be produced over much of the crystallization history as a result of aqueous fluid immiscibility. Two-phase (liquid + vapor) low to moderate salinity inclusions may be produced over a wide range of crystallization conditions. These inclusions can have homogenization temperatures as low as 300°C, depending on the PTX conditions of formation. These characteristics (low to moderate salinity, Th ≈ 300°C) are similar to those of typical late hydrothermal inclusions found in most granitic-hosted hydrothermal systems, and may be easily misidentified. These late hydrothermal inclusions and similar magmatic inclusions may be distinguished from one another based on mode of occurrence (quartz phenocrysts vs. veins), presence of tiny opaque daughter phases in magmatic inclusions, and relative ages. Success in being able to distinguish between these two inclusion types is forecast for the near future as techniques for trace or minor element and stable and radiogenic isotope analysis of individual inclusions are developed and perfected.

Rept. Geol. Surv. Japan, No. 279, p. 31-34, 1992

Physical and Chemical Constraints on Magmatic Aqueous Phase Exsolution: Toward an Integrated Field, Experimental and Computational Approach.

Philip A. CANDELA, Philip M. PICCOLI, Thomas J.WILLIAMS and Stephen, J. LYNTON

Laboratory for Mineral Deposits Research, Department of Geology, University of Maryland at College Park College Park, MD 20742, U.S.A.

The size and composition (i.e., bulk metal ratios) of magmatic-hydrothermal mineral deposits are affected by a number of processes including the nature of the source region and mode of emplacement of the associated plutons. The Magmatic-Hydrothermal Theory for the origin of porphyry, skarn and other deposits predicts that magma chemistry exerts strong controls on the composition of mineralized rocks, and much effort is concentrated on understanding the chemical controls on ore genesis. However, the means of egress of magmatic fluids and the focusing of these fluids into sites of alteration and mineralization are not well understood. To understand the role of source regions, and the role of aqueous phase/melt partitioning relative to crystal/melt partitioning of ore metals in ore genesis, and the means of egress of the magmatic aqueous phases from the pluton, we have:

1] investigated apatite chemistry in intrusive rocks;

2] performed experiments on the partitioning of metals and other elements between silicate melts and two phase mixtures of chloride-bearing aqueous fluids, and between silicate melts and crystalline phases; and

3] modeled the chemistry and physics of aqueous exsolution from a felsic magmatic system.

Apatite, and estimates of halogen contents of magma

The concentrations of Cl and F in apatites from the Tuolumne Intrusive Suite (TIS) have been measured. The ratio of the mole fraction of chlorapatite to hydroxyapatite (CAp/HAp) and fluorapatite to hydroxyapatite (FAp/HAp) within the TIS change from the outer to the inner units (0.08 to 0.02 and 1.7 to 8, respectively). From these data, the corresponding fugacity ratios can be calculated given reasonable estimates of apatite saturation temperatures. First order estimates of halogen concentrations in the melt can be calculated from these fugacities if estimates of the thermodynamic data for relating m^{aq}_{HCl} to $m^{aq}_{\Sigma Cl}$ can be made. These calculations have been attempted using experimental data on the relationship between aqueous HCl/(ΣCl) ratios and the composition of coexisting melts, and data on aqueous phase/melt partitioning of chlorine. Our calculations yield initial magmatic Cl of 620 ppm for the outer, most mafic unit (Sr_i = 0.7059) and 100 ppm for the inner, most felsic unit (Sr_i = 0.7066). This is evidence of a chloride-bearing slab-derived input to the zones of magma generation in the Sierra Nevada arc system. The Cl/water ratios estimated for the TIS would produce wide variations in the efficiency with which copper could be removed from an arc magma at a depth of a few kilometers.

Keywords: magma, volatiles, partitioning, dynamics, apatite

Ore metal partitioning in melt/crystal/vapor/brine systems

Partitioning experiments performed in our laboratory (Tacker and Candela, 1987; Candela and Bouton, 1990; Lynton *et al.*, 1990, and in prep.; and Williams *et al.*, 1991) suggest that oxygen fugacity-dependent crystal/melt partitioning of ore metals leads to different efficiencies of Cu, W, and Mo removal from silicate melts into ore-forming aqueous fluids (see table below). For example, the Mo/W ratio in magmatic-hydrothermal deposits should increase as the oxygen fugacity of the magma increases. Further, Cu should behave as a crystal-compatible element in water-undersaturated, sulfide-saturated magmas (as long as dissolved sulfur is present in sufficient quantity) with fO_2 <NNO due to the strong partitioning of Cu into pyrrhotite from the melt.

Experiments are also being performed on the partitioning of copper and other elements between silicate melts and mixtures of a brine and coexisting vapor (the aqueous mixture homogenizes upon quench). Variations in the chloride/water ratio of the starting material produces variations in the vapor/brine phase ratios at P and T. The composition range of our experiments approximates a haplogranitic - aqueous phase system. By using data on the chloride concentration of coexisting phases in the system NaCl-water, we can convert our (aqueous mixture)/melt partitioning data into model melt/vapor/brine partition coefficients. Our preliminary data show that [1] the (aqueous mixture)/melt partition coefficients of copper in these experiments are up to an order of magnitude higher than those determined by Candela and Holland (1984) which were performed with less aluminous melts, in the supercritical region, and at higher pressure; and [2] copper concentrates in the brine relative to the vapor; however, copper and sodium (not copper and chlorine) are distributed similarly between the two phases.

The physics of egress of the magmatic aqueous phases

High Lewis numbers (the ratio of heat to chemical diffusivity) for H_2O imply that water will accumulate within a marginal boundary layer or crystallization interval within magma chambers. This suggests: [1] magmatic water exsolution occurring at <<20% crystallization (at high initial magmatic water concentrations or low pressures), can induce the rise of bubble (+crystal)-laden plumes; [2] magmatic water exsolution occurring later (moderate initial magmatic water concentrations or moderate pressures), with vapor bubbles (trapped in an immobile crust) forms a spanning cluster at critical percolation through which the magmatic aqueous phase can upwardly advect; and [3] vapor exsolution occurring in an immobile crust but with lower initial water concentrations than in [2] (or at higher pressure), such that the spanning cluster at critical percolation is not achieved, results in the dispersal of the magmatic aqueous phase through the cracking front, which follows the solidus into the pluton. In the first case, the likelihood of plume rise (relative to the rise of individual bubbles) can be evaluated by calculating the characteristic rise time for individual bubbles, according to the Hadamard-Rybczynski law, relative to the characteristic rise time for bubble-laden plumes. Calculations show, for bubbles of r<1cm, that plume rise is likely. In the second case, percolation theory indicates that a spanning cluster of the aqueous phase on a simple three dimensional lattice is attained when the aqueous phase achieves a volume fraction of F = 0.31. Percolation is attained for initial magmatic water concentrations >1-2% at 0.5 kbar and >4-5% at

Table 1 Summary of experimental data on crystal/melt equilibria

SYSTEM	Metal	(O_2)	D(xl/melt)	Reference	Prob Value
Mt/Melt	Mo	NNO	0.21	1	<0.01
Mt/Melt	Mo	GM	0.52	1	
Ilm/Melt	Mo	NNO	0.22	2	0.06
Ilm/Melt	Mo	GM	0.42	2	
Ilm/Melt	W	NNO	0.50	2	0.33
Ilm/Melt	W	GM	0.39	2	
Po/Melt	Cu	NNO	566	3	0.15
Po/Melt	Cu	GM	908	3	

1- Tacker and Candela, 1987
2- Candela and Bouton, 1990
3- Lynton, Candela and Piccoli, 1990

2 kbar. For lower water concentrations and higher pressures, vapor will be dispersed through a rather diffuse cracking front. This analysis suggests that orthomagmatic-hydrothermal fluids can be transported and focused to sites of mineral deposition near the apical regions of magma chambers by either bubble-plume rise or advection through spanning clusters of vapor bubbles.

Summary

In summary, cycling of oxidized, hydrated, sulfidized and chlorine-enriched oceanic crust into the mantle can give rise to magmas that contain sulfur but are oxidized (NNO or greater). Further, rapid ascent of crystal-poor magmas with considerable water contents allows the melts to reach shallow levels in arc environments. The combination of high oxidation state, relatively hydrous but shallow conditions and a high Cl/H_2O ratio leads to saturation with respect to water early during crystallization and loss of a large proportion of magmatic copper to the aqueous phase. Ores formed from these oxidized magmas also possess high Mo/W ratios due to the effect of oxygen fugacity on the sequestering of Mo vs. W. In less oxidized magmas, Cu and Mo are partitioned into sulfides and Ti-bearing phases respectively, resulting in lower efficiencies of removal of Cu and Mo from melts into aqueous fluids. Further, the partitioning of W into crystallizing phases is reduced, producing a more efficient removal of W into ore-forming fluids. This ultimately leads to mineral deposits with higher W/(Mo + Cu) ratios relative to deposits associated with more oxidized systems. Silicic, high-fluorine magmas with fO_2 > NNO can be found in tensional environments (e.g., rocks associated with the Climax-type deposits of the Colorado Mineral Belt). High HF/H_2O activity ratios in the source regions yield melts that evolve an aqueous phase late during crystallization, leading to relatively low ratios of compatible/incompatible elements in the melt at water saturation.

There is little evidence that a high initial ore-metal content in magmas is the principal or sole factor in producing Cu, Mo or W-enriched ore fluids. Rather, intensive parameters such as Cl/H_2O and F/H_2O ratios, level of intrusion, initial H_2O concentration and oxygen fugacity act in concert with initial metal concentrations and depositional effects to determine the composition of magmatic-hydrothermal ore deposits.

References

Candela, P. A. and Bouton, S. L. (1990) The influence of oxygen fugacity on W and Mo partitioning between silicate melts and ilmenite. *Econ. Geol.*, vol. 85, p. 633-640.

——— and Holland, H. D. (1984) The partitioning of Cu and Mo between silicate melts and aqueous fluids. *Geochim. Cosmochim. Acta*, vol. 48, p. 373-380.

Lynton, S. J., Candela, P. A. and Piccoli, P. M. (1990) Experimental determination of copper partitioning between pyrrhotite and high-silica rhyolite. *Geol. Soc. Amer. abst. with Prog.*, vol. 22, p. 181.

Tacker, R. C. and Candela, P. A. (1987) The partitioning of Mo between magnetite and melt: a preliminary experimental study of the partitioning of ore metals between silicic magmas and crystalline phases. *Econ. Geol.*, vol. 82, p. 1827-1838.

Williams, T. J., Candela, P. A. and Piccoli, P. M. (1991) An experimental determination of Cu partitioning between a water saturated high silica rhyolite and a chloride bearing two-phase aqueous mixture at 800°C and 1 kilobar. *Geol. Soc. Amer. abst. with Prog.*, vol. 23, no. 5, p. 291.

Rept. Geol. Surv. Japan, No. 279, p. 35-38, 1992

Pre-eruption Hydrothermal Systems at Pinatubo, Philippines and El Chichon, Mexico: Evidence for Degassing Magmas beneath Dormant Volcanoes

Thomas J. CASADEVALL

U. S. Geological Survey
Box 25046 Mailstop 903, Denver Federal Center, Denver, CO 80225, U.S.A.

In terms of atmospheric impact and volume of new rock and sulfur produced, two of the largest explosive eruptions of the past decade occurred at Pinatubo, Philippines in June 1991 (bulk rock volume >7 km^3; Volcano Explosivity Index = 5+) and El Chichon, Mexico in March-April 1982 (bulk rock volume >1 km^3; VEI = 5). Both volcanoes had been dormant for about 600 years and both contained active hydrothermal systems that had been explored for their geothermal potential prior to their recent eruptions. In addition to similar pre-eruption geological settings (summit domes in small calderas), eruptive products from Pinatubo (SiO_2 = 63%) and El Chichon (SiO_2 = 56%) contain anhydrite as a primary microphenocryst phase, indicating high sulfur contents for their magmas (Luhr *et al.*, 1984; Bernard *et al.*, 1991). Both eruptions produced large amounts of sulfur dioxide gas (20 million metric tonnes [m.t.]-Pinatubo; 7 m.t.-El Chichon) (Bluth *et al.*, 1992) that was injected directly into the stratosphere.

Given the hazardous nature of both of these eruptions, and their impacts on the atmosphere, it is important to evaluate other dormant volcanoes with active hydrothermal systems for evidence of actively degassing magma. This paper reviews features of the pre-eruption hydrothermal systems at Pinatubo and El Chichon to determine criteria useful for detecting degassing magmas that may be contributing fluids as well as heat to hydrothermal systems at dormant volcanoes.

Pinatubo Prior to the 1991 eruption of Pinatubo volcano, there was an active hydrothermal system of hot springs and solfataras located from 1 to 2.5 km north-northwest of the summit at altitudes of 900 to 1180 m (Delfin, 1984). The location of this hydrothermal activity is approximately coincident with the epicentral area of both pre- and post-eruption seismicity and is located northwest of the new summit caldera. The initial eruption of April 2, 1991 produced a series of small craters along an east-west, 1.5 km fissure, which partly overlapped the active hydrothermal system. From April through early-June, several of these craters emitted vigorous clouds of steam and gas including sulfur dioxide (Daag *et al.*, 1991).

Before the 1991 eruptions, Pinatubo's active hydrothermal system was a source of elemental sulfur and had attracted geothermal exploration, including the drilling of three deep wells. Drilling encountered acidified reservoir fluids (pH to 2.3; temperatures to 336°C) (PNOC, 1990). Chemical and isotopic (helium, oxygen, and carbon) analyses of well fluids indicate the presence of magmatic components such as carbon dioxide and sulfur gases, as well as heat, in the Pinatubo reservoir (Ruaya *et al.*, this volume). One sample contained detectable sulfur dioxide gas (M. N. Ramos, personal communication, 1991). The high temperatures and acidic reser-

Keywords: pinatubo, El Chichon, crater lake, degassing magma

voir fluids indicate that a shallow, degassing body of magma was contributing heat and fluids to the Pinatubo geothermal system. Prior to and following the major eruption of June 1991, emission rates of sulfur dioxide were elevated (Daag *et al.*, 1991). These continuing high emission rates of sulfur dioxide through September 1991 suggest that a significant volume of magma continues to degas beneath the 1991 caldera.

Following the June eruptions, springs were observed discharging from the interior walls with water flowing directly into the central vent on the floor of the new caldera, possibly providing a phreatic triggering mechanism for the frequent ash explosions that have characterized activity since July 1991. Since September, a lake has been forming within the new caldera. Annual rainfall for the Pinatubo region is high and the annual volume of rainfall into the caldera is approximately 10 million cubic meters. In the absence of hot spring discharge or surface drainage out of the caldera, the new lake is likely to become acidified as magmatic gases condense in the lake water.

El Chichon After a repose of about 650 years, El Chichon volcano erupted on March 28 and April 4, 1982. Prior to the 1982 eruptions, the El Chichon hydrothermal system had also been explored for its geothermal potential. Thermal activity included fumaroles, hot springs, and altered ground concentrated in an irregular ring about 1.5 km in diameter around a 300 m high central dome in the summit of the volcano and along faults cutting the dome (Casadevall *et al.*, 1984). Maximum fumarole temperatures ranged from 93 to 98 degrees C, and gases emitted included hydrogen sulfide, but not sulfur dioxide. Summit hot springs, at altitudes between 930 and 950 m, had temperatures ranging from 20 to 71 degrees C. Wall rock near the fumaroles and hot springs was altered to an acid sulfate assemblage that included elemental sulfur (Molina-Berbeyer, 1974).

Following the April 4 activity, El Chichon quieted and had no additional eruptions. Due largely to accumulation of rainwater, a lake began to form within weeks in the 1.1 km-wide crater, and attained a maximum water volume of approximately 5 million cubic meters by early 1984 (Casadevall *et al.*, 1984). In early 1983, this lake was hot (temperatures as hot as 58 degrees C) and highly acidified (pH = 0.5) owing to condensation into the lake water of sulfur dioxide and hydrogen chloride of magmatic origin.

Other Volcanoes In addition to Pinatubo and El Chichon, several other volcanoes with similar periods of dormancy and containing active geothermal systems have erupted recently. Nevado del Ruiz volcano, Colombia, erupted disastrously in November 1985, claiming more than 22,000 lives. Post-eruption evaluation of geothermal reports made in the 1970s revealed evidence for input of magmatic fluids to the Ruiz pre-eruption hydrothermal system (Giggenbach *et al.*, 1990). Recent geothermal studies of dormant volcanoes with hydrothermal systems in the Philippines reveal similar evidence for input of magmatic heat and fluids at several Philippine volcanoes (Reyes, 1990). Indonesia alone contains about 30 dormant volcanoes in the "solfataric" stage of activity (van Padang, 1951). Few of these volcanoes have been examined to assess evidence for the presence of degassing magmas contributing fluids and heat to existing hydrothermal activity.

Evidence for magmatic involvement and hazards assessment

Geothermal assessments of dormant volcanoes with active hydrothermal systems

seldom consider the hazard posed by future eruptive activity. Recent advances in recognizing evidence for magmatic involvement of fluids and heat in hydrothermal activity at dormant volcanoes, especially in terms of the chemical and isotopic composition of fluids, chemical studies of alteration, and nature of fluid inclusions, make an assessment of volcanic hazards an important part of geothermal studies at dormant volcanoes with active hydrothermal systems. This type of assessment would be valuable for developing strategies for monitoring volcanoes such as Pinatubo, as well as for determining the suitability of such volcanoes for full-scale geothermal development.

References

Bernard, A., Demaiffe, D., Mattielli, N. and Punongbayan, R. S. (1991) Anhydrite-bearing pumice from Mt. Pinatubo eruption, new evidence of a sulfur-rich silicic magma: *Nature*, vol. 354, p. 139-140.

Bluth, G. J. S., Doiron, S. D., Schnetzler, C. C., Krueger, A. J. and L. S. Walter, (1992) Global tracking of the SO_2 clouds from the June, 1991 Mount Pinatubo eruption. *Geophys. Res. Lett.*, vol. 19, p. 151-154.

Casadevall, T. J., S. de la Cruz-Reyna, Rose, W. I. Jr., S. Bagley, Finnegan, D. L. and Zoller, W. H. (1984) Crater lake and post-eruption hydrothermal activity, El Chichon Volcano, Mexico. *Jour. Volcanol. Geotherm. Res.*, vol. 23, p. 169-191.

Daag, A. S., Tubianosa, B. S. and Newhall, C. G. (1991) Monitoring sulfur dioxide emissions at Pinatubo volcano, Central Luzon, Philippines (abs.). *EOS*, vol. 72, 1991 AGU Fall Meeting Supplement, p. 61.

de la Cruz-Reyna, J. S., Rose, W. I. Jr., Bagley, S., Finnegan, D. L. and Zoller, W. H. (1984) Crater lake and post-eruption hydrothermal activity, El Chichon Volcano, Mexico. *Jour. Volcanol. Geotherm. Res.*, vol. 23, p. 169-191.

Delfin, F. G. Jr. (1984), Geology and geothermal potential of Mt. Pinatubo: unpublished report, Philippine National Oil Company, 36p.

Giggenbach, W. F., Garcia N. P., Londono A. C., Rodriguez, L., V., Rojas, N. G. and Calvache, M. L. V. (1990) The chemistry of fumarolic vapor and thermal-spring discharges from Nevado del Ruiz volcanic-magmatic-hydrothermal system, Colombia. *Jour. Volcanol. Geotherm. Res.*, vol. 42, p. 13-39.

Luhr, J. F., Carmichael, I. S. E. and Varekamp, J. C. (1984) The 1982 eruptions of El Chichon Volcano, Chiapas, Mexico: mineralogy and petrology of the anhydrite-bearing pumices. *Jour. Volcanol. Geotherm. Res.*, vol. 23, p. 69-108.

Molina-Berbeyer, R. (1974) Preliminary report on the geochemistry of geothermal fluids from the Volcan del Chichonal, Chiapas (Mexico). Dept. Geotherm. Resources, Federal Energy Comission (in Spanish), 23 p.

van Padang, N. (1951) Indonesia; Part 1, Catalogue of the Active Volcanoes of the World including Solfataric Fields, International Volcanological Association, Naples, 271 p.

Philippine National Oil Company (PNOC) (1990) Mt. Pinatubo Resource Assessment (Draft Report), 51 p.

Reyes, A. G. (1990) Petrology of Philippine geothermal systems and the application of alteration mineralogy to their assessment. *Jour. Volcanol. Geotherm.*

Res., vol. 43, p. 279-309.

Ruaya, J. R., Ramos, M. N. and Gonfiantini, R. (1992) Assessment of magmatic components of the fluids at Mt. Pinatubo volcanic-geothermal system, Philippines from chemical and isotopic data. *Rept. Geol. Surv. Japan* no. 279, p. 142-152.

Rept. Geol. Surv. Japan, No. 279, p. 39-43, 1992

The Interaction of a Hydrothermal System with Its Intrusive Heat Source

Lawrence M. CATHLES

Department of Geological Sciences
Cornell University, Ithaca, NY 14853, U.S.A.

Observations at mid-ocean ridges over the last 15 years, taken together, suggest that the main (350°C) zone of water-rock interaction: (1) lies along the near vertical sides of a few km wide axial intrusive ~5 km high, (2) is very permeable (~300 millidarcies), and (3) is only a few meters wide. Land observations support this interpretation and there is every reason to expect the zone of water-rock interaction should be similar whenever a permeable environment is intruded by an igneous body.

The narrowness of the 350°C zone of water-rock interaction makes it highly vulnerable to physical and chemical perturbations. Because the thin flow zone is the most resistive element in the convective loop connecting seawater inflow to discharge, small physical perturbations can greatly affect its permeability and produce highly variable rates of discharge (e.g., changes form normal to the megaplume discharge rates observed at mid-ocean ridges). Episodic cracking of the thermal boundary layer that separates the flow zone from 1200°C portions of the axial intrusive can produce the half to twice seawater salinity variations commonly observed in ocean hydrothermal systems and inferred in massive sulfide hydrothermal systems. In fact, the episodic interactions with rock at >600°C that produce the salinity variations makes any simple distinction between magmatic fluids and circulating seawater difficult. Fluids forced out of an intrusive (magmatic fluids), vapor generated from seawater incursions to ~600°C, and brines recovered from the thermal boundary layer, all can significantly affect the chemistry of the water in the narrow flow zone.

In addition, buoyancy forces in the permeable flow zone are large enough to easily hydrofracture flow impediments within ~1 km of the surface. The hydrothermal system can therefore physically control the near surface ore deposition environment in ways that might normally be considered magmatic (breccia pipes, breccia dikes, etc.). In a broad sense the conference addresses the question of internal (magmatic) vs. external (hydrothermal) control of physical and chemical aspects of hydrothermal systems. The complexity of mid-ocean ridge hydrothermal systems, which probably occupy the hydrothermal end of a spectrum on which porphyry copper systems occupy the magmatic end, leads to an appreciation of the difficulties in identifying magmatic input at the hydrothermal end of the spectra.

The mid-ocean ridge observations that constrain the plumbing system of axial hydrothermal systems are: (1) The high temperature venting is at ~350°C. (2) The venting is at the ridge axis. (3) Axial magma chambers, from seismic evidence, are a few kilometers wide and extend from a few kilometers to the Moho depths (Dietrick, 1987). (4) The "normal" mass discharge rates of black smoker systems, Q, is ~150 kg/s and the normal heat discharge rate, $j = 5.3 \times 10^5$ cal/sec (Baker *et al.*,

Keywords: hydrothermal, convection, mid-ocean ridge, intrusive, permeability, porosity

Observations at Mid-Ocean Ridges Define the Hydrothermal System

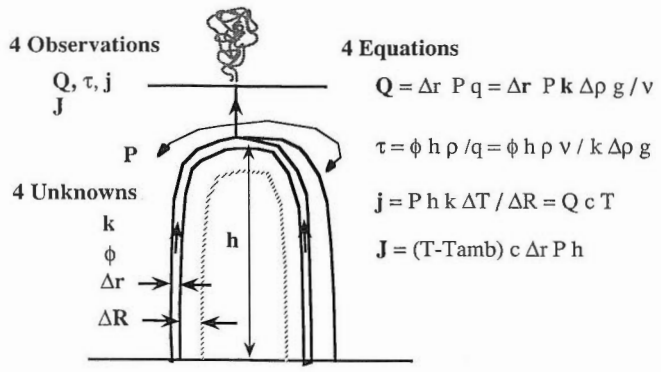

Fig. 1 Four observations of hydrothermal venting at mid-ocean ridges allow solution of 4 conservation equations for the 4 principle system unknowns. Symbols are defined and discussed in the text.

1989). (5) The residence time, t, of seawater at T>150°C in these "normal" systems is <10 years (Kadco and Moore, 1988). But (6) megaplume discharges, in systems that discharged "normally" both before and after, have released up to 0.08 km^3 of 350°C water or J = 2.9 × 10^{16} cal in a few days or weeks (e.g., have operated at discharge rates ~250 times normal for short periods (Baker *et al.*, 1989; Cann and Strens, 1989). (7) Discharging waters are on average of seawater salinity but salinities unequal to seawater are the rule rather than the exception and range from half to twice seawater salinity (Bischoff and Rosenbauer, 1989). (8) The heat flow is depressed within 7 km of the ridge axis (Fehn *et al.*, 1983). This indicates Moho-depth circulation, as does the profile of isotopic alteration observed in ophiolites (Gregory and Taylor, 1981; Cathles, 1983).

The near vertical walls of the magma chamber and the 350°C venting suggest permeability decreases strongly at temperatures greater than 350°C, and calculations show that if this is the case the flow will be concentrated in a thin flow zone adjacent to the axial intrusive and vent at ~350°C (Cathles, 1983). Observations of normal and megaplume discharge indicate just how narrow the flow zone may be. The principal observations, Q, t, j, and J defined and discussed above, are related to the principal unknowns of the hydrothermal system by 4 equations as indicated in Figure 1. The principal unknowns are: the permeability of the flow zone, k, the porosity of the flow zone, ϕ, the width of the flow zone Δr, and the average width of the thermal boundary layer, ΔR.

Solution of the set of equations shown in Figure 1 for Q=150 kg/sec, t=3 years, j=5.3 × 10^7 cal/sec, and J=2.9 × 10^{16} cal yields k=330 millidarcies, ϕ=9.6%, Δr=3.4 m, and ΔR=180 m, as fully described in Cathles (submitted). Basically the flow zone width and porosity are constrained by the fluid residence time and the ratio of the megaplume thermal discharge to the normal discharge rate. Megaplume discharge rates result from a large increase in flow zone permeability, which causes it to contract in width dramatically. The heat discharged by the megaplume thus provides a direct measure of the thermal volume of the flow zone under normal oper-

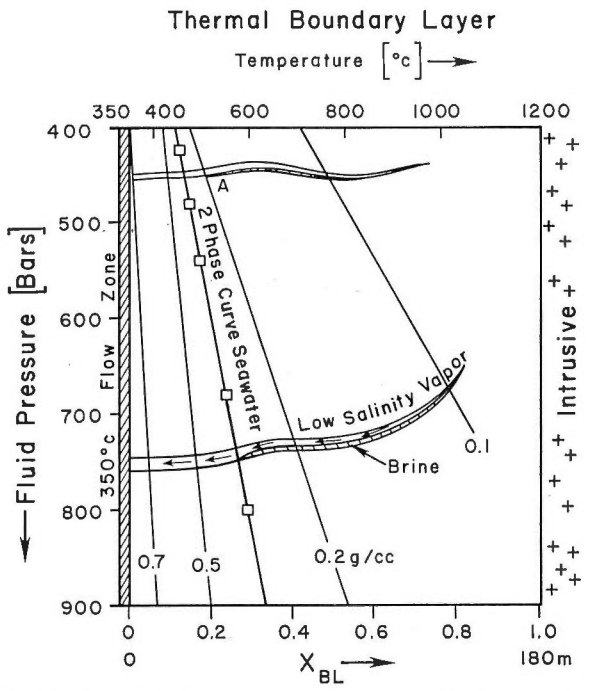

Fig. 2 Density of single phase seawater or vapor in fractures through the thermal boundary layer separating the 350°C flow zone and the 1200°C axial intrusive.

ating conditions. The width of the thermal boundary layer is measured by the geometry of the intrusive (area of its sides) and the normal thermal discharge rate, j. Given Δr and and the intrusive perimeter, Q measures the flow zone permeability. With a narrow flow zone, cracking of the thermal boundary layer can affect discharge chemistry. When fracturing occurs some cracks will penetrate across the thermal boundary layer at sonic velocities. Flow zone water will be drawn into much hotter rock, and after a short time the water filling the fracture will be heated to the temperature of the local rock environment. Water beyond the 2-phase boundary defined in Figure 2 will separate into a brine and low density vapor. The vapor will be expelled into the flow zone where it will recondense causing little increase in flow zone temperature (because of the large thermal mass of the rock compared to pore water) but a significant decrease in flow zone salinity. To reduce the salinity of the flow zone by 50%, cracking of the boundary layer must produce enough fractures to occupy 1% of the boundary layer and penetrate ~2/3 of the way across the boundary layer.

Veins observed in the Bushveld quantitatively confirm this model. Schiffries and Skinner (1987) have documented early high temperature veins with no halos that are >10 m long, contain calcic amphibole with <5 wt.% Cl, are cut by migmatites, and occupy 0.1 to 1% of the rock volume. Intermediate temperature veins (300°<T<600°C) with fluid inclusions with halite daughter minerals and narrow vein halos (~few mm to 1 cm wide) are typically traceable for >20 m and occupy 0.1 to 1% of the rock volume. Veins with wide alteration halos are extremely abundant in patches. In these patches the veins occupy ~10% of the rock volume. The high and

intermediate temperature veins with no or narrow halos are exactly those expected for very rapid seawater penetration of the thermal boundary layer (no time to develop diffusion alteration halos; Cl-rich amphiboles and halite daughter minerals attest to the presence of brine). The patchy lower temperature alteration is of the kind expected for the narrow flow zone. The porosity of ~10% is very close to that predicted from sea floor observations.

The narrow flow zone enables discharge compositions to respond rapidly to fracturing events. The migration of the flow zone need not, in fact probably will not, occur at the same time as cracking of the thermal boundary layer. Flow zone migrations will flush brine immediately but rock alteration will be delayed. Thus decreases in salinity will not in general correlate with changes in fluid composition that reflect interaction with fresh basalt. The absense of chemical correlation has been a puzzling aspect of ocean ridge hydrothermal systems.

Finally as shown in Figure 2, the density of the flow zone is ~0.3 g/cc less than the surrounding ~100°C environment. Buoyancy forces in the flow zone are thus ~30 bars/km. Normally they are balanced by the resistance offered by the porous media to upward flow. However, if precipitation of minerals in the upper parts of the system stop that flow, the full buoyancy force could be applied to break those restrictions. Over 7 km ~200 bars pressure could be delivered, and this is enough to hydrofracture restrictions to at least 1 km depth.

The mid-ocean ridge hydrothermal model sketched above provides a physical context for discussing magmatic contributions to hydrothermal systems.

References

Baker, E. T., Lavelle, J. W., Feely, R. A., Massoth, G. J., and Walker, S. L. (1989) Episodic venting of hydrothermal fluids from the Juan de Fuca Ridge. *Jour. Geophys. Res.*, vol. 94, p. 9237-9250.

Bischoff, J. L., and Rosenbauer, R. J. (1989) Salinity variations in submarine hydrothermal systems by layered double-diffusive convection. *Jour. Geol.*, vol. 97, p. 613-623.

Cann, J. R., and Strens, M. R. (1989) Modeling periodic megaplume emission by black smoker systems. *Jour. Geophys. Res.*, vol. 94, p. 12,227-12,237.

Cathles, L. M. (1983) An analysis of the hydrothermal system responsible for massive sulfide deposition in the Hokuroku Basin of Japan. *Econ. Geol. Monogr.* 5, p. 439-487.

Cathles, L. M. (submitted) A capless 350°C flow zone model to explain megaplumes, salinity variations, and high temperature veins in ridge axis hydrothermal systems. *Econ. Geol.*

Dietrick, R. S. *et al.* (1987) Multi-channel seismic imaging of a crustal magma chamber along the East Pacific Rise. *Nature*, vol. 326, p. 35-41.

Fehn, U. Green, K. E., Von Herzen, R. P., and Cathles, L. M. (1983) Numerical models for the hydrothermal field at the Galapagos spreading center. *Jour. Geophys. Res.*, vol. 88, p. 1033-1048.

Gregory, R. T., and Taylor, H. P. (1981) An oxygen isotope profile in a section of cretaceous oceanic crust, Samail Ophiolite, Oman: evidence for $\delta^{18}O$ buffering of the oceans by deep (>5km) seawater-hydrothermal circulation at mid-ocean ridges. *Jour. Geophys. Res.*, vol. 86, p. 2737-2755.

Kadko, D., and Moore, W. (1988) Radiochemical constraints on the crustal

residence time of submarine hydrothermal fluids: Endeavour Ridge. *Geochim. Cosmochim. Acta.*, vol. 52, p. 659-668.

Schiffries, C. M., and Skinner, B. J. (1987) The Bushveld hydrothermal system: field and petrologic evidence. *Amer. Jour. Sci.*, vol. 287, p. 566-595.

Rept. Geol. Surv. Japan, No. 279, p. 44-48, 1992

Search for Magmatic Signatures in Japanese Geothermal Fluids

Hitoshi CHIBA

Institute for Study of the Earth's Interior
Okayama University
*827 Yamada, Misasa, Tohaku, Tottori 682-01, Japan**

Many Japanese geothermal systems have been assessed and exploited for the purpose of electric power generation in the last two decades. The chemical compositions of the geothermal reservoir fluids of some of these systems were recently presented, and the mechanisms controlling fluid compositions were examined in detail (Chiba, 1991). In many systems, acidic fluids have been found during exploitation in addition to the more common neutral pH fluids. Acidic fluids may contain direct and indirect magmatic contributions. The purpose of the present study is to search for any magmatic signatures which remain in the major element chemical composition of the geothermal fluid, especially acidic fluid, and to assess the potential change in fluid composition from the magmatic to geothermal environment.

pH and major aqueous species

The pH of neutral geothermal fluids in Japan is controlled by the K-feldspar - K-mica buffer depending on the salinity of the fluid (Chiba, 1991). The reservoir pH values of acidic fluids discharged from wells in the same area as neutral pH geothermal wells are between 3.9 and 5.5, 1 to 2 pH units more acid compared with the neutral pH fluids. Major cations are not likely to be magmatic in origin, but rather are considered to be leached from country rocks or alteration minerals. As shown by Chiba (1991), in the mature Japanese geothermal systems the aqueous cation compositions are in equilibrium with alumino-silicate minerals. The cation/cation ratios of acidic geothermal fluids, except for ratios involving Mg, show a similar relationship with respect to temperature, as reported by Chiba (1991).

The sulfate concentrations in the neutral pH and acidic geothermal fluids are saturated with respect to anhydrite. The origins of sulfate and sulfide in Japanese acid geothermal fluids are suggested to be volcanic (Kiyosu and Kurahashi, 1983). However, in some areas, sulfate originated from seawater or fossil seawater may be involved in the geothermal fluid (Sakai and Matsubaya, 1974). All acidic fluids examined in this study are undersaturated with respect to calcite, although neutral pH geothermal fluids are nearly saturated with calcite (Chiba, 1991). The undersaturation with respect to calcite is likely due to the low pH of the fluid and may be an indirect indicator of a magmatic contribution. The origins of sulfate, carbonate and other anions are not clearly understood at present.

Keywords: neutral geothermal fluid, acidic geothermal fluid, aqueous speciation, oxygen fugacity

* Present address: Department of Earth and Planetary Sciences, Kyushu University, 6-10-1, Hakozaki, Higashi, Fukuoka 812, Japan.

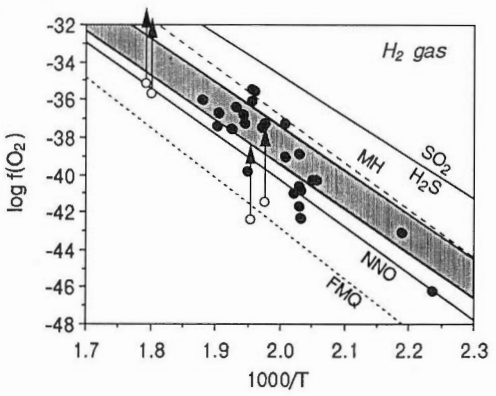

Fig. 1 Reservoir temperature versus oxygen fugacity calculated from H_2 concentration. MH: magnetite-hematite, NNO: nickel-nickel oxide, FMQ: fayalite-magnetite-quartz oxygen buffers. The shaded area is for fluid in equilibrium with volcanic rocks (Kishima, 1989). Solid circles: Japanese neutral pH geothermal fluids (Chiba, 1991). Open circles: Japanese acidic fluids from Kirishima (Kodama and Nakajima, 1988), Hatchobaru (Shimada *et al.*, 1985), Sumikawa (Ueda *et al.*, 1991) and Ohnuma (Sakai *et al.*, 1986) geothermal systems. The arrow above the open circle indicates the possible shift of oxygen fugacity when the hydrogen gas concentration is reduced to a hundredth of the measured composition to assess the steam gain. T in Kelvins.

Gaseous species

The concentration of CO_2 is controlled by a Ca-silicate - calcite - SiO_2 buffer in the neutral pH geothermal systems. In carbonate-hosted neutral pH geothermal system such as Nigorikawa, Japan, the CO_2 concentration is significantly higher than in other systems. This implies an indirect magmatic effect. The high CO_2 concentration is probably due to attack by acidic volcanic gases on the carbonate country rock. The acidic geothermal fluids studied here have a wider range of CO_2 partial pressures compared with the neutral pH geothermal fluids.

The concentration of H_2S is likely to be controlled by either the Fe-Al-silicate - pyrite (Giggenbach, 1980) or pyrite-pyrrhotite buffer in most Japanese neutral pH geothermal systems. In acidic geothermal systems, the ratio H_2/H_2S is much higher compared with that of neutral pH geothermal systems. Since the acidic fluids examined here have slight excess discharge enthalpies, they may have gained excess H_2 relative to H_2S from the vapor.

Oxygen fugacity of fluid

The oxygen fugacity of geothermal fluid can be calculated by several independent parameters, such as concentration of dissolved H_2, and the H_2S/SO_4^{2-} and CO_2/CH_4 ratios. These parameters differ in their reaction rates for approach to equilibrium. The dissolved H_2 concentration seems to follow most rapidly a change in the oxygen fugacity of the fluid, since it approaches the redox state of experimental solutions within three days at hydrothermal conditions (Kishima and Sakai, 1984). The oxygen fugacities calculated from the H_2 concentration and sulfide/sulfate activity ratios in Japanese neutral and acidic geothermal fluids are shown in Figures 1

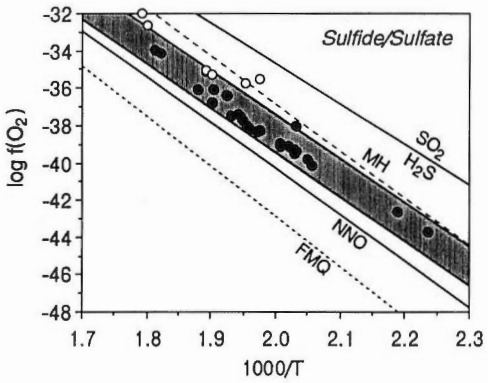

Fig. 2 Reservoir temperature versus oxygen fugacity calculated from sulfide/sulfate activity ratios. Symbols are as in Fig. 1.

and 2, and lie in a range of common buffers. Though the overall scatter in Figure 1 is large, the acid fluids appear to be slightly more reduced based on H_2 compositions. Kishima (1989) found that the oxygen fugacity of fluid between 200° and 500°C is controlled not by mineral buffers (e.g., FMQ or NNO), but by the rock itself. The calculated redox states of Japanese neutral pH geothermal fluids agree with Kishima's rock buffer. In contrast to the redox indicated by H_2 gas compositions, the sulfide/sulfate ratio points to the acid fluids being slightly more oxidized than the neutral pH fluids. The inconsistency may be due to artificially high H_2 gas concentrations in the acid fluids, due to excess discharge enthalpies, as noted previously and/or due to slow reaction rate among sulfur species (Ohmoto and Lasaga, 1982). The slightly higher oxygen fugacity estimated by sulfide/sulfate ratios might reflect the oxidized environment observed in volcanic gases.

In basic magma, the redox conditions lie between FMQ and NNO (Carmichael and Ghiorso, 1986). After formation of magmatic gas and/or fluid, the oxygen fugacity can be calculated from the composition of volcanic gases. The oxygen fugacities of volcanic gases of White Island, New Zealand, were calculated by Giggenbach (1987) using the H_2 and H_2O fugacity of volcanic gases. At a temperature higher than 600°C, the calculated oxygen fugacities lie between the NNO and (FeO)-($FeO_{1.5}$) buffers. The oxygen fugacities increase along the H_2S-SO_2 buffer line with decreasing temperature to 400°C. In this temperature range, the oxygen fugacity of the fluid is controlled by equilibrium among sulfur species and total sulfur concentration (Giggenbach, 1987). This means that the volcanic gas and/or fluid does not efficiently interact with rock matrix between 400° to 600°C. Presuming the existence of acid fluid at temperatures from 400° to 600°C, the change in the oxygen fugacity from acidic to neutral pH geothermal fluid below about 300°C will be largely a function of interaction with the rock buffer.

Transition from magmatic to geothermal fluid

The major cation composition of geothermal fluid is controlled by silicate mineral buffers. The cation composition of magmatic fluid is not clear at present. If it is acidic and is composed of HCl, CO_2 and SO_2 as assumed by Giggenbach (1988), it will attack the rock matrix along the ascending path and dissolve the rock leaving

only SiO_2. In this case, the transition of chemical composition from magmatic to geothermal fluid is accomplished by the neutralization of magmatic fluid with rock matrix and the production of hydrothermally-altered minerals. On the other hand, based on recent experiments on the partitioning of chlorine compounds between silicate melt and hydrothermal solutions at high temperature and low pressure (0.6 to 6 kbar) (Shinohara *et al.*, 1984; 1989), Shinohara (1991) suggests that magmatic fluid formed in the crust contains NaCl as a dominant chlorine compound and that its composition is different from the acidic volcanic gases. In this case, the geothermal fluid is originally Na-Cl dominant and its composition is modified through the formation of alteration minerals.

The main path of oxygen fugacity from magmatic to geothermal system is considered to trace follow the following stages: (1) between FMQ and NNO in volcanic rocks, (2) between NNO and (FeO)-($FeO_{1.5}$) in high temperature volcanic gas (>600°C) if the volcanic gas represents the oxygen fugacity of fluid exsolved from magma in the crust, (3) (FeO)-($FeO_{1.5}$) or rock buffer in the neutral pH geothermal environment. Direct evidence from the temperature range of 600°C to the geothermal environment is lacking, so this environment cannot be considered from the present study of Japanese acidic geothermal fluids. But this is the temperature range over which a drastic change in oxygen fugacity can be expected. In order to elucidate the entire evolutionary path of fluid from the magmatic to geothermal environment, knowledge is required about how and where the acidic fluid is formed.

References

Carmichael, I. S. E. and Ghiorso, M. S. (1986) Oxidation-reduction relations in basic magma: a case for homogeneous equilibria. *Earth Planet. Sci. Letters*, vol. 78, p. 200-210.

Chiba, H. (1991) Attainment of solution and gas equilibrium in Japanese geothermal systems. *Geochem. Jour.*, vol. 25, p. 335-355.

Giggenbach, W. F. (1980) Geothermal gas equilibria. *Geochim. Cosmochim. Acta*, vol. 44, p. 2021-2032.

——— (1987) Redox processes governing the chemistry of fumarolic gas discharges from White Island, New Zealand. *Appl. Geochem.*, vol. 2, p. 143-161.

——— (1988) Geothermal solute equilibria. Derivation of Na-K-Mg-Ca geoindicators. *Geochim. Cosmochim. Acta*, vol. 52, p. 2749-2765.

Kiyosu, Y. and Kurahashi, M. (1983) Origin of sulfur species in acid sulfate-chloride thermal waters, northeastern Japan. *Geochim. Cosmochim. Acta*, vol. 47, p. 1237-1245.

Kishima, N. (1989) A thermodynamic study on the pyrite-pyrrhotite-magnetite-water system at 300°-500°C with relevance to the fugacity/concentration quotient of aqueous H_2S. *Geochim. Cosmochim. Acta*, vol. 53, p. 2143-2155.

Kishima, N. and Sakai, H. (1984) A simple gas analytical technique for the Dickson-type hydrothermal apparatus and its application to the calibration of MH, NNO and FMQ oxygen buffers. *Geochem. Jour.*, vol. 18, p. 19-26.

Kodama, M. and Nakajima, T. (1988) Exploration and exploitation of the Kirishima geothermal field. *Jour. Geotherm. Research Soc. Japan.*, vol. 25, p. 201-230 (in Japanese).

Ohmoto, H. and Lasaga, A. C. (1982) Kinetics of reactions between aqueous sulfates and sulfides in hydrothermal systems. *Geochim. Cosmochim. Acta*, vol. 46, p. 1727-1745.

Sakai, H. and Matsubaya, O. (1974) Isotopic geochemistry of the thermal waters of Japan and its bearing on the Kuroko ore solutions. *Econ. Geol.*, vol. 69, p. 974-991.

Sakai, Y., Kubota, Y. and Hatakeyama, K. (1986) Geothermal exploration at Sumikawa, north Hachimantai, Akita. *Chinetsu*, vol. 23, p. 281-302 (in Japanese).

Shimada, K., Fujino, T., Koga, A. and Hirowatari, K. (1985) Acid hot water discharging from geothermal wells in the Hatchobaru geothermal field. *Jour. Geotherm. Research Soc. Japan.* vol. 22, p. 276-292 (in Japanese).

Shinohara, H., Iiyama, J. T. and Matsuo, S. (1984) Comportement du chlore dans le systeme magma granitique-eau. *C.R. Acad. Ac. Paris*, vol. 298, p. 741-743.

———, ——— and ——— (1989) Partition of chlorine compounds between silicate melt and hydrothermal solutions: I. Partition of NaCl-KCl. *Geochim. Cosmochim. Acta*, vol. 53, p. 2617-2630.

——— (1991) Geochemistry of magmatic hydrothermal system. *Chikyukagaku (Geochemistry)*, vol. 25, p. 27-38 (in Japanese).

Ueda, A., Kubota, Y., Katoh, H., Hatakeyama, K. and Matsubaya, O. (1991) Geochemical characteristics of the Sumikawa geothermal system, northeast Japan. *Geochem. Jour.*, vol. 19, p. 11-25.

Rept. Geol. Surv. Japan, No. 279, p. 49-52, 1992

The Composition of Ruapehu Crater Lake, New Zealand: Evolution of a Vent Hosted Hydrothermal System

Bruce W. CHRISTENSON[1] and C. Peter WOOD[2]

[1]. *DSIR Chemistry, Geothermal Research Centre*
Private Bag 2000, Taupo, New Zealand.
[2]. *DSIR Geology and Geophysics*
Private Bag, Rotorua, New Zealand.

Variations in Ruapehu Crater Lake composition during both eruptive and non-eruptive periods can be interpreted in terms of a sequence of stepwise hydrothermal reactions taking place in the vent complex, the effluent from which is expelled into the lake environment via a convective hydrothermal system.

The lake is roughly 500 m in diameter, has a maximum depth of 135 m, and ranges in temperature between ca. 10 and 60°C. Over the last twenty years, pH has varied between its present value of 0.6 and a high of 1.8 which was recorded during a period of phreatomagmatic activity in 1971 (Giggenbach, 1974). The low pH is attributed to inputs of magmatic HCl and H_2SO_4, the latter deriving from the disproportionation of SO_2 in the saturated vent environment. Recent bathometric and lake temperature studies (Christenson *et al.*, in prep.) reveal the presence of a molten sulphur pool over the vent region.

Phreatomagmatic activity has generally declined over the last 20 years. Juvenile material accompanied eruptions in 1969, 1971, 1975 and 1977, whereas smaller eruptions occurring in 1982 and 1988 were, strictly speaking, phreatic in nature. Alteration phases in the ejecta from these eruptions typically include cristobalite, elemental sulphur, natroalunite, anhydrite and pyrite, but lesser amounts of halite, sylvite, hematite, and pyrophyllite have also been identified.

The 1971 eruptions had a marked effect on the composition of the lake water (Giggenbach, 1974). Hydrolysis of the fresh magmatic material introduced into the vent environment resulted in increased pH, removal of SO_4^{-2} into natroalunite and anhydrite, and the release of conservative constituents (e.g., Mg^{++}) into solution.

The eruption in 1988, by comparison, had little effect on the lake composition. However, the relatively quiescent period which has ensued since that event has been characterised by steadily decreasing Mg/Cl ratios and increasing ratios of Mg/Na, Mg/K and Mg/SO_4 (Fig. 1). We attribute these changes to reaction path processes continuing in the vent, resulting in the dissolution of previously formed alteration phases (most notably natroalunite).

We have combined these observations with findings of Hurst *et al.* (1991) to generate the hydrothermal model depicted in Figure 2. A heat pipe is portrayed operating between the upper region of degassing magma and a zone of recirculating lake water in the upper portion of the vent. Condensate forming in the lower part of the two-phase envelope returns under gravity to the heat source whereas that forming higher in the system mixes with recirculating lake water and is convectively swept upward into the lake.

Such processes have obvious implications for the formation of high sulphidation ore deposits. Metals are introduced into the condensed aqueous phase both

Keywords: Ruapheu, volcanic crater lake, chemistry, computer models

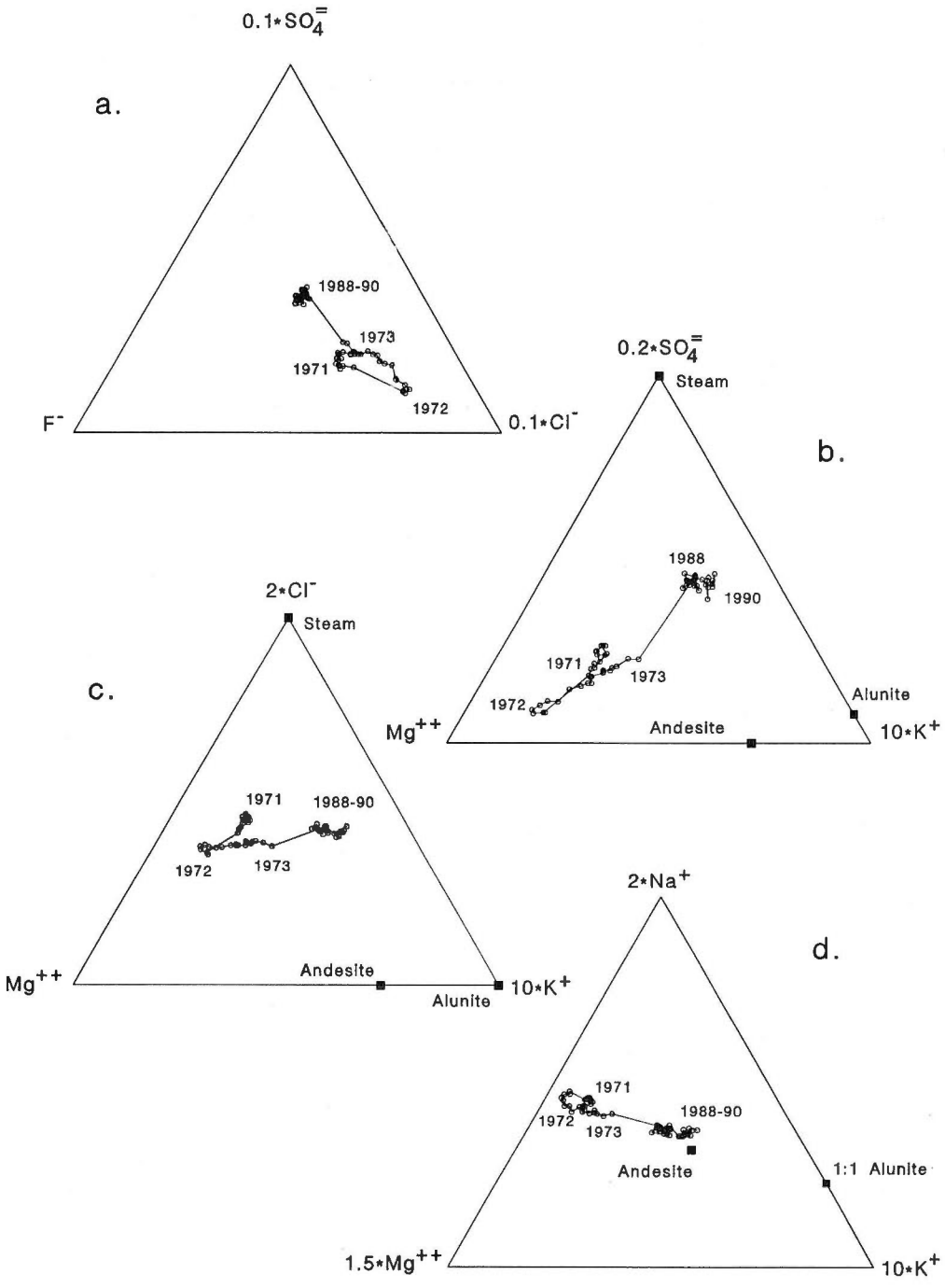

Fig. 1. Normalised variations between SO_4, Cl, F, Mg, Na and K in Ruapehu Crater Lake water. Eruptions in 1971 resulted in increases in Cl and Mg relative to SO_4, Na and K, but dissolution processes in the vent system have since reversed these trends.

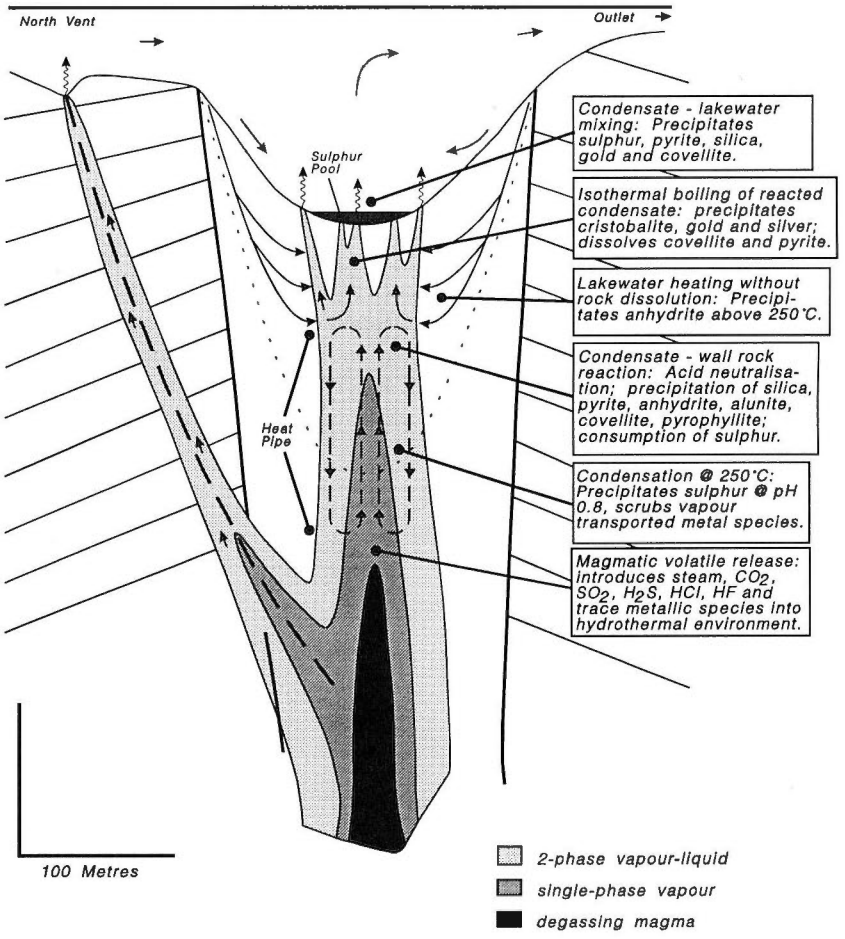

Fig. 2 Flow regime and major chemical processes in the vent-lake system. Drawn to scale, the dotted line represents the bathometric profile in 1965; sedimentation and volcanic activity brought lake depth close to its present level by 1970.

through dissolution of fresh andesitic material which is repeatedly introduced into the vent through time, but also through direct vapour phase transport into the two phase region of the vent where the metal species are condensed into the liquid phase.

Results of reaction path modelling using the computer code CHILLER (Reed and Spycher, 1984) and relevant end member fluid and rock compositions from Ruapehu and White Island volcanos are summarised in Figure 2. Acid neutralisation reactions between acidic condensate and wall rock are the dominant processes along the various flow paths in the vent system. Condensate formation is accompanied by the precipitation of elemental sulphur; dissolution of the enclosing andesite ensues, resulting in the sequential precipitation of cristobalite, pyrite, anhydrite, alunite, covellite, pyrophyllite, barite and fluorapatite, and the dissolution of the earlier formed sulphur. Further or continued titration of condensate into the reaction environment redissolves these alteration phases in approximately the reverse order of

their appearance. Boiling of both reacted and unreacted condensate in the vent precipitates gold, as does mixing of these solutions with the sulphide poor, oxidised lake waters.

References

Giggenbach, W. F. (1974) The chemistry of Ruapehu Crater Lake (New Zealand) during and after the 1971 active period. *N. Z. Jour. Sci.*, vol. 17, p. 33-45.

Hurst, A. W., Bibby, H. M., Scott, B. J. and McGuinness, M. J. (1991) The heat source of Ruapehu Crater Lake; deductions from the energy and mass balances. *Jour. Volcanol. Geotherm. Res.*, vol. 46, p. 1-21.

Reed, M. H. and Spycher, N. (1984) Calculation of pH and mineral equilibria in hydrothermal waters with application to geothermometry and studies of boiling and dilution. *Geochim. Cosmochim. Acta.*, vol. 45, p. 1479-1492.

Rept. Geol. Surv. Japan, No. 279, p. 53-56, 1992

Magmatic Hydrothermal System beneath Kuju Volcano, Central Kyushu, Japan

Sachio EHARA

Department of Mining, Faculty of Engineering, Kyushu University
Fukuoka 812, Japan

The Kuju volcano group, composed of many lava domes, is situated in the Beppu-Shimabara volcanic graben (Matsumoto, 1979), central Kyushu, Japan (Fig. 1). It is a typical andesitic island arc volcano. The main rock type is hornblende andesite (VSJ and IAVCEI, 1971). Volcanic activity started about 0.3 Ma, and the youngest radiometric age of Kuju volcanic rocks is several ten thousand years (Watanabe *et al.*, 1987; Hayashi, 1988). Historically, only phreatic explosions have occurred several times (JMA, 1975). An active solfatara field is present in an explosion crater of Mt. Hosshoyama, the most intense surficial geothermal activity in central Kyushu. The natural heat discharge is estimated at about 100 MW, most from steaming ground and fumaroles (Ehara *et al.*, 1981). Temperatures of fumaroles generally exceed 200°C and the maximum temperature measured was 508°C in 1960 (Mizutani *et al.*, 1986).

Heat flow in and around Kyushu island increases gradually from the Pacific side to the Japan Sea side (Ehara, 1989). Particularly high heat flows (up to 250 mW/m^2) are observed around Kuju Volcano. Curie point depths are shallower than 7 km below sea level around Kuju volcano (Okubo *et al.*, 1985). Both indicate high crustal temperature. The underground temperature calculated assuming a steady state is too high in the upper crust, given that seismic shear waves are transmitted beneath Kuju volcano. Therefore the high heat flows are interpreted to be due to conductive cooling of a relatively shallow magma reservoir beneath Kuju Volcano, based on finite element technique calculations (Lee *et al.*, 1980). It is assumed that the magma began to cool about 0.05 Ma, based on the youngest radiometric age of Kuju volcanic rocks. The magma is no longer molten but has a temperature of 400-700°C at 5 km depth (Fig. 2).

Mt. Hosshoyama is in the central part of the Kuju volcano group and the solfatara field (c.a., 0.2 km^2) is on its northern flank. Microseismic observations were conducted around the solfatara field, with an active seismic zone detected just beneath the solfatara field to 1.5 km depth below the surface. An aomalously low P wave velocity structure was also detected just beneath the solfatara field (Ehara *et al.*, 1990). These results indicate that the region beneath the solfatara field is fractured and therefore highly permeable.

ELF and ULF magnetotelluric soundings were made in and around Kuju Volcano (Mogi *et al.*, 1988). An extremely low resistivity value of 1 ohm-m was detected just beneath the solfatara field to depths greater than 1 km. The low resistivity zone is limited to an area of 900 m E-W by 500 m N-S. Such low resistivity beneath the solfatara field is most likely due to hot and saline geothermal fluids.

A conceptual thermal model is presented based on thermal, isotopic and struc-

Keywords: magmatic hydrotherml system, heat flow, thermal modelling, magma reservoir, geothermal reservoir

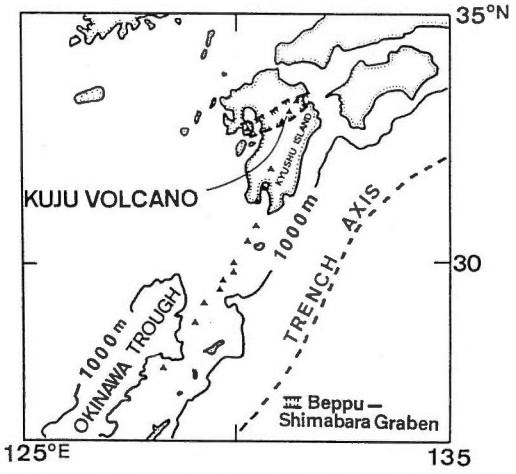

Fig. 1 Location map of Kuju Volcano in Kyushu. Solid triangles show active volcanoes along the Ryukyu Arc.

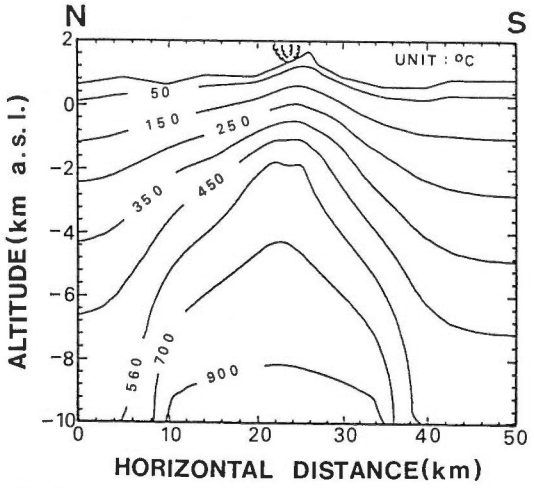

Fig. 2 Present temperature distribution beneath Kuju Volcano.

tural data (Fig. 3). The drilling (NEDO, 1988) and gravity (Komazawa and Kamata, 1985) data show the depth to basement is 1.5 to 2.0 km in and around the solfatara field. The low resistivity zone extends to the top of the basement. Microearthquakes occur at depths above the basement. The isotopic study of fumaroles, hot springs and groundwater shows mixing of meteoric water with magmatic fluid (Matsubaya *et al.*, 1975, Mizutani *et al.*, 1986).

Summarizing these data, the following conceptual thermal model was deduced. Magmatic fluid and deeply circulating meteoric water mix at about 2 km depth, near the top of the basement. A geothermal reservoir is present at this depth, from which hot fluids ascend through the low resistivity zone. Microearthquakes occur only in the upper part of the reservoir. Finally, hot water and steam discharge

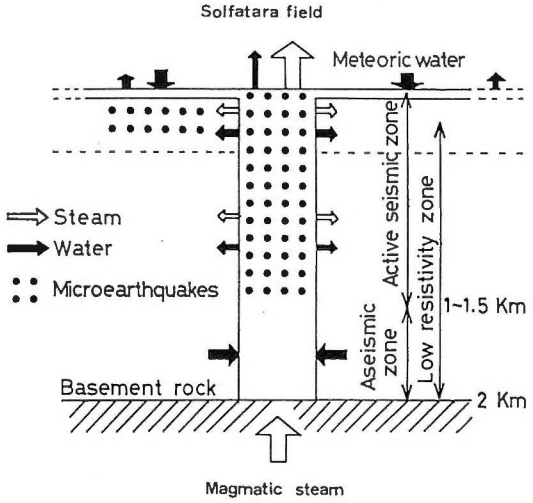

Fig. 3 Conceptual thermal model of the area beneath the solfatara field of Kuju Volcano.

at the ground surface.

Based on the magmatic fluid and meteoric water mixing model, the thermal process beneath the solfatara field was simulated by computer modelling (Pruess and Schroder, 1980; O'Sullivan, 1985), assuming a body of radial symmetry. The diameter and depth of the area concerned are 5 km and 2 km, respectively. The following parameters provide a good fit of the model. The magmatic fluid is supplied at a rate of 30 kg/sec (with an enthalpy of 3500 kJ/kg and temperature above 580°C), originating from the vicinity of the cooling magma body. This fluid mixes with a component of meteoric water amounting to about 10 kg/sec. Vapor (35.8 kg/sec) and hot water (4.3 kg/sec) subsequently discharge at the surface. The calculated heat discharge is 104.4 MW. These fluxes are minimum values, as the subsurface outflow of fluid is not considered. The central, high permeability zone contains two-phase fluids at all depths, with the temperature at 2 km depth exceeding 340°C. Considering the temperature of the upper crust and the magmatic fluid supplied to the geothermal reservoir, the original depth of the magmatic fluid is estimated to be about 5 km.

References

Ehara, S. (1989) Thermal structure and seismic activity in central Kyushu, Japan. *Tectonophysics*, vol. 159, p. 269-278.

———— , Bito, T., Ohi, T. and Kasai, H. (1990) Microseismic activity beneath active fumarolic areas - A case study at Kuju-Iwoyama in central Kyushu, Japan. *Jour. Geotherm. Research Soc. Japan*, vol. 12, p. 263-281(*).

———— , Yuhara, K. and Noda, T. (1981) Hydrothermal system and the origin of the volcanic gas of Kuju-Iwoyama volcano, Japan, deduced from heat discharge, water discharge and volcanic gas emission data. *Bull. Volcanol. Soc. Japan*, vol. 26, p. 35-56(*).

(*): in Japanese with English abstract. (**): in Japanese.

Hayashi, M. (1988) Quaternary volcanism as the heat source for some geothermal fields in Kyushu, Japan. In *Proceedings of the International Symposium on Geothermal Energy, 1988, Kumamoto and Beppu, Japan*, p. 446.

Japan Meteorological Agency (1975) National catalogue of the active volcanoes in Japan. p. 1-119(**).

Komazawa, M. and Kamata, H. (1985) The basement structure of the Hohi geothermal area obtained by gravimetric analysis in central-north Kyushu, Japan. *Rept. Geol. Surv. Japan*, no. 264, p. 303-333(*).

Lee, T. C., Rudmun, A. J. and Sjoreen, A. (1980) Application of finite-element analysis to terrestrial heat flow. *Indiana Geol. Surv. Occasional Paper*, vol. 29, p. 1-53

Matsubaya, O., Ueda, A., Matsuhisa, Y., Sakai, H. and Sasaki, A. (1975) Isotopic study of hot springs and volcanoes in Kyushu, Japan. *Bull. Geol. Surv. Japan*, vol. 26, p. 375-392(*).

Matsumoto, Y. (1979) Some problems on volcanic activities and depression structures in Kyushu, Japan. *Mem. Geol. Soc. Japan*, vol. 16, p. 127-139(*).

Mizutani, T., Hayashi, S., and Sugiura, T. (1986) Chemical and isotopic compositions of fumarolic gases from Kuju-Iwoyama, Kyushu, Japan. *Geochem. Jour.*, vol. 20, p. 273-285.

Mogi, T., Nakama, K. and Shimoizumi, M. (1988) Magnetotelluric study of the geothermal system in Kuju Volcano. In *Proceedings of the International Symposium on Geothermal Energy, 1988, Kumamoto and Beppu, Japan*, p. 539-542.

New Energy Development Organization (1988) An interim report, Kuju area. p. 65-120(**).

Okubo, Y., Graf, R. J., Hansen, R. O., Ogawa, K. and Tsu, H. (1985) Curie point depths of the Kyushu and surrounding areas, Japan. *Geophysics*, vol. 53, p. 481-494.

O'Sullivan, M. J. (1985) Geothermal reservoir simulation. *Energy Research*, vol. 9, p. 319-332.

Pruess, K. and Schroder, R. C. (1980) SHAFT79, User's manual. *Lawrence Berkeley Lab., Rept.* 10861, p. 1-47.

Volcanological Society of Japan and IAVCEI (1971) List of world active volcanoes. p. 1-160.

Watanabe, K., Hayashi, M. and Fujino, T. (1987) Fission track age of volcanoes in the Kuju volcanic region in relation to geothermal activity. *Jour. Geotherm. Research Soc. Japan*, vol. 9, p. 207-217.

Rept. Geol. Surv. Japan, No. 279, p. 57-59, 1992

The Influences of Depth of Burial and the Brittle-Plastic Transition on the Evolution of Magmatic Fluids

Robert O. FOURNIER

U. S. Geological Survey
MS-910, 345 Middlefield Road, Menlo Park, CA 94025, U.S.A.

In order to formulate realistic models of magmatic contributions to hydrothermal systems one must take into account the complex and dynamic multi-coupled processes that relate changes in chemical, hydrologic, and mechanical properties of rocks and fluids to each other and to changes in the temperature and pressure regime. The time and place of release of H_2O, CO_2, and other dissolved volatile constituents from upward moving and/or crystallizing magma depends mainly on the sum of the partial pressures of these constituents in the magma, and on the effective confining pressure. At the interface of magma with solid rock the effective confining pressure is the pore-fluid pressure in the encompassing rock. In brittle rock this may range from near lithostatic to considerably less than ideal hydrostatic (the pressure exerted by the weight of a column of cold water extending upward through relatively permeable rock to the ground surface). Where the encompassing rock behaves plastically, the effective confining pressure is likely to be close to lithostatic.

Based on what is currently known about concentrations of H_2O and chloride dissolved in silicic magmas in the continental crust, fluids that separate from these magmas where the partial pressure of H_2O (PH_2O) is greater than about 110 to 115 MPa would be brines with salinities generally in the range 10-30 weight percent. Magmatic fluids released into a hydrostatically pressured environment will encounter PH_2O >110 MPa only at depths greater than about 11-13 km (deeper at high partial pressures of CO_2 and other noncondensable gases). At shallower depths they will boil (or evaporate), yielding hypersaline brines with salinities greater than 40-80 weight percent plus coexisting gases. In contrast, magmatic fluids that remain at lithostatic effective confining pressure are likely to evolve to hypersaline brines with salinities greater than 40-80 weight percent only at depths less than about 5 km. Note that evolving brine will become more saline at lower pore-fluid pressures at a given temperature. However, at PH_2O less than about 20-30 MPa, cooling brine of magmatic origin is likely to enter a region in temperature-pressure space in which it completely evaporates, yielding gas plus precipitated Cl-rich salts that react with silicates and H_2O to produce HCl.

The effective confining pressure for magmatic volatiles at the interface of magma with country rock will remain at hydrostatic or less if permeability in the country rock adjacent to the contact is sufficiently great that fluids in pore spaces and fractures can escape from the system as fast as new fluids are added from the magma or are added by metamorphic reactions that liberate H_2O and/or gases such as CO_2. However, in shallow magmatic environments permeability is likely to change rapidly in response to competing processes that create and destroy interconnected porosity. At temperatures greater than about 300°C, chemical processes, including

Keywords: magmatic fluid, hydrothermal system, vein formation, hydrothermal brecciation, coupled chemical-mechanical processes, brittle-plastic transition

pressure solution and precipitation of minerals from convecting fluids, generally destroy permeability relatively quickly. Counteracting these chemical processes are mechanical processes; shear failure of rock (faulting) that mainly reopens old fractures, and the hydraulic opening of fractures when pore-fluid pressure becomes sufficiently high.

The brittle-plastic transition marks the limit of sustained convective fluid flow at hydrostatic pressure. In siliceous continental rocks in tectonically active regions, this transition probably occurs at about 400°C. At higher temperatures, pore-fluid pressures are likely to approach lithostatic, and fluids of magmatic and metamorphic origin may become trapped in nearly horizontal lenses with little vertical, but significant horizontal hydraulic communication. The horizontal movement of fluids at lithostatic pressure eventually may lead to their escape into cooler, brittle rock at or above the sides of a magmatic intrusion.

Episodes in which permeability barriers are breached, so that there is rapid discharge of fluids initially at lithostatic pressure and temperatures >400°C into regions of hydrostatic pressure and initial temperatures <400°C, are likely to result in local brecciation of two types. The first type is likely to occur within the initially high-pressure portion of the system, when a rapid pressure decline results in flashing of brine to gas in relatively confined spaces adjacent to more open channels. The second type is likely to occur within the initially lower-pressure and lower-temperature portion of the system, when liquid in relatively confined spaces adjacent to more open channels expands quickly as a result of rapid heating by the fluid propelled through the breached permeability barrier.

The temperature gradient extending outward from an intruding magma will be important in determining whether or not significant amounts of fluid become trapped at high pressure, either in the surrounding rock or in portions of previously crystallized magma. A steep temperature gradient can result in convective flow of fluid at hydrostatic pressure close to the magma and little, if any, entrapment of fluids at high pore-fluid pressures. In contrast, where relatively large volumes of crystalline rock are at temperatures in the range 400-500°C in the shallow crust, significant quantities of fluid may become trapped at high pressure. This possibly might arise as a result of previous magmatic injections that pre-heated the rock, or if a large body of magma had been cooling by transfer of heat to the surrounding rock over a considerable interval of time. Various mechanisms can transform plastic rock to brittle rock, with the result that fluids initially trapped at lithostatic pressure may induce fracturing that allows escape of the fluid to a hydrostatically pressured environment. One such mechanism is an increase in the strain rate in the surrounding rock, possibly caused by a new injection of magma. Another mechanism is simply cooling to temperatures less than about 400°C at the waning stage of igneous activity, when the latent heat of crystallization of molten material is no longer a factor in helping to maintain nearly isothermal conditions.

In addition to causing a change from plastic to brittle behavior, cooling and contraction result in the development of tensile stresses that favor the onset of hydraulic fracturing. It is commonly assumed that hydraulic fracturing will result in the upward expulsion of fluid as a result of cracks opening at their highly stressed upper ends and simultaneous closing at their lower ends. However, in a cooling and contracting rock, where tensile stresses are present and there is inherent shear and tensile strength, the gradient of the least principal stress with depth may be less than the hydrostatic gradient. In this situation hydraulic fracturing may propel fluid

downward into a shallow stock, rather than upward, by opening fractures at their more highly stressed lower ends while they simultaneously close at their tops.

A drop in pore-fluid pressure from lithostatic to near hydrostatic at initial temperatures >400°C will result in a major decrease in solubilities of many dissolved constituents, causing massive deposition of minerals in veins. This clogging of fractures by vein minerals, in turn, decreases permeability and may allow the redevelopment of high pore-fluid pressure to an extent that shear or hydraulic fracturing again occurs. An additional factor at temperatures in the 370-400°C range is the tendency for a rock that previously behaved in a brittle manner to switch to plastic behavior after a faulting episode and squeeze newly created fractures shut. This occurs because the faulting releases strain energy, thereby decreasing the difference between the principal stresses and lowering the strain rate. Thus, repeated cycles of pressure and stress buildup, fracturing, and vein deposition may occur.

Rept. Geol. Surv. Japan, No. 279, p. 60-62, 1992

Constant Magma Supply and Constant Generation of Pyroclastic Flows During Eruption of Unzen-dake, Kyushu, Japan

Toshitsugu FUJII[1], Setsuya NAKADA[2] and Hiroshi SATO[3]

[1] *Earthquake Research Institute, University of Tokyo, Yayoi, Tokyo 113, Japan*
[2] *Faculty of Science, Kyushu University, Hakozaki, Fukuoka 812, Japan*
[3] *Department Arts and Science, Hiroshima University, Hiroshima 730, Japan*

After 198 years of dormancy, Unzen-dake started eruption on November 17, 1990. Phreatic and phreatomagmatic eruptions at the summit continued intermittently until May 19, 1991, resulting in the formation of several new craters. On May 19, a new lava dome formed in one of the craters, the Jigoku-ato new crater, located at the east edge of the summit. The dacitic lava dome continued to grow, with failure of the edge of the lava dome resulting in the first pyroclastic flow on May 24. Continuation of growth of the dome and failure of lobes of lava resulted in numerous pyroclastic flows. One of the major pyroclastic flows killed 41 persons on June 3, 1991.

Estimation of the magma supply rate was made based on continuous observations of the dome and pyroclastic flow deposits. The cumulative volume of the supplied magma is calculated by summation of the cumulative volume of the pyroclastic flow deposits and the air fall deposit from the co-ignimbrite ash cloud and the volume of the dome on the date of estimation. The magma supply rate can be estimated from the slope of the accumulation curve of the supplied magma volume and is almost constant ($3\times10^5 m^3$ per day, Fig. 1). A constant supply of magma continued for more than 140 days from June 29, 1991.

The other significant feature of the Unzen-dake eruption is the constant generation of pyroclastic flows which contain very fine ash (Fig. 2) since the appearance of the lava dome.

Formation of fine ash associated with pyroclastic flows has been interpreted to be the result of explosive expansion of volatiles within the magmatic conduit (e.g., Sparks, 1978). The existence of fine ash within Merapi-type pyroclastic flows (block- and ash-flows) of Unzen volcano, however, suggests that magmatic explosion within the conduit is not necessary to produce fine ash.

Most of the pyroclastic flows at Unzen are triggered by detachment of lava blocks from the dome. Observation of video films of many pyroclastic flows from the dome lava shows a large amount of fine ash forms instantaneously when the dome lava fails near the edge of the lobe. Blocks and ash cascade down the slope, progressively forming more fine ash. Production of fine material is accelerated when blocks are jumping and rolling along the deep gulley and also when they go over a steep cliff. Sometimes small streams of hot ash continues to pour down the flanks of the dome after most of the rock fall has stopped. Rock falls from cold portions of the lava dome are much less mobile. These observations suggest that voluminous fine pyroclastic ash is produced without a discrete explosion at the dome or within the magmatic conduit. Similar observations have been made at Mt.

Keywords: Unzen volcano, pyroclastic flow, magma supply

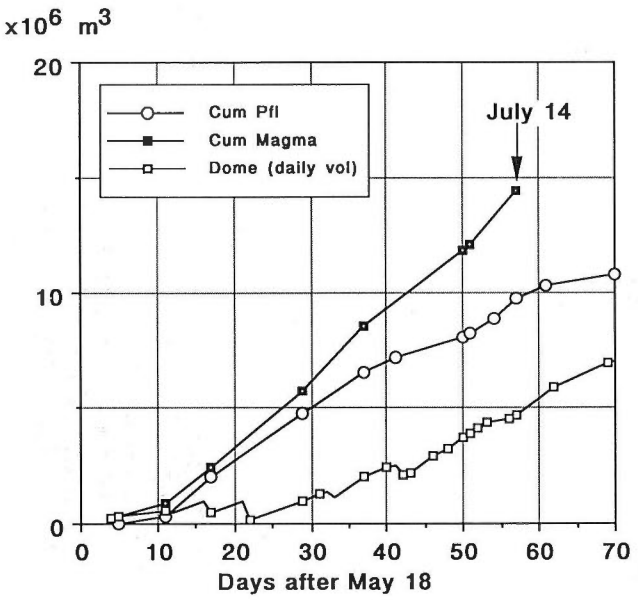

Fig. 1 Rate of magma supply at Unzen volcano. Open square, volume of lava dome. Open circle, cumulative volume of pyroclastic flows and air fall deposits. Solid square, cumulative magma supply estimated by summation of the cumulative volume of pyroclastic flows and air fall deposits and the volume of lava dome on the date of estimation.

St. Helens on 9 May 1986 (Mellors *et al.*, 1988) and at Augustine volcano in 1976 (Stith *et al.*, 1977).

The shape of fine ash is angular to subangular. The degree of vesiculation is not extensive and the bubble size ranges from submicron to ten microns, with a mean distribution of a few microns. No glass shards with bubble wall structure are observed, differing from the co-ignimbrite ash cloud deposit associated with pumice flow and the ash fall deposits from plinian or subplinean eruptions. These observations suggest that the fine ash was not produced by disruption of melt due to decompressional expansion of bubbles, but rather by the breakage of the glassy matrix. This may indicate that the glassy matrix of the dome lava is at its critical tensile strength when the dome lava extrudes. Expansion of volatiles during depressurization associated with ascent on magma may be prevented by a high viscosity of the magma, resulting in the build up of excess pore pressure. The experiments by Webb and Dingwell (1990) indicate melt may not show brittle failure up to a few kbar pressure at a low strain rate, suggesting that an excess pore pressure of few kbar could build up under certain conditions. The bubble-bearing glassy matrix of the dacite could be under a critical stress condition which is close to the yield strength of the matrix glass. Thermal stress may trigger the shattering of dome lava which is at its critical tensile strength due to the excess pore pressure. The rapid expansion of volatiles within the vesicles in glass may further generate fine ash and help the fluidization of the ash. Cooling of lava decreases excess pore pressure by contraction, resulting in rock fall from the cooled lava lobe not being well fluidized.

The feature of constant generation of pyroclastic flows over the period of eruption may be caused by continuous ascent of magma at a constant rate, with a

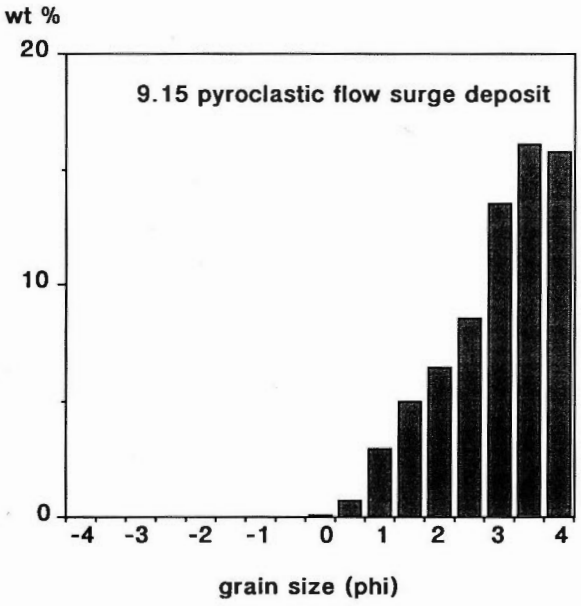

Fig. 2 Grain size distribution of a surge deposit associated with one of the major pyroclastic flows generated on September 15, 1991. Note that the grains finer than 4 in phi scale exceed 40% of the deposit.

consequent steady mechanism of degassing.

References

Mellors, R. A., Waitt, R. B. and Swanson, D. A. (1988) Generation of pyroclastic flows and surges by hot-rock avalanches from the dome of Mount St. Helens volcano, USA. *Bull. Volcanol.*, vol. 50, p. 14-25.

Sparks, R. S. J. (1978) The dynamics of bubble formation and growth in magmas: A review and analysis. *Jour. Volcanol. Geotherm. Res.*, vol. 3, p. 1-37.

Stith, J. L., Hobbs, P. V. and Radke, L. F. (1977) Observation of a nuee ardante from the St. Augustine volcano. *Geophys. Res. Lett.*, vol. 4, p. 259-262.

Webb, S. L. and Dingwell, D. B. (1990) Non-Newtonian rheology of igneous melts at high stresses and strain rates: experimental results for rhyolite, andesite, basalt and nephelinite. *Jour. Geophys. Res.*, vol. 95, p. 15695-15701.

Rept. Geol. Surv. Japan, No. 279, p. 63-67, 1992

Magmatic Gases in Fluid Inclusions from Hydrothermal Ore Deposits

Joseph R. GRANEY and Stephen E. KESLER

Department of Geological Sciences, University of Michigan
Ann Arbor, MI 48109, U.S.A.

Introduction

Subjacent intrusive rocks are the most obvious source of the gases dissolved in many hydrothermal systems, particularly epithermal systems. In acid-sulfate epithermal systems the pivotal role of magmatic gases in generating the low pH hydrothermal fluid is supported by stable isotope and chemical modelling studies (Rye *et al.*, 1991). In adularia-sericite epithermal systems, however, the most common assumption is that the gases are produced by reaction with surrounding host rocks. Several lines of evidence suggest that this might not be the case, and that gases from deeper sources might be important contributors to these systems. For instance, many vein deposits, including Quiruvilca (Bartos, 1987), contain zones of acid-sulfate-like ore and alteration that probably required the passage of small amounts of magmatic vapor. Secondly, gas concentrations in active geothermal systems differ by more than an order of magnitude, although it is not clear whether these variations reflect changes with time in the composition of the systems (Henley, 1985; Hedenquist and Henley, 1985). Finally, the pH of natural geothermal systems is lower than that of hydrothermal rock-water experiments involving similar rocks, and it has been suggested that this difference is due to the presence of CO_2 in natural systems (Kacandes and Grandstaffe, 1989). It is possible, therefore, that gases such as CO_2 and H_2S in high level hydrothermal (e.g., epithermal) systems, are derived at least in part from underlying sources, released by processes ranging from magmatic vapor separation to rock alteration or metamorphism. If this is the case, the pH and other chemical characteristics of the hydrothermal system will be controlled to some degree by this flux of gas. Episodic gas fluxes, might even raise the vapor pressure of the solution sufficiently to cause boiling and consequent mineral deposition.

Method of study

Direct evaluation of these possibilities has been limited by the scarcity of gas analyses in fluid inclusions from all types of hydrothermal systems. In a first step toward assembling a data base for the necessary comparisons, we have used a quadrupole mass spectrometer to determine the gas composition of fluid inclusions from a wide range of extinct hydrothermal systems as represented by different ore deposit types. These deposits, which include hot spring, epithermal vein, sediment-hosted micron gold, acid-sulfate, porphyry copper and molybdenum, tin-tungsten vein, and Mississippi Valley-type deposits (MVT), have associations with intrusive rocks that range from proximal to distal, and should show a corresponding variation in inclusion fluid gas contents if magmatic gas sources are important contributors to these

Keywords: fluid inclusion, fluid gas analysis, quadrupole mass spectrometry

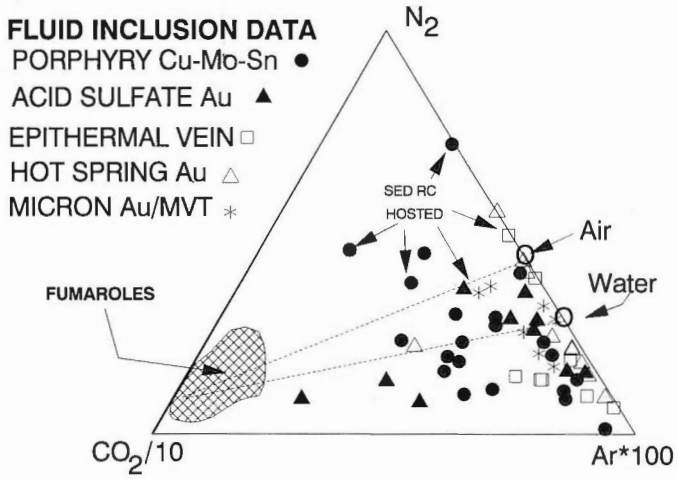

Fig. 1 Ternary diagram comparing the CO_2, N_2, and Ar contents of inclusion fluids from a variety of ore deposit types to volcanic fumaroles, air and air-saturated meteoric H_2O. The tie lines from air and water to CO_2 represent possible mixing lines between air and/or meteoric water with magmatic gas.

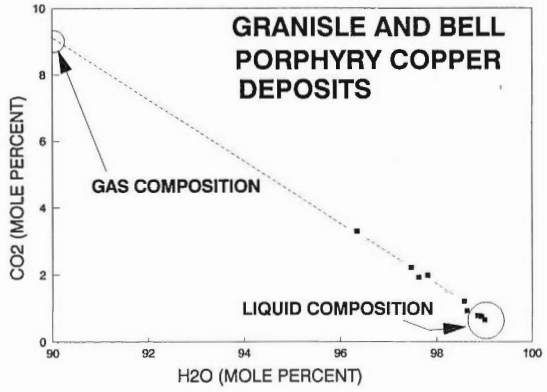

Fig. 2 H_2O-CO_2 binary depicting a method to approximate the vapor-rich inclusion composition from mixed populations of inclusions. If projected back to zero mole % H_2O, the dominant remaining volatile component is CO_2.

systems.

Most samples chosen for analysis consisted of transparent quartz, although barite, jasperoid, opal, sphalerite, pyrite, chalcopyrite, and bornite were also analyzed. Where possible, these samples were selected by optical study of polished fluid inclusion plates. Although efforts were made to include only a single type or generation of fluid inclusion in each analysis, coexisting vapor-rich and liquid-rich inclusions were analyzed in several samples, and inclusion of small secondary inclusions can not always be avoided. Mineral grains and chips from fluid inclusion plates for each analysis are typically less than 2 mm in diameter with a total mass of

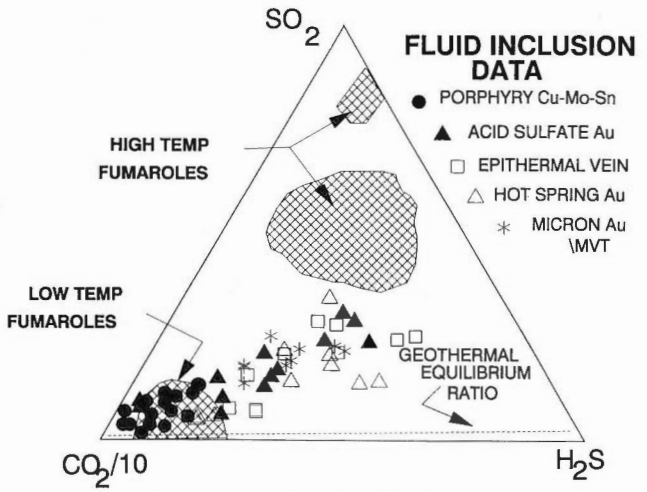

Fig. 3 Ternary diagram comparing the CO_2, SO_2, and H_2S contents of low and high temperature volcanic fumaroles to inclusion fluids from a variety of ore deposit types. The linear trend away from the CO_2 corner suggests subequal amounts of SO_2 and H_2S are present in inclusion fluids. Shown schematically are equilibrium H_2S/SO_2 ratios for geothermal systems which are much higher than the inclusion fluid ratios.

less than 50 mg. Gases were released by crushing the samples at 110°C under vacuum in a modified Nupro valve, from which they were passed directly into a VG SXP600 quadrupole mass spectrometer via a short conduit designed to maximize conductance and minimize adsorption. Data for 16 user-specified masses were collected in a cycling period of about 0.2 second, which permitted simultaneous determination of H_2O, CO_2, CH_4, C_2H_6, C_3H_8, N_2, Ar, O_2, H_2S, SO_2, H_2SO_4, HCl and H_2. Total response for each mass was obtained by integrating under the individual response-time curve for each mass from the time of crushing until the signal returned to background levels. The integrated response for each mass was converted to mole fraction for the gases of interest using a matrix-inversion procedure that takes into account fragmentation patterns and relative sensitivities (to N_2) determined for our instrument (Jones and Kesler, 1992).

Analytical results and discussion

H_2O is by far the dominant volatile component in fluid inclusions, and typically composes 95-99 mole percent of the inclusion fluid. CO_2 comprises most of the remaining volatile component and the other gases are generally present in amounts smaller than 0.1 mole percent. In a plot of CO_2-N_2-Ar abundances (Fig. 1), most of our fluid inclusion analyses extend outward from the composition of air-saturated water along a mixing line towards the composition of gases in high-temperature fumaroles of suspected magmatic origin (Giggenbach *et al.*, 1990). Analyses from porphyry and acid-sulfate deposits, in which magmatic gas contributions should be largest, plot closest to the fumarole compositions. The absence of air

contamination from our analyses is indicated by the fact that most analyses plot below a mixing line between air and these fumarole compositions. Samples such as porphyry-related tin-tungsten veins, MVT and micron-gold deposits, all associated with sedimentary rocks (a possible source of N_2) plot above this line. Note that many of the other samples contain more Ar than air-saturated water, perhaps due to Ar generation from the radiogenic decay of potassium, with subsequent incorporation into fluid inclusions.

Most of the porphyry copper deposit inclusion fluid analyses represent a mixture of liquid-rich and vapor-rich inclusions. That the H_2O-free composition of the vapor phase is largely CO_2 is shown in the H_2O-CO_2 plot (Fig. 2), where the analyses from the Granisle and Bell porphyry copper deposits plot along a line that projects to about 95 mole percent CO_2.

The inclusion fluid analyses define a linear trend in the CO_2-H_2S-SO_2 ternary (Fig. 3), with the porphyry copper deposits closest to the CO_2 corner. Acid-sulfate deposits plot nearer the sulfur gas species axis of the diagram, confirming the relatively greater importance of sulfur gases in these systems. The H_2S/SO_2 ratio of the inclusion fluid is nearly 1, much lower than the equilibrium ratio for gases from geothermal systems. This appears to reflect the presence in the inclusions of SO_2 and possibly thiosulfate (Landis and Rye, 1989; Kesler *et al.*, 1991). The relative scarcity of H_2 in the inclusion fluid analyses suggests that this SO_2 might be produced by post-depositional leakage of H_2 out of the inclusions, although this must be confirmed by further tests.

These inclusion fluid volatile component comparisons show that there are systematic differences in inclusion fluids from different hydrothermal systems. Although some of these variations probably reflect differences in wall rock compositions, the presence of high mole % CO_2 in inclusions from porphyry copper deposits and the enrichment of sulfur gases in acid-sulfate deposits supports the presence of magmatic gases in these deposits, and confirms that magmatic gases emanating from intrusions at intermediate and shallow depths will be enriched in CO_2. Further studies are necessary to demonstrate whether CO_2 abundances in epithermal systems reflect magmatic gas inputs or show systematic variations that can be related to other compositional or geologic parameters.

References

Bartos, P. J. (1987) Quiruvilca, Peru: mineral zoning and timing of wall rock alteration relative to Cu-Pb-Zn-Ag vein-fill deposition. *Econ. Geol.*, vol. 82, p. 1431-1452.

Giggenbach, W. F., Garcia, P. N., Londono, C. A., Rodriguez, V. L., Rojas, G. N. and Calcache, V. M. L. (1990) The chemistry of fumarolic vapor and thermal-spring discharges from the Nevado del Ruiz volcanic-magmatic hydrothermal system, Columbia. *Jour. Volcanol. Geotherm. Res.*, vol. 42, p. 13-39.

Hedenquist, J. W. and Henley, R. W. (1985) Effect of CO_2 on freezing-point depression measurements of fluid inclusions - evidence from active systems and application to epithermal studies. *Econ. Geol.*, vol. 80, p. 1379-1406.

Henley, R. W. (1985) The geothermal framework for epithermal deposits. In Berger, B. R. and Bethke, P. M., eds., Geology and geochemistry of epithermal

systems. *Reviews in Econ. Geol.*, vol. 2, p. 1-24.

Jones, H. D. and Kesler, S. E. (1992) Fluid inclusion gas chemistry in east Tennessee Mississippi Valley-type districts: evidence for immiscibility and implications for depositional mechanism. *Geochim. Cosmochim. Acta*, vol. 55, p. 137-154.

Kacandes, G. H. and Grandstaffe, D. E. (1989) Differences between geothermal and experimentally derived fluids: How well do hydrothermal experiments model the composition of geothermal reservoir fluids?. *Geochim. Cosmochim. Acta*, vol. 53, p. 343-358.

Kesler, S. E., Jones, H. D., and Arehart, G. B. (1991) Significance of O_2 and SO_2 in fluid inclusion analyses to hydrothermal geochemistry. *Geol. Assoc. Canada Program with Abstracts*, vol. 16, p. A65.

Landis, G. P. and Rye, R. O. (1989) Reconnaissance gas chemistry of the Creede, Colorado, hydrothermal system. *U.S. Geol. Surv. Open-File Rept.* 89-94, 51 p.

Rye, R. O., Bethke, P. M., and Wasserman, M. D. (1991) The stable isotope geochemistry of acid-sulfate alteration and vein forming alunite. *U.S. Geol. Surv. Open-File Rept.* 91-257, 59 p.

Rept. Geol. Surv. Japan, No. 279, p. 68-79, 1992

Recognition of Magmatic Contributions to Active and Extinct Hydrothermal Systems

Jeffrey W. HEDENQUIST

Mineral Resources Department, Geological Survey of Japan
1-1-3 Higashi, Tsukuba, Ibaraki 305, Japan

Introduction

Most high temperature geothermal systems active today are located in regions of extremely high heat flow (e.g., 700mW/m^2 over the 5000 km^2 area of the Taupo Volcanic Zone of New Zealand - about 14 times typical continental heat flow - with the heat flow on average 20 times higher over the geothermal systems themselves; Allis, 1980). Such heat flows can be sustained over geologic time only through emplacement of magma at shallow crustal depths. By analogy (as well as direct observation in some cases), many hydrothermal ore deposits also had a magma as the heat engine which drove hydrothermal convection.

Therefore, it is reasonable to consider situations where a magma may also contribute components (water, gases, metals, etc.) to the hydrothermal system, as it is unlikely that the exsolved aqueous phase remains constrained to the magma itself. I first examine the chemical and isotopic characteristics of demonstrably "magmatic fluids" at the surface, immediately adjacent to active volcanic vents. These hot springs are extremely acid (pH 0 to 2), and are closely related to high temperature (800°C+) volcanic fumaroles (the latter discussed elsewhere in this volume, e.g., by Matsuhisa, Shinohara, Symonds, and Taylor).

The next step is to examine the chemical and isotopic characteristics of neutral pH geothermal fluids (often considered to be meteoric-water dominated; Craig, 1963) to determine if any magmatic signatures can be recognized. That is, are there geothermal systems (and if so, in what situations) with magmatic fluids (or at least some magmatic components) entrained at depth in the convection cell? Examples mainly from New Zealand and Japan will be reviewed, though the data base is much larger, comprising well studied systems in Iceland, Indonesia, Italy, Philippines, Taiwan and the U.S.

The final step is to consider how magmatic contributions to extinct hydrothermal systems may be recognized, since fluids are no longer present (with the important exception as fluid inclusions; e.g., as discussed by Beane, Bodnar, Graney and Kesler, and Nedachi, this volume). One common problem is the overprint of late stage fluids which may erase or disguise the isotopic signature left by a magmatic fluid.

Volcanic-related hydrothermal fluids

Some of the most accessible and well studied volcanic hydrothermal systems are in Japan. Andesite-dacite volcanoes at Satsuma Iwojima (an island 40 km south

Keywords: magmatic fluid, meteoric water, geothermal system, volcanic hydrothermal system, metal sources

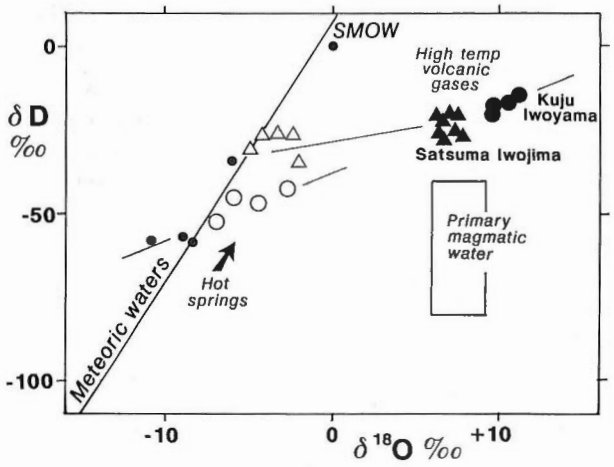

Fig. 1 Isotopic compositions of acid waters and fumaroles from Satsuma Iwojima (Matsuo *et al.*, 1974, Matsubaya *et al.*, 1975) and Kujyu (Mizutani *et al.*, 1986). Closed symbols are high temperature fumaroles, while open symbols are hot springs; small dots are local meteoric water values. Subsequent cooling at Kujyu of high temperature fumaroles resulted in a migration of compositions toward the local meteoric water value, indicating progressive groundwater entrainment.

of Kyushu; Matsuo *et al.*, 1974; Matsubaya *et al.*, 1975) and Kujyu (northeastern Kyushu; Mizutani *et al.*, 1986; Ehara, this volume) have been closely studied since the mid-1950s, with high temperature (500 to 900°C) fumaroles and associated acid springs repeatedly sampled. In the case in Kujyu, the fumaroles have cooled over time, followed by a systematic change of isotopic composition from the original volcanic gas value (Fig. 1) towards local meteoric water values along a simple mixing line. The isotopic compositions of acid waters discharging on the slopes of the volcano also fall on this simple volcanic gas - meteoric water mixing line, indicating that the springs are magmatic vapor condensates diluted by meteoric water. A similar trend is present in the acid springs around the base of Satsuma Iwojima, with the springs having approximately ≤ 30 % magmatic component (Fig. 1).

Thermal features on the volcanoes of Kirishima (southern Kyushu) and Esan (southern Hokkaido) were recently the subject of a comparative study (Hedenquist and Aoki, 1991). HCl-bearing fumaroles (170 to 225°C) are present near the summits of the Kirishima andesite massif and the Esan dacite dome. The isotopic compositions of these lower temperature vapors also define a trend from a Satsuma Iwojima-type high-temperature volcanic gas composition to local meteoric water values, with acid and neutral pH hot spring waters at Kirishima falling on the meteoric water end of the trend. The non-reactive gas signatures (N_2, Ar and He) of the vapors support the indication that Esan discharges are magmatic-dominant, whereas the large groundwater carapace at Kirishima greatly dilutes the ascending magmatic fluid.

The acid and neutral pH waters present at the surface of Kirishima have also been encountered during geothermal drilling on the northwest flank of the volcano (Kodama and Nakajima, 1988). These thermal waters show three types of endmem-

ber behavior in terms of chemical composition: 1) the compositions of highly acid waters (270°C) discharged from wells drilled into the Shiramizugoe Fault derive esentially from isochemical dissolution of andesite; 2) neutral pH waters from wells along the Ginyu Fault and hot springs in the Hayashida Valley have compositions controlled by a matrix of temperature-dependent reactions involving feldspars and clays, and are close to a "full equilibrium" assemblage (Giggenbach, 1988), and 3) dilute, steam-heated ephemeral waters are rich in bicarbonate and/or sulfate (the latter acid), and owe their composition to orders of magnitude less dissolution of rock, in comparison to the high temperature, acid Shiramizugoe waters. Given the isotopic and gas trends (Hedenquist and Aoki, 1991), one possible explanation for the acid Shiramizugoe waters is a direct input of magmatic gases, causing the acidity. Neutralization of these acid waters by water-rock interaction followed by mixing with meteoric water may account for the lower temperature and more dilute (in terms of chloride) neutral pH waters in wells only 500 m distant.

Similar trends in isotopic composition of acid waters associated with recent volcanic activity are also noted for acid hot springs, e.g., at Tamagawa (northern Honshu; Kiyosu, 1985) and Noboribetsu (southwestern Hokkaido; Matsubaya *et al.*, 1978). These positive shifts in $\delta^{18}O$ and δD from local meteoric water values are generally attributed to a magmatic component, while Kiyosu and Kurahashi (1983) used the $\delta^{34}S$ versus SO_4:Cl ratios to conclude a volcanic source of the sulfur (as SO_2 and H_2S). A similar isotopic trend of acid fluids in wells drilled into a geothermal system located on the flanks of the Pinatubo volcano, Philippines (Ruaya *et al.*, this volume) is also interpreted to be caused by the direct involvement of magmatic fluids.

The magmatic fluid discussed above has an isotopic composition related to a high temperature magmatic gas (Matsuhisa, Taylor, this volume). These fluids are relatively heavy in δD compared with the "magmatic water box", and are related to island arc (andestitic) volcanism (Giggenbach, 1992a). Such highly acid and mineralized fluids are common in association with recent volcanism, and have been studied, e.g., at Nevado del Ruiz, Colombia (Giggenbach *et al.*, 1990; Sturchio and Williams, 1990), White Island, New Zealand (Giggenbach and Sheppard, 1989) and Sirung volcano, Pantar, Indonesia (Poorter *et al.*, 1988), as well as at several acid crater lakes (e.g., El Chichon, Mexico, Casadevall *et al.*, 1984; Ruapehu, New Zealand, Christensen and Wood, this volume).

Neutral pH geothermal systems

Volcanic-hosted geothermal systems in New Zealand have been well studied in the course of their development, with their geochemical characteristics summarized by Giggenbach (1981, 1984, 1986, 1988) and Hedenquist (1986); they are characterized by low salinity, neutral pH fluids at 1 to 3 km depth. Giggenbach (1981) proposed that essentially all anions and much of the gases in such hydrothermal fluids are derived from an underlying magmatic source, whereas the cations in solution are largely the product of primary neutralization and reduction reactions between wall rock and the aggressive fluids (the latter resulting from proton generation during dissociation as the magmatic components cool upon ascent). A recent compilation of papers on the geochemistry of Japanese geothermal systems (Hedenquist, 1991) provides a review of the chemical and isotopic character of systems which are highly variable in physical features, though are rather constant in terms of

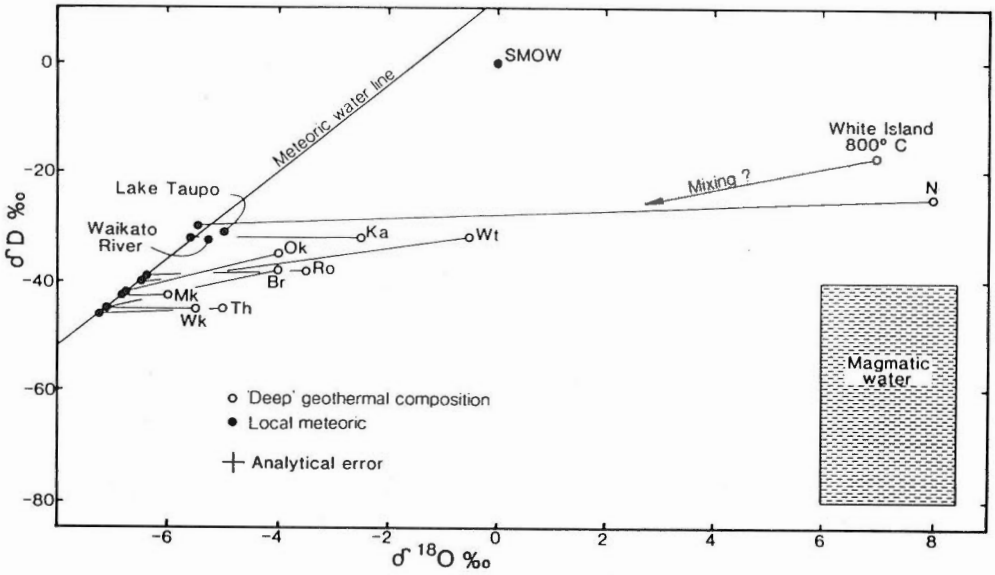

Fig. 2 Isotopic trends of neutral pH geothermal waters in New Zealand (Hedenquist, 1986). Mk, Mokai; Wk, Wairakei; Br, Broadlands; Ok, Orakeikorako; Ka, Kawerau; Wt, Waiotapu; N, Ngawha.

mineral-fluid equilibria (Chiba, 1991, and this volume). These Japanese systems are distinct chemically (Chiba, 1991) and physically from the generally larger and higher permeability geothermal systems of lower relief in New Zealand. Although most developed systems in Japan are dominated by neutral pH fluids, deep acid fluids also occur, and salinities range up to seawater values.

Geothermal systems in New Zealand, like many others around the world, are often dominated by meteoric water (Craig, 1963). However, more recent data and interpretation (Hedenquist, 1986) suggest that some systems (Waiotapu, Wt; Broadlands, Br) along the eastern (volcanic arc) margin of the Taupo Volcanic Zone have a distinct D-shift (Fig. 2) which can most simply be explained by a component of magmatic water similar in isotopic composition to that characteristic of volcanic discharges (e.g., White Island and volcanoes of Japan; Fig. 1). The geothermal systems along the eastern andesite margin of the Taupo Volcanic Zone also have the highest total gas concentrations in deep (300°C+) fluids (up to 1 molal), in contrast to 1-2 orders of magnitude lower gas concentrations in systems to the west (Wairakei, Wk; Mokai, Mk; Giggenbach, 1986). The gases are CO_2-dominant, followed by H_2S. The high gas systems have non-reactive gas proportions (N_2-Ar-He) which trend towards magmatic gas signatures, in contrast to the air-saturated meteoric water signatures of the low gas systems (Fig. 3; Giggenbach, 1986).

These trends in isotopic and gas composition, in conjunction with $\delta^{13}C$ and $^3He/^4He$ constraints (reviewed by Hedenquist, 1986), suggest that a component of magmatic water is entrained by the meteoric-dominated convection cells below drilled depths (>3 km) in some of the systems along the eastern andesitic margin of the Taupo Volcanic Zone. The high concentration of gas in some of these systems is also related to a magmatic contribution along the eastern margin, overprinting the low gas concentration, meteoric-water dominated signature in other systems to the

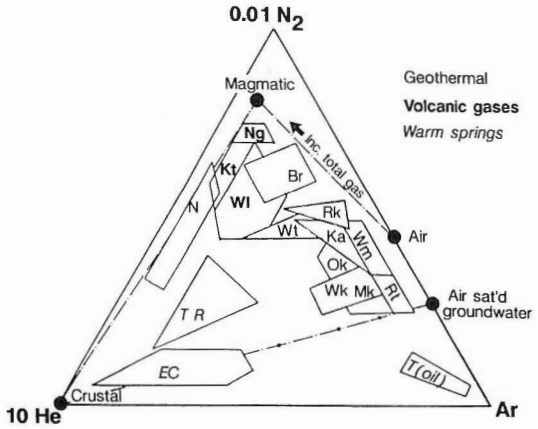

Fig. 3 Compositions of non-reactive gases from neutral pH geothermal fluids in New Zealand (from Giggenbach, 1986). The total gas concentration in the fluids increases in samples lying closer to the magmatic endmember. Abbreviations as in Fig. 2 caption, plus: WI, White Island; Ng, Ngauruhoe; Kt, Ketetahi (volcanic gases); Rk, Rotowawa; Wm, Waimangu (geothermal gases); EC, East Coast (warm springs).

west. Hedenquist *et al.* (1990) used ^{36}Cl isotopes of the Mokai waters to indicate that Cl cannot be derived from leaching of the sedimentary basement or silicic volcanics; it may be related to a more primitive source. A recent survey of the Pb isotopes of hydrothermal sulfides in five of these systems (Hedenquist and Gulson, 1992) indicates that high Pb concentrations (precipitated in the rocks along with precious metals) are closely related to an intrusive source in the high gas, D-shifted systems (Broadlands and Waiotapu), whereas Pb in the low gas, exclusively meteoric water systems is much lower in concentration and may be derived from leaching of sedimentary basement and possibly shallow volcanics. In other words, there is a constant source of Pb through leaching of the basement, though in some systems a component of magmatic fluid is present which contributes a higher concentration of Pb to the fluid, thus overprinting the background (leached) Pb signature (similar to the situation for residual gases).

The isotopic composition of waters in Japanese geothermal systems generally has two endmember trends. One trend is simply a small (few per mil) ^{18}O-shift from local meteoric water values, due to water-rock interaction (e.g., Takigami, Takenaka and Furuya, 1991; Hatchobaru, Hirowatari, 1991), while the other trend clearly extends from local meteoric water towards much heavier isotopic values (e.g, Nigorikawa, Yoshida, 1991; Okuaizu, Seki, 1991)(Fig. 4). Neutral pH hot springs at Osorezan, northern Honshu (Aoki, this volume), also show a strong shift in isotopic composition from local meteoric water towards isotopically heavy values. The isotopically heavy endmember of this second trend is identical in composition to the high temperature volcanic gas noted earlier (Fig. 1) and by others in this volume. A component of this magmatic fluid is my preference to explain the strong shift from meteoric water compositions in these geothermal systems. However, some workers (e.g., Matsubaya *et al.*, 1978) favor a modified seawater source of the isotopically-heavy fluid, since extrapolation of Cl - δD trends approximate seawater; however, a

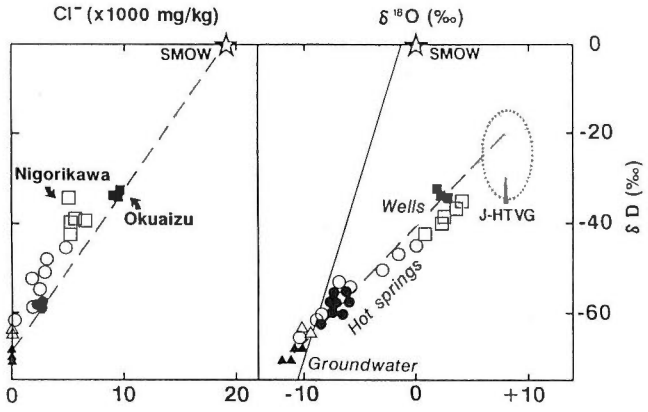

Fig. 4 Isotopic composition of neutral pH fluids from the Nigorikawa (Yoshida, 1991) and Okuaizu (Seki, 1991) geothermal systems, Japan. Squares are well discharges, circles are hot spring compositions, and triangles are local meteoric water values.

+10 per mil or more ^{18}O-shift from the seawater value must be accounted for if this is the case.

The trends of the non-reactive trace gases in Japanese geothermal systems (Chiba, 1991) are also similar to those of New Zealand systems, with the same correlation between D-shift and N_2 gas enrichment. The systems with large D-shift (Nigorikawa and Okuaizu; Fig. 4) have gas compositions trending towards the magmatic gas endmember. In contrast, systems with only an ^{18}O shift from local meteoric water values (e.g., Kakkonda and Sumikawa; Ueda *et al.*, 1991) have gas compositions similar to air-saturated groundwater (Chiba, 1991).

The neutral pH waters in Japanese geothermal systems indicate approximate equilibrium with the silicate assemblages present (Chiba, 1991 and this volume). However, in some systems (e.g., Sumikawa, Hatchobaru, Takigami and Kirishima; Ueda *et al.*, 1991; Hirowatari, 1991; Takenaka and Furuya, 1991; Kodama and Nakajima, 1988), relict disequilibrium assemblages of acid alteration minerals (kaolinite, alunite, pyrophylite, diaspore - the latter pair indicating paleo temperatures of at least 250°C; Hemley *et al.*, 1980) point to high temperature acid fluid having previously been present in some Japanese geothermal systems which are now dominated by neutral pH waters. However, some systems, notably Sumikawa and Kakkonda, and possibly Hatchobaru, have a few wells (generally the hottest and/or deepest) which discharge Cl and SO_4-rich acid fluids at depth (Hedenquist, 1991). However, such deep acid alteration and/or acid fluids have not been noted at drilled depths in New Zealand systems (due to more effective primary neutralization between a magmatic source and the depths now reached by drilling?).

Similar occurrences of acid minerals are common in Philippine geothermal systems now dominated by neutral pH fluids (Reyes, 1990, 1991; Reyes and Giggenbach, 1992; Ruaya *et al.*, this volume), and occur elsewhere as well (e.g., Indonesia). Philippine geothermal fluids often show a strong shift in isotopic and residual gas composition towards the magmatic fluid composition of andesitic affinity (Gig-

genbach, 1992a, 1992b; Reyes and Giggenbach, 1992), even in systems where the deep fluid has a neutral pH (e.g., Tongonan, Leyte; Alvis-Isidro and Solana, 1992; Bacon-Manito, Luzon; Buenviaje and Solis, 1992).

In summary, neutral pH geothermal fluids in New Zealand, Japan and the increasingly well-studied Philippines show distinct isotopic and non-reactive gas trends which indicate that a magmatic source contributes to a variable degree water and gases (at least) to meteoric water convection cells. The magmatic component in Japanese systems may not necessarily be larger than in New Zealand systems, but the acidity is less often fully neutralized by reaction with host rocks before reaching drilled depths or the surface, the latter in the vicinity of recently active volcanism. In contrast, the proximity of Philippine geothermal systems to recently active to active volcanoes accounts for the strong magmatic signatures to the fluids, particularly where the fluids are acid.

Consideration of extinct hydrothermal systems

Neutral pH geothermal systems are considered the active analogue of one class of epithermal ore deposits (e.g., Henley and Ellis, 1983), in which gold mineralization is associated with quartz, adularia and K-mica in veins, breccias and disseminations.

Hedenquist (1987) calls these deposits "low sulfidation", as they form from neutral pH, relatively reduced fluids (i.e., those having undergone primary neutralization by and equilibration with the host rock; Giggenbach, 1981); the term refers to the reduced state of the sulfur, and is a principal geochemical variable reflecting the evolution of the fluid (preferred to the uncertainties in using mineralogic assemblages for classification).

In contrast, recognition of an epithermal ore forming environment related to the highly acid and oxidizing fluids associated with volcanic discharges is more recent, with the relationship still not completely understood. Hedenquist (1987) terms this environment "high sulfidation", reflecting the relatively oxidized (and acid) nature of the fluids. Gold and copper mineralization is associated with highly leached rocks containing an assemblage of minerals indicating acid and relatively oxidizing conditions (enargite, terahedrite and other sulfides in direct association with gold, while minerals such as kaolinite, alunite, pyropyllite, diapore, etc., form a halo to the ore body which passes outwards into clay alteration and progressively to fresh rock; White and Hedenquist, 1990). Examples include the Nansatsu district in southern Kyushu (Urashima *et al.*, 1981; Hedenquist *et al.*, 1992), Nalesbitan (Sillitoe *et al.*, 1990), Lepanto, Philippines (Garcia, 1991), El Indio, Chile (Jannas *et al.*, 1990), Summitville, Colorado (Stoffregen, 1987), Rodalquilar, Spain (Arribas, 1992; Rye *et al.*, 1992) and Chinkuashih, Taiwan.

Identification of the source of fluid components in the extinct hydrothermal environment is more difficult since fluid inclusions are our only sample of fluid, and there is often the possibility that late stage (e.g., post-mineralization and different) fluids may overprint both the alteration assemblages and isotopic signatures. O'Neil and Siberman (1974) examined the general isotopic signature of fluids thought responsible for gold mineralization in the low sulfidation epithermal environment, and concluded that the fluids were dominantly meteoric, with various amounts of ^{18}O-shift due to water-rock interaction. More recent study of gases extracted from fluid inclusions by various workers have not yet been conclusive, due both to ana-

lytical uncertainties and the lack of an interpretive framework (Hedenquist *et al.*, 1992). However, present state-of-the-art gas extraction studies are now underway (e.g., Graney and Kesler, this volume), which should shed further light on both gas equilibria and gas signatures.

Recent detailed isotopic study of high sulfidation deposits (Rye *et al.*, 1992; Arribas, 1992; Hedenquist *et al.*, 1992), particularly on the composition of alunite and related hydroxyl-bearing minerals (clays), is revolutionizing our understanding of this ore environment. For example, the isotopic trend of fluids estimated from mineral compositions of the Summitville deposit (Rye *et al.*, 1992) is consistent with high temperature volcanic gases (Fig. 1) being related to alunite formation early in the life of the system; those fluid compositions lie on a dilution trend towards meteoric water. From the earlier discussion of acid volcanic fluids, it is clear that we do not have to constrain volcanic ("magmatic") fluids to have an isotopic composition of the "magmatic water box". This has also been confirmed by the detailed work of Arribas (1992) on the Rodalquilar high sulfidation deposit in Spain. Isotopic analysis of alunite, sericite and kaolinite closely associated with mineralization indicate the early stage fluids are similar in composition to high temperature volcanic fluids (Fig. 1). Late stage fluids are mixtures of the isotopically-heavy waters and surface waters. Similar patterns are also apparent based on isotopic analysis of alunite and marginal clays from the Nansatsu gold deposits of southern Kyushu (Hedenquist *et al.*, 1992). The alunites from the ore zone define a magmatic (andesitic) to meteoric water mixing trend, while the clays which form a halo to the deposit appear to be O-shifted meteoric waters. Similar isotopic results are also noted for some porphyry copper deposits (Matsuhisa, this volume).

A good framework of interpretation now exists for understanding the origin of components of fluids in geothermal systems, while a similar approach and understanding is now evolving for acid volcanogenic fluids. Using this information as a base, some of which was briefly outlined here, we should be able to make progress in designing analytical studies (in particular, detailed fluid inclusion and stable isotope study) of hydrothermal ore deposits which will give us the data necessary to constrain the geochemical environments of formation and identify sources of components to the hydrothermal fluid.

References

Allis, R. G. (1980) Heat flow. *Royal Soc. N.Z., Misc. Series*, no. 3, p. 47-48.

Alvis-Isidro, R. R. and Solana, R. R. (1992) Stable isotope geochemistry of the greater Tongonan geothermal field (abstract). *13th PNOC-EDC Geoscientific Workshop, Metro Manila,* February 19-21.

Arribas, A. (1992) The origin of the Rodalquilar gold deposit, Spain. Ph.D. dissertation, Univ. Mich., July.

Buenviaje, M. M. and Solis, R. P. (1992) Preliminary interpretations of the baseline isotopic data of the Bacon-Manito geothermal field (abstract). *13th PNOC-EDC Geoscientific Workshop, Metro Manila,* February 19-21.

Casadevall, T. J., de la Cruz-Reyna, S., Rose, W. I., Jr., Bagley, S., Finnegan, D. L. and Zoller, W. H. (1984) Crater lake and post-eruption hydrothermal activity, El Chichon volcano, Mexico. *Jour. Volcanol. Geotherm. Res.*, vol. 23, p. 25-36.

Chiba, H. (1991) Attainment of solution and gas equilibrium in Japanese geothermal

systems. In Hedenquist, J.W., ed., Geochemistry of newly developed geothermal systems in Japan, *Geochem. Jour.*, vol. 25, p. 335-355.

Craig, H. (1963) The isotopic geochemistry of water and carbon in geothermal areas. In Tongiorgi, E., ed., Nuclear Geology in Geothermal Areas, Cinsiglio Nazionale Delle Ricerche, Pisa.

Garcia, J. S., Jr. (1991) Geology and mineralization characteristics of the Mankayan mineral district, Benguet, Philippines. In Matsuhisa, Y., Aoki, M. and Hedenquist, J. W., eds., High temperature acid fluids and associated alteration and mineralization, *Rept., Geol. Surv. Japan,* no. 277, p. 21-30.

Giggenbach, W. F. (1980) Geothermal gas equilibria. *Geochim. Cosmochim. Acta*, vol. 44, p. 2021-2032.

——— (1981) Geothermal mineral equilibria. *Geochim. Cosmochim. Acta*, vol. 45, p. 393-410.

——— (1986) The use of gas chemistry in delineating the origin of fluids discharged over the Taupo Volcanic Zone. *Intl. Volcanological Congress, Proc. of Symp. 5, Hamilton, New Zealand*, p. 47-50.

——— (1988) Geothermal solute equilibria: Derivation of Na-K-Mg-Ca geoindicators. *Geochim. Cosmochim. Acta*, vol. 52, p. 2749-2765.

——— (1992a) Isotopic shifts in waters from geothermal and volcanic systems along convergent plate boundaries and the origin of "andesitic" waters. *Earth Planet. Sci. Lett.*, submitted.

——— (1992b) The composition of gases in geothermal and volcanic systems as a function of tectonic setting. *7th Water-Rock Interaction Symp., Park City,* July, in press.

———, Garcia P., N., Londono C., A., Rodriguez V., L., Rojas G., N. and Calvache V., M.L. (1990) The chemistry of fumarolic vapor and thermal-spring discharges from Nevado del Ruiz volcanic-magmatic-hydrothermal system, Colombia. *Jour. Volcanol. Geotherm. Res.*, vol. 42, p. 13-39.

——— and Sheppard, D.S. (1989) Variations in the temperature and chemistry of White Island fumarole discharges 1972-85. In Houghton, B.F. and Nairn, I.A., eds., The 1976-82 eruptions sequence at White Island volcano (Whakaari), Bay of Plenty, New Zealand. *N.Z. Geol. Surv. Bull.*, no. 103, p. 119-126.

Hedenquist, J.W. (1986) Geothermal systems of the Taupo Volcanic Zone, New Zealand: Their characteristics and relation to volcanism and mineralization. In Smith, I.E.M., ed., Late Cenozoic Volcanism in New Zealand. *Royal Soc. N.Z. Bull.*, no. 23, p. 134-168.

——— (1987) Mineralization associated with volcanic-related hydrothermal systems in the circum-Pacific basin. In Horn, M.K., ed., Transactions of the Fourth Circum-Pacific Energy and Mineral Resources Conference: Singapore, August, 1986, *American Assoc. Petroleum Geol.*, p. 513-524.

——— (1991) The geochemistry of newly developed geothermal systems in Japan. *Geochem. Jour.*, vol. 25, p. 199-202.

——— and Aoki, M. (1991) Meteoric interaction with magmatic discharges in Japan and the significance for mineralization. *Geology*, vol. 19, p. 1041-1044.

———, Goff, F., Phillips, F.M., Elmore, D. and Stewart, M.K. (1990) Groundwater dilution and residence times, and constraints on chloride

source, in the Mokai geothermal system, New Zealand, from chemical, stable isotope, tritium and ^{36}Cl data. *Jour. Geophys. Res.*, vol. 95, p. 19,365-19,375.

——— and Gulson, B.L. (1992) Intrusive and basement rock sources of lead in hydrothermal systems of the Taupo Volcanic Zone, New Zealand. *Geochim. Cosmochim. Acta.*, vol. 56(7), in press.

———, Reyes, A. G., Simmons, S. F., and Taguchi, S. (1992) The thermal and geochemical structure of geothermal and epithermal systems: A framework for interpreting fluid inclusion data. *Europ. Jour. Mineral.*, vol. 4, in press.

———, Matsuhisa, Y., Izawa, E., White, N. C., Giggenbach, W. F. and Aoki, M. (1992) Geology and geochemistry of high sulfidation gold mineralization in the Nansatsu district, Japan. *Econ. Geol.*, submitted.

Hemley, J. J., Montoya, J. W., Marinenko, J. W., and Luce, R. W. (1980) Equilibria in the system Al_2O_3-SiO_2-H_2O and some general implications for alteration/mineralization processes. *Econ. Geol.*, vol. 75, p. 210-228.

Henley, R. W. and Ellis, A. J. (1983) Geothermal systems, ancient and modern. *Earth Sci. Rev.*, vol. 19, p. 1-50.

Hirowatari, K. (1991) Development-related changes in the Hatchobaru geothermal system, Japan. In Hedenquist, J.W., ed., Geochemistry of newly developed geothermal systems in Japan, *Geochem. Jour.*, vol. 25, p. 283-299.

Jannas, R. R., Beane, R. E., Ahler, B. A., and Brosnahan, D. R. (1990) Gold and copper mineralization at the El Indio deposit, Chile. In Hedenquist, J.W., White, N.C, and Siddeley, G., eds., Epithermal gold mineralization of the Circum Pacific: Geology, geochemistry, origin and exploration, II., *Jour. Geochem. Explor.*, v. 36, p. 233-266.

Kiyosu, Y. (1985) Isotopic composition of acid sulfate-chloride waters and volcanic steam from some volcanoes in northeastern Japan. *Jour. Volcanol. Geotherm. Res.*, vol. 26, p. 25-36.

——— and Kurahashi, M. (1983) Origin of sulfur species in acid sulfate-chloride thermal waters, NE Japan. *Geochim. Cosmochim. Acta*, vol. 47, p. 1237-1245.

Kodama, M. and Nakajima, T. (1988) Exploration and exploitation of the Kirishima geothermal field. *Chinetsu*, vol. 25, p. 1-30 (in Japanese).

Matsubaya, O., Ueda, A., Kusakabe, M., Matsuhisa, Y., Sakai, H., and Sasaki, A. (1975) An isotopic study of the volcanoes and the hot springs in Satsuma Iwojima and some areas in Kyushu. *Bull. Geol. Surv. Japan*, vol. 26, p. 375-392 (in Japanese with English abs.).

———, Sakai, H., Ueda, A., Tsutsumi, M., Kusakabe, M. and Sasaki, A. (1978) Stable isotope study of the hot springs and volcanoes of Hokkaido. *Papers of the Institute for Thermal Spring Research, Okayama University*, no. 47, p. 55-67 (in Japanese with English abs.).

Matsuo, S., Suzuoki, T., Kusakabe, M., Wada, H., and Suzuki, M. (1974) Isotopic and chemical composition of volcanic gases from Satsuma Iwojima, Japan. *Geochem. Jour.*, vol. 8, p. 165-173.

Mizutani, Y., Hayashi, S. and Sugiura, T. (1986) Chemical and isotopic compositions of fumarolic gases from Kuju-Iwoyama, Kyushu, Japan. *Geochem. Jour.*, vol. 20, p. 273-285.

O'Neil, J. R. and Silberman, M. L. (1974) Stable isotope relations in epithermal Au-Ag deposits. *Econ. Geol.*, vol. 69, p. 902-909.

Poorter, R. P. E., Varekamp, J. C., Van Bergen, M. J., Kreulen, R., Sirwana, T., Vroon, P. Z. and Wirakusumah, A. D. (1988) The Sirung boiling spring: An extreme chloride-rich, acid brine on Pantar (Lesser Sunda Islands), Indonesia. Unpublished manuscript, *Third IAVCEI Workshop on Volcanic Gases, New Zealand,* February, 25 p.

Reyes, A. G. (1990) Petrology of Philipine geothermal systems and the application of alteration of alteration mineralogy to their assessment. *Jour. Volcanol. Geotherm. Res.*, vol. 43, p. 279-309.

——— (1991) Mineralogy, distribution and origin of acid alteration in Philippine geothermal systems. In Matsuhisa, Y., Aoki, M., and Hedenquist, J. W., eds., High temperature acid fluids and associated alteration and mineralization, *Rept. Geol. Surv. Japan*, no. 277, p. 59-65.

——— and Giggenbach, W. F. (1992) Petrology and fluid chemistry of magmatic-hydrothermal systems in the Philippines. *7th Water-Rock Interaction Symp., Park City,* July, in press.

Rye, R. O., Bethke, P. M., and Wasserman, M. D. (1992) The stable isotope geochemistry of acid-sulfate alteration. *Econ. Geol.*, vol. 87, p. 225-262.

Seki, Y. (1991) The physical and chemical structure of the Oku-aizu geothermal system. In Hedenquist, J. W., ed., The geochemistry of newly developed geothermal systems in Japan, *Geochem. Jour.*, vol. 25, p. 245-265.

Sillitoe, R. H., Angeles, C. A., Jr., Comia, G. M., Antioqua, E. C., and Abeya, R. B. (1990) An acid sulfate-type lode deposit at Nalesbitan, Luzon, Philippines. In Hedenquist, J. W., White, N. C, and Siddeley, G., eds., Epithermal gold mineralization of the Circum Pacific: Geology, geochemistry, origin and exploration, I., *Jour. Geochem. Explor.*, vol. 35, p. 387-412.

Stoffregen, R. E. (1987) Genesis of acid-sulfate alteration and Au-Cu-Ag mineralization at Summitville, Colorado. *Econ. Geol.*, vol. 82, p. 1575-1591.

Sturchio, N. C. and Williams, S. N. (1990) Possible eruption-induced variations in chemistry of acid-sulfate-chloride springs at Nevado del Ruiz volcano, Colombia: November 1985 through December 1988. In Williams, S. N., ed., *Jour. Volcanol. Geotherm. Res.*, vol. 42, p. 201-208.

Takenaka, T. and Furuya, S. (1991) Geochemical model of the Takigami geothermal system, northeast Kyushu, Japan. In Hedenquist, J. W., ed., The geochemistry of newly developed geothermal systems in Japan, *Geochem. Jour.*, vol. 25, p. 267-281.

Ueda, A., Kubota, Y., Katoh, H., Hatakeyama, K, and, Matsubaya, O. (1991) Geochemical characteristics of the Sumikawa geothermal system, northeast Japan, In Hedenquist, J. W., ed., The geochemistry of newly developed geothermal systems in Japan, *Geochem. Jour.*, vol. 25, p. 223-244.

Urashima, Y., Saito, M., and Sato, E. (1981) The Iwato gold ore deposits, Kagoshima prefecture, Japan. *Mining Geol., Spec. Issue* 10, p. 1-14 (in Japanese with English abs.).

White, N. C., and Hedenquist, J. W. (1990) Epithermal environments and styles of

mineralization: variations and their causes, and guidelines for exploration. In Hedenquist, J. W., White, N. C, and Siddeley, G., eds., Epithermal gold mineralization of the Circum Pacific: Geology, geochemistry, origin and exploration, II, *Jour. Geochem. Explor.*, vol. 36, p. 445-474.

Yoshida, Y. (1991) Geochemistry of the Nigorikawa geothermal system, southwest Hokkaido, Japan. In Hedenquist, J. W., ed., Geochemistry of newly developed geothermal systems in Japan, *Geochem. Jour.*, vol. 25, p. 203-222.

Rept. Geol. Surv. Japan, No. 279, p. 80-83, 1992

Complex Interaction Between Hydrothermal Activity and Basic Andesitic Magma, White Island Volcano, New Zealand 1976-1991

B. F. HOUGHTON and I. A. NAIRN

DSIR Geology and Geophysics, Rotorua, New Zealand

Events at White Island, New Zealand in 1976-91 record a complex yet direct interaction between basic andesitic magma and a long-lived hydrothermal system, related to the deeper magmatic system of the volcano. White Island is unusual because of a low discharge rate of magma over an extended time period, and because of the influence of the unique physical and hydrological setting. The low magma rise rate leads to very effective separation of magmatic volatiles which rise to interact with the hydrothermal system in a manner influenced by a delicate balance between erosion and collapse of the weak conduit walls. Very low permeability away from the volcanic conduits leads to very high laterial temperature gradients and telescoping of high temperature and acidic low temperature environments. Telescoping also results from migration of the magma from depths of 1 km or more to discharge at the surface, and from collapse of the conduit walls to form maar-like craters.

White Island is an active andesitic-dacitic composite volcano surrounded by sea, yet isolated from sea water by chemically sealed zones which confine a long-lived acidic hydrothermal system, within a thick sequence of fine-grained volcaniclastic sediment and ash (Fig. 1).

The volcano has a long history of frequent small phreatic and phreatomagmatic eruptions, interrupting long intervals of continuous intense fumarolic and hydrothermal activity (Cole and Nairn, 1975). Three large subcraters are infilled with unconsolidated fine grained, volcaniclastic sediments and tephra, saturated with hot brine acidified by dissolved volcanic gases. The rise of at least 10^6 m^3 of basic andesite magma to shallow levels between 1973 and 1976, has provided a unique opportunity to observe shallow interaction between geothermal and magmatic components during three eruption sequences in 1976-82, 1983-84 and 1986-91. During this period the brine-saturated but relatively impermeable deposits infilling the subcraters were cut by reactivated volcanic conduits enclosed by successive envelopes of vapour, and two-phase mixtures of vapour plus brine (Fig. 2).

The outstanding features at White Island are the low discharge rate of magma over this extended time period and the unusual physical setting, in which magma and magmatic volatiles interacted with abundant but finite quantities of groundwater in a confined hydrothermal system. Other influences are:

(1) the fine-grained and brine-saturated, unconsolidated nature of the conduit wall material, and

(2) the location of partially blocked pre-existing volcanic conduits in the vent area.

There is clear evidence that the low discharge rate of magma permits decoupling of magmatic volatiles at shallow depths beneath White Island. The average rise rate of magma between 1973-77 was c. 3×10^{-6} m/s (Houghton and Nairn, 1989), after which time the magma as remained stationary or receded. Rise rates for 1 cm

Keywords: magma:water interaction, magmatic volatiles, telescoping, White Island.

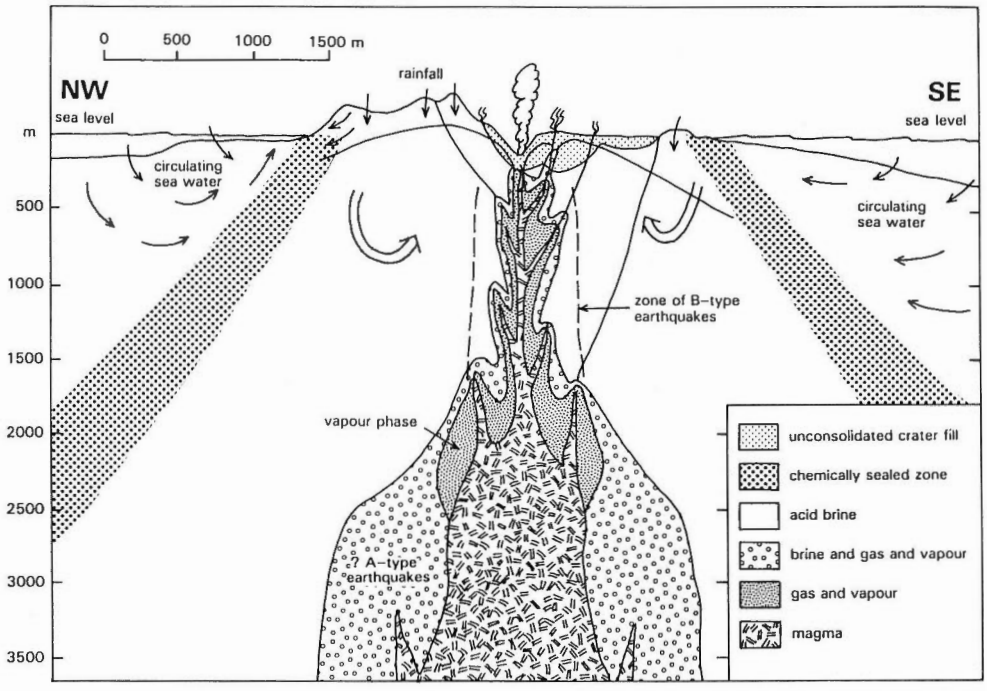

Fig. 1 Cartoon of the subsurface structure and hydrology of White Island volcano, inferred from structural, seismic and chemical data.

bubbles can be modelled, assuming magma viscosity of 10^4 to 10^5 poise, as 10^{-3} - 10^{-4} m/s. This velocity contrast between magma and gas bubbles led to effective decoupling of magma and exsolved volatiles and subsequent gas streaming. A key factor is the consistently significant flux of magmatic volatiles at White Island even during phreatic phases, which remained high even during the repose period after 1982 (Rose *et al.*, 1986). The long-term flux of SO_2 at White Island following the 1976-82 eruption (Rose *et al.*, 1986) is equivalent to degassing of c. 1 m^3/s of andesitic magma containing 0.1 wt% SO_2. Magma discharge rates even during the 1976-82 eruptions probably only reached 1 m^3/s for short intervals at the peak of Strombolian phases and averaged 10^{-2} m^3/s over the duration of the eruption. This means effectively far more magma is degassed at White Island than is ever discharged from the subaerial vents.

The hydrothermal discharges show no isotopic evidence for sea water in the system (Giggenbach, 1987), probably because of chemical sealing of the margins of the hydrothermal system. The sealed zone which excludes seawater also confines fumarolic condensates and meteoric groundwater obtained from the catchment areas of 0.4 km^2 draining directly into the western subcrater and 3.4 km^2 for the entire island. The rainfall is probably equivalent to 4000 tonnes/day, providing a significant but finite amount of fluid entering the shallow groundwater system.

Surface hydrothermal features at White Island have had relatively short lifespans during the recent intervals of volcanism, and are repeatedly disturbed or destroyed by deposition of volcanic ash and collapse of the volcanic vents. The preexisting conduits active in 1933-71 are important as channelways for both de-

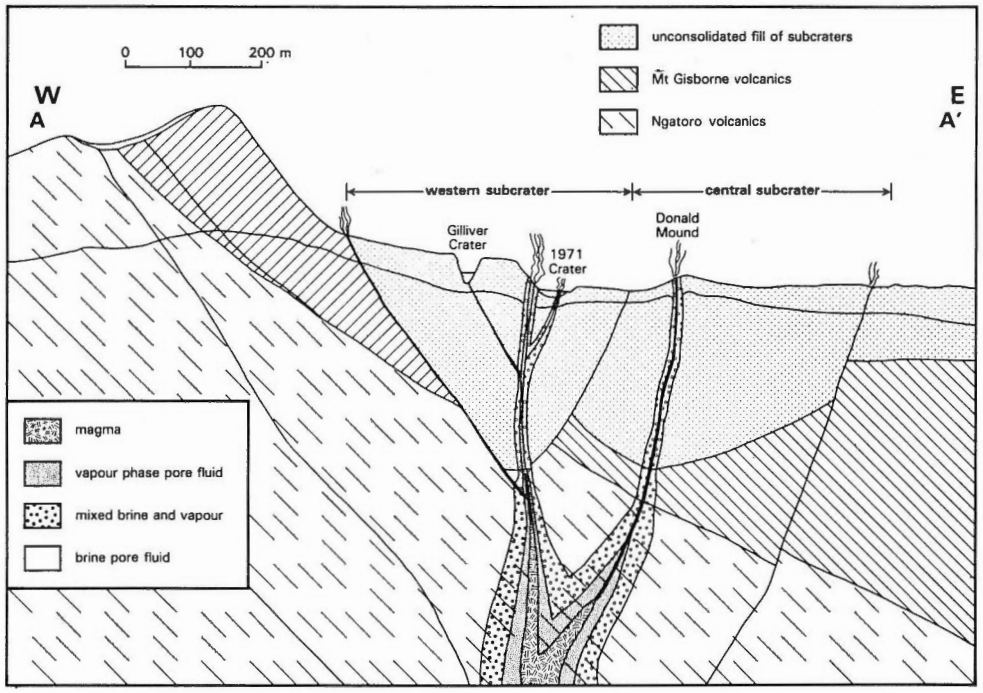

Fig. 2 Schematic section through the White Island vents in December 1976 immediately prior to the onset of the first eruption sequence. Envelopes of vapour and hot brine enclose conduits leading to vents formed in earlier historical eruptions.

coupled magmatic and hydrothermal fluids, but also serve as foci for development of the subterranean voids which permit sudden crater collapse, destroying both hydrothermal and volcanic features.

The White Island activity represents a very complex and fragile interaction at shallow levels between four heterogeneous components of the volcano: a long-lived hydrothermal system, prehistoric craters filled with weak unconsolidated fill, basic magma, and a sustained flux of magmatic gas. Even during repose periods, magmatic volatiles interact with shallow circulating meteoric groundwater, and the volcanic conduits provide zones of high vertical permeability in otherwise impermeable near-surface materials. These hydrological factors lead to an abrupt lateral juxtaposition of high and low temperature mineral assemblages. The hydrothermal activity also severely modifies the form of explosive eruptions, and has led to wall collapse and changes in vertical relief of up to 250 m. Rapid obliteration of near vent stratigraphy and structure in this fashion, which has occurred several times during the eruption, is also a factor in telescoping of contrasting hydrothermal assemblages.

References

Cole J. W. and Nairn I. A. (1975) Catalogue of the Active Volcanoes of the World including Solfatara Fields - Part 22: New Zealand. *International Association of Volcanology and Chemistry of the Earth's Interior*, Naples, 156 p.

Giggenbach W. F. (1987) Redox processes governing the chemistry of fumarolic gas discharges from White Island, New Zealand. *Appl. Geochem.*, vol. 2, p. 143-161.

——— and Sheppard D. S. (1989) Variations in the temperature and chemistry of White Island fumarole discharges 1972-85. *N. Z. Geol. Surv. Bull.* no. 103, p.119-126.

Houghton B. F. and Nairn I. A. (1991) The 1976-82 Strombolian and phreatomagmatic eruptions of White Island, New Zealand: eruptive and depositional mechanisms at a 'wet' volcano. *Bull. Volcanol.* vol. 54, p. 25-49.

Rose W. I., Chuan R. L., Giggenbach W. F. and Kyle P. R. (1986) Rate of sulfur dioxide and particle emission from White Island volcano, New Zealand, and an estimate of the total flux of major gaseous species. *Bull. Volcanol.*, vol. 48, p. 181-188.

Rept. Geol. Surv. Japan, No. 279, p. 84-88, 1992

Evolution of Volcanic and Hydrothermal Systems in Southern Kyushu

Eiji IZAWA

Department of Mining, Kyushu University
Hakozaki, Higashiku, Fukuoka, 812 Japan

Introduction

Late Cenozoic magmatism in southern Kyushu is characterized by two contrasting types of magmas; these are oxidized magma of the magnetite series (Ishihara, 1977) and reduced magmas of the ilmenite series. The difference in oxidation state affects, in particular, the degassing of sulfur species from the magmas. Sulfur may escape from oxidized magmas as SO_2-dominant fluids. On the other hand, sulfur tends to remain as sulfide (S^{2-}) in reduced magmas (Burnham and Ohmoto, 1980). Associated mineral deposits are consequently expected to have different characteristics. In the Circum-Pacific region, porphyry copper deposits and epithermal gold deposits occur with oxidized magmas, and tin deposits and silver-antimony-arsenic deposits tend to be associated with reduced magmas.

In this paper I present the spatial, temporal and geochemical characteristics of the two types of late Cenozoic magmatism in southern Kyushu.

Reduced magma (ilmenite-series)

Widespread magmatism of the ilmenite-series (I-type and S-type) occurred throughout the Outer Zone of southwest Japan, including southern Kyushu, in the middle Miocene (15-13 Ma; Shibata, 1978) (Fig. 1). The granitic magmas are considered to be generated by the melting of Shimanto sedimentary rocks (Nakada and Takahashi, 1979). Some of the granitic intrusives are closely associated with consanguineous ilmenite-series volcanic rocks (andesite, dacite and rhyolite). The shallow intrusive rocks at Okueyama, Osuzuyama and Suzuyama are associated with tin deposits.

In the Suzuyama district, cassiterite-bearing quartz veins occur near a small stock of granodiorite porphyry (Takenouchi and Imai, 1975). Sulfides in the vein consist of pyrrhotite, pyrite and arsenopyrite, and the assemblage indicates a reduced environment during mineralization. Thus, the sulfur isotopic ratio ($^{34}S/^{32}S$) of the ore probably represents that of the hydrothermal fluids. The $\delta^{34}S$ values for ore sulfur are about -8.0 per mil, and are similar to that of the intrusive rocks (-9.2 per mil) and the Shimanto sedimentary rocks (-9.4 per mil) (Hayashi *et al.*, 1991). This suggests that the ore sulfur has been derived from granitic magma but the ultimate source is the Shimanto sedimentary rocks. Sulfur has been transferred from surrounding carbonaceous sedimentary rocks into the pluton probably by means of a fluid phase. Although silver-antimony-arsenic deposits occur in the peripheral area of the Suzuyama district, no significant gold mineralization is known.

Keywords: volcanic evolution, hydrothermal mineralization, age dating, oxidized magma, reduced magma

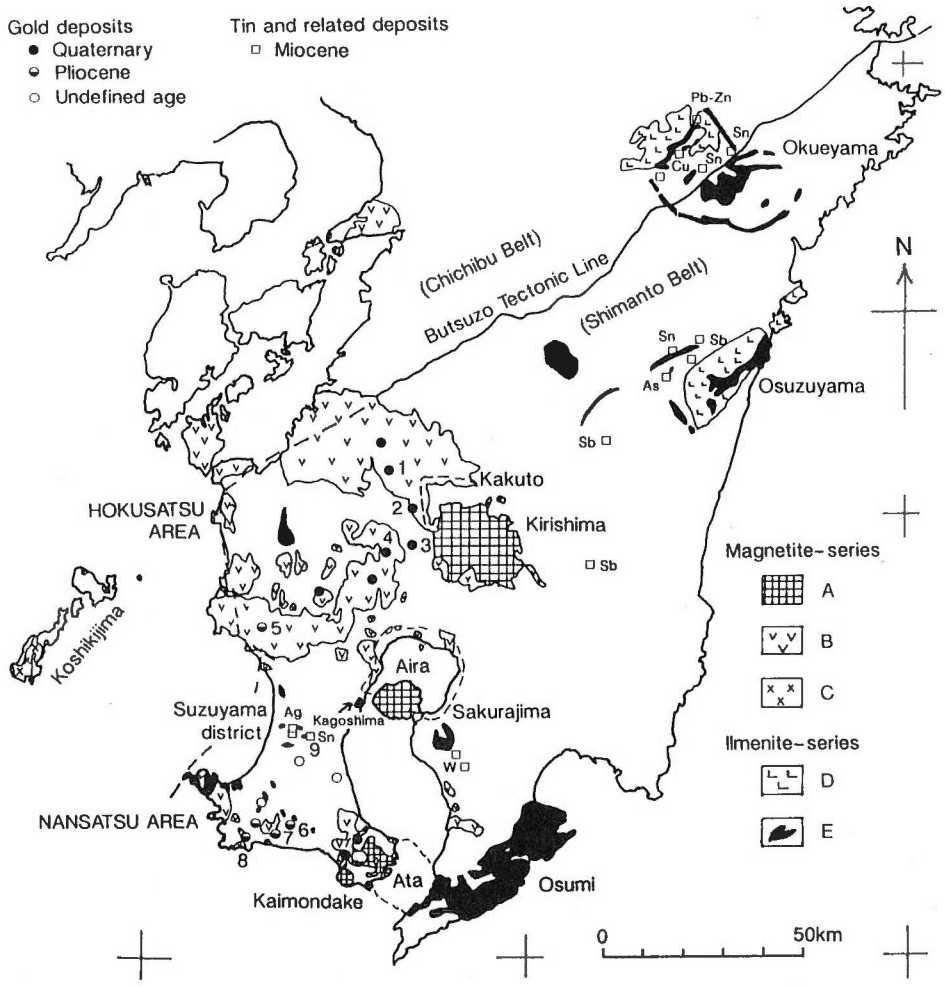

Fig. 1 Map showing the distribution of the Late Cenozoic volcanic rocks (excluding large-scale pyroclastic flow deposits), intrusive rocks and related metallic ore deposits in southern Kyushu. Location of Late Pleistocene large calderas (Kakuto, Ata and Aira) are also shown. A = Late Pleistocene to Holocene volcanic rocks, B = Late Miocene to Middle Pleistocene volcanic rocks, C = Late Miocene Koshikijima granodiorite, D = Middle Miocene volcanic rocks of the ilmenite-series, E = Middle Miocene intrusive rocks of the ilmenite-series. Gold deposits: 1 = Okuchi, 2 = Hishikari, 3 = Onoyama, 4 = Yamagano, 5 = Kushikino, 6 = Akeshi, 7 = Iwato, 8 = Kasuga. Tin deposit: 9 = Suzuyama.

Oxidized magma (magnetite-series)

Volcanism related to oxidized magma began along the west coast of southern Kyushu in the late Miocene (later than 9 Ma). The volcanic centers then shifted intermittently towards the east, in the direction of the convergent plate boundary

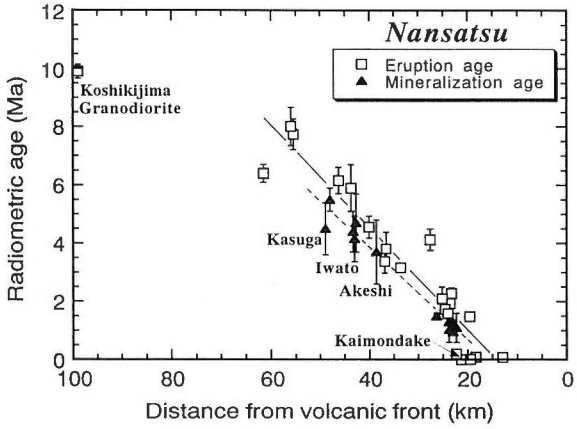

Fig. 2 Relationships between the radiometric age and the distance from volcanic front for volcanic rocks and gold deposits in the Nansatsu area, southern Kyushu. Regression lines are drawn for data of volcanic rocks (solid line) and those of gold deposits (broken line). The regular eastward migration of volcanism and mineralization is clearly indicated. Radiometric ages are taken from Togashi and Shibata (1984), Izawa *et al.* (1984), MITI (1985), Urashima and Ikeda (1987), and MITI (1991a and 1991b). Age data having large analytical errors are omitted. Unpublished radiometric ages for Koshikijima granodiorite and three volcanic rocks are also included.

(Izawa and Urashima, 1989). The eastward migration of volcanism was followed by geothermal activity resulting in epithermal gold mineralization in both the Hokusatsu and the Nansatsu areas. Many radiometric ages, newly obtained and previously reported on volcanic rocks and ores, reveal the close relationship between volcanism and gold mineralization in the area (Fig. 2). The slope of the regression line in Figure 2 shows that the rate of eastward migration of magmatism is about 6 cm per year, and that volcanic activity was followed by hydrothermal activity (gold mineralization) less than one million years later.

Two distinct styles of epithermal gold mineralization are recognized in southern Kyushu, and are typical for the Circum-Pacific region. The first type is characterized by adularia, smectite and calcite (the adularia-sericite type of Heald *et al.*, 1987). The second type is characterized by sulfate minerals such as alunite and barite (the acid-sulfate type). Adularia-calcite type gold deposits are far more important and include Hishikari (250 tonnes of contained gold; Izawa *et al.*, 1990), Kushikino, etc. Common sulfide minerals in the vein are pyrite and chalcopyrite. The sulfur isotopic ratio of ore sulfur was determined only from Hishikari and has an average of +0.3 per mil (Ishihara *et al.*, 1986). Since the contribution of sulfur from the Shimanto sedimentary rocks appears to be small, a magmatic source is assumed for sulfur in Hishikari gold ores.

Although the sulfate-type gold deposits (Nansatsu-type deposits) are minor in number and tonnage of gold produced, they form an important class of epithermal gold deposits by their distinct nature. The Nansatsu-type deposits, such as Kasuga, Iwato and Akeshi, consist of a central silicified zone enveloped by an argillic zone of acid alteration (alunite, kaolinite, dickite and pyrophyllite). Mineralization by high temperature acid-sulfate solutions indicates a direct magmatic contribution to

the hydrothermal systems. Sulfur isotopic ratios of sulfide and sulfate also indicate the disproportionation of magmatic SO_2 (Hedenquist *et al.*, 1988).

Concluding remarks

While gold mineralization was related to oxidized magmas, tin-silver mineralization was associated with reduced magmas during the late Cenozoic in the Shimanto basement area of southern Kyushu. This situation raises the question of how the two kinds of magma were generated and the difference in their mode of emplacement. The two types of magmatism clearly reflect the tectonic framework of the Ryukyu arc in the late Cenozoic (e.g., Hibbard and Karig, 1990). In addition to magma type, the diversity of mineral deposits in southern Kyushu is also related to the level of magma intrusion, local volcanic processes, the site of mineralization in relation to the volcanic vent, etc.

References

Burnham, C. W. and Ohmoto, H. (1980) Late-stage processes of felsic magmatism. In Ishihara, S. and Takenouchi, S., eds., Granitic magmatism and related mineralization. *Mining Geol. Spec. Issue,* no. 8, p. 1-11.

Hayashi, S., Izawa, E., Motomura, Y. and Taguchi, S. (1991) Geochemistry of Sn-Ag deposits in the Suzuyama district, Kagoshima Prefecture (abstract). *Mining Geol.*, vol. 41, p. 187 (in Japanese).

Heald, P., Foley, N. K. and Hayba, D. O. (1987) Comparative anatomy of volcanic-hosted epithermal deposits: acid-sulfate and adularia-sericite types. *Econ. Geol.*, vol. 82, p. 1-26.

Hedenquist, J. W., Matsuhisa, Y., Izawa, E., Marumo, K., Aoki, M. and Sasaki, A. (1988) Epithermal gold mineralization of acid-leached rocks in the Nansatsu district of southern Kyushu, Japan. *Geol. Soc. Australia Abstracts*, no. 22, p. 183-190.

Hibbard, J. P. and Karig, D. E. (1990) Alternative plate model for the early Miocene evolution of southwest Japan margin. *Geology*, vol. 18, p. 170-174.

Ishihara, S. (1977) The magnetite-series and ilmenite-series granitic rocks. *Mining Geol.*, vol. 27, p. 293-305.

———— , Sakamaki, Y., Sasaki, A., Teraoka, Y. and Terashima, S. (1986) Role of the basement in the genesis of the Hishikari gold-quartz vein deposit, southern Kyushu, Japan. *Mining Geol.*, vol. 36, p. 495-509.

Izawa, E. and Urashima, Y. (1989) Quaternary gold mineralization and its geologic environments in southern Kyushu, Japan. *Econ. Geol. Monogr.* 6, p. 233-241.

———— , ———— , Ibaraki, K., Suzuki, R., Yokoyama, T., Kawasaki, K., Koga, A. and Taguchi, S. (1990) The Hishikari gold deposit: high-grade epithermal veins in Quaternary volcanics of southern Kyushu, Japan. *Jour. Geochem. Expl.*, vol. 36, p. 1-56.

———— , ———— and Okubo, Y. (1984) Age of mineralization of the Nansatsu type gold deposits, Kagoshima, Japan: K-Ar dating of alunite from Kasuga, Iwato and Akeshi. *Mining Geol.*, vol. 34, p. 343-351 (in Japanese with English abs.).

MITI (Ministry of International Trade and Industry) (1985) Report of regional

geological survey: Nansatsu area, 1984 fiscal year. Tokyo, 180 p. (in Japanese).

——— (1991a) Report of regional geotectonic survey: Nansatsu area, 1990 fiscal year. Tokyo, 51 p. (in Japanese).

——— (1991b) Report of detailed survey: Nansatsu area, 1990 fiscal year. Tokyo, 76 p. (in Japanese with English abs.).

Nakada, S. and Takahashi, M. (1979) Regional variation in chemistry of the Miocene intermediate to felsic magmas in the Outer Zone and the Setouchi Province of Southwest Japan. *Jour. Geol. Soc. Japan*, vol. 85, p. 571-582 (in Japanese with English abs.).

Shibata, K. (1978) Contemporaneity of Tertiary granites in the Outer Zone of Southwest Japan. *Bull. Geol. Surv. Japan*, vol. 29, p. 551-554 (in Japanese with English abs.).

Takenouchi, S. and Imai, H. (1975) Glass and fluid inclusions in acidic igneous rocks from some mining areas in Japan. *Econ. Geol.*, vol. 70, p. 750-769.

Togashi, Y. and Shibata, K. (1984) K-Ar age for alunite-bearing rock from the Iwato gold deposit, Kagoshima Prefecture, southern Japan. *Mining Geol.*, vol. 34, p. 281-285 (in Japanese with English abs.).

Urashima, Y. and Ikeda, T. (1987) K-Ar ages for adularia from the Fuke, Okuchi, Hishikari, Kuronita, and Hanakago gold-silver deposits, Kagoshima Prefecture, Japan. *Mining Geol.*, vol. 37, p. 205-213 (in Japanese with English abs.).

Rept. Geol. Surv. Japan, No. 279, p. 89-92, 1992

Geophysical Background of Kirishima Volcanoes

Tsuneomi KAGIYAMA

Kirishima Volcano Observatory, Earthquake Research Institute, The University of Tokyo 1489, Suenaga, Ebino, Miyazaki 889-43, Japan

The volcanoes of Kirishima, located in southern Kyushu, are a group of more than 20 volcanoes occupying an area of about 20 × 30 km elongated northwest-southeast. At least three volcanoes have historic records of eruptions; Shinmoe-dake, Ohachi and Iwo-yama, and more than 10 volcanoes were active in the past 22,000 years. This indicates that Kirishima is a multi-active volcanic group. Intense geothermal activity and frequent earthquake swarms are also characteristic features of Kirishima. Through seismological and other geophysical observations, the nature of the Kirishima 'multi-active volcanic system' has been revealed (Ida *et al.*, 1986; Kagiyama *et al.*, 1990).

Seismological research

The distribution of recent earthquake hypocenters in the Kirishima area are shown in Figure 1. Some hypocenters are shallow (< 5 km) beneath Kirishima, while others are deeper (10 km) around Kirishima. The majority of the hypocenters are distributed along several trends that are elongate either NE-SW or NW-SE. The dominant focal mechanism solutions indicate normal faulting with a NW-SE tensile axis in the NE-SW segments and of strike slip in the NW-SE segments. Active volcanoes are located along these lines, and extremely shallow earthquakes are distributed just beneath the craters of these volcanoes. The seismicity and focal mechanism indicate that the Kirishima area is subject to NW-SE extensional stress. The slight extensional stress is favorable for a fault system that allows magma to ascend at various points. For this reason, a multi-active volcanic group was generated in this area instead of a large stratovolcano.

Geothermal and electromagnetic research

Hot springs, fumaroles and steaming ground are scarce on the northeastern side of Kirishima, but are abundant on the southwestern side. The distribution of apparent electrical resistivity measured by VLF-MT has a consistent feature. Fumarolic activity is observed at the historically active volcanoes, Iwo-yama, Shinmoe-dake and Ohachi. Heat discharge from these three sites has been determined to be 61, 22, and 2.1 MW, respectively, based on the surface temperature distribution and the rise velocity of the fumarolic plumes. In the Iwo-yama region, which has the most active geothermal features at Kirishima, precise geothermal and electromagnetic surveys have been carried out. Ground temperature distribution reaches a maximum around the high temperature fumaroles located at the summit, with a significant thermal anomaly higher than 1 watt/m^2 around the summit. The distribution of

Keywords: Kirishima Volcanoes, active volcanic group, tensile stress field, VLF, ELF, ULF-MT, water saturated layer, volcano

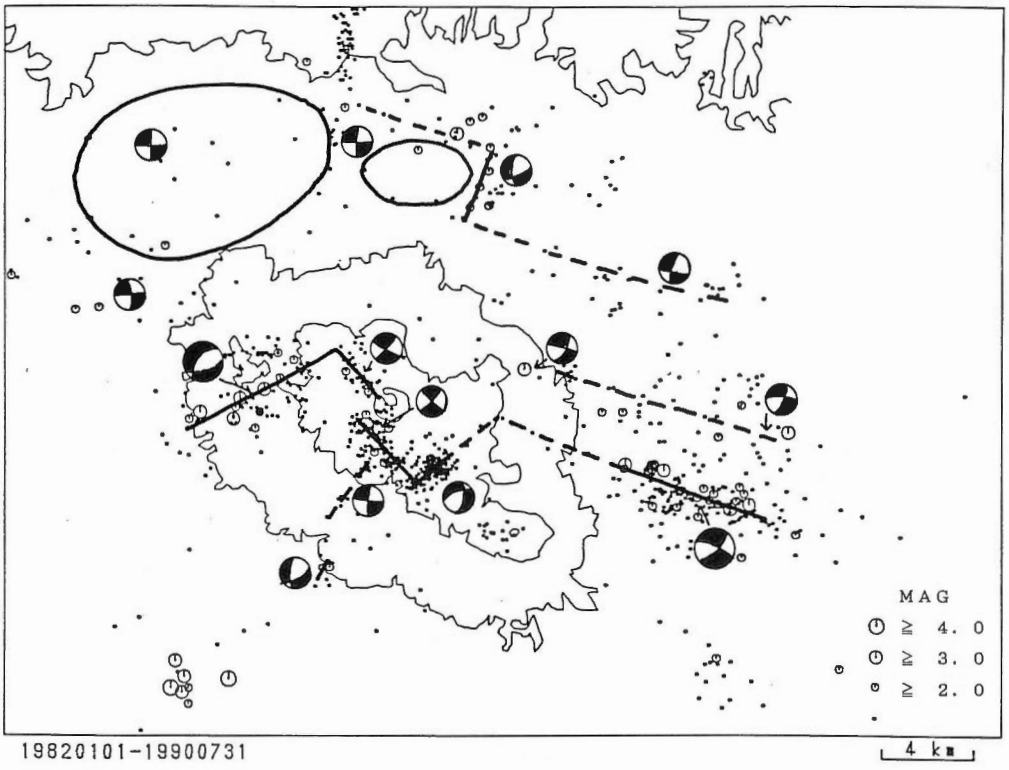

Fig. 1 Distribution of hypocenters of earthquakes observed over the period 1982 - 1990, and typical focal mechanism solutions for each area. Two ovals indicate the epicentral area of earthquake swarms in 1968 and 1975 in the Kakuto Caldera. Line and dashed line represent linear trends of hypocenters.

apparent resistivity measured by ELF-MT has a similar feature (Fig. 2); the summit area, which shows middle resistivity (5 ohm-m), is enclosed by an extremely low resistive zone (< 3 ohm-m). These zones correspond to the high temperature fumarolic zone and low temperature steaming ground, respectively. Through an inversion analysis using VLF, ELF and ULF-MT, a low resistivity second layer is found throughout the Kirishima area beneath the more resistive surface layer, which is about 100 m thick.

The resistivity of the second layer decreases dramatically just around the summit of Iwo-yama. This is interpreted as being caused by a saturated porous layer with wide distribution around Kirishima (Fig. 3), while high temperature volcanic gas supplied from beneath Iwo-yama creates the acid and extremely low resistive hydrothermal zone around the summit. The depth of the heat and gas source is estimated about 10 km by ULF-MT. Since a similar system is expected for each active volcano in Kirishima, an extensive MT survey is now being conducted.

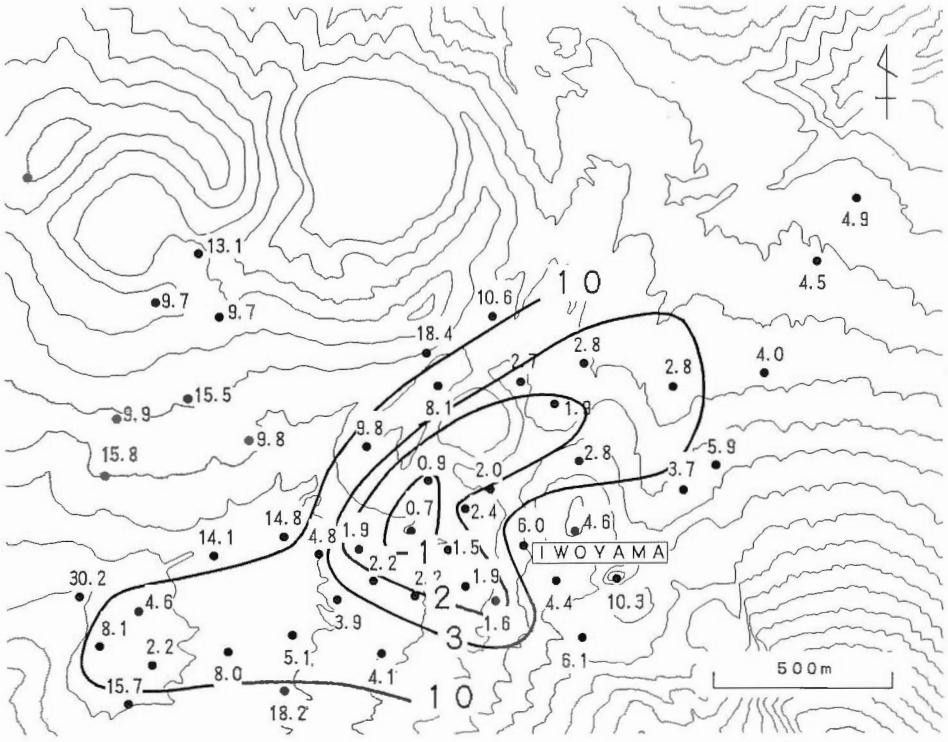

Fig. 2 Distribution of apparent electrical resistivity around Iwo-yama, measured by ELF-MT. 8 Hz, unit in ohm-m.

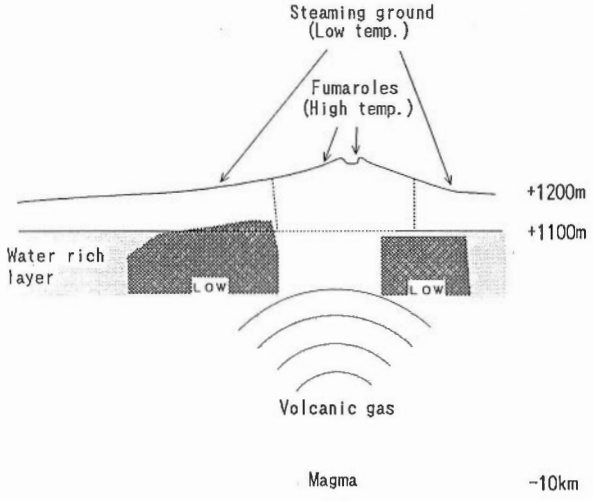

Fig. 3 Schematic model of geothermal system of Iwo-yama revealed by VLF, ELF and ULF-MT. "LOW" indicates the extremely low resistive (< 1 ohm-m) hydrothermal zone around the summit.

Significance of the saturated layer beneath volcanoes

In recent years, a low resistivity zone interpreted as a saturated porous layer has been revealed by MT surveys beneath some volcanoes; Izu-oshima Volcano by Utada *et al.* (1990), Suwanose-jima Volcano by Kagiyama *et al.* (1992), and Unzen Volcano by Kagiyama *et al.* (1991). In Izu-oshima and Suwanose-jima, volcanic tremor and geothermal precursors occurred before their volcanic eruptions. These precursors are caused by the ascent of magmatic gas to the water-rich layer. At Unzen Volcano, a phreato-magmatic eruption occurred on April 9, 1991, where it was thought that the magma penetrated the saturated layer. These results indicate the significance of the saturated layer beneath a volcanic body with respect to precursors of volcanic eruptions.

Acknowledgements

The author would like to express his sincere appreciation to Dr. J. W. Hedenquist for reviewing the manuscript and to Dr. H. Utada for his helpful suggestions on MT survey. He also thanks Mr. Yamaguchi and Mr. Masutani, Kirishima Volcano Observatory, for their assistance.

References

Ida, Y., Yamaguchi, M. and Masutani, F. (1986) Recent seismicity and stress field in Kirishima Volcano. *Bull. Seismol. Soc. Japan*, vol. 39, p. 111-121 (in Japanese).

Kagiyama, T., Ida, Y., Yamaguchi, M. and Masutani, F. (1990) Multi-active volcanic group generated in a slightly tensile stress field (abstract). *Eos*, vol. 71, p. 964.

———, Masutani, F., Utada, H., Matuo, H., Shimizu, H. and Umakoshi, K. (1991) Magma rising process estimated from ELF-VLF MT and sight observation at the volcanoes Unzen (abstract). *Volcanol. Soc. Japan.*, no. 2, p. 25 (in Japanese).

———, ——— and Iguchi, M. (1992) ELF, VLF-MT survey of the volcano Suwanose-jima. *Report Joint Geophys. Geochem. Obs. Suwanose-jima* (in press, in Japanese).

Utada, H. and Shimomura, T. (1990) Resistivity structure of Izu-oshima volcano revealed by the ELF-VLF magnetotelluric method. *Jour. Geomag. Geoelectr.*, vol. 42, p. 169-194.

Rept. Geol. Surv. Japan, No. 279, p. 93-96, 1992

Sulfur Isotopic Effects in the Disproportionation Reaction of Sulfur Dioxide at Hydrothermal Temperatures

Minoru KUSAKABE and Yasuo KOMODA*

Institute for Study of the Earth's Interior, Okayama University
Misasa, Tottori 682-01, Japan

Sulfur isotopic effects during disproportionation of sulfur dioxide were studied experimentally under hydrothermal temperatures and saturated water vapor pressures. Sulfur dioxide and water, sealed in a Pyrex glass tube with the total sulfur concentration ranging from 0.03 to 1.2 mol/kg, were reacted at 50° to 330°C for a variety of reaction periods up to 600 hours. Chemical and isotopic compositions of the run products were measured after quenching. Taking high reaction rates into consideration, "in-situ quenching" and "in-situ mixing" techniques were developed. In-situ quenching means that H_2S produced during the reaction is fixed as CdS at the temperature of the reaction by breaking a seal containing Cd^{2+} in order to avoid "retrograde" reactions during quenching. In-situ mixing means that SO_2 is mixed with a solution after a desired temperature has been reached by releasing the gas through a breakable seal into the solution. This avoided the effects of various reactions taking place during the initial temperature rise.

The final products of the disproportionation reaction of sulfurous acid were either sulfate plus elemental sulfur or sulfate plus hydrogen sulfide, the latter combination being favored when temperature was high or the total sulfur concentration was low. The "in-situ quenching" and "in-situ mixing" techniques revealed that, at the initial stage of the reaction, elemental sulfur as well as thiosulfate and polythionate ions were present even in the case where H_2S should eventually be stable. A large sulfur isotopic fractionation, up to 23 per mil in terms of $\Delta^{34}S_{SO_4\text{-}S^\circ}$, which is weakly temperature dependent, accompanied the initial stage of reactions that produced sulfate, elemental sulfur, hydrogen sulfide and other unstable sulfur species with intermediate valencies (Figures 1a, 1b and 2). Based on these observations, the disproportionation reaction of sulfurous acid (tetra-valent sulfur) is interpreted to proceed in the following way.

When HSO_3^- concentration is high in the initial stage, the following reactions take place:

$$2HSO_3^- \rightarrow S_2O_5^{2-} + H_2O \rightarrow SO_4^{2-} + H_2SO_2 \quad (1)$$

$$H_2SO_2 + HSO_3^- \rightarrow HSO_4^- + S^* + H_2O \quad (2)$$

$$S^* + HSO_3^- \rightarrow S_2O_3^{2-} + H^+ \quad (3)$$

where S* denotes a nascent state of sulfur. If the total sulfur concentration is high or temperature is low where elemental sulfur becomes stable, then,

$$S_2O_3^{2-} + 2HSO_3^- \rightarrow 2SO_4^{2-} + 2S^\circ + H_2O \quad (4)$$

and the overall reaction can be written as

$$H^+ + 3HSO_3^- \rightarrow 2HSO_4^- + S^\circ + H_2O \quad (5)$$

If the total sulfur concentration is low or temperature is high where H_2S becomes

Keywords: sulfur isotopic effects, disproportionation reaction, sulfur dioxide

* Present address: Kamioka Mining & Smelting Co. Ltd.,
Kamioka, Yoshiki-gun, Gifu-ken 506-12, Japan

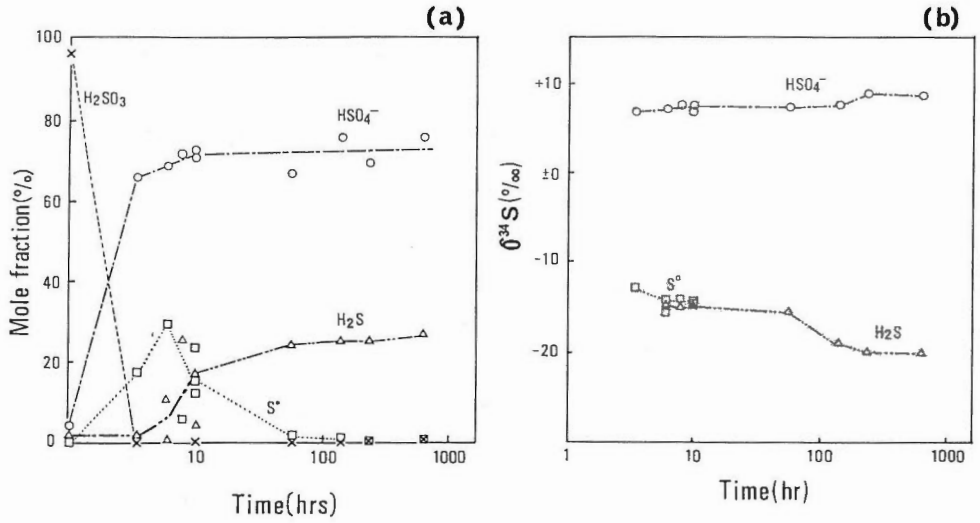

Fig. 1 Variations with time in the chemical composition (a) and isotopic composition (b) of the run products at 200°C with the total sulfur concentration of 0.031 mol/kg. Elemental sulfur was present until the end of the run and thiosulfate until 56 hrs, although their concentrations were not high enough for isotopic measurements.

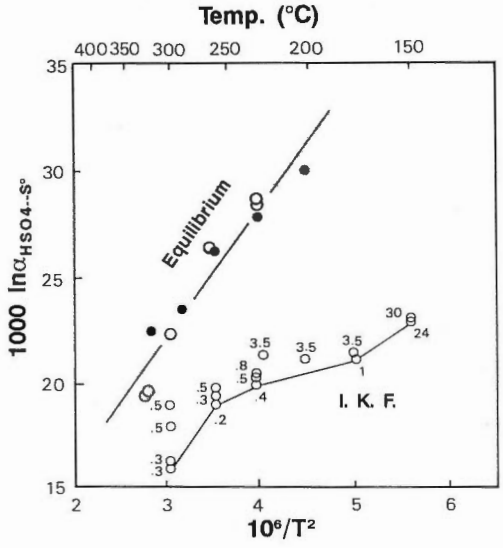

Fig. 2 Sulfur isotopic fractionation between HSO_4^- and S° as a function of temperature. The equilibrium values were estimated from the runs with long durations. The present results are indicated by open circles and those of Robinson (1973) by solid circles. The fractionation factors obtained from the runs with the shortest durations (indicated by numerals in hr) are connected to show the initial kinetic fractionation (I. K. F.).

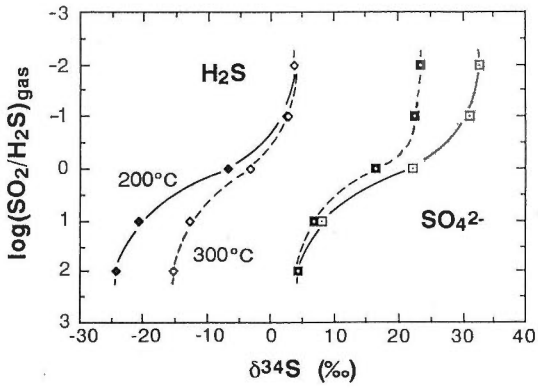

Fig. 3. Variation in $\delta^{34}S$ values of sulfate and hydrogen sulfide in isotopic equilibrium under hydrothermal conditions at 200° and 300°C as a function of SO_2/H_2S ratios of volcanic gases that are supplied to the hydrothermal system. A $\delta^{34}S_{\Sigma S}$ of the volcanic gases of 4 per mil was assumed to construct this diagram.

stable, then,

$$S_2O_3^{2-} + H_2O \rightarrow SO_4^{2-} + H_2S \quad (6)$$

and the overall reaction can be expressed as

$$H^+ + 4HSO_3^- \rightarrow 3HSO_4^- + H_2S \quad (7)$$

The initial, kinetically-controlled fractionation factors (I.K.F.) for the HSO_4^--S° pair and its equilibrium fractionation factors obtained from runs with long durations are illustrated in Figure 2, together with similar experimental results by Robinson (1973). The equilibrium fractionation factors (E.F.) in the temperature range between 230° to 330°C are approximated by the equation :

$$1000\ln\alpha_{HSO_4\text{-}S^\circ} = 6.21\times10^6/T^2 + 3.62 \quad (8)$$

which is close to the HSO4--H2S fractionation given by Ohmoto and Lasaga (1982). The HSO_4^--S° fractionation given by Oana and Ishikawa (1966), who first studied sulfur isotopic behavior during sulfurous acid disproportionation, ranges from 16 to 22 per mil, probably representing I.K.F. of our experiments, judging from their short reaction periods (up to only 3.5 hrs).

Kinetic treatment of the sulfur isotopic behavior during the initial stage of disproportionation indicates that the rates at which I.K.F.'s approach E.F.'s depend on temperature and the total sulfur concentration. Assuming that the rate is expressed as:

$$\ln[(\alpha_e-\alpha)/(\alpha_e-\alpha_i)] = -kC_st \quad (9)$$

where α_e, α_i and α are E.F., I.K.F. and an apparent fractionation at time t, respectively, while k and C_s are the rate constant and the total sulfur concentration of the system, respectively (Ohmoto and Lasaga, 1982). The rate constant k (kg H_2O/mol/hr) is approximated by an equation

$$\log k = -4.92(10^3/T) + 9.16 \quad (10)$$

From the above results, the reaction rates are found to become smaller as temperature decreases; e.g., the rate at 200°C is more than 2 orders of magnitude slower that at 300°C if the concentration of total sulfur is constant. When the total sulfur concentration is low, the overall reaction rate may be further reduced.

When sulfur dioxide from depths is supplied in the form of volcanic gases to a low-temperature, shallow hydrothermal environment where the disproportionation reaction takes place, the initial disequilibrium fractionation between sulfate and elemental sulfur (or hydrogen sulfide) may remain almost unchanged due to slow reaction rates at low temperatures. The sulfur isotopic compositions of sulfate and hydrogen sulfide in isotopic equilibrium in the aquifer are highly dependent on temperature and SO_2/H_2S ratios in the original volcanic gases (Figure 3). A large range of variations in the $\delta^{34}S$ values of SO_4^{2-} and H_2S in the acid hydrothermal environment (Kiyosu and Kurahashi, 1983) can be satisfactorily explained by disproportionation of sulfurous acid at low temperatures (<200°C).

References

Kiyosu, Y. and Kurahashi, M. (1983) Origin of sulfur species in acid-chloride thermal waters, northeastern Japan. *Geochim. Cosmochim. Acta*, vol. 47, p. 1237-1245.

Oana, S. and Ishikawa, H. (1966) Sulfur isotopic fractionation between sulfur and sulfuric acid in the hydrothermal solution of sulfur dioxide. *Geochem. Jour.*, vol. 1, p. 45-50.

Ohmoto, H. and Lasaga, A. C. (1982) Kinetics of reactions between aqueous sulfates and sulfides in hydrothermal systems. *Geochim. Cosmochim. Acta*, vol. 46, p. 1727-1745.

Robinson, B. W. (1973) Sulphur isotope equilibrium during sulphur hydrolysis at high temperatures. *Earth Planet. Sci. Lett.*, vol. 18, p. 443-450.

Rept. Geol. Surv. Japan, No. 279, p. 97, 1992

Evidence for Extreme Partitioning of Copper into a Magmatic Volatile Phase

Jacob B. LOWENSTERN[1)]*, Gail A. MAHOOD[1)], Mark L. RIVERS[2)] and Stephen R. SUTTON[2)]

[1)] *Department of Geology, Stanford University, Stanford, CA 94305, U.S.A.*
[2)] *Department of Applied Science, Brookhaven NL, Upton, NY 11973, U.S.A.*

Synchrotron x-ray fluorescence analysis of melt inclusions in quartz and sanidine phenocrysts and in matrix glass of Cl-rich (0.9 wt.%) pantellerites (peralkaline rhyolites) from Pantelleria, Italy, reveals the presence of a magmatic volatile phase within the pantellerite magma chamber.

Experiments were run on beamline X26A at the National Synchrotron Light Source of Brookhaven National Lab, New York. Twenty inclusions in quartz were prepared such that the trace-element-free, host quartz was doubly-polished and the inclusions within them were not opened. Single spectra were collected by rastering the entire inclusions under the synchrotron beam. Eighteen of the inclusions contain less than 30 ppm copper, whereas two of the inclusions have copper in excess of 100 ppm. High-resolution scans revealed that the copper is concentrated in bubbles within Cu-rich melt inclusions. The bubbles contain several hundred times more copper than the coexisting glass (melt). The presence of copper within bubbles and the presence of these copper-rich bubbles within a minority of melt inclusions is consistent with the random entrapment of a copper-rich magmatic volatile phase in some of the melt inclusions (Lowenstern *et al.*, 1991). Analysis of these bubbles by EDS and FTIR showed that they also contain CO_2, Cl, S and H_2O.

Similar experiments on melt inclusions in quartz from the high-silica rhyolite erupted in 1912 at the Valley of Ten Thousand Smokes (VTTS), Alaska showed that a copper-bearing volatile phase also resided in the VTTS magma chamber. The presence of these volatile phases in magma chambers with <10% phenocrysts shows that crystallization-induced volatile saturation (second boiling) is not necessary for the creation of Cu-rich vapors/fluids in silicic magma chambers. Occasionally, Cu-rich vapors will escape during volcanic eruptions. We calculate that the eruption of the Green Tuff, 45,000 years ago at Pantelleria, released 5×10^5 tons of Cu during catastrophic degassing, roughly ten times the annual anthropogenic contribution of Cu to the atmosphere.

Reference

Lowenstern, J. B., Mahood, G. A., Rivers, M. L., Sutton, S. R. (1991) Evidence for extreme partitioning of Cu into a magmatic vapor phase. *Science*, vol. 252, p. 1402-1405.

Keywords: copper, vapor, volatile phase, chlorine, peralkaline

* Present address: Mineral Resources department, Geological Survey of Japan, Higashi 1-1-3, Tsukuba 305, Japan

Rept. Geol. Surv. Japan, No. 279, p. 98-103, 1992

Magmatic Heating and Brine Diapirism in the Salton Trough Rift

Michael A. McKIBBEN

Dept. of Earth Sciences - 036, University of California
Riverside, CA 92521-0423, U.S.A.

The metal-rich brines of the Salton Sea geothermal system (SSGS) are the most accessible and well studied saline hydrothermal fluids in the world. The chemical behavior and hydrodynamics of brines are critical in processes of hydrothermal ore formation near crystallizing hydrous magmas. Therefore, it is fruitful to review the thermal, physical and chemical behavior of the Salton Sea geothermal brines for this Seminar.

Although these brines have evolved chemically as a consequence of sedimentary and metamorphic processes in the continental rift environment of the Salton Trough, it is the interplay between underlying magmatic heat input and overlying lake levels which controls the topology and level of ascent of the internally-convecting diapiric brine reservoir of the SSGS. Without focused magmatic heat input, these brines would otherwise remain several kilometers deeper in the rift basin. Magmatic heating also drives extensive brine-rock interaction in the deltaic host sediments, yielding concentrations of metals and other solutes which mask any direct magmatic chemical contribution to the brines.

Geological setting

The SSGS is located in the Salton Trough, an active continental rift representing the tectonic transition from the divergent East Pacific Rise spreading system of the Gulf of California to the strike-slip San Andreas fault system of western North America. The Trough is underlain by a fragmented oceanic ridge spreading system, and has been gradually filled and bisected transaxially by the delta of the Colorado River over the past 5 Ma. This has resulted in a persistent hydrologically closed saline lake environment in the northern Trough, of which the Salton Sea is the modern expression. The combination of underlying MORB magmatic heat sources, thick porous deltaic-lacustrine sediments, recurrent tectonic activity, and persistent saline lakes has provided a unique environment for the localized accumulation and movement of metalliferous hydrothermal brines.

Within the Trough, high-intensity hydrothermal systems (Salton Sea, Brawley, Cerro Prieto) tend to occur in sediment filled structural pull-apart basins (rhombochasms) which overlie the spreading center fragments; these are structurally analogous to the Guaymas Basin farther south in the Gulf of California. These Trough systems exhibit high heat flow, strong gravity and magnetic anomalies, and often have surface manifestations such as Quaternary volcanoes and thermal springs.

Keywords: metals, brine, magma-fluid interactions, Salton Sea, geothermal system, rift

Reservoir structure

The reservoir of the SSGS has recently been mapped out in detail by Williams and McKibben (1989). The saline brine reservoir has a domal upper surface defined by a coincidence of the 260°C isotherm with a sharp fluid interface, where salinities increase rapidly with depth from <12 % TDS to >15 % TDS. This fluid interface occurs at a depth of only 500 m in the hot, central part of the field and is density-stabilized (non-convective) due to a balance between salinity and temperature (Williams, 1988; Williams and McKibben, 1989). The interface effectively chemically isolates the underlying brine volume, with heat transfer across the interface occurring mainly by conduction. The underlying reservoir of hypersaline brine appears to have a density gradient that permits convection, a scenario that is supported by the chemical and stable isotopic homogeneity of the brine. The lower limits to the brine reservoir, if any, are not known, but saline brine has been encountered at depths of at least 4 km in locations peripheral to the SSGS. Unfortunately there is no economic incentive for the geothermal companies to drill to produce brine from depths greater than 2-3 km, to explore the peripheral topology of the brine diapir.

Expanding on the ideas of Rex (1983, 1985), a model for the evolution of the brine reservoir was proposed by Williams and McKibben (1989). Rift basinal brines that have accumulated in the closed Salton Sea basin have been magmatically heated above oceanic spreading center fragments to generate an internally-convecting brine diapir that has advected to within 0.5 km of the surface. Rather than being limited by any lithologic "cap", the depth to the top of the brine diapir is controlled by the density of the hot brine under the current hydrologic head of the Trough. Williams and McKibben proposed that the brine interface therefore had oscillated vertically with time due to changes in brine temperature (magmatic heat influx) and paleo lake levels (hydrologic head changes).

Brine chemistry and metamorphism

The hot (up to 365°C), hypersaline Na-Ca-K-Cl brines contain up to 26 % TDS and are rich in B, NH_3, Fe, Mn, Zn, Pb and other metals. Interestingly, there are only 5 water molecules per ion in these brines, so that if each ion is even partially hydrated there is effectively no free solvent left! Undoubtedly a large fraction of the ionic constituents are chloride-complexed or ion-paired rather than hydrated, but in effect the brines must behave more like molten salts or molecular fluids than dilute aqueous solutions. The brines therefore are quite viscous and very slow to convect and mix with shallower, more dilute fluids. U-Th decay-chain measurements imply that the hypersaline brines have relatively long residence times in the SSGS, on the order of 10^4 years (Zukin *et al.*, 1987). For this reason their gradual ascent and persistence as a discrete internally-convecting diapir within the Salton Trough is a reasonable scenario.

Numerous stable isotopic studies of the brines indicate that their water originated as Colorado River water that has undergone near-surface evaporation and subsequent water-rock interaction at elevated temperatures. The hypersaline brines are oxygen-isotope equilibrated with the host metasediments and have a hydrogen isotopic composition that is distinct from the less-equilibrated, less saline overlying fluids (Williams and McKibben, 1989). This implies that they may represent older

(Plio-Pleistocene?) fluids that accumulated under different climatic or recharge conditions than more recent surface waters.

Patterns of metamorphic mineral zonation with depth track the diapiric topology of the heated brine reservoir (McDowell, 1987), and record greenschist and amphibolite facies assemblages at depths of less than 4 km (Muffler and White, 1969; McDowell and Elders, 1980; Cho *et al.*, 1988). Substantial water-rock interaction has strongly modified both the host rock and brine diapir upon its ascent; the host sediments have effectively been transformed to a dense, fractured hornfels that behaves as a homogeneous porous medium on a gross scale.

Shales in the host metasediments of the SSGS show a progressive, nearly complete depletion in their base metal contents with increasing depth (McDowell, 1987), implying that the hot brines have effectively stripped the sediments of their detrital metal content as the brine diapir advected upwards through the sedimentary section. Mass balance calculations by McDowell and McKibben indicate that the content of most of the metals in the brines can be accounted for by this hydrothermal leaching of the host sediments. There is no need to invoke magmatic or other external sources for the base metals.

Ore mineralization

In contrast to the spectacular metal contents of the brines, ore mineralization within the system is presently rather feeble (McKibben and Elders, 1985; McKibben *et al.*, 1988). The metals apparently precipitate only infrequently, when tectonic movements generate vertical fractures that transgress the fluid interface and allow shallow, more oxidized dilute fluids to mix with the metalliferous hypersaline brines (McKibben *et al.*, 1988). The most common ore minerals in these open veins are pyrite, hematite, chalcopyrite, sphalerite and galena. Common gangue minerals are calcite, quartz, epidote and chlorite. Fluid inclusion salinities in these veins are intermediate between those of the endmember fluids, further supporting a transient fluid interface mixing model.

The sampled brines have a relatively high oxidation state, corresponding to the hematite-pyrite and SO_4-H_2S redox couples (McKibben and Elders, 1985). Most of the brine samples come from well production zones just below the fluid interface, so it is not known if the brines may become more reduced at depth within the heart of the diapir. However, sulfur isotopic data imply that the brine redox state may be uniformly buffered at this high value by metamorphic redox reactions between Fe^{2+} in the brines and abundant evaporitic anhydrite in the host metasediments (McKibben and Eldridge, 1989; Osborn *et al.*, 1988). The $\simeq 0$ per mil sulfur isotopic composition of H_2S in the brines can be accounted for by this hydrothermal sulfate reduction mechanism, and no major magmatic sulfur component is required.

The high oxidation state and high Ca^{2+} content of the brines thus keep the dissolved H_2S and SO_4 contents quite low ($<10^{-3}$ m each). The low activity of reduced sulfur coupled with high chloride activity permit the spectacular metal contents of the brines, while at the same time inhibiting the amount of metal sulfide precipitation. The persistent saline lake environment generated in the northern Salton Trough for the past 4 Ma by the growth of the Colorado River delta has therefore significantly influenced the metal-carrying capacity of these brines, by providing a brine-filled sedimentary section rich in metalliferous shales and lacustrine sulfate (McKibben *et al.*, 1988).

The low content of Cu relative to Zn and Pb in these brines may be caused by the high Fe content, which stabilizes chalcopyrite as a vein mineral phase and keeps Cu solubility low.

A future ore deposit?

The SSGS will not likely form a major concentrated base metal ore deposit in its present configuration, unless precipitation by episodic mixing at the fluid interface is allowed to continue for a protracted length of time. Given the tectonically dynamic nature of the Trough, this seems unlikely. The quantitative precipitation of the contained in the brine metals will instead require some catastrophic event, such as sudden magmatic heating and advective expulsion of the fluids onto the floor of the Salton Sea.

Because the ascent of the diapiric brine reservoir is controlled by a temperature-density balance which responds both to magmatic heat from below and the hydrologic head created by lake levels above, a sudden increase in magmatic heat input coupled with a high lake level could allow the brine diapir to advect upward and breach the surface.

The modern Salton Sea is quite shallow and well-mixed, so that an expulsive event would likely generate a stratiform Fe-Mn oxide deposit. However, some of the Pleistocene lakes that were present in the northern Trough were considerably larger and deeper (Waters, 1983) and could have had anoxic, H_2S-rich bottom waters. In this case lake-floor expulsion of the brines could generate a massive stratiform base metal sulfide deposit.

The expulsive ore-forming capacity of the SSGS brines can be estimated by calculating the total mass of metals that the brines contain (McKibben *et al.*, 1990). This can be estimated very conservatively by taking the volume between the domal upper surface of the hypersaline brine diapir and the maximum commercially exploited depth of 2 km. This volume excludes portions of the explored field containing lower-salinity fluids, and yields $\simeq$55 km^3 of total reservoir. With a 20% fracture and granular porosity, the resulting hypersaline brine volume is $\simeq$11 km^3. At a brine density of $\simeq$1.0 at 300°C, this volume contains $\simeq 1.1 \times 10^{13}$ kg of brine. Using typical SSGS metal contents, the following amounts are calculated for a few selected metals:

Fe	1600 mg/kg	18 million metric tons
Zn	500 mg/kg	6 million metric tons
Ag	1 mg/kg	350 million ounces
Pd	1 μg/kg	350,000 ounces

These estimates are approximate, because they consider only the currently exploited hypersaline geothermal system and assume a uniform metal content. Hypersaline brines are found at depths below 2 km, both within and outside of the exploited Salton Sea field. It has been proposed that the total hypersaline brine volume is at least 10 times that which is presently exploited in the SSGS (Rex, 1983; Williams and McKibben, 1989). If the metal content of these brines is uniform, then the entire hydrothermal system could contain ten times the amounts of dissolved metals calculated above.

The tonnage estimates above compare favorably with those for several major

types of stratiform sediment-hosted base metal ore deposits (Cox and Singer, 1986). The SSGS thus may be a reasonable and useful analog for modeling the accumulation and subaqueous expulsion of metalliferous brines to form stratiform ores in continental rift environments.

References

Cho, M., Liou, J. G. and Bird, D. K. (1988) Prograde phase relations in the C.S. 2-14 well meta-sandstones, Salton Sea geothermal field, California. *Jour. Geophys. Res.*, vol. 93, B11, p. 13081-13103.

Cox, D. P. and Singer, D. A. (1986) Mineral Deposit Models. *U. S. Geol. Surv. Bull.* 1693, 379 p.

McDowell, S. D. (1987) Geothermal alteration of sediments in the Salton Sea scientific drillhole: petrophysical properties and mass changes during alteration. *Final Research Report, Department of Energy*, Grant DE-FG02-85ER13409, 62 p.

——— and Elders, W. A. (1980) Authigenic layer silicate minerals in borehole Elmore 1, Salton Sea geothermal field, California, U.S.A. *Contrib. Mineral. Petrol.*, vol. 74, p. 293-310.

McKibben, M. A. and Elders, W. A. (1985) Fe-Zn-Cu-Pb mineralization in the Salton Sea geothermal system, Imperial Valley, California. *Econ. Geol.*, vol. 80, p. 539-559.

———, Andes, J. P., Jr. and Williams, A. E. (1988) Active ore formation at a brine interface in metamorphosed deltaic lacustrine sediments: the Salton Sea geothermal system, California. *Econ. Geol.*, vol. 83, p. 511-523.

——— and Eldridge, C. S. (1989) Sulfur isotopic variations among minerals and aqueous S species in the Salton Sea geothermal system: a SHRIMP ion microprobe and conventional study of active ore genesis in a sediment-hosted environment. *Amer. Jour. Sci.*, vol. 289, p. 661-707.

———, Williams, A. E. and Hall, G. E. M. (1990) Solubility and transport of platinum-group elements and Au in saline hydrothermal fluids: constraints from geothermal brine data. *Econ. Geol.*, vol. 85, p. 1926-1934.

Muffler, L. J. P. and White, D. E. (1969) Active metamorphism of upper Cenozoic sediments in the Salton Sea geothermal field and the Salton Trough, southeastern California. *Geol. Soc. Amer. Bull.*, vol. 80, p. 157-182.

Osborn, W. L., McKibben, M. A. and Williams, A. E. (1988) Formation, diagenesis and metamorphism of lacustrine sulfates under high geothermal gradients in an active continental rift zone. *Geol. Soc. Amer., Abstracts with Program*, vol. 20, no. 7, p. 51.

Rex, R. W. (1983) The origin of the brines of the Imperial Valley, California. *Transactions Geotherm. Resources Council*, vol. 7, p. 321-324.

——— (1985) Temperature-chlorinity balance in the hypersaline brines of the Imperial Valley, California. In Stone, C., ed., *Intl. Symp. on Geotherm. Energy, Geotherm. Resources Council*, p. 351-356.

Waters, M. R. (1983) Late Holocene lacustrine chronology and archaeology of ancient Lake Cahuilla, California. *Quat. Res.*, vol. 19, p. 373-387.

Williams, A. E. (1988) Fluid density distribution in a stratified geothermal reservoir: Salton Sea geothermal system, California. *Geol. Soc. Amer.*,

Abstracts with Program, vol. 20, no. 7, p. A98.

——— and McKibben, M. A. (1989) A brine interface in the Salton Sea geothermal system, California: fluid geochemical and isotopic characteristics. *Geochim. Cosmochim. Acta*, vol. 53, p. 1905-1920.

Zukin, J. G., Hammond, D. E., Ku, T. L. and Elders, W. A. (1987) Uranium-thorium series radionuclides in brines and reservoir rocks from two deep geothermal boreholes in the Salton Sea geothermal field, southeastern California. *Geochim. Cosmochim. Acta*, vol. 51, p. 2719-2732.

Rept. Geol. Surv. Japan, No. 279, p. 104-109, 1992

Origin of Magmatic Waters in Subduction Zones: Stable Isotopic Constraints

Yukihiro MATSUHISA

Geological Survey of Japan
1-1-3 Higashi, Tsukuba, Ibaraki 305, Japan

Introduction

Hydrogen and oxygen isotopic ratios (D/H and $^{18}O/^{16}O$ in terms of δD and $\delta^{18}O$) have been used as a good indicator of the origin of hydrothermal waters, since the ratios have distinct values for the three major sources of the waters: magmatic, meteoric and seawater. Later modification of the waters by mixing, boiling and interaction with rocks is also recognizable on a δD-$\delta^{18}O$ diagram. Among the three major sources of the waters, the latter two are directly accessible. For the magmatic water, which is more ambiguous as compared to the other two, the compositional range of "Primary Magmatic Water (PMW)" (δD = -40 to -80 per mil, $\delta^{18}O$ = +6 to +9 per mil) was estimated by Taylor (1974) on the basis of isotope data of igneous rocks and minerals, and has long been accepted as a common reference point. High temperature volcanic gases discharging directly from magma should be a suitable source to approximate the composition of magmatic water. However, there is a discordance between the hydrogen isotope ratios of the PMW and volcanic discharges from subduction zones of the Circum-Pacific region; the latter has waters with δD values higher than the PMW by 20 to 40 per mil. The objective of this paper is to discuss and evaluate whether this discrepancy in the hydrogen isotope ratios of the "two" magmatic waters reflects the difference in source material of magma, i.e., the contribution of subducted oceanic slab, or is due to isotopic fractionation associated with the degassing of magma.

Isotopic ratios of volcanic discharge

Figure 1 shows two examples of isotopic ratios of waters in island-arc volcanic discharges: Satsuma-Iwojima and Showa-Shinzan, Japan. Satsuma-Iwojima, an active dacite volcanic cone situated on the edge of a submerged caldera, has intensive fumarolic activity in the summit crater with temperatures up to 877°C. The water condensates from the fumarolic gases have a uniform isotopic composition of δD = -23 to -27 per mil, and $\delta^{18}O$ = +6.3 to +7.6 per mil (Matsuo *et al.*, 1974; Matsubaya *et al.*, 1975). They appear to have little contamination by meteoric water and seawater. On the other hand, volcanic gases from Showa-Shinzan show a wide spread of isotopic composition, ranging between that of high-temperature volcanic gas (the highest temperature is 830°C) and local meteoric waters. Mizutani (1978) estimated an isotopic composition of δD = -32 and $\delta^{18}O$ = +7.4 per mil for the initial magmatic water of this volcano. Similar mixing lines between high-temperature volcanic gas and local meteoric water are seen for samples from several other volcanoes in Japan (e.g., Mizutani *et al.*, 1986). We also have several examples of hy-

Keywords: hydrogen isotope, oxygen isotope, volcanic discharge, volcanic rock, magma degassing, subduction zone.

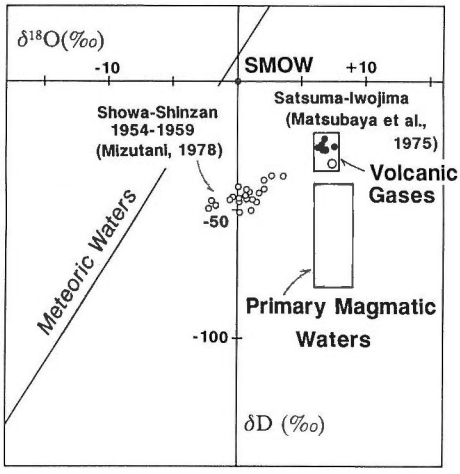

Fig. 1 δD-$\delta^{18}O$ plot showing the compositional ranges of three end-members of hydrothermal waters: Primary Magmatic Waters (PMW), Meteoric Waters, and Seawater (SMOW), and that of high-temperature volvanic gases (VG). Also shown are volcanic gases from Satsuma-Iwojima (solid circles) (Matsubaya *et al.*, 1975) and Showa-Shinzan (open circles) (Mizutani,1978). The large open circle denotes the primary magmatic water of Showa-Shinzan volcano estimated by Mizutani (1978).

drothermal waters whose isotopic compositions extend toward that of the high-temperature volcanic gases (Aoki, this volume). In conclusion, a compositional range of δD = -20 to -35 and $\delta^{18}O$ = +6 to +8 is recognized for water of high-temperature volcanic discharges in Japan, enriched in D by 20 to 40 per mil as compared to the PMW (Fig. 1). The $\delta^{18}O$ values of the volcanic gases are identical to that of the PMW, and indicate isotopic equilibrium with silicate rocks or melt at magmatic temperatures. This composition range for volcanic gases is also accordant with data for other volcanoes of the Circum-Pacific region, including White Island (Stewart and Hulston, 1975), several in Kamchatka (Taran *et al.*, 1988), Mt. St. Helens (Barnes, 1984) and Augustine (Viglino *et al.*, 1985). Therefore, this compositional range can be generalized as that related to volcanoes of island-arcs and plate margins of the Circum-Pacific region. Since the available data are limited to this region, however, it is difficult to conclude whether or not the D-enriched feature is characteristic of subduction-related magmas. In this context, Pineau and Javoy (1986) reported an interesting δD value of -25 per mil for the gas recovered from "Popping Rock" of the Mid Atlantic Ridge.

D/H ratios of volcanic rocks

Volcanic rocks may have preserved the composition of primary magmatic waters. Individual data of volcanic rocks, however, indicate a large deviation from the primary composition due to degassing of magma and alteration of volcanic glass and minerals. By eliminating secondary modification, well-defined primary magmatic δD values are deduced to be -70 to -80 per mil for MOR (e.g., Craig and Lupton, 1976; Kyser and O'Neil, 1984; Poreda *et al.*, 1986), and -60 to -70 per mil for

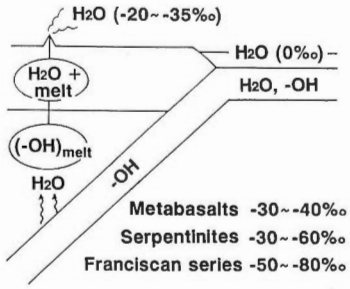

Fig. 2 A schematic diagram showing the processes involved in the formation of magmatic water in subduction-related magmatism.

Hawaii (Friedman, 1967; Moore, 1970). For island-arcs, slightly higher δD values of -50 to -60 per mil are estimated for boninite (water-rich, high-magnesium andesite) and sanukite (glassy andesite) from Japan (Satake *et al.*, 1984; Dobson and O'Neil, 1987; Sato and Kusakabe, 1991). The δD values of pre-eruption rhyolitic magmas in the continental margin of western US are also in the same range (Taylor *et al.*, 1983). In contrast, high δD values of -30 to -40 per mil are reported for alkalic members from back-arc basins (Poreda, 1985). Therefore, 10 to 30 per mil enrichment in D could exist in the subduction-related magmas as compared with the MOR system. This D-enrichment may indicate the involvement of fluids derived by dehydration of the downgoing oceanic slab (δD = -30 to -60 per mil) into the magma source. However, the δD values of -50 to -60 per mil for the island-arc magmas are within the compositional range of the PMW, and are not high enough to explain the the difference between the PMW and the volcanic gases. Besides, the volcanic gases are the final product of processes with multiple stages involving dehydration of the subducted oceanic slab, hydration of the overlying mantle wedge, partial melting of the mantle and water-dissolution into magma, degassing of magma due to pressure decrease and crystallization, and migration of liberated water, all of which could be associated with isotopic fractionation to a various degree (Fig. 2). Therefore, it is essential to evaluate the nature and degree of isotope fractionation in these processes.

D/H fractionation associated with degassing of magma

If we have the isotope composition of magma, we can estimate the composition of volcanic gas by assuming degassing models of magma and isotopic fractionation factors between gas and melt phases. Figure 3 shows the δD variation of water being released from a hydrous melt for three degassing models: continuous degassing in an open system, accumulation of water derived by continuous degassing, and degassing in a closed system. Similar degassing models have been discussed for the systematic depletion of rhyolite magma in D/H ratio by B. E. Taylor and his coworkers (Taylor *et al.*, 1983; Taylor, 1986; Taylor, this volume). The primary δD value of magma was assumed to be -60 per mil, with a D/H fractionation factor of 40 per mil between gas and melt taken from Dobson *et al.* (1989). Although we have large uncertainties in the primary δD value of magma (± 10 per mil or larger) and in the fractionation factor between gas and melt (it may decrease with increasing water content of magma, down to 20 per mil, e.g., Newman *et al.*, 1988; Taylor, this vol-

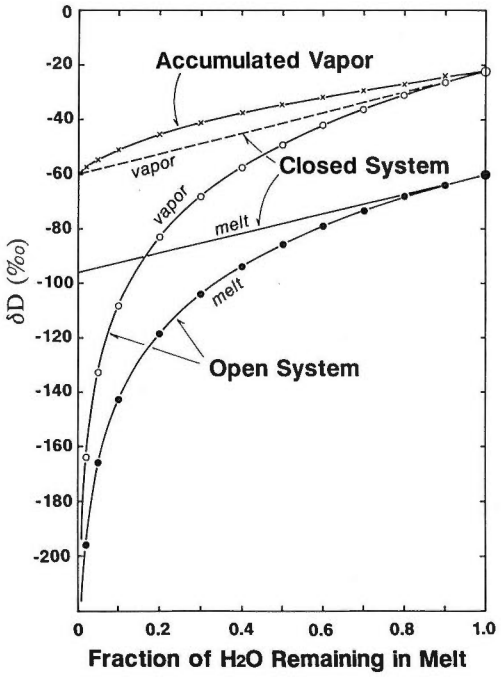

Fig. 3 δD-variation of vapor and melt phases with the degree of degassing of hydrous magma. Calculation was made for three degassing models: continuous degassing in an open system, accumulation of vapor derived by continuous degassing, and degassing in a closed system. In the diagram a maximum D/H fractionation factor of 40 per mil between vapor and melt is taken by assuming dissolved water in the melt to be hydroxyl H2O. Actually, the fractionation factor is a function of the water content of the melt, and becomes larger with decreasing water content (Newman *et al.*, 1988). In an early stage of degassing, the fractionation factor may be smaller than 40 per mil due to the existence of dissolved molecular H2O in the melt (Stolper, 1989), then gradually become larger with progressive degassing, increasing to 40 per mil.

ume), it is evident that water vapor with a reasonably narrow range of δD values (-20 to -40 per mil with up to 60% degassing of magma) can form in a closed system or in a vapor reservoir isolated from magma. Continuous degassing in an open system will create a large variation in isotopic composition of both gas and melt phases, which should be detected but is never recognized in volcanic discharges. The degassing of magma may not continue until the last drop of water is released. However, a more realistic idea would be that the volcanic discharges we generally observe may represent only the early stages of degassing of magma, and that fumarolic activity may rapidly decline, with surface activity stopping with decreasing temperature of the magma. If that is the case, the δD values of released water may not change significantly even in an open system (-20 to -40 per mil with up to 35% degassing), and the balance of the water may remain within solidified rocks (-66 per mil in this case).

Therefore, the apparent enrichment of volcanic gases in D relative to the

PMW may be attributed to isotope fractionation associated with the degassing of magma. The relatively uniform composition of volcanic gases does not conflict with this degassing model. The D-enrichment relative to the PMW is observed in hydrothermal fluids responsible for porphyry copper mineralization (Kusakabe *et al.*, 1990), and some acid-sulfate alteration associated with high-sulfidation mineralization (Rye *et al.*, 1992). These fluids may have been derived directly from an underlying magma by degassing.

References

Craig, H. and Lupton, J. E. (1976) Primordial neon, helium, and hydrogen in oceanic basalts. *Earth Planet. Sci. Lett.*, vol. 31, p. 369-385.

Barnes, I. (1984) Volatiles of Mount St. Helens and their origins. *Jour. Volcanol. Geotherm. Res.*, vol. 22, p. 133-146.

Dobson, P. F., Epstein, S. and Stolper, E. M. (1989) Hydrogen isotope fractionation between coexisting vapor and silicate glasses and melts at low pressure. *Geochim. Cosmochim. Acta*, vol. 53, p. 2723-2730.

——— and O'Neil, J. R. (1987) Stable isotope compositions and water contents of boninite series volcanic rocks from Chichi-jima, Bonin islands, Japan. *Earth Planet. Sci. Lett.*, vol. 82, p. 75-86.

Friedman, I. (1967) Water and deuterium in pumice from the 1959-60 eruption of Kilauea Volcano, Hawaii. *U. S. Geol. Surv. Prof. Paper*, no. 575-B, p. B120-B127.

Kusakabe, M., Hori, M. and Matsuhisa, Y. (1990) Primary mineralization-alteration of the El Teniente and Rio Blanco porphyry copper deposits, Chile: Stable isotopes, fluid inclusions and $Mg^{2+}/Fe^{2+}/Fe^{3+}$ ratios of hydrothermal biotite. *Geol. Dept. and Univ. Extension, Univ. of Western Australia, Pub.* no. 23, p. 244-259.

Kyser, T. K. and O'Neil, J. R. (1984) Hydrogen isotope systematics of submarine basalts. *Geochim. Cosmochim. Acta*, vol. 48, p. 2123-2133.

Matsubaya, O., Ueda, A., Kusakabe, M., Matsuhisa, Y., Sakai H. and Sasaki, A. (1975) An isotopic study of the volcanoes and the hot springs in Satsuma Iwo-jima and some areas in Kyushu. *Bull. Geol. Surv. Japan*, vol. 26, p. 375-392.

Matsuo, S., Suzuoki, T., Kusakabe, M., Wada, H. and Suzuki, M. (1974) Isotopic and chemical compositions of volcanic gases from Satsuma-Iwojima, Japan. *Geochem. Jour.*, vol. 8, p. 165-173.

Mizutani, Y. (1978) Isotopic compositions of volcanic steam from Showashinzan Volcano, Hokkaido, Japan. *Geochem. Jour.*, vol. 12, p. 57-63.

———, Hayashi, S. and Sugiura, T. (1986) Chemical and isotopic compositions of fumarolic gases from Kuju-Iwoyama, Kyushu, Japan. *Geochem. Jour.*, vol. 20, p. 273-285.

Moore, J. (1970) Water content of basalt erupted on the ocean floor. *Contr. Mineral. Petrol.*, vol. 28, p. 272-279.

Newman, S., Epstein, S. and Stolper, E. (1988) Water, carbon dioxide, and hydrogen isotopes in glasses from the ca. 1340 A.D. eruption of the Mono Craters, California: Constraints on degassing phenomena and initial volatile content. *Jour. Volcanol. Geotherm. Res.*, vol. 35, p. 75-96.

Pineau, F. and Javoy, M. (1986) The volatile record of a 'popping' rock from the

Mid-Atlantic Ridge at 15°N: Concentrations and isotopic compositions. *Terra Cognita*, vol. 6, p. 191.

Poreda, R. (1985) Helium-3 and deuterium in back-arc basalts: Lau Basin and the Mariana Trough. *Earth Planet. Sci. Lett.*, vol. 73, p. 244-254.

———, Schilling, J-G. and Craig, H. (1986) Helium and hydrogen isotopes in ocean-ridge basalts north and south of Iceland. *Earth Planet. Sci. Lett.*, vol. 78, p. 1-17.

Rye, R. O., Bethke, P. M. and Wasserman, M. D. (1992) Diverse origin of alunite and acid sulfate alteration: Stable isotope systematics. *Econ. Geol.*, vol. 87, p. 225-262.

Satake, H., Tanaka, M., Hirai, A., Urano, H., Shiraki, K. and Kuroda, S. (1984) Oxygen and hydrogen isotopic ratios of boninites from Chichi-jima, Bonin islands and their origin. *Abstracts, Annual Meeting of Geochem. Soc. Japan*, p. 211.

Sato, H. and Kusakabe, M. (1991) Water content and hydrogen isotopic composition of glassy bronzite andesite (sanukite) and glassy rhyolite from Goshikidai and Kanayama, northeast Shikoku, Japan. *Jour. Geol. Soc. Japan*, vol. 97, p. 755-758.

Stewart, M. K. and Hulston, J. R. (1975) Stable isotope ratios of volcanic steam from White Island, New Zealand. *Bull. Volcanol.*, vol. 39, p. 28-46.

Stolper, E. (1989) Temperature dependence of the speciation of water in rhyolitic melts and glasses. *Amer. Mineral.*, vol. 74, p. 1247-1257.

Taran, Y. A., Pokrovsky, B. G. and Esikov, A. D. (1988) Deuterium and oxygen-18 in fumarolic steam and amphiboles from some Kamchatka volcanoes: "Andesitic" waters. *Commission on the Chemistry of Volcanic Gases, IAVCEI, Newsletter*, no. 1, p. 15-18.

Taylor, B. E. (1986) Magmatic volatiles: Isotopic variation of C, H, and S. In Valley, J. W., Taylor, H. P., Jr. and O'Neil, J. R. eds., Stable isotopes in high temperature geological processes., *Reviews in Mineralogy, Mineral. Soc. Amer.*, vol. 16, p. 185-225.

———, Eichelberger, J. C. and Westrich, H. R. (1983) Hydrogen isotopic evidence of rhyolitic magma degassing during shallow intrusion and eruption. *Nature*, vol. 306, p. 541-545.

Taylor, H. P., Jr. (1974) The application of oxygen and hydrogen isotope studies to problems of hydrothermal alteration and ore deposition. *Econ. Geol.*, vol. 69, p. 843-883.

Viglino, J. A., Harmon, R. S., Borthwick, J., Nehring, N. L., Motyka, R. J., White, L. D. and Johnston, D. A. (1985) Stable-isotope evidence for a magmatic component in fumarole condensates from Augustine Volcano, Cook Inlet, Alaska, U.S.A. *Chem. Geol.*, vol. 49, p. 141-157.

Rept. Geol. Surv. Japan, No. 279, p. 110-114, 1992

The Geological Setting of Coupled Igneous-Hydrothermal Systems: A Geothermal Perspective

L. J. Patrick MUFFLER

U. S. Geological Survey
MS 910, 345 Middlefield Road, Menlo Park, CA 94025, U.S.A.

Over the past forty years, the understanding of the drilled parts of modern geothermal fields has become quite sophisticated, particularly with the aid of numerical models (e.g., Ingebritsen and Sorey, 1988; Bodvarsson *et al.*, 1990; Lowell, 1991). This strictly geothermal perspective, however, is restricted to the distal end of coupled igneous-hydrothermal systems and thus is limited in its ability to deal with any related igneous rocks and the coupling of igneous and hydrothermal systems. Furthermore, the geothermal perspective is limited by drilling capability, not only because of depth and resultant cost but also because of high temperature, high fluid pressure, and corrosive environments. Finally, even with great future advances in drilling technology, our human perspective of less than 30 years on any active geothermal system will remain just a snapshot in geologic time. Accordingly, modern conceptual models such as those of Hedenquist (1987) have come to reflect geological, geophysical, geochemical and hydrologic constraints from both modern geothermal systems and older mineral deposits in the geologic record. Despite this generalized understanding, however, the nature of the interaction of specific modern geothermal systems with the underlying or adjacent igneous systems is poorly known and usually addressed in a stylized fashion.

There is little question that most high-temperature geothermal systems are associated primarily with igneous systems at plate margins and intra-plate melting anomalies ("hot spots"; Muffler, 1976). Examples at spreading ridges include Krafla and various other systems along the mid-Atlantic ridge in Iceland, and the Salton Sea and Cerro Prieto systems along the landward extension of the East Pacific Rise in the United States and Mexico. Examples at oceanic subduction zones include the geothermal systems in the Philippines and Japan, whereas examples at subduction zones beneath continents include the Lassen hydrothermal system of the Cascade Range. Mid-oceanic melting anomalies are exemplified by Kilauea volcano in Hawaii, and Yellowstone is the preeminent geothermal system over a continental hot spot. In a continental setting, the general association of silicic volcanic rocks with geothermal systems has long been emphasized as a tool for regional geothermal exploration, and attempts have been made to reason from the volume and age of silicic volcanic rocks the amount of heat that might still be stored beneath the volcanic center (Smith and Shaw, 1975).

Studies of the petrology of volcanic centers have given much insight to the general nature of the igneous structure at depth beneath volcanic areas. It is now widely recognized that igneous activity is fundamentally basaltic and that the evolved silicic rocks seen at the surface and as intrusions are the result of complex interaction with the crust. The influence of crustal thickness in the Chilean Andes

Keywords: geothermal, igneous, heat source, intrusions, magma

has been elucidated by Hildreth and Moorbath (1988), who reason from trace-element and isotopic petrology to a zone of melting, assimilation, storage, and homogenization at the base of the crust. Various models, in great part derivative from Hildreth (1981), have been applied to Cascade volcanoes. Some, like those of Donnelly-Nolan (1988) at Medicine Lake and of Bullen and Clynne (1990) at Lassen Peak display a plexus of relatively small feeders and intrusive bodies. Other situations, such as Crater Lake, where over 50 km^3 of andesite and rhyodacite magma was erupted essentially instantaneously ~7000 years B.P. (Bacon, 1983), require that a large, single magma chamber exist, at least for short periods of time. And certainly the geologic record documents that igneous bodies of batholithic size have existed often in the earth's upper crust.

Various geophysical techniques have identified anomalies that can reasonably be interpreted to be caused by intrusive rocks beneath geothermal areas. Aeromagnetic data in the Salton Sea geothermal system clearly delineate near-surface intrusions of igneous rock (Griscom and Muffler, 1971). The large negative gravity anomaly at The Geysers in northern California has long been interpreted as resulting from the density contrast of a young body of igneous rock with the heavier rocks of the Franciscan Complex (Chapman, 1975). A similar negative gravity anomaly at Larderello has been interpreted in various ways, most convincingly as a body of intrusive rock. Seismic refraction surveys at Larderello have defined a very conspicuous reflector at 3-6 km, interpreted by Batini *et al.* (1985) as "intensely fractured rocks to a thickness of some hundreds of metres, just above and within the top of the Alpine batholiths". Fournier (1991) emphasizes that the fractures in this zone are clogged by hydrothermal minerals, thus allowing separation of a shallower zone of hydrostatic pressure from a deeper zone where pressures are greater than hydrostatic.

Geophysical detection of bodies of still-molten igneous rock in the upper crust has been frustrating and difficult, although a variety of seismic techniques should be able to detect such bodies in modern volcanic areas. Teleseismic P-delay experiments have defined general anomalies at Yellowstone and elsewhere (Iyer, 1988), but the smallest body that can be detected has a diameter approximately equal to the wavelength of the teleseismic signal (6 km). In an attempt to get around this wavelength limitation, Achauer *et al.* (1988) and Evans and Zucca (1988) have carried out experiments at Newberry volcano in Oregon and Medicine Lake volcano in California using explosive sources to produce high-frequency seismic waves that travel steeply upward through the crust to dense arrays of seismographs. After analysis by tomographic methods, in both cases a small low-velocity anomaly at depths of 3-5 km can be interpreted as a possible magma body. A combination of seismic, geodetic, and geologic methods has allowed analysis of the Medicine Lake region in terms of thermal weakening of the crust by mafic intrusions (Dzurisin *et al.*, 1991). Sanders (1984) has inferred bodies of magma under Long Valley, California, from attenuation of S-wave amplitude data from local and regional earthquakes. Perhaps the most successful case history to date, however, is Yellowstone, where a major teleseismic P-delay anomaly correlates well with gravity, magnetics, earthquake hypocenters, and magnetotellurics, all pointing towards magma at shallow depth (Eaton *et al.*, 1975).

Very young igneous rocks have been encountered in several geothermal systems. Indeed, at Namafjall along the mid-Atlantic Ridge in Iceland, basaltic scoria was ejected briefly from a geothermal well on 08 September 1977 (Larsen *et al.*,

1979). Basaltic dikes are injected laterally at very shallow levels both at the Krafla geothermal field in Iceland (Stefansson, 1981) and in the East Rift Zone of Kilauea volcano (Delaney *et al.*, 1990). In both areas, the chemical and physical characteristics of the associated geothermal reservoir are spatially heterogeneous and temporally variable (Armannsson *et al.*, 1982; Thomas, 1987), reflecting the transitory and rapidly changing local thermal regimes. At The Geysers, deep drilling in the heart of the geothermal field has identified a large felsite body of Pleistocene age, interpreted as related to the igneous heat source responsible for the geothermal system (Thompson, 1989). At Larderello, several drillholes at depths of 3-4 km have sampled sporadic granitic dikes with K-Ar and Rb-Sr ages up to 4 Ma cutting the metamorphic basement (Del Moro *et al.*, 1982; Villa *et al.*, 1987; Puxeddu and Villa, 1989; Cavarretta and Puxeddu, 1990), but the granitic batholith commonly inferred to underlie the region has not yet been encountered.

References

Achauer, U., Evans, J. R. and Stauber, D. A. (1988) High-resolution seismic tomography of compressional wave velocity structure at Newberry Volcano, Oregon Cascade Range. *Jour. Geophys. Res.*, vol. 93, p. 10,135-10,147.

Armannsson, H., Gislason, G. and Hauksson, T. (1982) Magmatic gases in well fluids aid the mapping of the flow pattern in a geothermal system. *Geochim. Cosmochim. Acta*, vol. 46, p. 167-178.

Bacon, C. R. (1983) Eruptive history of Mount Mazama and Crater Lake caldera, Cascade Range, U.S.A. *Jour. Volcanol. Geotherm. Res.*, vol. 18, p. 57-115.

Batini, F., Bertini, G., Gianelli, G., Pandeli, E., Puxeddu, M. and Villa, I. M. (1985) Deep structure, age and evolution of the Larderello-Travele geothermal field. *Geotherm. Resources Council Trans.*, vol. 9, part 1, p. 253-259.

Bodvarsson, G. S., Pruess, K., Haukwa, C. and Ojiambo, S. B. (1990) Evaluation of reservoir model predictions for the Olkaria East geothermal field, Kenya. *Geothermics*, vol. 19, p. 399-414.

Bullen, T. D. and Clynne, M. A. (1990) Trace element and isotopic constraints on magmatic evolution at Lassen volcanic center. *Jour. Geophys. Res.*, vol. 95, p. 19,671-19,691.

Cavarretta, G. and Puxeddu, M. (1990) Schorl-dravite-ferridravite tourmalines deposited by hydrothermal magmatic fluids during early evolution of the Larderello geothermal field, Italy. *Econ. Geol.*, vol. 85, p. 1236-1251.

Chapman, R. H. (1975) Geophysical study of the Clear Lake region, California. *Calif. Div. Mines Geol., Spec. Rept.*, no. 116, p. 23.

Delaney, P., Fiske, R. S., Miklius, A., Okamura, A. T. and Sato, M. K. (1990) Deep magma body beneath the summit and rift zones of Kilauea Volcano, Hawaii. *Science*, vol. 247, p. 1311-1316.

Del Moro, A., Puxeddu, M., Radicati di Brozolo, F. and Villa, I. M. (1982) Rb-Sr and K-Ar ages on minerals at temperatures of 300°-400°C from deep wells in the Larderello geothermal field (Italy). *Contrib. Mineral. Petrol.*, vol. 81, p. 340-349.

Donnelly-Nolan, J. M. (1988) A magmatic model of Medicine Lake volcano, California. *Jour. Geophys. Res.*, vol. 93, p. 4412-4420.

Dzurisin, D., Donnelly-Nolan, J. M., Evans, J. R. and Walter, S. R. (1991) Crustal subsidence, seismicity, and structure near Medicine Lake volcano, California. *Jour. Geophys. Res.*, vol. 96, p. 16,319-16,333.

Eaton, G. P., Christiansen, R. L., Iyer, H. M., Pitt, A. M., Mabey, D. R., Blank, Jr., R. H., Zietz, I. and Gettings, M. E. (1975) Magma beneath Yellowstone National Park. *Science*, vol. 188, p. 787-796.

Evans, J. R. and Zucca, J. J. (1988) Active high-resolution seismic tomography of compressional wave velocity and attenuation structure at Medicine Lake volcano, Northern California Cascade Range. *Jour. Geophys. Res.*, vol. 93, p. 15,016-15,036.

Fournier, R. O. (1991) The transition from hydrostatic to greater than hydrostatic fluid pressure in presently active continental hydrothermal systems in crystalline rock. *Geophys. Res. Lett.*, vol. 18, p. 955-958.

Griscom, A. and Muffler, L. J. P. (1971) Aeromagnetic map and interpretation of the Salton Sea geothermal field, California. *U.S. Geol. Surv. Geophys. Invest. Map* GP-754, scale 1:62,500.

Hedenquist, J. W. (1987) Mineralization associated with volcanic-related hydrothermal systems in the Circum-Pacific basin. *Fourth Circum-Pacific Energy and Mineral Resources Conf. Trans.*, p. 513-524.

Hildreth, W. (1981) Gradients in silicic magma chambers: implications for lithospheric magmatism. *Jour. Geophys. Res.*, vol. 86, p. 10,153-10,192.

——— and Moorbath, S. (1988) Crustal contributions to arc magmatism in the Andes of central Chile. *Contrib. Mineral. Petrol.*, vol. 98, p. 455-489.

Ingebritsen, S. E. and Sorey, M. L. (1988) Vapor-dominated zones within hydrothermal systems: evolution and natural state. *Jour. Geophys. Res.*, vol. 93, p. 13,635-13,655.

Iyer, H. M. (1988) Seismological detection and delineation of magma chambers beneath intraplate volcanic centers in western U.S.A. In King, C.-Y. and Scarpa, R. eds., Modeling of Volcanic Processes., Friedr. Vieweg & Sohn, Braunschweig/Wiesbaden, Germany, p. 1-56.

Larsen, G., Gronvold, K. and Thorarinsson, S. (1979) Volcanic eruption through a geothermal borehole at Namafjall, Iceland. *Nature*, vol. 278, p. 707-710.

Lowell, R. P. (1991) Modeling continental and submarine hydrothermal systems. *Rev. Geophys.*, vol. 29, no. 3, p. 457-476.

Muffler, L. J. P. (1976) Tectonic and hydrologic control of the nature and distribution of geothermal resources. *Proc. Second United Nations Symp. Develop. and Use of Geothermal Resources*, San Francisco, 1975, vol. 1, p. 499-507.

Puxeddu, M. and Villa, I. M. (1989) Larderello revisited: new data uphold the 4 Ma age (abs). *New Mexico Bureau of Mines and Mineral Resources, Bulletin* 131, p. 199.

Sanders, C. O. (1984) Location and configuration of magma bodies beneath Long Valley, California determined from anomalous earthquake signals. *Jour. Geophys. Res.*, vol. 89, p. 8287-8302.

Smith, R. L. and Shaw, H. R. (1975) Igneous-related geothermal systems. In White, D. E. and Williams, D. L. eds., Assessment of geothermal resources of the United States--1975. *U.S. Geol. Surv. Circ.* 726, p. 58-83.

Stefansson, V. (1981) The Krafla geothermal field, northeast Iceland. In Rybach, L. and Muffler, L. J. P. eds., Geothermal Systems: Principles and Case

Histories, John Wiley & Sons, p. 273-294.

Thomas, D. (1987) A geochemical model of the Kilauea east rift zone. In Decker, R. W., Wright, T. L. and Staufer, P. H. eds., Volcanism in Hawaii, *U. S. Geol. Surv. Prof. Pap.* 1350, p. 1507-1525.

Thompson, R. C. (1989) Structural stratigraphy and intrusive rocks at The Geysers geothermal field. *Geotherm. Resources Council Trans.*, vol. 13, p. 481-485.

Villa, I., Gianelli, G., Puxeddu, M., Bertini, G. and Pandelli, E. (1987) Granitic dykes of 3.8 Ma age from a 3.5 km deep geothermal well at Larderello (Italy). *Proc. Conf. Granites and Their Surroundings, Verbania (Italy)*, 28 September-3 October, 1987, Ricerca Scientifica ed Educazione Permanente, Universita di Milano, Supplemento, no. 59, p. 163-164.

Rept. Geol. Surv. Japan, No. 279, p. 115-120, 1992

Compositional Zoning and the Genesis of Pegmatite Garnet: A Product of Final Stage Crystallization of Granitic Magma

Takanori NAKANO and Yukiko NISHIYAMA

Institute of Geoscience, University of Tsukuba
Tennoudai, Tsukuba, Ibaraki 305, Japan

Introduction

Spessartine-almandine garnet is a major accessory mineral in metamorphic rocks as well as in aluminous granite or pegmatite. Compositional growth zoning of metamorphic garnet has been studied extensively, since it records well the metamorphic event. The bell-shaped rim to rim profile of Mn in metamorphic garnets has been called normal zoning, and ascribed to an increase of temperature of metamorphism during garnet growth. However, Leake (1967) found a similar normal zoning pattern of Mn in garnet from a granitic pegmatite in France. This finding suggests that normal zoning of Mn in garnet could be formed during the crystallization of pegmatitic magma, presumably in accordance with a falling temperature. In addition to major elements of Mn and Fe, compositional zoning of minor elements such as Ca and Mg has also been reported for garnets in metamorphic (Banno and Kurata, 1972) and granitic rocks (Leake, 1967). A quantitative model to explain the compositional pattern of pegmatite garnet with respect to multiple elements would therefore provide valuable information on the crystallization of granitic magma and the internal differentiation process of pegmatite, and by extension, on the metamorphic process. However, no detailed compositional pattern of garnet from a granitic pegmatite has been reported subsequent to the study by Leake. Furthermore, a quantitative multi-element model of pegmatite garnet has yet been presented. The lack of such a model is probably due to the complexity resulting from a large number of factors (i.e., magma composition, partition coefficient of elements between garnet and granitic melt, growth rate of garnet and associated mineral chemistry, etc.) which may affect the compositional pattern of granitic garnet. In this paper, we describe the compositional pattern of garnets from granitic pegmatites in the Ishikawa and Yamanoo area, northeastern Japan. The compositional patterns are subsequently analysed by a model incorporating the factors mentioned above.

Sample description

Garnets analysed in this study were collected from the feldspar zone in the Ishikawayama mine and from the muscovite-feldspar-quartz zone in the Yamanoo pegmatite, northeastern Japan. The grain size of two garnets from the Ishikawayama mine (termed hereafter as I-1 and I-2) is 7 mm and 1 cm, respectively, while that of the Yamonoo garnet (Y-1) is 1 cm. They display a well preserved 24-faced crystal form. Although all garnet crystals have some internal cracks, they are optically isotropic. The Ishikawayama garnets contain no mineral inclusions whereas the Yamanoo garnet contains muscovites in the core. In order to elucidate the elemental

Keywords: pegmatite, garnet, compositional zoning, crystallization, partitioning

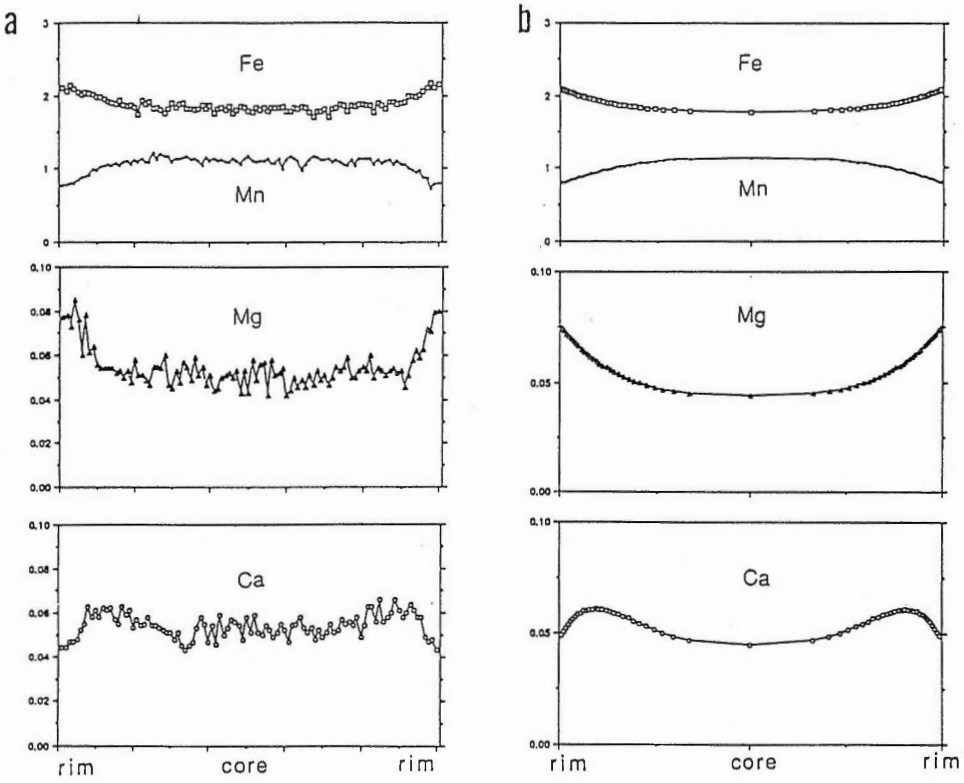

Fig. 1 Comparison of rim to rim compositional profile of garnet I-1 (left) with calculated profile (right).

distribution pattern in the garnet crystal, polished thin sections were made for the garnets, each of which was cut through the crystal center.

Garnet composition

Figures 1, 2 and 3 represent rim to rim compositional profiles for garnet grains I-1 and I-2 and Y-1, respectively. In these figures, the numbers on the vertical axis denote values of each cation assuming 12 oxygens total. Of the cations, Mn and Fe are dominant whereas Ca, Mg and Y are minor. As the Al contents are virtually constant over a narrow range of 1.99-2.02, the andradite components can be neglected. Thus the pegmatite garnet chemistry can be expressed as a mixture of almandine-spessartine-grossular-pyrope component.

Figures 1 to 3 indicate that individual garnets show a different compositional pattern and concentration with respect to the four cations (Fe, Mn, Ca and Mg). Garnet I-2 does not display any distinct compositional zoning, whereas other garnets show a systematic compositional trend from core to rim. The latter garnets have a tendency to increase in Fe content and decrease in Mn content, from core to rim. This depletion pattern in Mn content is rather consistent with previous studies of metamorphic garnets. Despite trace contents, it is also conspicuous that all compositionally-zoned garnets have a tendency to increase monotonically in Mg content

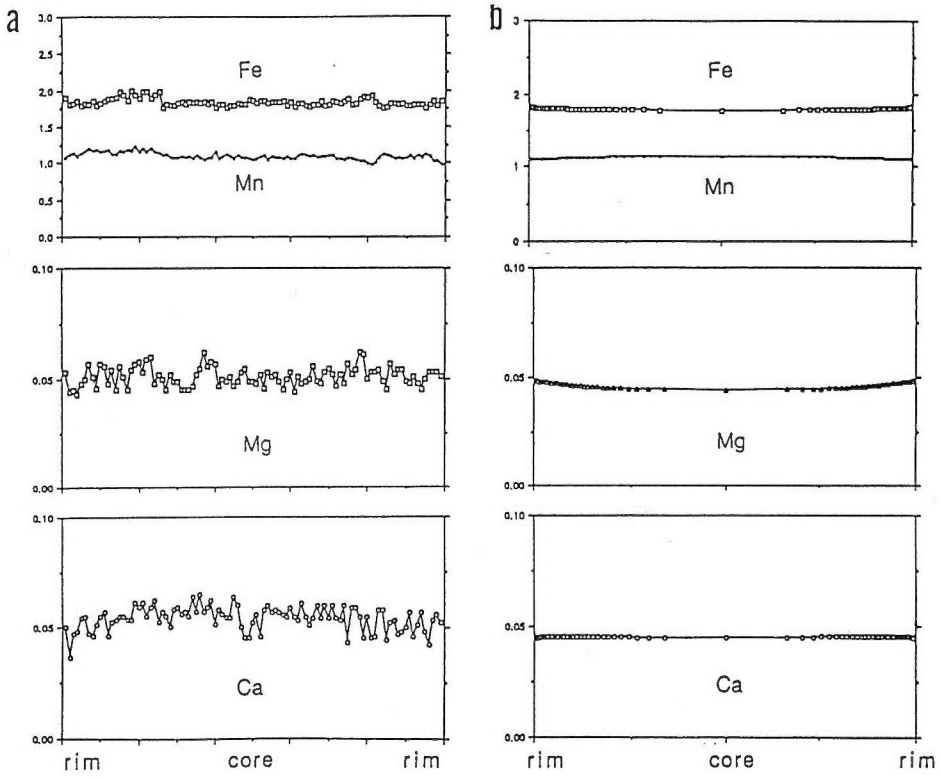

Fig. 2 Comparison of rim to rim compositional profile of garnet I-2 (left) with calculated profile (right).

from core to rim. The most characteristic feature is the compositional pattern of Ca in garnet. Garnet I-1 tends to increase in Ca content from core to margin and then to decrease again at the rim. This Ca compositional pattern, with a peak between core and rim, has also been noted for some metamorphic garnets (Banno and Kurata, 1972) and pegmatite garnets (Leake, 1967), indicating that the pattern is not accidental.

Model for garnet crystallization

(1) Partition coefficient between garnet and granitic melt

The following exchange reaction of cations between garnet and granitic melt was assumed. Considering of garnet that the 8-coordinated site is entirely occupied by cations Fe, Mn, Mg and Ca, the reaction may be expressed as follows:

$$Mn_3Al_2Si_3O_{12}gar + Fe^{2+}Al_2Si_3O_{12}melt = Fe^{2+}Al_2Si_3O_{12}gar + Mn_3Al_2Si_3O_{12}melt$$
$$Mg_3Al_2Si_3O_{12}gar + Fe^{2+}Al_2Si_3O_{12}melt = Fe^{2+}Al_2Si_3O_{12}gar + Mg_3Al_2Si_3O_{12}melt$$
$$Ca_3Al_2Si_3O_{12}gar + Fe^{2+}Al_2Si_3O_{12}melt = Fe^{2+}Al_2Si_3O_{12}gar + Ca_3Al_2Si_3O_{12}melt$$

where gar and melt denote garnet and melt phase, respectively. These relations are given by:

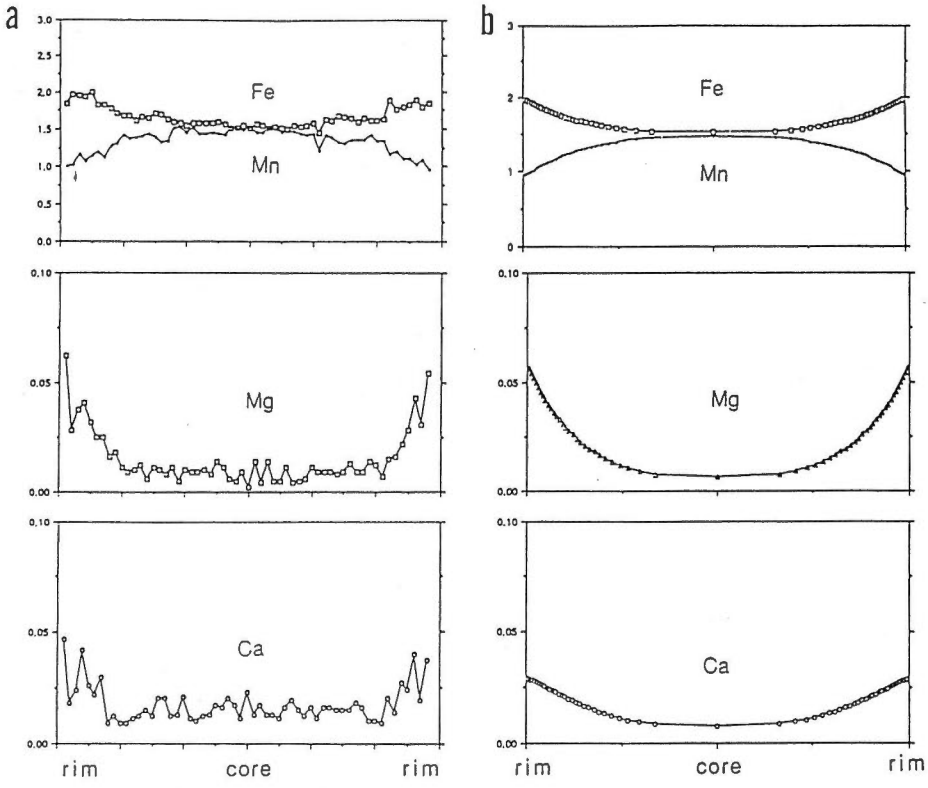

Fig. 3 Comparison of rim to rim compositional profile of garnet Y-1 (left) with calculated profile (right).

$$(Mn/Fe)\ gar = K1 \times (Mn/Fe)\ melt \quad (1)$$
$$(Mg/Fe)\ gar = K2 \times (Mg/Fe)\ melt \quad (2)$$
$$(Ca/Fe)\ gar = K3 \times (Ca/Fe)\ melt \quad (3)$$

where K1, K2 and K3 are partition coefficients which are variable, primarily dependent on temperature. Although values of K1, K2 and K3 are not experimentally determined, it is possible from these equations to calculate the proportion of Fe, Mn, Mg and Ca in the garnet which was in equilibrium with a granitic melt of a given composition. The value of partition coefficients should be variable if garnets grow as the temperature falls. It is assumed in the calculation that the concentration of cations Fe, Mn, Mg and Ca in the melt phase was homogeneous throughout a whole stage of garnet crystallization, and the diffusion rate of those cations in garnet was slow enough to preserve the growth record of garnet (Hollister, 1966).

(2) Initial melt composition

The pegmatitic melt composition from which the garnet crystallized is difficult to determine. Cerny (1982), however, reported that bulk composition of granitic pegmatite magma is almost identical to that of associated granitic rocks. Hence it is assumed in this study that the composition of garnet-forming pegmatite

Table 1. Initial and boundary condition to calculate compositional profiles of the Ishikawayama and Yamanoo pegmatitic garnets

Garnet		I-1	I-2	Y-1
Mass ratio of crystallized garnet	R	0.10%	0.03%	0.10%
Melt composition (ppm)	Fe	15049	15049	23435
	Mn	787	787	757
	Mg	2333	2333	4265
	Ca	10882	10882	13753
Partition coefficient	Mn/Fe	12→8	12→11	30→18
	Mg/Fe	0.07→0.10	0.07→0.08	0.01→0.07
	Ca/Fe	0.03→0.07	0.03→0.03	0.006→0.03
Ca concentration of other minerals (ppm)		7500	2000	5000

Calculation was made by simplifying garnet as a sphere.
Partition coefficients vary linearly with the growth of garnet from the initial value at which the garnet begins to crystallize to the final value at which the garnet is completely crystallized.

melt is given by its associated granitic rocks (young biotite granodiorite for Ishikawayama garnets and the Yamanoo granodiorite for Yamanoo garnets).

(3) Proportion of garnet crystallized from pegmatitic magma

Garnet composition is affected by the proportion of garnet which crystallized from granitic melt within a given mass. The proportion of amounts of crystallizing garnet to the initial pegmatitic mass (given by R) was considered as an independent factor in the calculation.

(4) Composition of minerals accompanying garnet

Effect by other solid phases coprecipitated with garnets from the granitic melt may also have been an important factor. Major associated minerals with the garnet are K-feldspar, quartz and muscovite. As these minerals contain trace content of Fe, Mn and Mg, the Fe, Mn and Mg content in the garnet may have not been significantly affected by the solidification of these minerals. Feldspars are composed of K-feldspar and plagioclase ($An_{1\text{-}6}$). As they contain minor Ca, the Ca content in garnet is affected by solidification of feldspars.

Results and discussion

Calculations were made for each garnet by considering the factors mentioned above. The result of calculation is illustrated in Figures 1 to 3, and compared with raw compositional data. The calculation result provides a good simulation of the compositional pattern of three pegmatite garnets. Table 1 shows the values of factors used for the calculation.

It is assumed in the calculation that the Ca content in the solids co-crystallizing with garnet is different between the two Ishikawayama garnet grains, 7000 ppm for crystal I-1 and 2000 ppm for crystal I-2, respectively. These values are reasonable when taking the local variation of Ca content in the pegmatite zone into account. Other important factors to simulate the different compositional patterns in the Ishikawayama garnets are R values and the variation of the partition coefficients. Variation of partition coefficients is larger for the zoned garnet I-1 than for

the unzoned garnet I-2. As the partition coefficients are strongly affected by temperature, a large variation in the partition coefficients infers that a large temperature change occurred during the garnet growth, most likely a falling temperature. In the case of the crystal I-2, a small change in the partition coefficients suggests that this garnet formed under constant temperature conditions. This indicates that garnet I-2 grew faster than garnet I-1, considering that garnet I-2 is larger in size than crystal I-1. A smaller value of R for garnet I-2 than for garnet I-1 suggests that garnet I-2 was enclosed in the feldspar zone more rapidly than garnet I-1. It is likely that the growth rate varied locally in coarse-grained pegmatite minerals. The R value corresponds to the volume ratio of the garnet in the feldspar zone. This value is a measureable parameter, although it is not determined here due to the local distribution of garnet and field conditions. However, values of R from 0.03 to 0.1 % are qualitatively reasonable.

The conditions and values of factors for forming the Yamanoo garnet are slightly different from those for the Ishikawayama garnets, except for R value and the concentration of Ca removed by minerals accompanying the garnet. The major difference is the initial composition of granitic melt, especially for Fe and Mg concentration, and the partition coefficients. As the partition coefficient is a function of temperature, the temperature condition may have differed between the Ishikawayama and Yamanoo pegmatites.

This study demonstrates that falling temperature of pegmatite magma is necessary to form a compositionally-zoned garnet. The growth rate of associated pegmatite minerals and local variation of pegmatite magma composition would have produced various compositional patterns of the pegmatite garnet even within a single zone.

References

Banno, S., and Kurata, H. (1972) Distribution of Ca in zoned garnet of low-grade pelitic schists. *Jour. Geol. Soc. Japan.*, vol. 78, p. 507-512.

Cerny, P. (1982) Petrogenesis of granitic pegmatites. In Cerny, P. ed. Short course in granitic pegmatites in science and industry. *Mineral. Assoc. Canada Short Course Handbook*, vol. 8, p. 405-462.

Hollister, L. S. (1966) Garnet zoning: An interpretation based on the Rayleigh fractionation model. *Science*, vol. 154, p. 1147-1151.

Leake, B. E. (1967) Zoned garnets from the Galway granite and its aplites. *Earth Planet. Sci. Lett.*, vol. 3, p. 311-316.

Rept. Geol. Surv. Japan, No. 279, p. 121-126, 1992

Pyroxene Composition as an Indicator to Classify Magmatic-hydrothermal Skarn Deposits

Takanori NAKANO[1], Takashi YOSHINO[2], Hidehiko SHIMAZAKI[3] and Masaaki SHIMIZU[4]

[1] *Institute of Geoscience, University of Tsukuba, Tennoudai, Tsukuba, Ibaraki 305, Japan*
[2] *Institute of Applied Physics, University of Tsukuba, Tennoudai, Tsukuba, Ibaraki 305, Japan*
[3] *Geological Institute, Faculty of Science, University of Tokyo, Hongo, Tokyo 113, Japan*
[4] *University Museum, University of Tokyo, Hongo, Tokyo 113, Japan*

Introduction

Skarn deposits vary regionally in metal compositions and other geochemical characteristics. Einaudi and Burt (1982) noted that the chemical composition of pyroxenes in skarn deposits is variable, depending on the dominant economic metal, and thereby has potential as a metallogenetic indicator. However, more comprehensive analytical data for skarn pyroxenes are necessary to confirm the validity of the suggestion of Einaudi and Burt, since their classification is based on mineral chemistry data from only fifteen skarn deposits.

Skarn deposits in Japan are suitable for the study of skarn metallogenesis, since there are a large number of various skarn deposits located in the country. In addition, geological and geochemical information have been gathered on these deposits over the recent decade by Shimazaki and his coworkers (e.g., Shimazaki, 1980, 1986; Shimazaki and Shimizu, 1984; Nakano *et al.*, 1990). In addition to the major elements of Mg, Mn and Fe, skarn pyroxenes contain other minor or trace elements such as Na and Al. Recently Nakano *et al.* (1991) have shown that mafic silicates contain Zn at a sufficient concentration level (>50 ppm) to allow its measurement by EPMA. Their preliminary data indicate the presence of some meaningful relationships between the Zn content of skarn pyroxene and the metal-type. This EPMA analytical study was attempted to elucidate the variability of pyroxene in skarns and its usefulness in characterizing skarn metallogenesis.

Results and Discussions

(1) Mg, Mn, Fe ratio of pyroxene

Previous EPMA studies have revealed that the Mg:Mn:Fe proportion varies widely in a single deposit, dependent on the mineral assemblage and the protolith composition (e.g., Morgan, 1975; Einaudi, 1977). However, some systematic relation seems to exist in the pyroxene from several deposits. Figure 1A illustrates a ternary Mg-Mn-Fe proportion of pyroxenes from the Kamaishi Cu-Fe and Yaguki W-Cu mine. It is notable that the Fe and Mg content (in other words Mg/Fe ratio) of pyroxenes are significantly variable, whereas their Mn/Fe ratios lie within a relatively restricted range for each mine. Figure 1B shows a ternary plot of pyroxene compositions from the Nakatatsu Pb-Zn mine with data taken from Yamada (1989) and Shimizu and Iiyama (1982). Although the Mg/Fe ratio of Nakatatsu pyroxenes diverges from 0 to nearly infinity on the ternary diagram, a majority of the Mn/Fe

Keywords: skarn metallogenesis, pyroxene, Mn/Fe ratio, Zn content

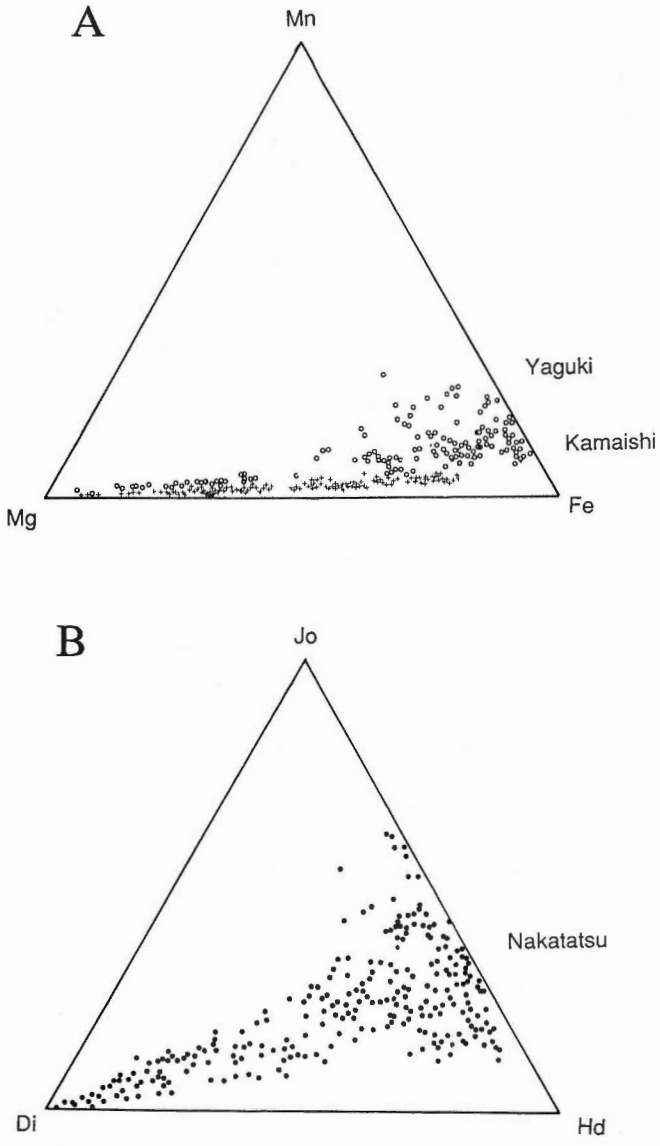

Fig. 1 Mg-Mn-Fe (or diopside(Di)-johannsenite(Jo)-hedenbergite(Hd)) relation of pyroxenes in skarn deposits from the Kamaishi Cu-Fe and Yaguki W-Cu mine (A) and from the Nakatatsu mine (B), taken from Yamada (1989) and Shimizu and Iiyama (1984).

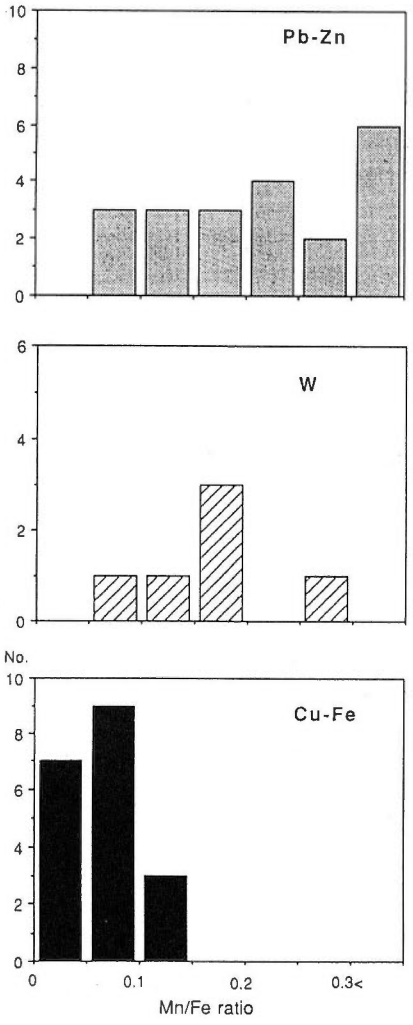

Fig. 2 Histogram of mean Mn/Fe ratio of pyroxenes for each class of deposit.

ratios have more restricted values over a range of 0.25-1.5. The mean Mn/Fe ratio of pyroxenes for each deposit is shown in Figure 2. It is evident from this figure that the Mn/Fe ratio of pyroxenes in the Cu-Fe deposits is lower (<0.1) than in the Pb-Zn deposits (>0.1); pyroxenes in W deposits have an intermediate Mn/Fe ratio (0.1-0.3) between both other types. These data thus strongly support the proposition of Einaudi and Burt (1982) that pyroxenes with high a johannsenite component, or pyroxenes with high Mn/Fe ratio in our expression, occur mostly in Pb-Zn deposits.

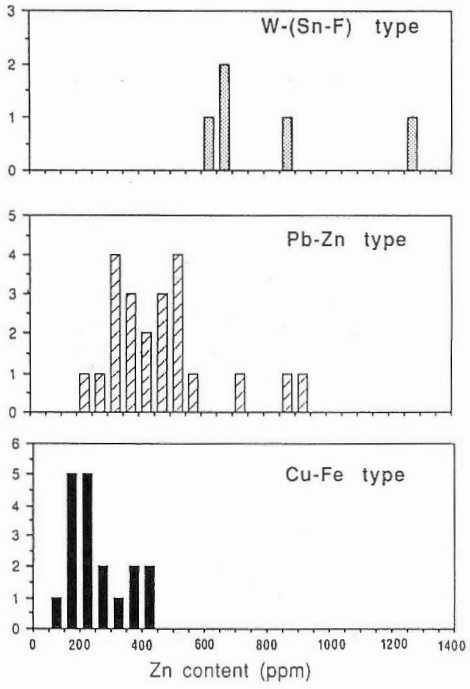

Fig. 3 Histogram of mean Zn content of pyroxenes for three skarn types (Cu-Fe, Pb-Zn and W-Sn-F).

(2) Zn content of pyroxene

Pyroxenes in contact with sphalerites have a zone enriched in Zn along the boundary with the sphalerite. Textural analysis and compositional mapping data indicate that the Zn enrichment zone probably formed after sphalerite growth through an influx of Zn from the sphalerite into the pyroxene. Zn is heterogeneously distributed in pyroxene grains away from the sphalerite, suggesting that such Zn was incorporated into the pyroxene during its growth. The width of the Zn zone is less than 100 μm as far as we could determine. In order to avoid such secondary alteration by sphalerites, Zn analysis of skarn pyroxenes was done at points at least 200 μm from a boundary with sphalerite.

The Zn content of pyroxene varies regionally. The pattern of variation is related to the metal type (Fig. 3). The Zn content of skarn pyroxene in Cu-Fe type deposits (50-450 ppm; mostly <200 ppm) is lower than in Pb-Zn type deposits (150-500 ppm; mostly >200 ppm). It is high but variable in W type deposits; pyroxenes of six W-Sn-F type deposits (Kagata, Kasugayama, Kuga, Fujigatani, Kiwada and Ishida mine) contain a high Zn content, above 500 ppm, while those of two W-Cu type skarn deposits (Yaguki and Yamaguchi mine) contain low Zn content of 171 and 302 ppm, respectively. This tendency is qualitatively consistent with the classification based on the Sr isotopic data of skarns (Nakano *et al.*, 1990).

Shimazaki and Shimizu (1984) analysed FeS, MnS and CdS content of sphalerites from skarn deposits in Japan. They showed that CdS content of sphalerites is relatively constant throughout an individual skarn deposit, allowing them to assume that the activity ratio, a_{Cd}/a_{Zn}, in the ore-forming fluids was nearly constant for each

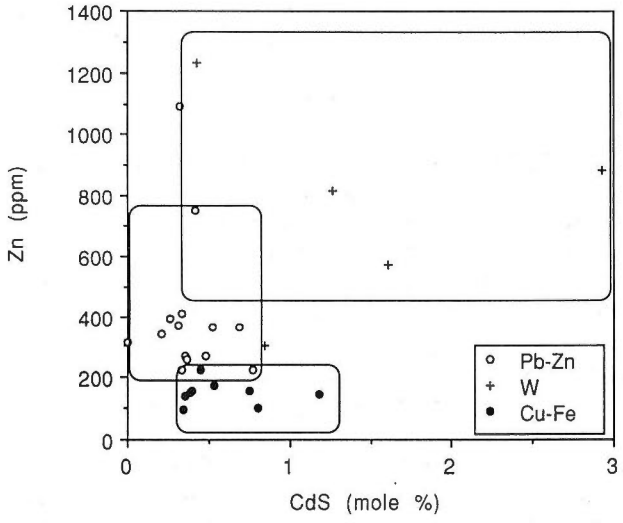

Fig. 4 Relation between mean Zn content of pyroxene and CdS content of sphalerite for each skarn type.

deposit, probably due to the similar geochemical behavior of Zn and Cd. They reported that sphalerites in the W-Sn-F type contain a high CdS content (1 mole %) compared to sphalerites in other type deposits (<1 mole %). Analysis of data from Shimazaki indicates that the sphalerite composition tends to vary in accordance with the metal type, as classified in this study. Figure 4 shows the relation between the CdS content of sphalerites and the Zn content of pyroxene in Japanese skarn deposits, indicating that each class occupies a distinct region in this figure. A high Zn content of pyroxenes and a high CdS content of sphalerites seems to be a diagnostic feature of the W-Sn-F type deposits.

Summary

The chemical compositions of pyroxenes from forty-six skarn deposits in Japan were statistically examined by compiling published data and newly analysed data in order to put constraints on the skarn metallogeny. Pyroxenes along the contact with sphalerite have a concentration halo enriched in Zn about 100 μm in width, which was probably formed by influx of Zn from the sphalerite into the pyroxene. Sphalerite-bearing pyroxenes excluding such a Zn halo have similar Zn contents to ummineralized pyroxenes. The Mn/Fe ratio and Zn content of pyroxenes in a single deposit are relatively constant, and tend to vary regionally in accordance with the metal type. Most pyroxenes in the Cu-Fe deposits are characterized by a low Mn/Fe ratio (<0.1) and low Zn content (<200 ppm), whereas those in the Pb-Zn deposits have a high Mn/Fe ratio (>0.2) and high Zn content (>200 ppm). Pyroxenes in W type deposits have an intermediate Mn/Fe ratio (around 0.15) between the two types, and a very high Zn content, especially of the W-Sn-F deposits (>500 ppm). The systematic relation between pyroxene composition and metal type seems to extend to the Mn and Cd content of skarn sphalerites as well (Shimazaki and Shimizu, 1984). The Mn/Fe ratio and Zn content of skarn pyroxene, together with the Mn/Fe ratio and Cd

content of sphalerite, can serve as an additional aid in skarn classification and in defining environments of their formation.

References

Einaudi, M. T. (1977) Petrogenesis of the copper-bearing skarn at the Mason valley mine, Yerington district. *Econ. Geol.*, vol. 72, p. 764-783.

——— and Burt, D. M. (1982) Introduction, terminology, classification and composition of skarn deposits. *Econ. Geol.*, vol. 77, p. 745-753.

Morgan, B. A. (1975) Mineralogy and origin of skarns in the Mount Morrison pendent, Sierra Nevada, California. *Amer. Jour. Sci.*, vol. 275, p. 119-142.

Nakano, T., Shimazaki, H. and Shimizu, M. (1990) Strontium isotope systematics and metallogenesis of skarn deposits in Japan. *Econ. Geol.*, vol. 85, p. 794-815.

———, Yoshino, T. and Nishida, N. (1991) Rapid analytical method for trace Zn contents in some mafic minerals using the electron microprobe: potential utility as a metallogenetic and petrogenetic indicator. *Chem. Geol.*, vol. 89, p. 379-389.

Shimazaki, H. (1980) Characteristics of skarn deposits and related acid magmatism in Japan. *Econ. Geol.*, vol. 75, p. 173-183.

——— (1986) Regional variation of isotopic composition of hydrothermal ore sulfur in Japan. *Jour. Fac. Sci., Univ. Tokyo*, Sec, II, vol. 21, p. 81-100.

——— and Shimizu, M. (1984) Compositional variation of sphalerites from skarn deposits in Japan. *Jour. Fac. Sci., Univ. Tokyo*, Sec. II., vol. 21, p. 1-37.

Shimizu, M. and Iiyama, J. (1982) Zinc-lead skarn deposits of Nakatatsu mine, central Japan. *Econ. Geol.*, vol. 77, p. 1000-1012.

Yamada, K. (1989) Skarn forming process at the Senno deposit, Nakatatsu mine, central Japan. *Jour. Fac. Sci., Univ. Tokyo*, Sec. II, vol. 22, p. 11-37.

Rept. Geol. Surv. Japan, No. 279, p. 127-130, 1992

Composition of Fluids Related to Ok Tedi Mineralization, Papua New Guinea

Munetomo NEDACHI

Department of Geology, College of Liberal Arts, Kagoshima University
Kagoshima, 890 Japan

The Ok Tedi ore deposit is an epicontinental porphyry copper system in Papua New Guinea. Chivas *et al.* (1984) estimated the isotopic composition of fluid from hydrothermal biotite, with the fluid having a magmatic signature; $\delta^{18}O$=+9.2 and δD=-57. They considered that the ore fluid emanated from a magma, and gold and copper minerals precipitated due to mixing with meteoric water. Nedachi *et al.* (1990b) conducted a preliminary study of the chemical composition of fluid inclusions in quartz coexisting with biotite and apatite from the deposit. In the present study, fluid inclusions were semi-quantitatively analyzed by two means; microanalysis of unopened inclusions hosted by quartz, and analysis of materials left on the surface of quartz after inclusion decrepitation and subsequent fluid evaporation. The chemical features are discussed for the fluid emanated from the magma.

Geology, igneous activity and mineralization

The Ok Tedi ore deposit is located in a continental platform of the Australian Plate near the New Guinea Mobile Belt. The basement is composed of Paleozoic metamorphic rocks and granites. Mesozoic to Cenozoic shelf sediments unconformably cover the basement, and are intruded by the Upper Miocene to Pleistocene Ok Tedi complex.

The Ok Tedi complex is of calc-alkaline rock series, and is characterized by enrichment of incompatible elements; K, Rb, F and light REE, in contrast to other porphyry copper deposits in the island arc system (Arnold and Griffin, 1978; Nedachi *et al.*, 1991). The complex might be of continental crust origin or highly contaminated with crustal materials. In the mine area, the Ok Tedi complex is mainly composed of two intrusive bodies; Sydney monzodiorite and Fubilan monzonite porphyry. Skarn development is associated with the Ok Tedi complex. Phlogopite dissemination, phlogopite-quartz-apatite veining, Cu mineralization and argillic alteration are distinct in the Fubilan monzonite porphyry. Late stage quartz veining and silicification are very intense in the center of the Fubilan monzonite porphyry ("Quartz Core"). The Fubilan monzonite porphyry is genetically related to mineralization.

Hydrous minerals suggest a high fugacity ratio of HCl to H_2O, and its increase during the solidification of hydrous magma and the early hydrothermal stage (Nedachi *et al.*, 1991), which are essential features of the Ok Tedi mineralization, as recognized elsewhere in Papua New Guinea (e.g., Nedachi *et al.*, 1990a).

Keywords: Ok Tedi, porphyry copper deposit, fluid inclusion analysis, electron probe microanalyser

Occurrence of fluid inclusions

Quartz in the "Quartz Core" in the Fubilan monzonite porphyry contains occasional fluid inclusions, which consist mainly of three phases; vapor, liquid and halite.

On the other hand, numerous fluid inclusions are observed in quartz in the hydrothermal phlogopite-quartz-apatite veins in the Fubilan monzonite porphyry. Although some are vapor-rich, other fluid inclusions are multiphase, suggestive of fluid boiling. The multiphase fluid inclusions are mainly composed of vapor, liquid, halite and sylvite. In some fluid inclusions, anhydrite, fluorite, opaque minerals and unidentified phases (Fe-K-Cl phases?; Quan *et al.*, 1987) are also observed. The filling temperature of multiphase fluid inclusions ranges from 380 to 470°C. Neglecting the effect by other components, halite disappearence temperatures indicate that NaCl contents of the fluid range from 27 to 45 wt%, while the KCl contents range from 15 to 40 wt%, which are rather high and possess a large scatter. Fluid compositions do not vary along the halite trend (Cloke and Kesler, 1979). In the "Quartz Core" of the later stage of the Ok Tedi mineralization, sylvite is rare as a daughter mineral in quartz, and biotite does not coexist with the quartz. The precipitation of phlogopite during fluid trapping by the coexisting quartz might be a reason for the wide range of K content observed. The compositions of coexisting phlogopite and apatite (Nedachi *et al.*, 1991), and the $\delta^{18}O$ and δD compositions of the hydrothermal phlogopite (Chivas *et al.*, 1984) suggest that the fluid examined in the present study is magmatic. The K content of the magmatic fluid of the Ok Tedi epicontinental porphyry copper system is significantly higher than that of island arc porphyry copper systems (e.g., Panguna; Eastoe, 1978).

Composition of fluid inclusions by non-destructive analysis

The chemical compositions of the inclusion fluids were non-destructively analysed using electron microanalyzer. With an increasing accelerating voltage, Cl, S, K, Ca, Na, Mn, Fe, Cu, Zn and Ag can be detected from the fluid inclusion near the polished surface of quartz. Many kinds of base metals have been detected in the fluid. Almost all daughter minerals homogenize to the liquid at elevated temperature. Therefore, the original fluid might have been quite rich in base metals. The Maaskant method (Maaskant, 1986) was applied to semi-quantitative analysis of the fluid inclusions. The chemical compositions were calculated from the X-ray intensity by Heinrich's correction. Subtracting H_2O, normalized values of Na content were from 6 to 22 wt%, K from 6 to 15 wt%, Cl from 54 to 74 wt%, Ca from 0.1 to 1.9 wt%, Fe from 2.0 to 21 wt%, Mn from 0.8 to 2.2 wt%, Cu from 0 to 0.2 wt%, and S from 0.1 to 2.4 wt%. It is remarkable that Cl is higher than the calculated value of the combined cations on a molecular equivalent basis. The K/Na atomic ratios range from 0.2 to 0.8, which coincide with those determined from microthermometric measurement.

Composition of precipitate formed after decrepitation

The samples studied were heated up to about 100°C above the homogenization temperature, resulting in the fluid inclusions being destroyed by decrepitation. The homogenized fluid erupted through a crack, and the volatile portion immediately

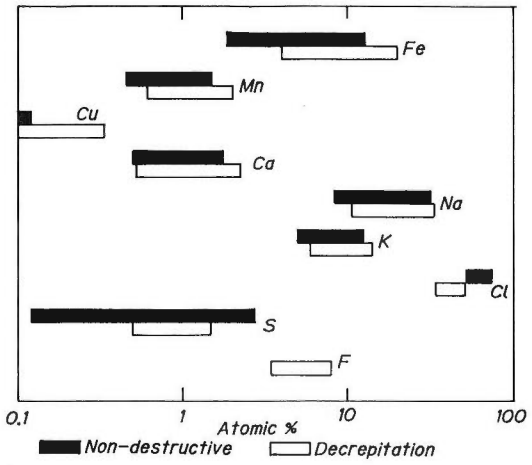

Fig. 1 Compositional range of inclusion fluids, determined by two means.

evaporated while the non-volatiles precipitated on the polished surface of quartz. The bulk chemical compositions of precipitates were semi-quantitatively determined by electron microanalyzer with ordinary ZAF correction. Subtracting SiO_2, the normalized data are compared with those by non-destructive method mentioned above. As shown in Fig. 1, the following features are recognized.

1) The contents of major cations, Na, K, Fe and Ca are almost same between the two methods, indicating that these elements were completely dissolved in the liquid at elevated temperature, removed to the sample surface during decrepitation, and did not evaporate during subsequent treatment.

2) F is detected only from the precipitate on the surface. The absorption of the F Kα line by SiO_2 may be too large to be detected from a fluid inclusion enclosed in quartz, suggesting that the quantitative analysis of light elements in fluid inclusions may be difficult by non-destructive means. Some data for base metals differ slightly between the two methods. In those fluid inclusions, small grains of opaque minerals probably remained after decrepitation.

3) Recalculated anion contents (Cl+F+2S) in the precipitate roughly coincide with the cation values (Na+K+2Fe+2Ca+2Mn+2Cu).

As mentioned above, however, the Cl contents of inclusion fluids analyzed by non-destrucive means are apparently higher than those in the precipitate. The differences between the anions and cations, and the detection of F from precipitate by decrepitation, suggest that the anions combine not only with the estimated cations, but also acids such as HCl might be dissolved in the enclosed fluid inclusions. Up to $n\times10^{-1}$ mole% HCl content is estimated for the fluid.

References

Arnold, G. O. and Griffin, T. J. (1978) Intrusions and porphyry copper prospects of the Star Mountains, Papua New Guinea. *Econ. Geol.*, vol. 73, p. 785-795.

Chivas, A. R., O'Neil, J. R. and Katchan, G. (1984) Uplift and submarine formation of some Melanesian porphyry copper deposits; stable isotope evidence. *Earth Planet. Sci. Lett.*, vol. 68, p. 326-334.

Cloke, P. L. and Kesler, S. E. (1979) The halite trend in hydrothermal solutions. *Econ. Geol.*, vol. 74, p. 1823-1831.

Eastoe, C. J. (1978) A fluid inclusion study of the Panguna porphyry copper deposit, Bougainville, Papua New Guinea. *Econ. Geol.*, vol. 73, p. 703-720.

Maaskant, P. A. (1986) Electron probe microanalysis of unopened fluid inclusions, a semiquantitative approach. *N. Jb. Miner. Mh.*, Jg. 1986, H7, p. 297-304.

Nedachi, M., Enjoji, M., Yamamoto, M., Malagun, S., Taguchi, S., Shiga, Y., Higashi, S. and Manser, W. (1990a) Role of halogen elements on the Panguna porphyry copper mineralization, Bougainville, Papua New Guinea. *South Pacific Study* (Kagoshima Univ.), vol. 11, no. 1, p. 23-36.

———, Shin-yama, T. and Ueno, H. (1990b) Electron probe microanalysis on fluid inclusions in quartz from the Ok Tedi Mine (in Japanese with English abstract). *Sci. Rept. Kagoshima Univ.*, no. 39, p. 41-46.

———, Malagun, S., Yamamoto, M., Taguchi, S., Shiga, Y. and Higashi, S. (1991) Halogen geochemistry in the Ok Tedi porphyry copper system, Papua New Guinea. *South Pacific Study* (Kagoshima Univ.), vol. 11, no. 2, p. 69-81.

Quan, R. A., Cloke, P. L. and Kesler, S. E. (1987) Chemical analyses of halite trend inclusions from the Granisle porphyry copper deposit, British Columbia. *Econ. Geol.*, vol. 82, p. 1912-1930.

Rept. Geol. Surv. Japan, No. 279, p. 131-134, 1992

Synorogenic Hydrogeological Systems in the Canadian Cordillera and their Impact on the Formation of Ores by Igneous Processes

Bruce E. NESBITT

Department of Geology, University of Alberta
Edmonton, Alberta T6G 2E3, Canada

Introduction

Magmas pass through or are emplaced into a hydrodynamically complex middle and upper crust. Results of deep continental drilling and EM studies indicate that this portion of the crust is universally saturated with a liquid or gas phase, usually an aqueous solution. In addition, permeability studies and results from deep drilling indicate that crustal fluid pressures are highly heterogeneous, ranging from hydrostatic to lithostatic. Models of fluid flow associated with igneous intrusions often assume relatively simplistic and temporally invariant hydrogeological characteristics of the host units. Whereas in reality, crustal hydrogeological systems are quite complex and variable with time.

It is the objective of this presentation to characterize some of the variability in the hydrogeologic characteristics of the middle and upper crust and to explore the impact of crustal hydrogeology on the development of ores related to igneous intrusions or extrusions. As will be seen, one answer to the perennial question of why some plutons are mineralized and other, very similar plutons are not, can be found in constraints on mineralization processes exerted by regional hydrogeological factors.

Synorogenic fluid flow in the Canadian Cordillera

The Mesozoic-Cenozoic orogenic event in the Canadian Cordillera encompassed a wide variety of tectonic styles ranging from compression to extension to transpression, offering an opportunity to compare differences in the hydrogeological regimes of different tectonic styles within a single region.

In the Rocky Mountains, a classic, thin-skinned fold and thrust belt involving late Precambrian to Early Tertiary sedimentary rocks developed during the Cretaceous and early Tertiary. Stable isotope studies of Phanerozoic carbonate units and undeformed carbonate veins yield relatively normal $\delta^{13}C$ values of 0 to -2.0 per mil. However, $\delta^{18}O$ values of the same samples indicate that the carbonate units have undergone regionally variable ^{18}O depletion from initial values of approximately 23 per mil (SMOW) to values as low as 14 to 16 per mil. Such widespread and substantial depletion of $\delta^{18}O$ values can only be a product of the massive influx of low $\delta^{18}O$ meteoric water. This is confirmed by δD studies of extracted inclusion fluids.

In the underlying Precambrian units, $\delta^{13}C$ and $\delta^{18}O$ values of vein carbonate are substantially lower ($\delta^{13}C$= -10.0±2.5 per mil, $\delta^{18}O$= +13.3±1.5 per mil), indicating little hydrodynamic interaction between the Phanerozoic and the Precambrian

Keywords: syntectonic fluid regimes, ore formation

units. In addition, δD studies of inclusion fluids indicate that veins in these units formed from two different fluids. An early, metamorphic fluid (δD= -70±18 per mil) formed minor veins in joints and a later fluid of a meteoric origin (δD= -130±16 per mil) formed large, subvertical veins related to postcompression normal faults.

The data from the geochemical studies in the Rockies indicate that at deep levels in compressional environments vertical movements of fluids are inhibited and the fluid regime is dominated by subsurface fluids. At shallower levels, synorogenic influx of surface fluids may have occurred. During post-compression relaxation and normal faulting, surface fluids appear to have penetrated to depths of several kilometers.

The other extreme of tectonic environments in the Cordillera is represented by the Tertiary extensional complex of the southern Omineca. During the Jurassic, this region underwent widespread thrust and nappe development associated with plutonism and high grade metamorphism. During the Eocene, the same region was exposed to an extensional event with associated plutonism, volcanism and metamorphism.

Immediately below the extensional detachment zone, para- and orthogneisses and syndeformation plutons are depleted in ^{18}O relative to primary, whole rock values (Nesbitt and Muehlenbachs, 1989; 1991). Deeper into the footwall, whole rock $\delta^{18}O$ values are undepleted; however, low δD values of micas and amphiboles document the penetration of surface fluids to these levels. Above the zone of detachment, widespread quartz±carbonate veins with moderately high $\delta^{18}O$ values and low δD values document the formation of these veins on the ascending limb of convection cells involving meteoric water. In addition, the Eocene volcanics of the upper plate are locally depleted in ^{18}O, indicating the activity of epithermal circulation cells.

The results from the southern Omineca extensional complex document widespread and deep (at least 10 km) convection of surface fluids during or shortly following deformation. Surface fluids dominated the system to such as extent that little evidence has been found indicating the involvement of magmatic or metamorphic fluids.

The overall results of these studies indicate that tectonic style plays a major role in controlling synorogenic hydrogeological regimes. Compressional environments inhibit vertical fluid movement, either the influx of surface fluids or ascent of subsurface fluids. Vertical fracturing produced in extensional and transcurrent environments facilitates the influx of large volumes of surface fluids. In the following section, the impact of these phenomena on the generation of ores associated with igneous intrusions or extrusions in the Canadian Cordillera will be examined.

Ore formation in British Columbia in relation to Mesozoic and Cenozoic igneous events

Five major tectonic stages characterize the accretionary event in the British Columbian portion of the Canadian Cordillera. Early Jurassic, island arc magmatism preceded terrane collision. Plutonism, volcanism, metamorphism and thrusting characterized the Middle Jurassic collisional event, which formed the Omineca Crystalline Belt. Late Jurassic-Early Cretaceous was a period of uplift, initiation of transcurrent faulting and a lull in magmatism and metamorphism. Plutonism, metamorphism and thrust faulting were common during the Middle Cretaceous col-

lisional event generating the Coast Plutonic Complex. The Late Cretaceous-Eocene witnessed widespread extension and magmatism.

In British Columbia, absolute and relative dating reveals that the generation of significant porphyry Cu±Mo,Au and skarn deposits was restricted to the Early Jurassic and Late Cretaceous-Eocene events (Nesbitt, in press). Both the Middle Jurassic and Middle Cretaceous plutonic events, though widespread and voluminous, are barren of significant porphyry-skarn development. Similarly terrestrial volcanics of the Early Jurassic and Late Cretaceous-Eocene host epithermal Au-Ag, while terrestrial volcanics of the Middle Jurassic and Middle Cretaceous are barren. It appears that the limitations on vertical fluid movement imposed by the compressional-thrusting events of the Middle Jurassic and Middle Cretaceous were sufficient to prevent the deep penetration of meteoric water dominated convection.

The major mesothermal Au deposits of the Omineca were formed between 130 and 140 Ma (Early Cretaceous) during uplift and a lull in magmatic and metamorphic activity. Timing constraints indicate that neither magmatic or metamorphic devolatilizational fluids could have been significantly involved in ore generation. Permeability generated during uplift would facilitate deep convection of surface fluids and permit their involvement in ore generation.

These results indicate that three intervals, Early Jurassic, Late Jurassic-Early Cretaceous, and Late Cretaceous-Eocene were responsible for the formation of the bulk of the epigenetic ores formed during accretion in British Columbia. The Middle Jurassic and Middle Cretaceous collisional events, in spite of widespread, voluminous plutonism and volcanism, were notably lacking in the generation of mineralization. This correlates directly with variations in the crustal hydrogeology of the different regimes and indicates that regional crustal hydrogeology plays a key role in the ability of orogenic events to generate ores.

Case studies of ores associated with plutons and volcanics in the Canadian Cordillera

Isotopic studies of ores associated with igneous bodies in the Canadian Cordillera indicate variable degrees of involvement and importance of magmatic fluids in ore generation. Epithermal style mineralizations have been investigated in Eocene volcanics of southern B.C. and in Paleozoic limestones of the Yukon. In both settings large (10s-100 km^2) zones of whole rock ^{18}O depletion have been noted. The magnitude of these depletion zones, together with low δD values from inclusion fluids, indicates that large scale circulation of surface fluids occurred in these systems. In general, there is little evidence for the involvement of magmatic fluids in these deposits; however, in the Yukon deposits there is some indication from δD data that a small proportion of magmatic fluids was involved.

Studies of deeper porphyry-skarn deposits indicate greater roles for magmatic fluids. The initial results from an ongoing study of Eocene porphyry Cu-Mo mineralization in central B.C. suggest that either magmatic fluids or highly evolved surface fluids were involved in most stages of porphyry development. In the Yukon, studies of skarn mineralization by Bowman *et al.* (1985) indicate high levels of involvement of magmatic fluids with up to 75 % of the ore-forming fluids being composed of putative magmatic fluids.

Conclusions

The results of these studies indicate that regional structural-hydrogeological conditions play a major role in determining whether mineralization will develop in response to the emplacement of a pluton. As our understanding of regional synorogenic hydrogeological regimes improves, we will be simultaneously improving our ability to decipher the role of magmatic fluids in the formation of various types of igneous associated mineralization.

References

Bowman, J. R., Covert, J. J., Clark, A. H. and Mathieson, G. A. (1985) The CanTung E - Zone scheelite skarn orebody, Tungsten, Northwest Territories: Oxygen, hydrogen and carbon isotope studies. *Econ. Geol.*, vol. 80, p. 1872-1896.

Nesbitt, B. E. (in press) Orogeny, crustal hydrogeology and the generation of epigenetic ore deposits in the Canadian Cordillera. *Mineral. and Petrol.*, 35p.

——— and Muehlenbachs, K. (1991) Stable isotopic constraints on the nature of the syntectonic fluid regime of the Canadian Cordillera. *Geoph. Res. Lett.*, vol. 18, p. 963-966.

——— and ——— (1989) Origins and movement of fluids during deformation and metamorphism in the Canadian Cordillera. *Science*, vol. 245, p. 733-736.

Rept. Geol. Surv. Japan, No. 279, p. 135-140, 1992

Origin of Diverse Hydrothermal Fluids by Reaction of Magmatic Volatiles with Wall Rock

Mark H. REED

Department of Geological Sciences
University of Oregon, Eugene, OR 97403, U.S.A.

Introduction

Many volcanic gases sampled from active fumaroles are extremely acidic and some contain relatively large concentrations of metals (e.g. Augustine, Alaska, Symonds *et al.*, 1990). Such magmatic fluids may condense into an overlying meteoric hydrothermal system, supplying metals, sulfur, and acidity to the hydrothermal fluids. Numerical experiments using Augustine gas condensates show that although magmatic fluid could be the major contributor of sulfur and acid, most of the metals must be leached out of wall rock. Wall rock reaction gradually neutralizes the acidic magmatic-meteoric fluid, yielding a range of alteration assemblages from advanced argillic through sericitic to propylitic. Depending on the stage of neutralization when a liquid is tapped off to ascend in a fracture, the fluid may boil either with decreasing pH or with increasing pH, producing a Cu-Au mineral assemblage in the former instance and a Zn-Pb-Ag-(Au) assemblage in the latter.

The numerical experiments reported here were executed using computer program CHILLER (Reed, 1982) in the following series: a) Mix Augustine fumarole gas with water; b) React the mixture with Augustine andesite wall rock at 300°C and P>110 bars; c) Isolate reacted waters from the wall rock reaction at five different water/rock reaction ratios and boil them isoenthalpically from 300°C to 100°C.

Starting fluids and rock

For an H_2O-dominated, 900°C magmatic gas condensing into cold meteoric ground water, a mixing ratio of 1:10 (magmatic gas:cold water, by weight) yields a mixture with a temperature of approximately 300°C. Using the Augustine Dome-3 bulk gas analysis (including trace metals) of Symonds *et al.* (1990) mixed with pure H_2O, the mixture has a pH at 300°C of 0.78. The source of the acidity is nearly evenly divided between hydrochloric and sulfuric acids. The saturation pressure of the mixture is 109.7 bars, which is 24 bars greater than the saturation pressure of pure water at 300°C. About half of the excess pressure is contributed by CO_2 and half by SO_2 with small contributions from HCl and H_2S. The bulk fluid composition is given in Table 1. The mixed fluid is postulated to react with an andesitic wall rock, for which an analysis of an Augustine andesite was used (Symonds *et al.*, 1990), including a full suite of trace metals, some of which were taken from analyses of other andesites (Table 2).

Keywords: hydrothermal alteration, magmatic fluids, boiling, ore precipitation, acidic fluid, acid neutralization, epithermal

Table 1 Composition of Diluted Augustine Gas

Species	Molality	Species	Molality
H+	1.3125	Na+	.92367e-04
Cl-	.39849	Mn++	.11216e-06
SO_4--	.27892	Zn++	.42225e-05
HCO_3-	.15967	Cu+	.45523e-06
HS-	.19083	Pb++	.15836e-05
SiO_2	.54760e-03	Ag+	.65976e-10
Al+++	.17814e-05	Au+	.65976e-10
Ca++	.30349e-05	Hg++	.11875e-07
Mg++	.31668e-06	Ba++	.18473e-08
Fe++	.10556e-04	Sb+++	.25070e-06
K+	.57399e-04	As+++	.65316e-05

Table 2 Reactant Andesite Composition (wt.%)

SiO_2	61.36	$CuO_{.5}$	.0052
Al_2O_3	16.83	PbO	.00107
FeO	3.38	ZnO	.0138
Fe_2O_3	2.00	Au	.1500E-06
MgO	3.56	$AgO_{.5}$	.7500E-05
CaO	6.82	Hg	.1500E-05
K_2O	.98	NaCl	.033
Na_2O	3.56	Sb_2O_3	.000401
MnO	.12	As_2O_3	.000134
BaO	.0965	H_2O	1.240

Wall rock reaction

The initial fluid is saturated with liquid sulfur (Fig. 1). As rock is titrated into the aqueous phase, the pH steps through a series of mineral buffer assemblages while increasing from 0.78 to 5.71 (Fig. 1b). The following series of overlapping mineral assemblages forms (Fig. 1a) (minerals* are listed in their order of precipitation with increasing pH within each group; key minerals are highlighted): 1) S-qz-bar-anh-py (pH 0.78 - 1.6), 2) S-qz-bar-anh-py-al-pyro (pH 1.6 - 3.5), 3) qz-bar-anh-py-pyro-chl-hem-musc-par-mar (pH 3.5 - 4.9), 4) qz-bar-anh-py-chl-hem-musc-par-mar-ep-ab-micr-mt-trem (pH 4.9 - 5.7). These mineral groups constitute a series ranging from intense advanced argillic (qz-S) to advanced argillic (qz-al-pyro) to sericitic (qz-musc-chl) to propylitic (ab-ep-micr-chl-musc).

The initial acidic aqueous phase is dominated by H^+, Cl^-, SO_4^{2-} and H_2CO_3, all derived from the magmatic fluid (Fig. 1b, 1c). The final aqueous composition in equilibrium with the propylitic assemblage is dominated by Cl^-, H_2CO_3 and Na^+ with lesser K^+, Ca^{2+}, and Ba^{2+} (Fig. 1b). Thus, overall, H^+ is exchanged for base cations

* Mineral abbreviations used in the text and figures are as follows: ab, albite; ac, acanthite (Ag_2S); al, alunite; anh, anhydrite; bar, barite; bn, bornite (Cu_5FeS_4); cal, calcite; cc, chalcocite (Cu_2S); cinn, cinnabar (HgS); chl, chlorite; cv, covellite (CuS); en, enargite, (Cu_3AsS_4);ep, epidote; gn, galena (PbS); hem, hematite; kaol, kaolinite; mar, margarite; micr, microcline; mt, magnetite; musc, muscovite; par, paragonite; py, pyrite; pyro, pyrophyllite; qz, quartz; rn, rhodonite; S, liquid sulfur; sil, silver; sl, sphalerite (ZnS); tr, tremolite end member of amphibole.

and sulfate is removed by reduction to sulfide as ferrous iron is oxidized to ferric iron which precipitates in hematite and epidote.

The aqueous concentrations of each of the ore metals, Au, Ag, Cu, Pb and Zn increase by more than an order of magnitude (Fig. 1d) as they are leached from the andesite during the alteration reactions. The concentration of each is limited when a solid phase containing the metal saturates (gold, ac, bn, sl, gn; Fig. 1d). The points of saturation of the metal-limiting minerals differ; thus the ore metal concentration ratios in the aqueous phase change radically as the wall rock reaction proceeds, yielding a spectrum of ore-bearing fluid compositions. It is apparent from Figure 1d that fluids extracted from the water-rock system just before saturation with respect to bornite and electrum (pH 4.1; between points B and C, Fig. 1d) contain a relative maximum of Cu and Au; fluids extracted at the point just before sphalerite precipitates (pH 5.3; point D) contain a relative minimum of Cu but maxima of Zn and Au with lesser Pb and Ag; finally, fluids extracted just at the point of paragonite dissolution, before pH increases from 5.4 to 5.7 (to the left of point F), contain relative maxima of Zn, Pb and Ag, but little Au and Cu.

The overall process of reaction of the acidic magmatic-meteoric fluid with the andesitic wall rock is one of progressive neutralization of the acid by exchange of H^+ ion for base cations. The maximum concentrations of the ore metals in the aqueous phase depend on how much andesite has been destroyed, thereby liberating its metals, before the requisite pH (and sulfide activity, etc.) is reached where a metal-limiting phase saturates. Thus, a less acidic initial fluid than the one explored here would yield smaller metal concentrations. Furthermore, even if the initial magmatic fluid contained much larger metal concentrations than the Augustine example used here, to the extent that the fluid equilibrates with its wall rock, those concentrations would be limited by the same processes outlined above. The evidence is very strong that geothermal fluids are almost always in equilibrium with their host wall rock alteration minerals (e.g., Reed and Spycher, 1984). Thus it appears likely that wall rock reactions commonly limit metal concentrations in epithermal fluids with slightly acidic to neutral pHs (e.g., pH 4.5 - 5.5 at 300°C), regardless of the metal concentrations in the magmatic fluid.

Fluid ascent and boiling

Imagine that the magmatic-meteoric hydrothermal fluids described above migrate through their wall rock, react with it to one extent or another, then ascend through open fractures and boil. This process was modeled by picking six different fluids (identified by A, B, C, D, E and F in Fig. 1a, 1d) from the above wall rock reaction and numerically boiling them. Depending on the amount of wall rock with which they have already reacted, the six fluids yield diverse ores when they boil: initially acidic waters boil with decreasing pH and precipitate a qz-cv-gold-kaol or qz-gold-cc-kaol assemblage while neutral-pH waters boil with increasing pH and precipitate a qz-cal-sl-gn-silver-cc-micr assemblage (Fig. 2). In two of the three acidic waters, gold chloride complex predominates over gold bisulfide and gold precipitates with decreasing temperature because the chloride complex is less stable at lower temperature. In the others, gold bisulfide predominates, and gold precipitates by desulfidation of the fluid as H_2S gas boils off (Reed and Spycher, 1985; Spycher and Reed, 1989).

In contrast to the "normal" boiling with pH increase caused by CO_2 loss to the

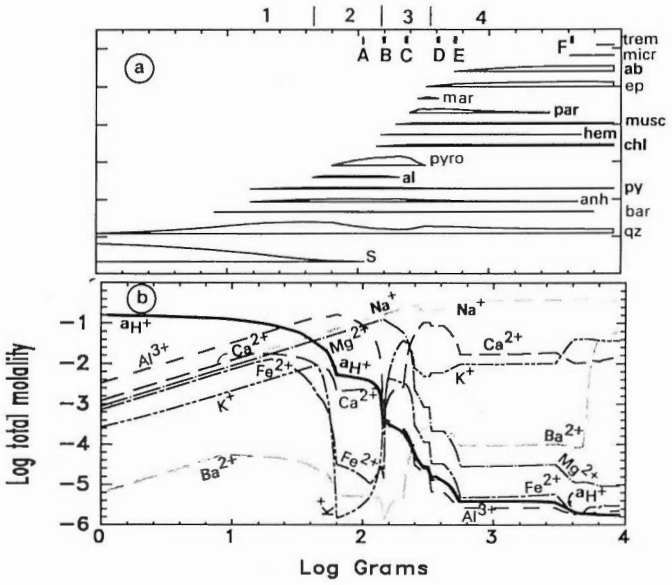

Fig. 1 Reaction of Augustine andesite with a fluid composed of an Augustine volcanic gas condensed into meteoric water at 300°C. The abscissa shows the log of the number of grams of andesite titrated into 1.051 kilogram of the fluid.

a) Paragenetic-style diagram showing the presence and relative abundance (wt. %) of the major minerals* that precipitate as the andesite is altered. Rhodonite and calcite are not shown, but they precipitate with assemblages 3 and 4, respectively. Sulfides and electrum are shown in Fig. 1d. The numbers at the top identify alteration assemblages discussed in the text: 1) intense advanced argillic, 2) advanced argillic, 3) sericitic with chlorite and 4) propylitic. The letters A - F at the top identify the pick-off points for fluids that were boiled, as shown in Fig. 2.

b) pH (identified by aH^+) and total molalities of major cations in the aqueous phase. The plateaus in the aH^+ curve are caused by mineral pH buffers that can be identified in Fig. 1a. The dominant trend is the replacement of aqueous H^+ by base cations as the andesite neutralizes the acidic fluid.

c) Total molalities of major anionic and neutral species and aH^+. Chloride and carbonate concentrations are slightly affected by the rock reaction, but sulfate is strongly depleted as it is reduced to sulfide by reaction with ferrous iron that precipitates in epidote and hematite. Sulfide is depleted by precipitation of pyrite and base metal sulfides (Fig. 1d).

d) Total molalities of ore metals. Concentrations of all metals increase markedly as they are leached from the andesite. Au concentration is limited by precipitation of alteration native gold (Au-rich electrum); the other metals are limited by sulfide precipitation, as shown at the top of the graph. The indicated minerals* are present to the right of the vertical bars. The letters A - F at the bottom identify the pick-off points for fluids that were boiled, as shown in Fig. 2.

gas phase, boiling with decreasing pH occurs in waters that are initially acidic enough to contain significant concentrations of associated HCl and HSO_4^- whose dissociation, upon boiling-induced temperature decrease, yields more H^+ to the aqueous phase than CO_2 degassing consumes from the aqueous phase (Reed, 1989, 1992). The difference in boiling behavior, depending on initial pH and metal content, clearly determines the nature of the resulting vein "ores". Thus, it is possible

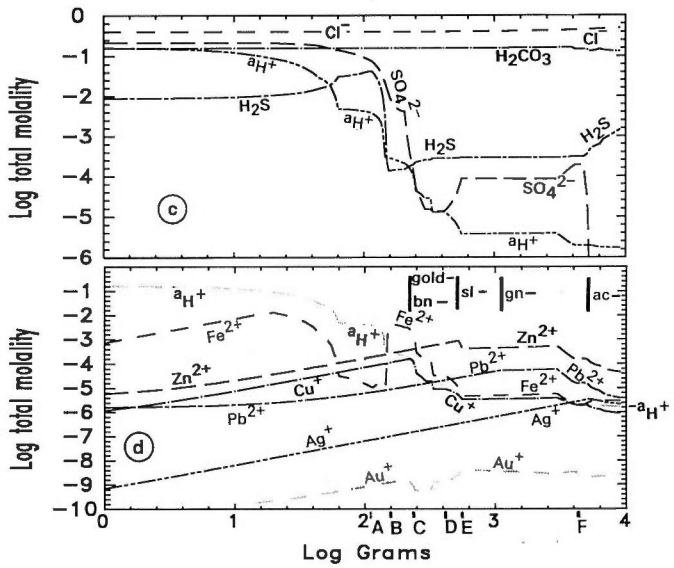

Fig. 1 (continued)

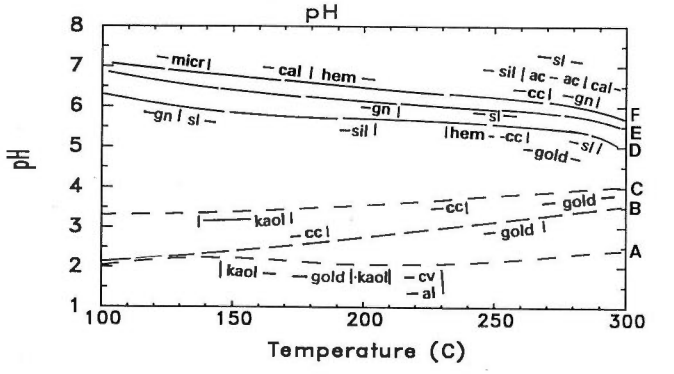

Fig. 2 Boiling-induced pH changes for fluids A - F, as marked in Fig. 1. Curves A, B and C demonstrate boiling with decreasing pH with the precipitation of Cu and Au minerals. Curves D, E and F demonstrate boiling with increasing pH with precipitation of Pb, Zn and Ag minerals. The curves are marked with the minerals* that precipitate upon boiling (except for curve E, for which only sl and gn are shown). The indicated minerals are present on the side of the vertical bar on which the name is shown and their presence extends in the direction indicated by the hyphen. Quartz is present over the whole range of temperatures in all cases except A, where it precipitates only where kaolinite is absent.

that a single magmatic-hydrothermal system could yield a range of geothermal fluid types and a range of epithermal ore types--from "acid-sulfate" Cu-Au (cv-en-gold) to "adularia-sericite" Pb-Zn-Ag-Au. In the absence of repeated pulses of magmatic volatiles (and excluding surficially-produced acidic waters; Reed and Spycher, 1985), we would expect a single hydrothermal system and its product ores to evolve from the acid-sulfate to neutral-pH type.

Acknowledgements

A. Michaels and J. DeBraal assisted with graphics and computing. P. Condon executed preliminary calculations on this system in 1990. Discussions with G. Plumlee, R. Symonds, J. Margolis and A. Getahun helped to shape the project. I thank all of these people. This research was supported by funding from NSF EAR-8915854 and EAR-9105490.

References

Reed, M. H. (1982) Calculation of multicomponent chemical equilibria and reaction processes in systems involving minerals, gases and an aqueous phase. *Geochim. Cosmochim. Acta*, vol. 46, p. 513-528.

——— (1989) Epithermal boiling with decreasing pH: Selective precipitation of gold and silver vs. base metal sulfides. *Geol. Soc. Amer. Abstracts with Programs*, vol. 21, no. 6, October 1989, p. 350.

——— (1992) Computer modeling of chemical processes in geothermal systems: Examples of water-rock reaction, boiling and mixing. In Applications of Geochemistry in Geothermal Reservoir Development, United Nations Institute for Training and Research, United Nations Development Program (in press).

——— and Spycher, N. (1984) Calculation of pH and mineral equilibria in hydrothermal waters with application to geothermometry and studies of boiling and dilution. *Geochim. Cosmochim. Acta*, vol. 48, p. 1479-1492.

——— and ——— (1985) Boiling, cooling and oxidation in epithermal systems: A numerical modeling approach. In Berger, B. R. and Bethke, P. M. eds., Geology and Geochemistry of Epithermal Systems, *Rev. Econ. Geol.*, vol. 2, p. 249-272.

Spycher, N. F. and Reed, M. H. (1989) Evolution of a Broadlands-type epithermal ore fluid along alternative P-T paths: Implications for the transport and deposition of base, precious, and volatile metals. *Econ. Geol.*, vol. 84, p. 328-359.

Symonds, R. B., Rose, W. I., Gerlach, T. M., Briggs, P. H., and Harmon, R. S. (1990) Evaluation of gases, condensates, and SO_2 emissions from Augustine volcano, Alaska: the degassing of a Cl-rich volcanic system. *Bull. Volcanol.*, vol. 52, p. 355-374.

Rept. Geol. Surv. Japan, No. 279, p. 141-151, 1992

Assessment of Magmatic Components of the Fluids at Mt. Pinatubo Volcanic-geothermal System, Philippines from Chemical and Isotopic Data

J. R. RUAYA[1], M. N. RAMOS[1] and R. GONFIANTINI[2]

[1] *PNOC Energy Development Corporation*
Ft. Bonifacio, Makati, Metro Manila, Philippines
[2] *Isotope Hydrology Section, International Atomic Energy Agency*
A-1400 Vienna, Austria

Introduction

The presence of magmatic components in geothermal fluids has been documented on the basis of chemical and isotopic data (e.g., Kiyosu and Yoshida, 1988; Yoshida, 1984; Kiyosu and Kurahashi, 1983; D'Amore *et al.*, 1990). The inferred contributions of magmatic fluids to the hot spring waters and fumarolic gases at Suretimeat field in Vanuatu were used to form a general model of a volcanic geothermal system (Heming *et al.*, 1982). Recently, a detailed geochemical model of the volcanic-magmatic-hydrothermal system at Nevado del Ruiz volcano, Colombia (Giggenbach *et al.*, 1990; Sturchio *et al.*, 1990) has significantly increased our understanding of these systems.

Data from surface exploration and deep drilling (up to 2733 m vertical depth; VD) at Mt. Pinatubo, Philippines (Fig. 1) reveal a volcanic-geothermal system akin to those described in the above papers.

Thermal features and deep drilling

Mt. Pinatubo is an andesitic composite volcano (elevation: 1745 m) which lies along the west Luzon volcanic arc (Wolfe and Self, 1983). The natural thermal features associated with Mt. Pinatubo volcanism consist of hot and warm springs, solfatara, gas seepages and hydrothermally-altered ground (Fig. 1). Water and gas sampling from the natural thermal manifestations were conducted from 1982 to 1984, and again in early 1990 mainly for isotope analysis.

Three exploratory wells were drilled in 1988 and 1989. Well Pin-1 discharged slightly acidic fluid. Well Pin-2D had a maximum temperature of 336°C but had to be shut after three days due to highly acidic discharge fluid (pH as low as 2.30). Well Pin-3D also discharged, but had low permeability. Water samples were taken from the weirbox while the gas samples were obtained by a tapping the horizontal discharge line using a Webre separator.

Water chemistry

An initial assessment of the origins of these waters can be made based on their relative Cl, HCO_3 and SO_4 concentrations (Fig. 2). In terms of these anions, there is

Keywords: Mt. Pinatubo, magmatic fluid, magmatic contribution, geothermal, volcanic-geothermal system, stable isotope

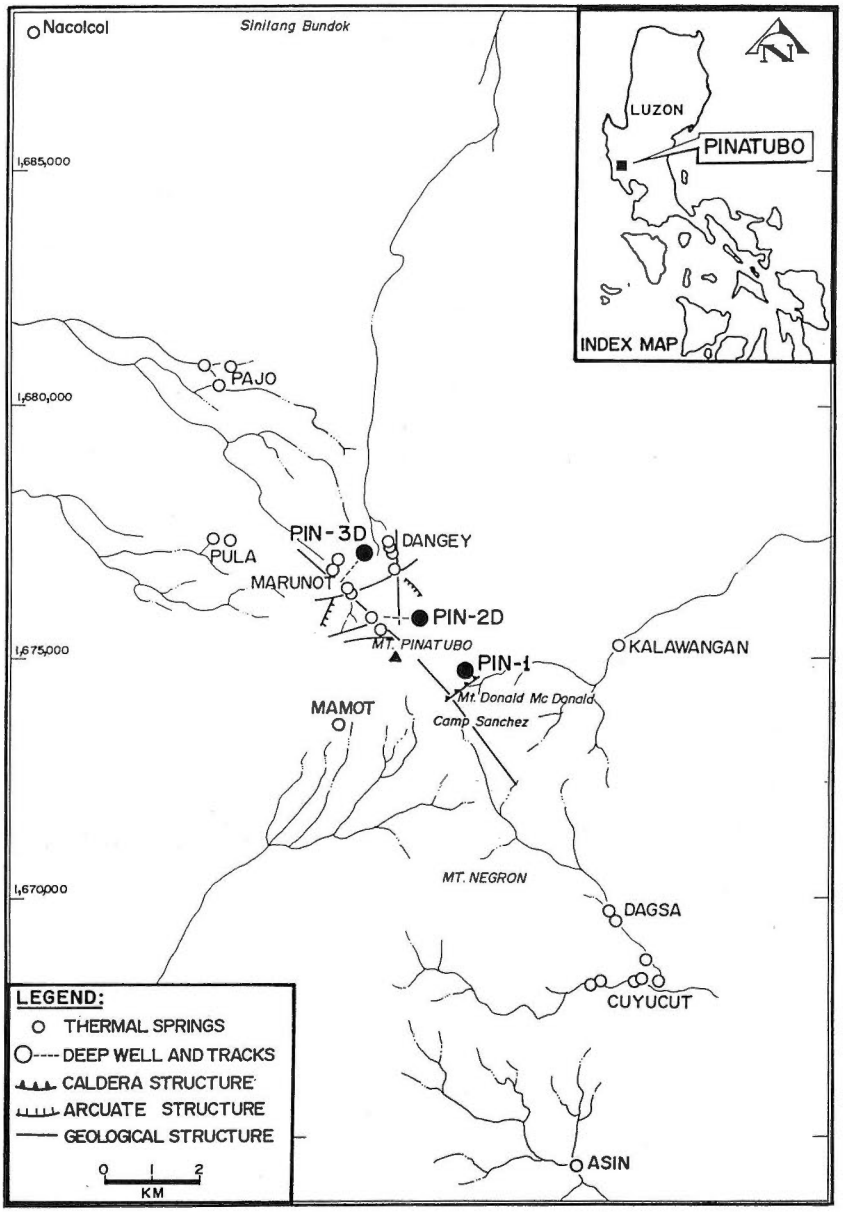

Fig. 1 Location map of the thermal features and wells drilled in Mt. Pinatubo, Philippines, volcanic-geothermal area.

a pronounced gradation of the springs from the highlands to the lowlands: from the highly acidic Cl-SO_4 Pinatubo solfatara pool, to SO_4-HCO_3 at Upper Marunot, to HCO_3-SO_4 at Dangey, Mamot, Pula and Lower Marunot; to distinctly Cl-HCO_3-rich at Dagsa, Asin, Cuyucut and Kalawangan. The dominance of SO_4-HCO_3 for the highland springs indicates extensive steam condensation, while the presence of chloride springs diluted by near surface waters (indicated by HCO_3) in the lowlands suggest a

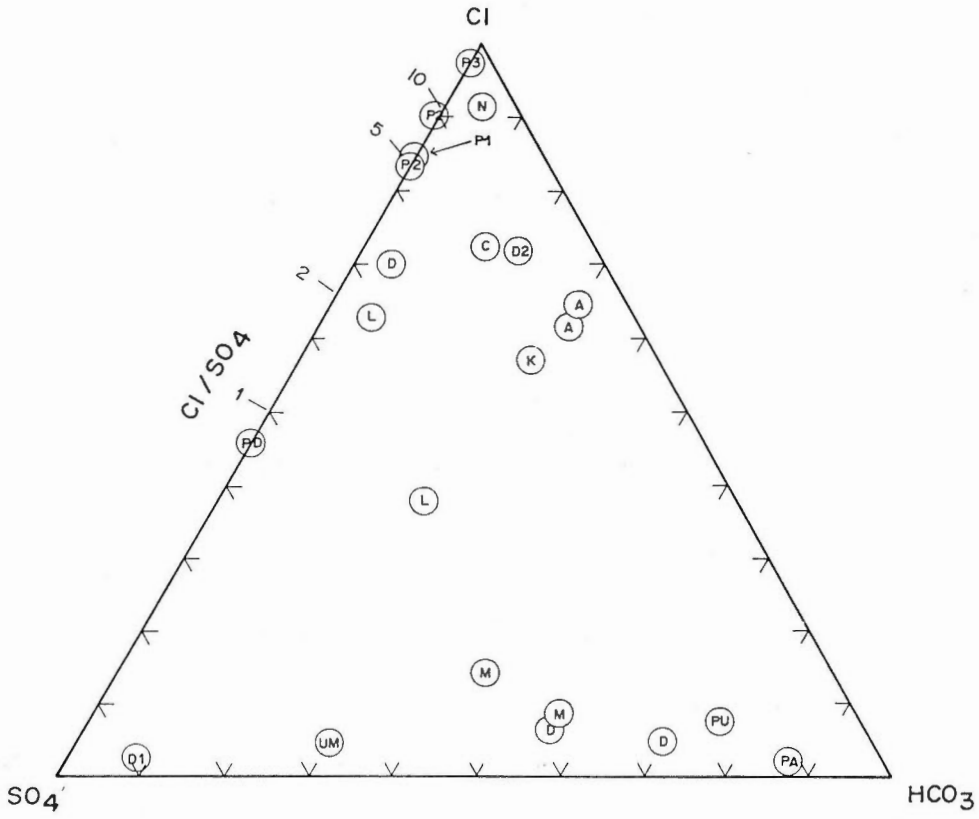

Fig. 2 Classification of the thermal waters from hot and warm springs and wells at Mt. Pinatubo thermal area in terms of the relative amounts of Cl, HCO_3 and SO_4.

probable alkali-chloride reservoir within the system. However, the presence of appreciable Cl in many highland springs (Mamot, Dangey, Marunot and Pinatubo pool) suggests that the chloride may be genetically related to active volcanism.

On a Na-K-Mg diagram (Giggenbach, 1988) shown in Figure 3, most of the surface waters plot near the Mg apex, signifying that these are predominantly meteoric in origin. Only the southern chloride-containing springs (Asin, Dagsa and Cuyucut) have signatures of geothermal water components. However, the well discharges follow two distinct trends. The Pin-1 discharge water roughly falls along a trend coinciding with Dagsa, Asin and Cuyucut. A second trend is defined by the Pin-2D downhole and discharge fluids, the Pinatubo solfataric pool and roughly, the Pin-3D discharge. Thus, the fluids feeding the Pinatubo pool are likely to be the same fluid tapped by wells Pin-2D and Pin-3D. These trends suggest two possibilities: One, there are at least two convective systems about the Pinatubo dome; and two, there is only one large system, but the fluids have undergone distinct subsurface processes (e.g., dilution and cooling) prior to discharge.

Despite the fact that the discharged well waters come from considerable depths, these are still far from equilibrium with the altered rocks, unlike most ex-

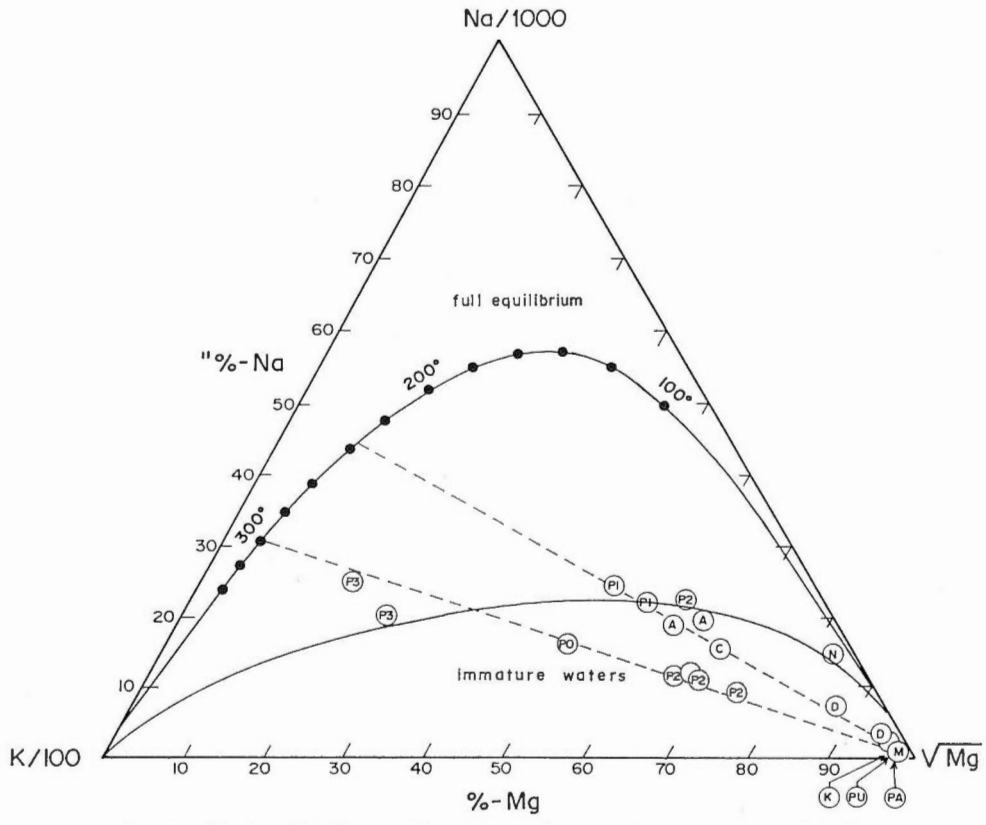

Fig. 3 Relative Na, K, and Mg contents of thermal waters from the Mt. Pinatubo volcanic-geothermal area.

plored alkali chloride geothermal fluids, which are close to chemical equilibrium with altered rocks (Giggenbach, 1988). The non-attainment of equilibrium with rocks is a distinctive characteristic of the fluids at Pinatubo.

Gas chemistry

Magmatic gases have a chemical signature which allows them to be distinguished from gases of diverse origins. For magmatic gases from andesitic volcanoes in Japan, the CO_2/N_2 and N_2/Ar ratios are 270 and 4250, respectively (Kiyosu, 1985; Kiyosu and Yoshida, 1988), while the corresponding ratios from White Island volcano, New Zealand, exhalations have average values of 180 and 800, respectively (Giggenbach, 1987). These values have been superimposed in Figure 4 together with a dilution line from White Island magmatic gases to air (which has a N_2/Ar ratio of 83) and to an air-saturated groundwater.

The Pinatubo gases lie very close to the andesitic magmatic steam composition. In particular, the Pin-2D gas sample is almost coincident with the "average" White Island gas (Giggenbach, 1987). This sample is therefore considered represen-

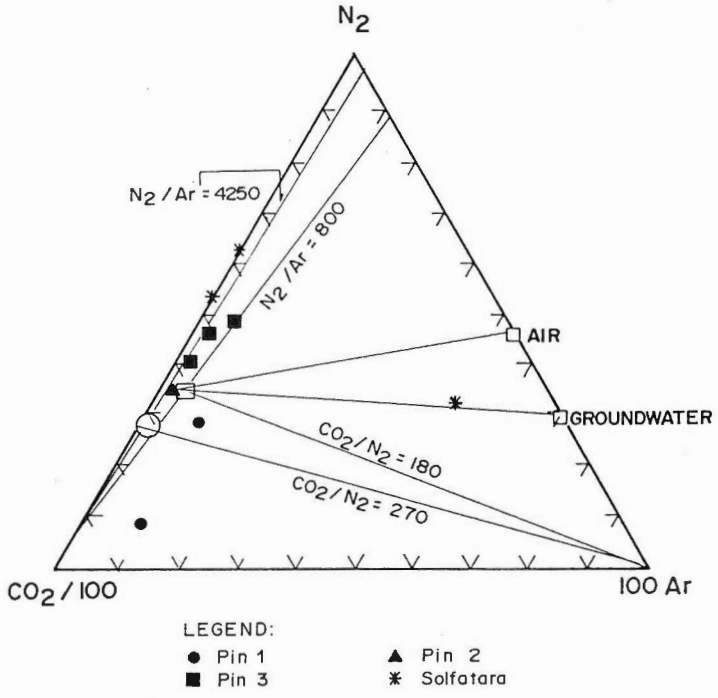

Fig. 4 Relative amounts of CO_2, N_2 and Ar in gases taken from Mt. Pinatubo volcanic-geothermal area. Also shown are the average White Island, New Zealand, gas composition with CO_2/N_2 and N_2/Ar ratios of 180 and 800, respectively, and the average gas compositions from Japanese volcanoes, which have the corresponding ratios of 270 and 4250, respectively. Lines are drawn connecting the White Island gases to air and air-saturated groundwater.

tative of the magmatic fluid in the Mt. Pinatubo system.

The discharged gas ratios $(X_1/X_2)_d$ of gases 1 and 2 would depend on the relative amounts of magmatic gases and meteoric water in the given mixture. In such case, the following relation holds (Kiyosu, 1985; Kiyosu and Yoshida, 1988):

$$(X_1/X_2)_d = f(X_1/X_2)_M + (1 - f)(X_1/X_2)_m \qquad (1)$$

where f is the fraction of magmatic gases, and M and m stand for magmatic gases and meteoric water respectively. In addition, these mixed fluids may lose or gain vapor, thus modifying the measured gas ratios. The effects of vapor gain and loss with respect to the composition expected for the discharge of a pure equilibrium phase $(X_{1,i})$ have been discussed by Giggenbach (1980).

Following Kiyosu and Yoshida (1988), the gas ratio at the discharge can be related to the original liquid phase, which has undergone vapor gain or loss:

$$(X_1/X_2)_d = (X_1/X_2)l(D_1/D_2)^{\pm 1} \qquad (2)$$

where the plus or minus signs refer to vapor gain or loss, respectively; $D_i = 1 - y +$

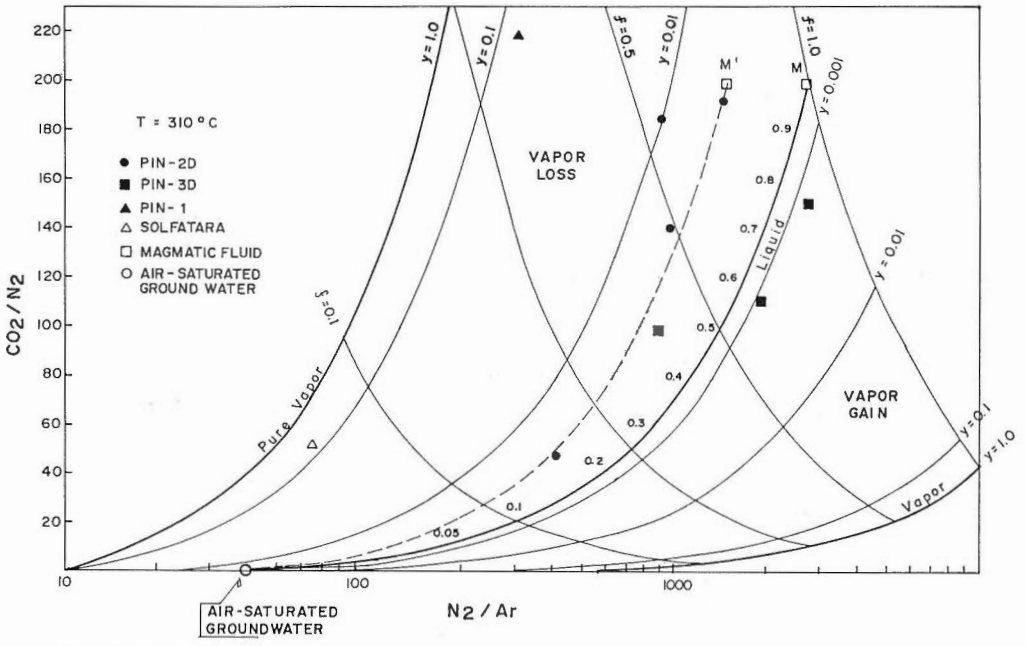

Fig. 5 Plot of CO_2/N_2 versus N_2/Ar for Pinatubo gas samples. A mixing line connecting the inferred magmatic gas composition denoted by M and air-saturated groundwater is shown. Numbers in this line are the fractions of magmatic gases in the mixture. Shown also are vapor gain and loss lines for several vapor fractions (y) and several lines of constant magmatic gas fraction (f).

yB_i; y = equilibrium vapor fraction, and B_i is the distribution coefficient of gas i between vapor and liquid phases.

As noted earlier, the Pin-2D gas is closest in composition to magmatic gases. Therefore, the CO_2/N_2 ratio for the magmatic fluid is taken to be 200. However, considerably higher N_2/Ar ratios are observed for well Pin-3D, and thus, the magmatic N_2/Ar ratio is set at 2800, although a significant vapor gain at very high temperatures (>300°C), a mixed fluid at low gas ratio could also cause the observed ratios at Pin-3D.

Using these end member values, Eqs. 1 and 2 can be solved simultaneously (at a temperature of 310°C) to evaluate the effects of vapor gain or loss on the gas ratios; the results are shown in Figure 5. The mixed fluids resulting from the condensation of magmatic gases in air-saturated groundwater is shown as a line labeled 'liquid' while the magmatic endmember is labeled 'M'. Numbers on this line are the fractions of magmatic fluids. Also shown are vapor loss or gain lines for selected values of y, and a few lines of constant f. It can be seen that all of the Pin-2D and Pin-3D samples are essentially mixed fluids if the region on the plot bounded by the lines y = 0.01 is considered, within uncertainty, to be liquid. As to be expected, the solfatara sample lies on the vapor loss region at a high y value, and low f.

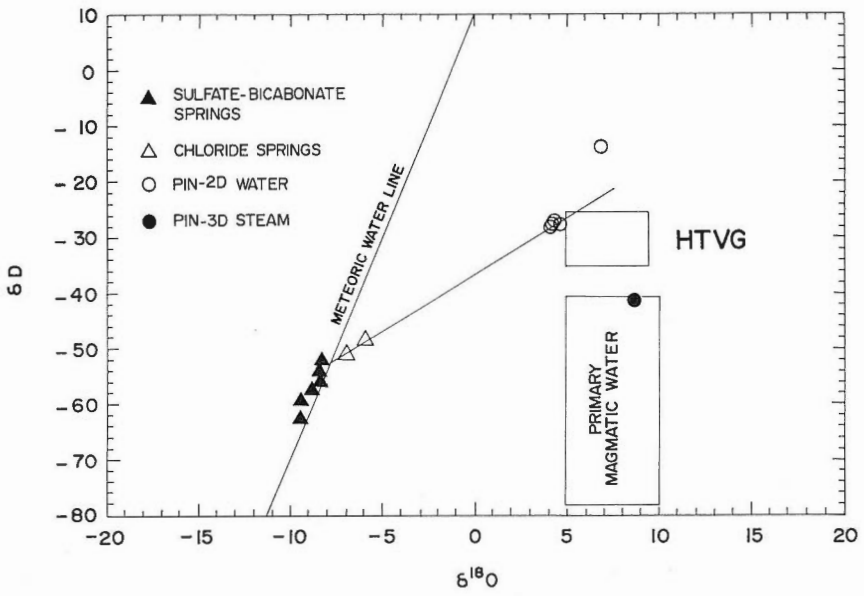

Fig. 6 Oxygen-18 versus deuterium plot for the waters at Mt. Pinatubo. Shown is the area (box, labeled HTVG) where most of the high temperature volcanic gases from Japanese volcanoes plot. The previously accepted "primary magmatic fluid" region is also shown for comparison.

Stable isotope data

Figure 6 is a plot of $\delta^{18}O$ versus δD, showing that most of the thermal features fall near the meteoric water line, indicating these are either essentially meteoric or diluted steam condensate. The Dagsa-1 sample, while warm (T = 35°C) is essentially meteoric (e.g., low chloride, and lies close to the Mg apex in Fig. 2); it is heated locally during passage through hot ground without significant modification.

The $\delta^{18}O$ and δD of well waters are strongly shifted relative to meteoric water compared with those of other geothermal systems (Panichi and Gonfiantini, 1978). The values for Pin-2D (ave: δD = -27.3, $\delta^{18}O$ = 4.34 per mil) are close to the average values for high temperature fumarolic steam (δD = -25.0, $\delta^{18}O$ = 6.6) from volcanic areas of Japan (Matsuo *et al.*, 1974; Sakai and Matsubaya, 1977). The latter are likely to be in isotopic equilibrium with andesitic magma on the basis of the $\delta^{18}O$ values of the fresh andesites ($\delta^{18}O$ = 6.6 to 7.0) (Matsuo *et al.*, 1974). The well waters plot above the "primary magmatic water" composition (Taylor, 1979), though are consistent with the water compositions of andesitic volcanoes (see Matsuhisa, and Taylor, this volume). The stable isotope data indicate that volcanic fluids have intruded into the system. There appears to be a mixing line connecting Pin-2D, Asin and Cuyucut to the surface waters with the hot springs having only a small volcanic component. On a Cl vs. δD plot (Fig. 7), simple evaporation of surface waters to obtain the $\delta^{18}O$ and δD values for Pin-2D is readily ruled out, while the chloride-containing springs, Asin, Cuyucut and Nacolcol, can be connected by a straight line with groundwater, which likely represents mixing.

The relationship, if any, between the Pin-2D and Pin-3D samples is somewhat

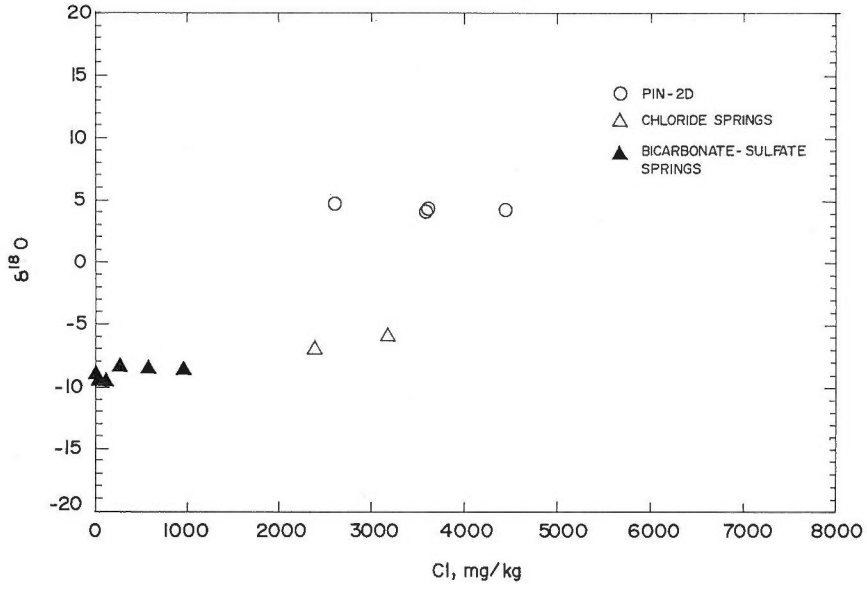

Fig. 7 A plot of chloride contents versus deuterium shifts for Mt. Pinatubo thermal waters.

unclear. Vaporization of the former at 310°C results in changes in $\delta^{18}O$ and δD of the residual fluid towards the direction of Pin-3D in Figure 6, but the magnitude is too small. A possible explanation of the isotope data for the latter is that this steam sample comes from liquid water which has been modified by water-rock interactions. This is consistent with the fact that the chemical data suggests that Pin-3D water is partly equilibrated with the rocks as shown previously by the Na-K-Mg plot.

A conceptual geochemical model

The chemical and isotopic data presented above show that the hydrothermal fluids of Mt. Pinatubo have not attained chemical equilibrium with the host rocks. There is no evidence of a "mature" (that is, chemically equilibrated) convecting meteoric water heated by contact with hot rocks. Temperatures in excess of 300°C suggest that a more efficient heat transfer mechanism operates.

A conceptual geochemical model for the Mt. Pinatubo magmatic-geothermal system is shown in Figure 8. The temperature contours and the approximate location of the two-phase zone are based on downhole observations. Hot magmatic vapors rise through fractures, heating the volcanic rocks, and condensing in shallow groundwaters, producing acidic waters that have been tapped by Pin-2D and Pin-3D and, to some extent, by Pin-1. Some of these waters leak through fractures, interact with the rocks, and appear as neutral SO_4-HCO_3-Cl hot springs (Mamot, Dangey, Pajo, Pula and Kalawangan). The chemical signatures of the original magmatic vapors are largely retained in gas ratios and isotopic data obtained from discharges of wells Pin-2D and Pin-3D.

The thermal energy of the convecting magmatic vapor induces the formation

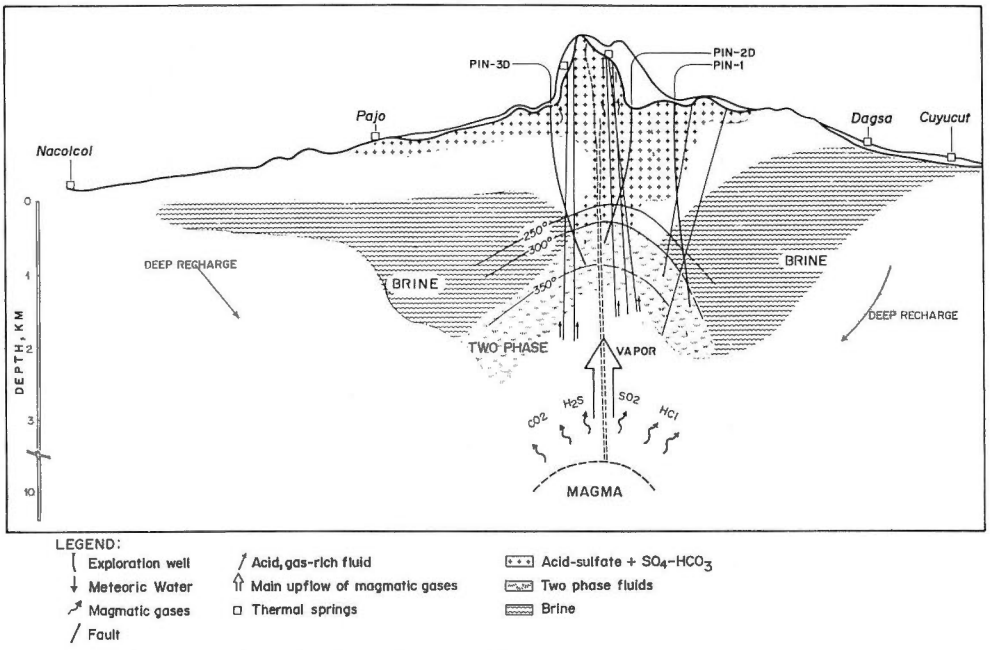

Fig. 8 A conceptual physico-chemical model of the Mt. Pinatubo volcanic-geothermal system.

of convective cells of largely meteoric water on the periphery of the Mt. Pinatubo dome. At least two separate brine systems have evolved. One is located towards the northwest direction, and a portion of this--probably near the transition between the brine and two-phase region--has been intersected by well Pin-3D. The other system lies towards the southeast. The fluid tapped by Pin-1 is probably the northern and upper portion of this system, while its major outflow is manifested by the chloride springs at Dagsa, Asin and Cuyucut.

Permeability within the wells is generally limited. This is compatible with the Giggenbach *et al.* (1990) model of such systems, where an entensive, hydrothermally-sealed carapace is likely to form. These workers pointed out that several processes are conducive to the formation of this carapace; evaporation of locally formed brines, deposition of solids such as silica from rising waters, and conversion of volcanic rocks to more voluminous secondary hydrothermal alteration products. In Figure 8, the location of this carapace would lie along the boundary of the two-phase zone with groundwater, which would place it near the 300°C contour.

The Pinatubo system is in marked contrast to the nearby Mt. Natib system (Ruaya and Panem, 1991), where the waters are mostly of the neutralized SO_4-HCO_3-Cl type. The major difference is that fluids at Mt Natib have substantially reacted with the rocks while the fluids at Mt. Pinatubo have not reached chemical equilibrium with the rocks, due to continuous input of magmatic components at the latter. In a sense, the two systems represent windows into a continuous spectrum ranging from purely magmatic to fully matured (that is, chemically equilibrated) geothermal systems.

Acknowledgement

This study is part of Research Contract PHI-6/019 between PNOC and IAEA on isotopic investigations of geothermal fields in the Philippines.

References

D'Amore, F., Rivera, J. R., Giusti, D. and Rossi, R. (1990) Preliminary geochemical and thermodynamic assessment of the geothermal resoures, Sulphur Springs area, St. Lucia, W. I. *Appl. Geochem.*, vol. 5, p. 587-604.

Giggenbach, W. F. (1980) Geothermal gas equilibria. *Geochim. Cosmochim. Acta*, vol. 44, p. 2021-2032.

——— (1987) Redox processes governing the chemistry of fumarolic gas discharges from White Island, New Zealand. *Appl. Geochem.*, vol. 2, p. 143-161.

——— (1988) Geothermal solute equilibria. Derivation of Na-K-Mg-Ca geoindicators. *Geochim. Cosmochim. Acta*, vol. 52, p. 2749-2765.

———, Garcia, P. N., Londono, C. A., Rodriguez, V. L., Rojas, G. N. and Calvache, V. M. L. (1990) The chemistry of fumarolic vapor and thermal-spring discharges from the Nevado del Ruiz volcanic-magmatic-hydrothermal system, Colombia. *Jour. Volcanol. Geotherm. Res.*, vol. 42, p. 13-39.

Heming, R. F., Hochstein, M. P. and McKenzie, W. F. (1982) Suretimeat geothermal system: an example of a volcanic geothermal system. *Proc. Pacific Geothermal Conference 1982, Part 1*, Auckland, New Zealand, p. 247-250.

Kiyosu, Y. (1985) Variations in N_2/Ar and He/Ar ratios of gases from some volcanic areas in Northeastern Japan. *Geochem. Jour.*, vol. 19, p. 275-281.

——— and Kurahashi, M. (1983) Origin of sulfur species in acid sulfate-chloride thermal waters, northeastern Japan. *Geochim. Cosmochim. Acta*, vol. 47, p. 1237-1245.

——— and Yoshida, Y. (1988) Origin of some gases from the Takinoue geothermal area in Japan. *Geochem. Jour.*, vol. 22, p. 183-193.

Matsuo, S., Suzuki, T., Kusakabe, M., Wada, H. and Suzuki, M. (1974) Isotopic and chemical compositions of volcanic gases from Satsuma-Iwojima, Japan. *Geochem. Jour.*, vol. 8, p. 165-173.

Panichi, C. and Gonfiantini. R. (1978) Environmental isotopes in geothermal studies. *Geothermics*, vol. 6, p. 143-161.

Ruaya, J. R. and Panem, C. C. (1991) Mt. Natib, Philippines: a geochemical model of a caldera-hosted geothermal system. *Jour. Volcanol. Geotherm. Res.*, vol. 45, p. 255-265.

Sakai, H. and Matsubaya, O. (1977) Stable isotopic studies of Japanese geothermal systems. *Geothermics*, vol. 5, p. 97-124.

Sturchio, N. C. and Williams, S. N. (1990) Variations in chemistry of acid-sulfate-chloride springs at Nevado del Ruiz volcano, Colombia: November 1985 through December 1988. *Jour. Volcanol. Geotherm. Res.*, vol. 42, p. 203-210.

Taylor, H. P. Jr. (1979) Oxygen and hydrogen isotope relationships in hydrothermal mineral deposits. In Barnes, H. L. ed., Geochemistry of Hydrothermal Ore

Deposits, 2nd ed., Wiley-Interscience, New York, p. 236-277.

Wolfe, J. A. and Self, S. (1983) Structural lineaments and Neogene volcanism in southwestern Luzon. In Hayes, D. E. ed., The Tectonic and Geologic Evolution of Southeast Asian Seas and Islands, Part 2. *Geophys. Monogr. Ser.*, Am. Geophys. Union, Washington, D. C., vol. 27, p. 157-172.

Yoshida, Y. (1984) Origin of gases and chemical equilibrium among gas species in steam from Matsukawa geothermal area, Northeast Japan. *Geochem. Jour.*, vol. 18, p. 195-202.

Rept. Geol. Surv. Japan, No. 279, p. 152-155, 1992

Does Acid Volcanic Gas Represent Magmatic Discharge at Depth?

Hiroshi SHINOHARA

Mineral Resources Department, Geological Survey of Japan
Higashi, 1-1-3, Tsukuba, Ibaraki 305, Japan

Introduction

Acid volcanic gases from high temperature fumaroles are often assumed to represent the composition of the fluids released from magma. However, high pressure experiments clearly show that the magmatic discharge at depth contains a smaller amount of acid species (e.g., HCl) and a larger amount of neutral species (e.g., NaCl) than the volcanic gases (Burnham, 1979; Shinohara *et al.*, 1984; 1989). In this paper, I will compare the difference in compositions of the magmatic discharge at depth with volcanic gases, and discuss the possible differentiation processes of the volcanic gas originating from a deep magmatic discharge.

Volcanic gas and magmatic discharge

High temperature volcanic gas is a sample of the hydrothermal fluid evolved from a magma, and is often believed to represent the composition of the magmatic discharges. Obviously, some volcanic gases, which originate from an extruded magma body (i.e., lava lake, lava flow or lava dome), are the magmatic discharge itself, and the identity of the magmatic discharge and the volcanic gas is clear under the low pressure condition. Since the difference in composition between volcanic gases which originate from magmas at the surface and at depth is not clear, the magmatic discharge at depth has also been assumed to have an acidic composition similar to the near surface magmatic discharge.

Classically, volcanic gas studies have been concerned only about the volatile species (i.e., H_2O, CO_2, SO_2, H_2S, HCl, HF, and other non-condensable gases). Although the condensation process of less-volatile species (i.e., NaCl, KCl, Fe_2O_3, FeS and others) in the volcanic gas was also discussed by several authors, concentrations of these species in the volcanic gas are generally low and the differentiation process of the main volatile species is little affected by the consideration of the less-volatile species. The condensation process has been investigated with decreasing temperature, but only at atmospheric pressure. Since the volcanic gas sampled at atmospheric pressure has inevitably experienced a large pressure decrease, differentiation due to pressure decrease is believed to be an important consideration in the discussion of the origin of the volcanic gas.

In contrast with volcanic gas studies, the composition of a hydrothermal solution is often approximated by a NaCl-H_2O mixture in studies of hydrothermal ore deposits based on analyses of fluid inclusions. Burnham (1979) estimated the composition of magmatic hydrothermal solutions based on his laboratory experiments,

Keywords: volcanic gas, magmatic discharge, water-rock interaction, pressure dependence, HCl/NaCl ratio

Table 1 Composition of the magmatic aqueous phase in equilibrium at 1.0 kb with a granodioritic melt whose chlorine content is 0.1 wt % (Burnham, 1979).

Phenocrysts	Total Cl (m)	Major Cationic Constituents (m)				
		Na	K	Fe	H	Ca
Pl, Mt,	1.0	0.40	0.23	0.10	0.09	0.02
Pl, Mt, Hb,	1.0	0.17	0.47	0.11	0.03	0.02
Pl, Mt, Bi,	1.0	0.32	0.32	0.11	0.03	0.02

Pl; Plagioclase, Mt; Magnetite, Hb; Hornblende, Bi; Biotite.

as shown in Table 1. Shinohara *et al.* (1984; 1989) conducted high pressure experiments in the simple system of Ab-Or-Q-NaCl-KCl-HCl-H_2O at 810°C and over the pressure range of 0.6 to 6.0 kb. These studies showed that the concentration of HCl in the aqueous phase is always less than that of NaCl and KCl, unless the silicate melt is aluminous. These experimental results agree with the approximation of the hydrothermal ore fluids as a NaCl-H_2O mixture, but show a significant departure from the composition of acid volcanic gas, which contains abundant HCl and little NaCl.

How does the acid volcanic gas, which contains little NaCl, differentiate from the magmatic discharge at depth? Two processes are proposed; 1) deposition of NaCl by phase separation, or 2) conversion of NaCl to HCl by reactions which have a large pressure dependence. Because of the lack of experimental data on multicomponent systems which include sulfur species or chlorine compounds (except NaCl and HCl), the following discussion will be limited to the NaCl-HCl-H_2O system.

Differentiation process of volcanic gas

1) *Phase separation of NaCl*

Numerous experimental and theoretical studies have been conducted on the phase equilibrium of the system NaCl-H_2O. Under sub-critical conditions, the solubility of NaCl in the vapor phase decreases with decreasing pressure as shown in Figure 1, with a solubility minimum at high temperature and low pressure conditions (Pitzer and Pabalan, 1986). For example, the minimum NaCl solubility in the vapor phase is 50 ppm at 800°C, while it is 600 ppm at 1000°C. Consequently, the large amount of NaCl which is contained in the magmatic discharge at depth is separated as NaCl-rich liquid and/or NaCl solid during ascent of the fluids, and the NaCl concentration in the volcanic gas decreases to the solubility minimum.

Where do the large amounts of separated NaCl-rich liquid and NaCl solids disappear to? As HCl accounts for only less than 10 % of the chlorine compounds in the magmatic discharge at depth (Table 1), the flux of NaCl (and other salt species) from the magma amounts to about ten times that of HCl. NaCl-rich hot springs are often found near volcanoes, and are one sink NaCl from the magma. In active volcanic systems, however, the NaCl flux from hot springs is not sufficient to account for all the NaCl released from the magma. For example, the chlorine flux from Satsuma-Iwojima volcano, Japan, was estimated to be $1x10^5$ ton/year, with 70% of this released from fumaroles as HCl, and only 30% released to the surface from hot springs as a mixture of NaCl, KCl, $CaCl_2$, $MgCl_2$ and others (Yoshida and Ozawa, 1981). Since the concentration of neutral species in the deep magmatic discharge is higher

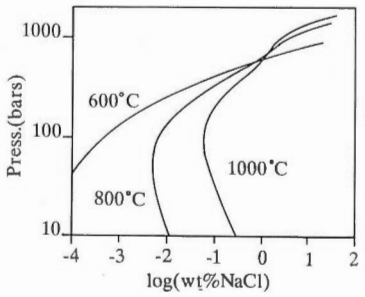

Fig. 1 Calculated solubilities of NaCl in water vapor phase at several isotherms as a function of pressure (after Pitzer and Pabalan, 1986).

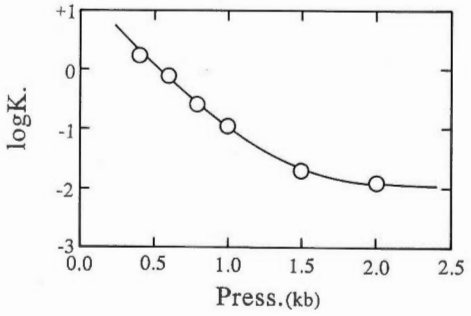

Fig. 2 Variation of equilibrium constant of reaction (1) at 600°C. The equilibrium constant K is experimentally obtained from the HCl/NaCl ratio in the aqueous phase (Shinohara and Fujimoto, in prep.).

than that of HCl, a significant amount of NaCl and other neutral species must be accumulated in the volcanic edifice or are consumed by other processes.

2) *Reaction of NaCl to HCl*

Shinohara and Fujimoto (in prep.) experimentally obtained the equilibrium constants of the following reaction at a temperature of 600°C and over the pressure range of 400 to 2000 bars; they found a large pressure dependence on the equilibrium constants (Fig. 2).

$$\underset{\text{(Andalusite)}}{1/2Al_2SiO_5} + \underset{\text{(Quartz)}}{5/2SiO_2} + \underset{aq}{1/2H_2O} + \underset{aq}{NaCl} = \underset{\text{(Albite)}}{NaAlSi_3O_8} + \underset{aq}{HCl} \qquad (1)$$

Thermodynamic analysis of the experimental result reveals that the large pressure dependence is due to the large difference in the partial molar volumes of NaCl and HCl in the hydrothermal fluid. Accepting the above discussion, Shinohara (1990) concluded that the equilibrium constant of any reaction which has NaCl and HCl on opposite sides will also have a large pressure dependence, i.e., the HCl/NaCl ratio in the hydrothermal solution will increase with decreasing pressure. Volcanic gas which originates from a magma at depth inevitably experiences a pressure decrease, and the reaction of the ascending hydrothermal fluids with silicate materials thus consumes NaCl and produces HCl.

Summary

The volcanic gas which originates from magma at depth experiences a large pressure gradient during ascent. Two important pressure dependent effects on the equilibrium constants of related reactions were discussed; 1) phase equilibrium in the NaCl-H_2O system, and 2) reaction equilibrium which converts NaCl to HCl. Both reactions will remove NaCl from the ascending hydrothermal fluid, and the latter reaction will add HCl to the fluid. The magmatic discharge at depth is differentiated to the volcanic gas through these reactions, with a large pressure dependence along the large pressure gradient.

The reaction of NaCl with silicate to form HCl should also produce Na-rich silicate minerals. Although Na-rich alteration is expected to occur in such high temperature acid environments according to the above discussion, it is not a widespread observation (though albite alteration is associated with the margins of some porphyry copper systems; R.H. Sillitoe, pers. comm., 1991). Since the stability field of the Na-rich silicates is limited to high temperature and low pressure conditions, Na-rich alteration may be decomposed by later, lower temperature alteration processes (such as overprinting propylitic alteration). NaCl released from magma should accumulate as NaCl-rich brine, NaCl deposits or Na-rich silicates around the degassing magma, until the thermal anomaly is sufficiently mature to establish a convecting cell interacting with overlying meteoric (or sea) water, with NaCl subsequently dissipated.

This discussion is limited to chlorine compounds purely because of the lack of experimental and theoretical studies of other species in hydrothermal solution, and these studies are needed for a more quantitative discussion. Since several forms of sulfur compounds including neutral salt species are expected under magmatic conditions, experimental studies on sulfur species may be the most important to consider next.

Reference

Burnham, C. W. (1979) Magmas and hydrothermal fluids. In Barnes, H. L., ed., Geochemistry of Hydrothermal Ore Deposits, John Wiley and Sons, p. 71-136.

Pitzer, K. S. and Pabalan, R. T. (1986) Thermodynamics of NaCl in steam. *Geochim. Cosmochim. Acta*, vol. 50, p. 1445-1454.

Shinohara, H. (1990) Pressure dependence of water/rock reaction and control of HCl/NaCl ratio. In Matsuhisa, Y., Aoki, M., and Hedenquist, J. W., eds., High temperature acid fluids and associated alteration and mineralization., *Rept. Geol. Surv. Japan*, vol. 277, p. 97-99.

———, Iiyama, J. T. and Matsuo, S. (1984) Comportement du chlore dans le systeme magma granitique-eau. *C. R. Acad. Sc. Paris*, vol. 298, p. 741-743.

———, ——— and ——— (1989) Partition of chlorine compounds between silicate melt and hydrothermal solutions: I. Partition of NaCl-KCl. *Geochim. Cosmochim. Acta*, vol. 53, p. 2617-2630.

Yoshida, M. and Ozawa, T. (1981) Amounts of some chemical components discharged from Satsuma-Iwo-jima volcano in relation to their feeding sources. *Kazan*, vol. 26, p. 25-34 (in Japanese with English abstract).

Rept. Geol. Surv. Japan, No. 279, p. 156-160, 1992

The Porphyry-epithermal Transition

Richard H. SILLITOE

27 West Hill Park, Highgate Village, London N6 6ND, England

Introduction

Epithermal mineralization in the shallow parts of porphyry systems has been recognized for nearly 20 years (Sillitoe, 1973; Wallace, 1979), but exploration and academic work during the gold boom of the last decade have added appreciably to both the number of documented examples and their interpretation. Selected geologic aspects of this work are highlighted here.

Overall relationships and metal associations

Epithermal gold and/or silver deposits of high-sulfidation (acid-sulfate) type are commonplace above porphyry copper deposits (Fig. 1A; Sillitoe, 1983), whereas those of low-sulfidation (adularia-sericite) type are less common and, where present, tend to be located peripheral to high-sulfidation environments and the uppermost parts of underlying porphyry deposits (Fig. 1A; Sillitoe, 1988). There is little concrete evidence for direct down-dip or along-strike transitions between high- and low-sulfidation gold and/or silver deposits. Given the broadly intermediate, commonly andesitic-dacitic compositions of the calc-alkaline or, locally, alkaline magmatism responsible for these porphyry copper systems, the epithermal mineralization is generally, but not exclusively, hosted by stratovolcanoes (Fig. 1A).

The porphyry copper deposits central to these I-type, magnetite-series magmatic systems contain subsidiary amounts of gold and/or molybdenum. However, less-studied, precious-metal-bearing epithermal settings hosted by volcanic domes are also present above tin deposits associated with felsic, reduced (ilmenite-series) porphyries in Bolivia (Fig. 1B), and are inferred above stockwork molybdenum deposits of Climax type in high-silica rhyolite stocks (Fig. 1C).

Spatial separations

The vertical intervals between porphyry-hosted and high-sulfidation epithermal environments are observed to be extremely variable, and range from zero to more than 1 km (Fig. 1; e.g., Vila and Sillitoe, 1991) - a parameter of considerable concern to the explorationist. Where the two environments are separated, the intervening "barren gaps" are characterized by one or more of intermediate argillic, sericitic, chloritic, and propylitic alteration, all of which are pyritic. Juxtaposition of the two environments in telescoped systems (Fig. 1D) places advanced argillic (quartz-alunite) alteration in contact with sericitic or intermediate argillic alteration which, in turn, are generally superimposed on preexisting K-silicate assemblages. Indeed, high-sulfidation assemblages, with or without copper and/or gold, are present locally as structurally localized overprints to K-silicate and/or sericitic alteration to deep levels within porphyry stocks (e.g., Sillitoe and Angeles, 1985).

Keywords: stratovolcano, dome, telescoping, magmatic fluid

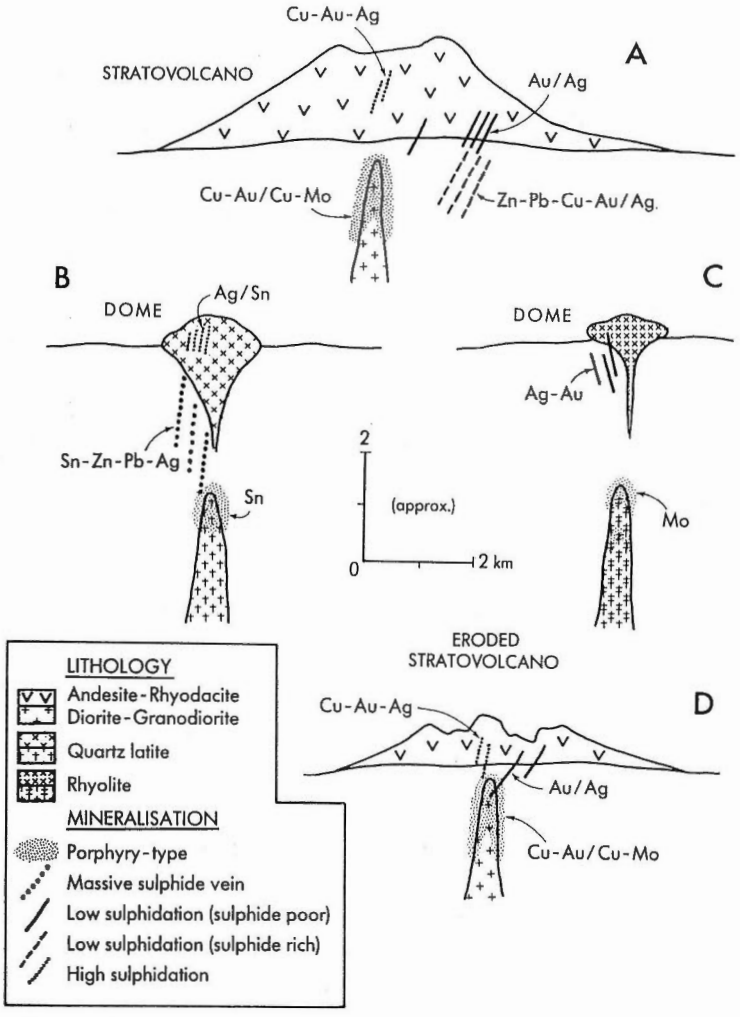

Fig. 1 Types of epithermal mineralization in porphyry-related copper, tin, and molybdenum systems.

Juxtaposition of low-sulfidation and porphyry deposits is apparently much less widespread, but takes place locally (e.g., Moyle *et al.*, 1990). Moreover, upward transitions from sulfide-rich, tin- and base-metal-bearing veins to low-sulfidation, silver-rich veins are present in some Bolivian districts (Fig. 1B).

Telescoping in intrusion-centered systems is believed to be due primarily to degradation of paleosurfaces during hydrothermal activity. Paleosurface lowering may be caused by high erosion rates (Fig. 1D) under tropical or glacial climatic conditions and/or gravitational collapse of volcanic edifices (Sillitoe, 1989). The latter process is capable theoretically of transforming porphyry into epithermal environments almost instantaneously.

Evidence for magmatic influence

A direct connection between porphyry and epithermal environments is suggested by several observations. First, appreciable amounts of copper, tin, and molybdenum attain the epithermal environments above porphyry-hosted copper, tin, and molybdenum deposits, respectively. Indeed copper, as enargite and/or covellite, is important economically in the high-sulfidation parts of some porphyry copper systems.

Second, high Ag/Au ratios characterize the epithermal environment in Bolivian tin systems, which suggests that these reduced, ilmenite-series magmas are incapable of releasing much gold. Third, high-sulfidation alteration and mineralization do not seem to be developed in rhyolite-hosted, epithermal environments (e.g., Berger and Bonham, 1990), such as those above Climax-type stockwork molybdenum deposits (Fig. 1C), which may suggest that the hydrothermal fluids are either released completely at depth and thereby neutralized before they reach epithermal levels (cf., Berger and Henley, 1989) or, more probably, are inherently far less sulfur-rich than those evolved from more basic magmas.

Consequently, magmatic components and conditions seem to exert a profound influence on the epithermal environment, which therefore cannot be a product exclusively of magmatically heated meteoric water. This conclusion is supported further by the worldwide distribution of epithermal deposits and, in particular, by the apparent absence of epithermal mineralization in many high heat flow extensional settings, such as the East African rift system and Iceland.

Aspects of a model

The role of magmatic fluids in the generation of copper, tin, and molybdenum deposits associated with porphyry stocks is well documented (e.g., Burnham and Ohmoto, 1980), and contrasts with the dominance of meteoric fluids in the epithermal environment (e.g., Hedenquist, 1987). However, given the evidence for magmatic input to epithermal deposits, a means of transforming magmatic to meteoric-dominated fluids is required. Condensation of magmatic volatiles into meteoric fluid regimes is an attractive possibility, and has been proposed specifically as a means of creating the low-pH fluids necessary to form high-sulfidation deposits (e.g., Sillitoe, 1983; Heald *et al.*, 1987).

Acid fluids responsible for high-sulfidation mineralization may be neutralized and transformed to fluids capable theoretically of generating low-sulfidation precious-metal deposits (e.g., Hedenquist, 1987; Berger and Henley, 1989). However, geologic relationships do not provide much support for operation of this mechanism, but rather suggest that high-sulfidation deposits above porphyry coppers and low-sulfidation deposits peripheral to them are the products of discrete fluids (Sillitoe, 1989). Indeed, an analogous situation is documented from many hydrothermally active stratovolcanoes, where acid fluids underlie the summit regions and neutral fluids are found beneath their flanks (e.g., Henley and Ellis, 1983). The acid and neutral fluids in at least some volcanoes seem to be generated independently (Giggenbach *et al.*, 1990).

Furthermore, intimate associations of advanced argillic assemblages and precious metals in high-sulfidation deposits confirm metal precipitation from acid fluids (e.g., Muntean *et al.*, 1990) rather than during introduction of late-stage

fluids of low-sulfidation type (e.g., Berger and Henley, 1989).

Concluding remark

Conclusive evidence for transitions between porphyry and epithermal environments will necessarily be geologic in nature, and increased efforts are required to obtain it. The varied spatial connections between the two environments are documented, at least preliminarily, but need the added support of detailed alteration, metal-ratio, fluid-inclusion, and isotopic studies.

References

Berger, B. R. and Bonham, H. F. Jr. (1990) Epithermal gold-silver deposits in the western United States: time-space products of evolving plutonic, volcanic and tectonic environments. *Jour. Geochem. Expl.*, vol. 36, p. 103-142.

——— and Henley, R. W. (1989) Advances in the understanding of epithermal gold-silver deposits, with special reference to the western United States. *Econ. Geol. Mongr.* no. 6, p. 405-423.

Burnham, C. W. and Ohmoto, H. (1980) Late-stage processes of felsic magmatism. *Mining Geol. Spec. Issue*, no. 8, p. 1-11.

Giggenbach, W. F., Garcia P. N., Londono, C. A., Rodriguez V. L., Rojas G. N. and Calvache V. M. L. (1990) The chemistry of fumarolic vapor and thermal-spring discharges from the Nevado del Ruiz volcanic-magmatic-hydrothermal system, Colombia. *Jour. Volcanol. Geotherm. Res.*, vol. 42, p. 13-39.

Heald, P., Foley, N. K. and Hayba, D. O. (1987) Comparative anatomy of volcanic-hosted epithermal deposits: Acid-sulfate and adularia-sericite types. *Econ. Geol.*, vol. 82, p. 1-26.

Hedenquist, J. W. (1987) Mineralization associated with volcanic-related hydrothermal systems in the Circum-Pacific basin, In Horn, M. K., ed., *Trans. Fourth Circum-Pacific Energy & Mineral Resources Conf.*, Singapore, 1986, p. 513-524.

Henley, R. W. and Ellis, A. J. (1983) Geothermal systems ancient and modern: a geochemical review. *Earth Sci. Rev.*, vol. 19, p. 1-50.

Moyle, A. J., Doyle, B. J., Hoogvliet, H. and Ware, A. R. (1990) Ladolam gold deposit, Lihir Island, In Hughes, F. E. ed., Geology of the Mineral Deposits of Australia and Papua New Guinea, vol. 2: *Australia. Inst. Mining Metallurgy Mongr.*, no. 14, p. 1793-1805.

Muntean, J. L., Kesler, S. E., Russell, N. and Polanco, J. (1990) Evolution of the Monte Negro acid sulfate Au-Ag deposit, Pueblo Viejo, Dominican Republic: Important factors in grade development. *Econ. Geol.*, vol. 85, p. 1738-1758.

Sillitoe, R. H. (1973) The tops and bottoms of porphyry copper deposits. *Econ. Geol.*, vol. 68, p. 799-815.

——— (1983) Enargite-bearing massive sulfide deposits high in porphyry copper systems. *Econ. Geol.*, vol. 78, p. 348-352.

——— (1988) Gold and silver deposits in porphyry systems, In Schafer, R. W., Cooper, J. J. and Vikre, P. G., eds., Bulk Mineable Precious Metal Deposits of the Western United States, *Proc. Symp., Reno, Nevada, 1987,*

Geol. Soc. Nevada, p. 233-257.

——— (1989) Gold deposits in western Pacific island arcs: The magmatic connection. *Econ. Geol. Mongr.*, no. 6, p. 274-291.

——— and Angeles, C. A., Jr. (1985) Geological characteristics and evolution of a gold-rich porphyry copper deposit at Guinaoang, Luzon, Philippines, In Asian Mining '85: London, *Inst. Mining Metallurgy*, p. 15-26.

Vila, T. and Sillitoe, R. H. (1991) Gold-rich porphyry systems in the Maricunga belt, northern Chile. *Econ. Geol.*, vol. 86, p. 1238-1260.

Wallace, A. B. (1979) Possible signatures of buried porphyry-copper deposits in middle and late Tertiary volcanic rocks of western Nevada. *Nevada Bur. Mines Geol. Rept.* no. 33, p. 69-76.

Rept. Geol. Surv. Japan, No. 279, p. 161-169, 1992

Fluids in the Source Regions of Subduction Zone Magmas: Clues from the Study of Volatiles in Mariana Trough Magmas

Edward M. STOLPER and Sally NEWMAN

Division of Geological and Planetary Sciences
California Institute of Technology, Pasadena, California 91125, U.S.A.

We have measured H_2O, CO_2, uranium, and chlorine concentrations in submarine basaltic glasses from the Mariana back-arc trough ("MT") at 18°N, whose chemical and isotopic compositions have been previously well characterized. The results conform to simple trends that allow us to derive relationships about the nature of heterogeneity and melting processes in the oceanic mantle in this region. In particular, we have been able to constrain the composition of the H_2O-rich fluid that is widely believed to have been added to the mantle wedge beneath volcanic arcs and its influence on petrogenesis. In the context of this meeting, the results may be compared and contrasted with estimates of the compositions of fluids exsolving from and coexisting with magmas in crustal environments.

(1) The dissolved H_2O and CO_2 contents of primitive Mariana trough basalts ("MTBs") are negatively correlated and plot near the vapor saturation curve for basaltic melt at a pressure of 400 bars (Fig. 1), approximately the pressure at which the samples erupted. When examined more closely, there is a good correspondence between the pressure at which each sample would have been vapor-saturated and the pressure at the depth at which it was collected. The vapors that would coexist with basaltic melts of these compositions ranges from nearly pure H_2O at one end of the trend to nearly pure CO_2 at the other. We conclude that these samples erupted on the sea floor under vapor-saturated conditions.

(2) Dissolved H_2O contents of submarine glasses are little influenced by bubble-growth (unless volatile-loss has been massive and/or the eruption is at a depth of a few hundred meters or less), whereas their CO_2 contents are usually modified by the exsolution of even small amounts of vapor. Thus, the H_2O contents of the MT glasses are expected to reflect accurately those of liquids prior to de-

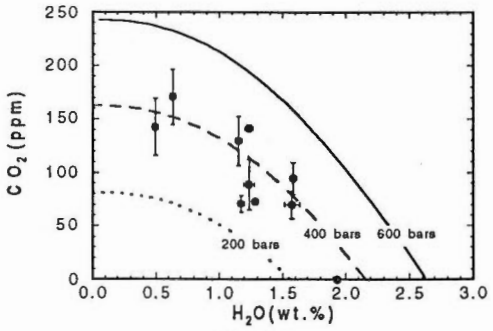

Fig. 1

Keywords: Mariana trough, back-arc basin, metasomatism, subducted slab, water, carbon dioxide, basalt

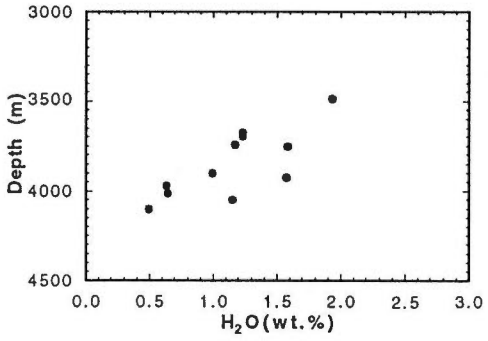

Fig. 2

gassing on ascent or cooling on the sea floor. This is consistent with measured H_2O and CO_2 contents of glass inclusions in phenocrysts in these samples and with the fact that the H_2O contents of the samples collected from the shallowest depths have the highest H_2O contents (Fig. 2). The extent of degassing must be greater at lower pressures, so it would be difficult to explain this latter observation by variable amounts of degassing since the samples that must have degassed the least (i.e., those erupted at the highest pressures) have the lowest H_2O contents. The observed inverse correlation between H_2O content and eruption depth must reflect something fundamental about magma genesis.

(3) The H_2O contents (0.5-2.0 wt%) of primitive basaltic glasses (MgO=6.5-8.1 wt%) from the MT are highly correlated with concentrations of major and trace elements and radiogenic and stable isotope ratios based on data in the literature (two examples are given in Fig. 3). The H_2O contents are positively correlated with the following elemental concentrations and isotopic ratios: Al, Ba, Ca, Cl, K, La, Rb, $^{87}Sr/^{86}Sr$, Sr, Th, and U. They are negatively correlated with the following elemental concentrations and isotopic ratios: C, Fe, Mn, Na, Nd, $^{143}Nd/^{144}Nd$, Sm, Ti, V, Y, and Zr. Silica shows little or no variation with H_2O content.

(4) Given that the samples on which these correlations are based have a limited MgO range and typically contain only olivine ± spinel as phenocryst phases, these correlations cannot be readily explained by high level fractionation (except for the variations V, which may reflect a correlation between the amount of spinel fractionation experienced by these liquids and their water contents and oxygen fugacities). We conclude that these correlations are inherited from the magmas parental to MTBs.

(5) To a good first approximation, primitive glasses from the MT define a linear array in composition space. This array extends from NMORB toward an end member defined by lavas similar in composition to primitive basaltic glasses from the Mariana island arc (Fig. 5). The concentrations of some incompatible elements (e.g., K, Rb, Sr) in the most arc-like MT samples are higher than the extension of the trend established by the bulk of the primitive MT samples (Fig. 5b).

(6) Except for the scatter at the arc-like end of the trend, the variations in chemical and isotopic composition observed among primitive Mariana back arc basin basalts can be explained by melting of mixtures of two mantle components. The characteristics of these components can be quantified given certain assumptions:
(a) We chose the source of the NMORB end of the observed compositional range of

Table 1 Compositions of end members in Mariana trough mantle sources (by wt.)

	NMORBS component	H_2O-rich component	
Ba	1.3	1120(78)	ppm
Cl	0.0003	1.19(0.09)	%
Cu	4.8	1997(201)	ppm
H_2O	0.026	44.15(0.89)	%
K_2O	0.0069	8.51(0.09)	%
La	0.26	99(8)	ppm
Na_2O	0.272	42.59(1.31)	%
Nd	0.67	147(9)	ppm
P_2O_5	0.0098	2.23(0.07)	%
Pb	0.031	16.9(0.6)	ppm
Rb	0.062	147(7)	ppm
Sc	9.0	1285(142)	ppm
Sm	0.24	34.5(2.9)	ppm
Sr	9.6	4682(146)	ppm
Ta	0.011	2.6(0.4)	ppm
Th	0.0059	13.2(0.5)	ppm
TiO_2	0.199	0.0	%
U	0.0042	4.4(0.1)	ppm
Y	2.4	294(26)	ppm
Zn	4.1	2070(239)	ppm
Zr	6.9	985(62)	ppm
δD	-55	-25	per mil
$^{87}Sr/^{86}Sr$	0.7026	0.7032	
$^{143}Nd/^{144}Nd$	0.5132	0.5129	
$^{206}Pb/^{204}Pb$	17.7	18.77(0.08)	
$^{207}Pb/^{204}Pb$	15.4	15.56(0.01)	
$^{208}Pb/^{204}Pb$	37.3	38.50(0.11)	

the MT samples as one end of this mixing line. The NMORB end member is assumed to have been generated by 5% melting, and the source (referred to as NMORBS) was constructed by adding 5% of NMORB to 95% of a residue assumed to have equilibrated with it, based on a set of reasonable partition coefficients (D's).

(b) The other end of the mixing line was calculated by an iterative procedure. We first guessed a composition of this second end member. Then, for each primitive MTB (~70 samples, excluding the most arc-like samples), we determined the best fit fraction (y) of this component in its source and the degree of melting (x) by which it was generated. We used these values of x and y to obtain a new, best fit estimate of the composition of the second mixing component. We then refit x and y for each sample and repeated the procedure until x and y for each sample and the concentration of each element in the end member converged to 1 part in 10^6. After convergence, best fit isotopic ratios of the second end member were obtained. In following this procedure, we assumed the second end member contained 0% TiO_2 and the elements whose concentrations were solved for summed to 100%. In practice, the assumption regarding TiO_2 is equivalent to assuming the TiO_2 contents of the mixed sources of the basalts are essentially constant. The constraint that the constituents of the second end member must sum to 100% has little effect on the ratios among these constituents; if the sum were constrained to 50%, all concentrations would change by about a factor of 2 (the isotopic ratios of this end member would change in a more complicated way).

(c) The fitting procedure succeeds in that it accounts for the chemical and isotopic

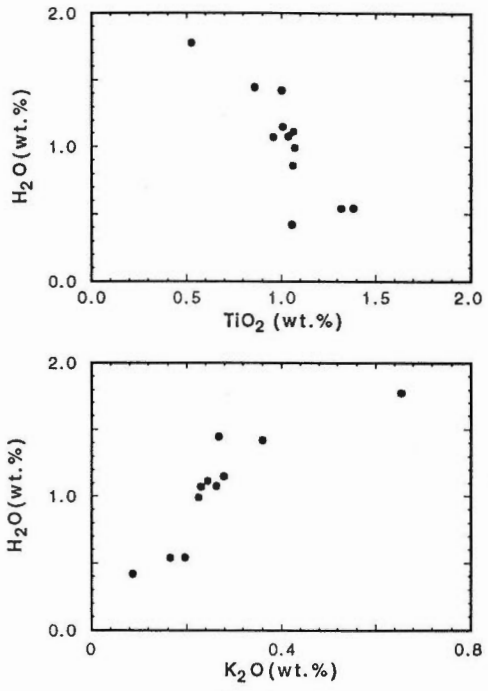

Fig. 3

compositions of each primitive MTB with only the variables x and y and two mantle components of constant composition.

(7) Although values of x and y for each sample depend on the D's we used, the composition of the second, H_2O-rich end member depends only weakly on them. The compositions of the two mantle end members given one set of D's are listed in Table 1. We emphasize that the H_2O-rich component represents an extreme because the components listed in Table 1 sum to 100%; there are infinite permissible H_2O-rich components, but all must lie on a line in composition space between the NMORBS end member and an end member with element ratios similar to the H_2O-rich end member given in Table 1.

(8) For a given set of D's, the degree of melting by which MTBs are generated is positively and approximately linearly correlated (Fig. 4) with the proportion of the second mantle component (referred to as the H_2O-rich end member). The ranges in x and y depend on the D's, but the slope is well defined. This result has several implications:

(a) Source enrichment in the H_2O-rich component is accompanied by an increase in the degree of melting (Fig. 4). If a doubling of the H_2O content of the source were accompanied by a doubling in the degree of melting, then the H_2O contents of melts would be independent of the degree of melting. However, for the MTBs, the degree of melting increases more slowly than the H_2O content of the source, so the H_2O contents of the melts increase with increasing degree of melting. All components that are positively correlated with H_2O in the MT samples are likewise being enriched in the mixed sources more rapidly than the degree of melting increases with addition of the H_2O-rich component. For elements such as La that vary little in the

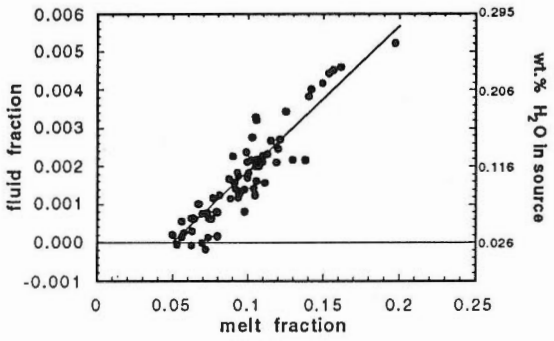

Fig.4

MT suite, the degree of enrichment in the source accompanying enrichment in the H_2O-rich component is roughly balanced by the increasing degree of melting. For elements that are negatively correlated with H_2O in the MT suite, their concentrations are either not enriched by addition of the H_2O-rich component or the increase is insufficient to compensate for the increased degree of melting (e.g., Na, Zr). Note that even though the H_2O-rich component is rich in Na_2O (H_2O/Na_2O~1), the Na_2O content of the melts decreases with increasing degree of melting because the Na_2O content of NMORBS is so high that the increase in the Na_2O content of the mixed sources is small relative to the increase in the degree of melting accompanying addition of the H_2O-rich component.

(b) The higher degrees of melting of the sources richer in the H_2O-rich component probably reflect the well known influence of H_2O on the solidus of mantle peridotite, although alternative explanations cannot be ruled out (e.g., temperatures could be systematically higher in sources with larger amounts of the H_2O-rich component). If this is correct, our work provides a quantitative estimate of the influence of water on degree of melting of mantle sources.

(c) Assuming that variation in H_2O content of the source is the major factor governing observed trends in major element composition among the primitive MT samples (and their extensions to primitive Mariana arc samples), these trends give insights into the influence of H_2O on phase equilibria and on the compositions of liquids generated by melting of wet mantle peridotite. With increasing degrees of melting, the Ca and Al contents of the melts go up, the Fe content goes down, and the Si content remains approximately constant. The increase in Ca is similar to the trend observed with progressive melting of dry sources provided Ca-rich pyroxene remains in the residue. The increase in Al content is opposite the trend in dry magmas and likely reflects the contraction of the liquidus volume of aluminous phases with the addition of H_2O. The decrease in Fe is similar to local trends but opposite to the global trend observed in MORB magmas. Reconstruction of the Mg contents of primary magmas parental to the primitive basalts from the MT by incremental addition of an equilibrium olivine component until the liquid can coexist with Fo90 olivine suggests that MgO contents of primary magmas in this suite decrease from ~13-14 wt% at the NMORB end of the trend to ~10-11 wt% at the arc-like end. We suggest that the well known progressive expansion of the olivine liquidus volume with H_2O content is responsible for the trends of decreasing Fe and Mg with increasing H_2O content and degree of melting; i.e., at a given degree of melting, wet liquids will

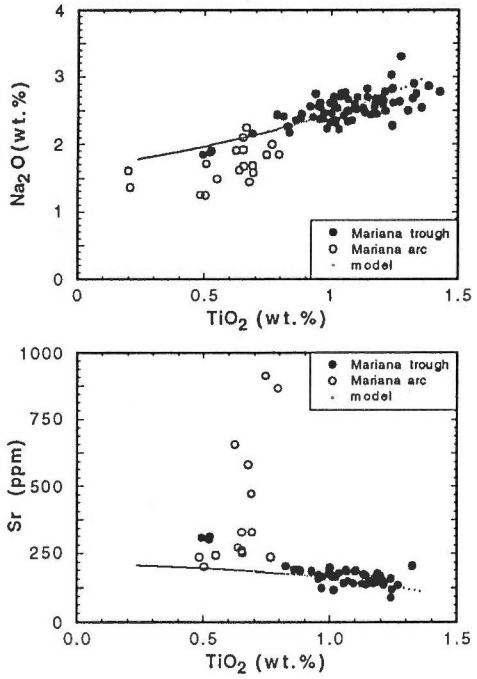

Fig. 5

have lower normative olivine contents than dry liquids. There is, however, a competition between this effect due to increasing water in the source and the increase in normative olivine that will be observed in progressive melts of a source of constant composition. The approximately constant Si content also reflects competition between these opposing effects.

(d) The high degrees of melting inferred for the arc-like end of the MT trend suggest, a priori, that the parental magmas of Mariana arc basalts are Mg-rich. The reconstruction described above of a parental liquid that could coexist with residual mantle olivine indicates MgO contents of 10-11% and supports this suggestion.

(e) Our analysis suggests that the degree of melting by which primitive basalts are generated increases from back-arc basin NMORB, through more H_2O-enriched back arc basin basalts, to island arc basalts. This effect is not a subtle one: according to our treatment, the degree of melting increases by a factor of 5 or more from MT NMORB to the Mariana island arc basalts (Fig. 4). According to this view, the low HFSE (e.g., Ti, Nb) concentrations of island arc basalts relative to NMORB are simple consequences of the higher amounts of melting involved in their generation (plus the fact that these elements are not sufficiently enriched in the H_2O-rich mantle component to overwhelm the effects of enhanced melting; see (8a) above). Depletions of HFSE relative to neighboring elements on "spider diagrams" reflect the enrichment of the H_2O-rich component in the neighboring elements relative to HFSE.

(f) The observation that magmas richer in H_2O are erupted at shallower water depths (Fig. 2) and previous recognition that arc-like MTBs are from higher elevations on the ridge are consistent with our conclusion that H_2O-rich, arc-like magmas were

generated by higher degrees of melting than. NMORB-like samples. Such a correlation between degree of melting and eruption depth has previously been observed for mid-ocean ridge basalts and in the MT probably reflects primarily the greater crustal thickness accompanying larger amounts of melt production and to a lesser extent density changes in the mantle accompanying melt production and segregation.

(g) Because H_2O causes a lowering of the solidus and is also an incompatible component, if fractional fusion were the dominant melting process in hydrous sources, no further melting would occur after the exhaustion of hydrous phases (crystals or vapor) until the solidus of the anhydrous residue were reached. The high degrees of melting implied for the H_2O-rich MT samples, which would not be saturated with hydrous vapor or a hydrous crystalline phase on their liquidi at mantle pressures, would thus appear to be inconsistent with simple fractional fusion and instead to favor a batch fusion process. Fractional fusion could occur, however, if more H_2O were resupplied to the source after each increment of melt extraction. Although the MT is not underlain by an actively subducting slab, ascent of H_2O-rich fluid generated by the subsolidus breakdown of hydrous phases at depths below the zone of melt generation might be a source of such resupply. Fractional fusion is plausible for melt generation beneath the Mariana arc where the nearby dehydrating slab can supply water to the mantle wedge continuously. The very high degrees of melting implied for the primitive arc basalts and the even higher degrees of melting inferred for boninitic magmas and their highly depleted sources are consistent with melting processes approaching fractional fusion in sources fluxed and refluxed with H_2O-rich fluids released from the underlying slab.

(9) Concentrations in primitive Mariana arc basalts and arc-like MT samples of compatible elements enriched in the H_2O-rich component (e.g., Na) and of incompatible elements not significantly enriched in this component (e.g., Ti, Ta, Nb, Zr) fall near the high degree of melting end of the trend established by the bulk of primitive MT samples (Fig. 5a). However, the concentrations in these samples of most incompatible elements enriched in the H_2O-rich component (e.g., K, Rb, Sr, Sm, Nd) are greater than or equal to the concentrations predicted by extension of the simple trends established by the bulk of the MT samples (Fig. 5b). We emphasize that although the concentrations of these elements in the arc samples can be up to a factor of 10 higher (e.g., Ba) than the concentrations predicted by the MT trends, the range of their concentrations appears to be floored by this trend.

(a) We propose the following explanation for this observation: Fluids escaping from the downgoing slab are initially out of equilibrium with the overlying mantle. We envision their interaction with the mantle as they flow through it to be similar to an ion exchange column. Compatible elements (i.e., with respect to fluid-mantle interaction) in the fluid come into equilibrium with the mantle after the fluid has flowed a relatively short distance, whereas fluids must flow along longer mantle paths before they lose their slab signature of more incompatible elements. We propose that the H_2O-rich component in the sources of most MT samples is formed by addition to NMORBS of H_2O-rich fluid that has interacted with sufficient NMORBS mantle that, for all but the most incompatible of components (e.g., H_2O), it has lost its slab signature and is almost fully equilibrated with NMORBS. If this is correct, then the ratio of the concentration of each element in the H_2O-rich component listed in Table 1 to its concentration in NMORBS represents an upper limit to the fluid/mantle partition coefficient for that element.

(b) By whatever paths fluid is transferred from the slab to the sources of MT

samples, such paths are undoubtedly typically longer and more complex than those followed by fluids moving from the slab to the sources of island arc basalts and the total amount of fluid reaching them is less. We thus expect that the fluids introduced into the sources of island arc lavas would, a priori, be more likely than those introduced into BABB sources to retain remnants of the slab signature in their most incompatible elements; for sufficiently compatible elements, the length of mantle column between the slab and the sources would always be sufficient to erase the slab signature. Given the complexity and variability of the paths followed by fluids to the sources of island arc magmas, the total effective length of the column for individual parcels of fluid may be quite variable, sufficient to have completely erased the slab signature in some cases but to have only partially erased it in others. For those samples from sources infiltrated by fluids in which this signature was completely erased, the fluid added to the source will have equilibrated with the mantle column (~NMORBS) and thus the sample will plot on the extension of the MT trend; note that there is no way (other than higher degrees of melting for the same degree of enrichment in the H_2O-rich component) that a sample can get below this trend. For a sample from a source infiltrated by fluids in which this signature was only partially erased, the fluid added to the source still has elevated concentrations of the most incompatible elements, and thus for those elements the sample would plot variably above the trend of the MT samples. Note that for the MT samples generated by the highest degrees of melting (and thus in our view from sources with the largest influxes of H_2O), fluid not fully equilibrated with the mantle column must have infiltrated their sources. Note also that the characteristics of a simple ion exchange column would approximate a mixing process for isotopes of a single element; thus it is possible for the elemental composition of the fluid to closely approach equilibrium with the mantle column but for its isotopic composition to retain a larger residual slab signature.

(10) Taking the H_2O-rich component listed in Table 1 as an estimate of fluid added to the sources of MT samples and assuming it is in equilibrium with NMORBS, we have estimated fluid/mantle partition coefficients for the elements listed in Table 1. Using these D's, we have evaluated the influence on mantle composition of the extraction and addition of such a fluid. Note that some partition coefficients (e.g., Cu, Pb) are poorly determined by our analysis because of limited data and that some would be expected to be highly sensitive to the major element composition of the fluid, which could be highly variable (e.g., CO_2 or Cl could dominate some mantle fluids).

(a) To a good approximation, NMORBS mantle can be generated by extraction of a few tenths of a percent of such a fluid from primitive mantle. Continental crust can be generated by several percent melting of primitive or NMORBS mantle enriched by several tenths of a percent in such a fluid. Local heterogeneities in MORB can also be explained by enrichments or depletions of a few hundredths of a percent of this fluid. Given the H_2O-rich nature of this fluid, correlations between H_2O contents and various trace element ratios would be expected if mobility of such fluid were indeed responsible for heterogeneity of mantle sources. Enrichments and depletion of only very small amounts of such a fluid are implied by this analysis. Note further that this fluid is rich in Th and U and has a high Th/U; it thus could be an effective agent for generating variations in Th/U in the mantle.

(b) We have avoided giving a name to the fluid we have invoked to explain mantle heterogeneity in the Mariana oceanic mantle and elsewhere; it could be a "H_2O-rich

silicate melt or a dense hydrous "vapor" rich in dissolved constituents. Our prejudice is that the agent of the enrichment of MT and arc sources in H_2O is a hydrous "vapor" rather than a silicate melt. If this is valid, then mobility of vapor in the mantle may be an important factor in generating mantle heterogeneity. Although the evolution of much of this heterogeneity could have been associated with subduction, other mantle environments in which hydrous fluid ("vapor"?) mobility is likely important (such as beneath mid-ocean ridges, around rising diapirs and deep intrusions of hydrous magma, and in ancient environments -- not necessarily restricted to subduction-- in which wet mantle dehydrated and melted) are also possibilities.

Rept. Geol. Surv. Japan, No. 279, p. 170-175, 1992

Getting the Gold from the Gas: How Recent Advances in Volcanic-Gas Research have Provided New Insight on Metal Transport in Magmatic Fluids

Robert B. SYMONDS*

Mineral Resources Department, Geological Survey of Japan
1-1-3 Higashi, Tsukuba, Ibaraki 305, Japan

High-temperature (600-1200°C) volcanic gases contain a number of trace metals including Zn and Cu, and it has often been presumed that these metals are degassed from magma (Zeis, 1929). However, recent advances in sampling and analytical techniques, and in thermochemical modeling provide new insight on the suite of transported elements and their origins, the volatile trace-element species, and on reaction processes in volcanic fumaroles.

In the past decade, much has been learned about the abundances of trace elements in volcanic gases by analyzing samples of condensed volcanic gas by modern analytical techniques (AAS, ICP-AES, ICP-MS, INAA, PLES) (Gemmell, 1987; Le Guern, 1987; Symonds *et al.*, 1987). Condensates have long been analyzed for common rock-forming elements (e.g., Na, K, Al, Ca, Fe, Mg), but the new methods make it feasible to obtain data for 20 to 40 elements, including highly volatile metals (e.g., Cd, Bi, Pb). Well-analyzed, high-temperature (>500°C) condensates are now available from Augustine (Symonds *et al.*, 1990), Merapi (Symonds *et al.*, 1987), Momotombo (Gemmell, 1987; Quisefit *et al.*, 1989), Mount St. Helens (Le Guern, 1988), Poas (Gemmell, 1987), San Cristobal (Gemmell, 1987), Showashinzan (Mizutani, 1970; Symonds and Mizutani, unpublished), Tolbachik (Menyailov and Nikitina, 1980), Usu (Le Guern, unpublished), and White Island (Christenson, unpublished). Selected analyses of volcanic gases, including metal contents from condensates, are shown in Table 1.

Our knowledge of trace element concentrations in volcanic gases has also benefited from the development of the treated filter method, whereby volcanic fume is pumped through base-treated filters to collect metals and acid gases, and the filters are later analyzed by INAA (Finnegan *et al.*, 1989). One advantage of this method is that it can be used to sample the plume downwind of an erupting volcano when it is not possible to collect condensates. Also, analyzing the filters by INAA allows detection of many trace elements. Treated-filter data are available from Augustine (Lepel *et al.*, 1978), Etna (Buat-Menard and Arnold, 1978), Heimaey (Mroz and Zoller, 1975), Kilauea (Olmez *et al.*, 1986; Crowe *et al.*, 1987), and Mount St. Helens (Phelan *et al.*, 1982).

Unfortunately, extracting the magmatic-gas component from analyses of condensates or treated-filters is difficult because the samples may have been contaminated by rock particles (Crowe *et al.*, 1987; Symonds *et al.*, 1987; Symonds *et al.*, 1990) or, for condensates, by the sampling materials (Symonds *et al.*, 1987; Gemmell, 1987). The use of enrichment factors, whereby the ratio of an element to

Keywords: volcanic gases, magmatic fluid, metal, condensate, sublimate

*Present address: U. S. Geological Survey, Cascades Volcano Observatory, 5400 MacArthur Blvd., Vancouver, WA 98661, U.S.A.

Table 1 Some analyses of high-temperature volcanic gases, excluding data for N2, rare gases, Dy, Eu, Hf, I, La, Lu, Sc, Ta, Th, U and Zr. All data in moles per 100 moles of gas.

Volcano:	AUGUSTINE	ETNA	MERAPI	MOMOTOMBO	SHOWA-SHINZAN	MOUNT ST. HELENS	TOLBACHIK	USU
Magma:	andesite	basalt	andesite	basalt	dacite	dacite	basalt	dacite
Date:	1987	1983	1979,1984	1986	1955	1981	1976	1985
T (^{o}C):	870	928	915	886	800	710	1010	649
log (fO_2):	-12.59	---	-12.49	---	---	-15.77	---	-17.00
Ref:	1	2	3,4	5	6,7	2	8	9,10
				Gas Species				
H_2O	83.91	91.9	88.87	92.87	98.0	98.6	97.95	99.33
H_2	0.63	0.7	1.54	1.06	0.63	0.39	0.75	0.22
CO_2	2.40	1.4	7.07	3.45	1.2	0.886	0.07	0.39
CO	0.020	0.0007	0.16	0.045	0.0033	0.0023	---	0.00041
SO_2	5.72	2.8	1.15	2.0	0.043	0.067	0.08	0.016
H_2S	1.00	---	1.12	0.16	0.004	0.099	0.11	0.026
S_2	0.20	---	0.08	---	---	---	---	---
HCl	6.04	0.1	0.59	0.35	0.047	0.076	0.75	0.011
NaCl	1.4×10^{-3}	1.2	1.3×10^{-3}	7.6×10^{-4}	---	4.1×10^{-4}	1.6×10^{-2}	1.2×10^{-4}
KCl	8.7×10^{-4}	1.2	8.2×10^{-4}	4.0×10^{-4}	4.5×10^{-4}	1.8×10^{-4}	7.6×10^{-3}	2.6×10^{-5}
HF	0.086	0.5	0.04	0.01	0.024	0.03	0.20	0.0056
HBr	6.8×10^{-4}	---	1.6×10^{-4}	8.4×10^{-4}	---	6.7×10^{-7}	8.1×10^{-4}	4.5×10^{-7}
				Other Elements				
Li	6.7×10^{-6}	---	5.6×10^{-6}	---	---	---	---	---
B	4.5×10^{-3}	---	2.8×10^{-3}	7.7×10^{-2}	5.6×10^{-3}	---	5.4×10^{-3}	5.8×10^{-3}
Mg	4.8×10^{-6}	5.5×10^{-3}	1.5×10^{-4}	3.9×10^{-4}	---	---	3.7×10^{-4}	2.2×10^{-5}
Al	2.7×10^{-5}	---	1.5×10^{-3}	7.8×10^{-4}	5.2×10^{-4}	1.6×10^{-4}	3.1×10^{-3}	3.7×10^{-5}
Si	8.3×10^{-3}	---	---	2.0×10^{-3}	8.8×10^{-3}	---	---	8.3×10^{-5}
Ca	4.6×10^{-5}	3.4×10^{-7}	---	3.6×10^{-4}	2.6×10^{-3}	4.9×10^{-7}	1.0×10^{-3}	2.8×10^{-5}
Ti	6.5×10^{-7}	---	---	3.5×10^{-5}	---	---	6.8×10^{-5}	---
V	1.5×10^{-7}	---	6.9×10^{-7}	---	6.9×10^{-8}	1.7×10^{-7}	---	3.9×10^{-9}
Cr	1.2×10^{-7}	---	1.5×10^{-6}	---	---	4.1×10^{-7}	8.7×10^{-7}	2.9×10^{-6}
Mn	1.7×10^{-6}	---	6.4×10^{-7}	1.5×10^{-5}	4.8×10^{-6}	1.0×10^{-7}	1.2×10^{-5}	1.1×10^{-4}
Fe	1.6×10^{-4}	5.0×10^{-3}	3.2×10^{-4}	4.6×10^{-4}	3.5×10^{-5}	6.4×10^{-6}	1.2×10^{-3}	1.6×10^{-5}
Co	---	2.2×10^{-6}	5.5×10^{-8}	---	---	1.2×10^{-8}	3.7×10^{-7}	5.2×10^{-8}
Ni	2.2×10^{-7}	---	1.4×10^{-6}	---	---	---	3.3×10^{-5}	---
Cu	6.9×10^{-6}	---	1.1×10^{-6}	2.4×10^{-5}	6.1×10^{-7}	1.5×10^{-6}	1.7×10^{-4}	3.3×10^{-7}
Zn	6.4×10^{-5}	4.0×10^{-4}	2.5×10^{-4}	2.3×10^{-5}	9.7×10^{-6}	5.4×10^{-7}	2.7×10^{-4}	1.1×10^{-6}
Ga			2.3×10^{-7}	---	---	---	---	1.7×10^{-7}
As	9.9×10^{-4}	1.7×10^{-4}	2.1×10^{-5}	8.9×10^{-5}	8.0×10^{-5}	3.3×10^{-5}	5.8×10^{-4}	3.6×10^{-7}
Se	---	1.1×10^{-4}	---	8.5×10^{-5}	---	6.8×10^{-7}	---	9.1×10^{-9}
Rb	---	-----	---	---	---	1.0×10^{-7}	1.6×10^{-5}	1.0×10^{-7}
Sr	5.3×10^{-8}	---	3.5×10^{-6}	---	7.3×10^{-7}	1.5×10^{-5}	---	1.3×10^{-7}
Mo	1.8×10^{-5}	---	2.0×10^{-6}	8.7×10^{-6}	9.4×10^{-7}	1.8×10^{-6}	---	1.1×10^{-6}
Ag	---	2.2×10^{-6}	---	7.8×10^{-8}	---	2.5×10^{-10}	1.0×10^{-7}	8.3×10^{-9}
Cd	2.1×10^{-6}	4.5×10^{-5}	5.7×10^{-7}	4.5×10^{-7}	1.4×10^{-7}	6.6×10^{-7}	8.0×10^{-6}	8.0×10^{-8}
Sn	---	---	---	1.4×10^{-5}	---	---	1.4×10^{-6}	1.1×10^{-4}
Sb	3.8×10^{-6}	3.9×10^{-7}	$<6.6\times10^{-7}$	2.3×10^{-5}	2.0×10^{-6}	1.2×10^{-7}	2.0×10^{-4}	7.3×10^{-9}
Te	---	---	---	---	---	1.3×10^{-7}	---	5.6×10^{-9}
Cs	---	8.1×10^{-5}	---	---	---	2.7×10^{-8}	5.2×10^{-6}	8.3×10^{-9}
Ba	2.8×10^{-8}	---	---	---	2.2×10^{-6}	2.6×10^{-9}	---	1.8×10^{-7}
W	---		6.1×10^{-7}	---	---	2.9×10^{-8}	---	2.9×10^{-8}
Ir	---	---	---	---	---	1.9×10^{-11}	---	5.4×10^{-12}
Au	---	2.5×10^{-7}	---	4.2×10^{-8}	---	3.0×10^{-10}	4.0×10^{-8}	6.5×10^{-11}
Hg	---	---	---	---	---	1.8×10^{-7}	---	7.1×10^{-10}
Pb	2.4×10^{-5}	1.2×10^{-4}	1.2×10^{-5}	2.8×10^{-6}	6.0×10^{-7}	4.7×10^{-6}	5.0×10^{-6}	5.2×10^{-8}
Bi	2.4×10^{-7}	3.6×10^{-5}	1.0×10^{-6}	---	2.5×10^{-7}	1.0×10^{-6}	---	---

--- = Below detection or no data reported. References: (1) Symonds et al. (1991); (2) Le Guern (1988); (3) Symonds et al. (1987); (4) Le Guern et al. (1982); (5) Quisefit et al. (1989); (6) Nemeto et al. (1957); (7) Symonds, Mizutani, and Briggs (unpublished); (8) Menyailov and Nikitina (1980); (9) Giggenbach and Matsuo (1991); (10) Le Guern (unpublished).

Table 2 Sublimates collected by artifically cooling volcanic gases in silica tube.

Volcano:	Augustine		Merapi		Momotombo		Mount St. Helens	
Ref:	1		2,3		4		5	
Sampling range:	870°-400°C		900°-100°C		890°-100°C		675°-400°C	
	Phase	T (°C)	Phase	T (°C)	Phase	T (°C)	Phase	T (°C)
	Magnetite	>710	Magnetite	900	Magnetite	>830	Magnetite	>570
	Cristobalite	>710	Cristobalite	900	Cristobalite	>830	Cristobalite	>570
	Mb	710	Hy (Mn,Zn)	900	Halite	>830	Mb (Fe,Re)	570
	Bornite	710	Acmite	650	Sylvite	>830	Fb (MN)	570
	Halite	650	Mb (Re)	650	Aphthitalite	>830	Halite	550
	Sylvite	610	Wf (Mn)	630	$CuFeS_2$	>830	Sylvite	550
	Pyrite	540	Halite	630	Mb	>830	Gr (Cu,Zn,Fe)	520
	Sph (Cd, In)	540	Sylvite	630	Pyrite	650	Galena (Bi,Sn)	480
	Fe-K sulfate	<500	Pyrite	550	Salammoniac	550	$Pb_3Bi_2S_6$ (Sn)	450
			Sph (Cd,Fe)	550	Thenardite	550	AsS (Fe)	400
			Galena (Bi,Sn)	450	Jarosite	450		
			Gb (Sn)	450	Cu-Fe sulfide	450		
			Pb Chlorides	300	Pb-As sulfide	350		
			Salammoniac(Br)	250	Galena	250		
			S (As,I,Tl,Se)	150	Pb	250		
					As	250		
					Se	250		
					Tl	250		
					S	250		

Temperature is maximum temperature of deposition. Elements between parentheses have concentrations of > 1 wt.% in the solid phase. Gb = galenobismutite, Gr = greenockite, Hy = hercynite, Mb = Molybdenite, Sph = sphalerite, Wf = wolframite. References: (1) Symonds (unpublished), (2) Le Guern and Bernard (1982), (3) Bernard (1985), (4) Quisefit et al. (1989), (5) Bernard and Le Guern (1986).

a non-volatile element is compared to the same ratio in the parent magma, is one way to interpret the origin of elements in such samples (Lepel *et al.*, 1978; Symonds *et al.*, 1987). Studies using this methods have shown that some rock-forming elements (e.g., Al, Ba, Ca, Mg, Sr, Ti) typically have enrichment factors near unity and therefore probably originate from rock-particle contaminants in the condensate or treated-filter samples (Symonds *et al.*, 1987; Symonds *et al.*, 1990). In contrast, the samples are often enriched by factors of 10 to 10^5 in a large suite of elements that may include Hg, Se, I, Te, Re, Bi, Cd, Au, Br, In, Pb, W, Mo, Cs, Sn, Ag, As, Zn, Rb, Cu, Li, K, Na, and Sb (Ir is also highly enriched in gases discharging from hot-spot volcanoes). These highly-enriched elements clearly represent products of magma degassing (Symonds *et al.*, 1987; Quisefit, 1989). Some elements (Cr, Fe, Ga, Mn, Si, V) have moderate enrichments (between 2 and 10); they may come from degassing magma, the wall rocks, or from both sources (Symonds *et al.*, 1990).

The advent of the silica-tube method to sample sublimates (Le Guern and Bernard, 1982) has also advanced the understanding of metal transport in volcanic gases. Using this technique, silica tubes are inserted into fumaroles and sublimates form on the inner walls of the tubes in an environment buffered by the volcanic gas; this isolates sublimates from solids that form (in natural incrustations) by reactions with the atmosphere or the wall rocks. Silica-tube sublimate studies have been carried out at Augustine (Symonds and Bernard, unpublished), Etna (Bernard, 1985; Le Guern, 1988), Kilauea (Bernard, 1985), Merapi (Le Guern and Bernard, 1982; Bernard, 1985; Symonds *et al.*, 1987), Momotombo (Bernard, 1985; Quisefit *et al.*, 1989), Mount St. Helens (Bernard and Le Guern, 1986), Poas (Toutain and Meyer, 1989; Toutain, 1987), Piton de la Fournaise (Toutain *et al.*, 1990), and Usu (Bernard, 1985; Bernard and Symonds, 1988). Selected examples of the sublimates collected in silica tubes are shown in Table 2.

Analyses of the Merapi sublimates show that these deposits are enriched by factors between 20 and 10^5 in Se, Re, Bi, Cd, Au, Br, In, Pb, W, Mo, Cl, Cs, Sn, Cl,

S, Ag, Zn, F, As, Rb, Cu, K, Na, and Sb (Symonds *et al.*, 1987), clearly indicating that these elements are products of degassing magma. Similar enrichments are observed at Augustine, except that Pb is much less enriched (Symonds, unpublished). Sublimates from hot-spot volcanoes are also enriched in Ir (Toutain and Meyer, 1989).

Recent advances in thermodynamic modeling of volcanic gases have provided insight on metal transport and reaction processes in volcanic gases. Constrained with samples of gases, condensates, sublimates, and magmas, the modeling can be used to predict (1) the amounts of trace elements degassed from magma, and (2) the solids that should precipitate from the gas upon cooling. The model's predictions are tested by comparing them with the measured trace-element concentrations and the observed sublimate sequence. Such modeling for Augustine (Symonds and Bernard, unpublished), Etna (Le Guern, 1988), Merapi (Symonds *et al.*, 1987), Momotombo (Quisefit *et al.*, 1989), and Usu (Bernard and Symonds, 1988) predicts that: (1) trace elements are volatilized from near-surface magma as chlorides (AgCl, BiCl, CuCl, CsCl, $FeCl_2$, LiCl, KCl, NaCl, $PbCl_2$, RbCl, $SbCl_3$, $ZnCl_2$), sulfides (AsS, AuS, BiS, PbS, SbS), oxyacids (H_3BO_3, H_2MoO_4, H_2WO_4), oxychlorides (MoO_2Cl_2, WO_2Cl_2), hydroxides ($Fe(OH)_2$), hydrides (H_2Se), and elemental species (Ag, Cd, Hg, Te, Zn) with the dominant species (i.e., BiCl or BiS) for each element dependent on the specific gas composition involved; (2) some rock-forming elements (e.g., Al, Ba, Ca, Sr) exist as rock particles---not gases---in the gas stream, as is also predicted by enrichment factor arguments; (3) near-surface cooling of the gases causes sublimates to precipitate in the order of their saturation temperatures; (4) equilibrium cooling of the gas below 200°C causes >99% of the metal to be removed from the gas by sublimation; and (5) condensates should be collected from vents hotter than 600°C to minimize the loss of metals by subsurface deposition.

Future studies should focus on improving the volcanic gas data base and on studying long-term degassing trends. We need a much larger data base on volcanic gases, especially on the concentrations of trace elements in volcanic gases. There are only a handful of volcanoes for which high-quality data exist for the major gases and the trace components. Clearly more data are needed, especially for very high-temperature gases (>800°C) that are most likely to yield direct information on magmatic fluids. We also need to study the temporal evolution of trace-element gases from active volcanoes. Ideally, this would involve a frequent and detailed sampling program (gases, isotopes, condensates, treated filters, sublimates) over many years and during various periods of volcanic activity.

References

Bernard, A. (1985) Les mecanismes de condensation des gaz volcaniques (chimie, mineralogie et equilibre des phases condensees majeures et mineures). Ph. D. dissertation, University of Brussels, Belgium, 412 p.

——— and Le Guern, F. (1986) Condensation of volatile elements in high temperature gases of Mt. St. Helens. *Jour. Volcanol. Geotherm. Res.*, vol. 28, p. 91-105.

——— and Symonds, R. B. (1988) The speciation of trace metals in high-temperature gases from Usu Volcano, Japan. *EOS*, Trans. Amer. Geophys. Union, vol. 69, p. 514-515.

Buat-Menard, P. and Arnold, M. (1978) The heavy metal chemistry of atmospheric

particulate matter emitted by Mount Etna Volcano. *Geophys. Res. Lett.*, vol. 4, p. 245-248.

Crowe, B. M., Finnegan, D. L., Zoller, W. H. and Boynton, W. V. (1987) Trace-element geochemistry of volcanic gases and particles from 1983-1984 eruptive episodes of Kilauea volcano. *Jour. Geophys. Res.*, vol. 92, p. 13708-13714.

Finnegan, D. L., Kotra, J. P., Hermann, D. M. and Zoller, W. H. (1989) The use of ^{7}LiOH-impregnated filters for the collection of acidic gases and analysis by instrumental neutron activation analysis. *Bull. Volcanol.*, vol. 51, p. 83-87.

Gemmell, J. B. (1987) Geochemistry of metallic trace elements in fumarolic condensates from Nicaraguan and Costa Rican volcanoes. *Jour. Volcanol. Geotherm. Res.*, vol. 33, p. 161-181.

Giggenbach, W. F. and Matsuo, S. (1991) Evaluation of results from Second and Third IAVCEI Field Workshops on Volcanic Gases, Mt Usu, Japan, and White Island, New Zealand. *Appl. Geochem.*, vol. 6, p. 125-141.

Le Guern, F. (1988) Ecoulements gazeux reactifs ahautes temperatures, mesures et modelisation. Ph. D. dissertation, Univ. of Paris (in French), 314 p.

———— and Bernard, A. (1982) A new method for sampling and analyzing sublimates. Application to Merapi Volcano, Java. *Jour. Volcanol. Geotherm. Res.*, vol. 12, p. 133-146.

————, Gerlach, T. M. and Nohl, A. (1982) Field gas chromatograph analyses of gases from a glowing dome at Merapi volcano, Java, Indonesia, 1977, 1978, 1979. *Jour. Volcanol. Geotherm. Res.*, vol. 14, p. 223-245.

Lepel, E. A., Stefansson, K. M. and Zoller, W. H. (1978) The enrichment of volatile elements in the atmosphere by volcanic activity: Augustine volcano 1976. *Jour. Geophys. Res.*, vol. 83, p. 6213-6220.

Menyailov, I. A. and Nikitina, L. P. (1980) Chemistry and metal contents of magmatic gases: the new Tolbachik volcanoes gas (Kamchatka). *Bull. Volcanol.*, vol. 43, p. 197-207.

Mizutani, Y. (1970) Copper and zinc in fumarolic gases of Showashinzan volcano, Hokkaido, Japan. *Geochem. Jour.*, vol. 4, p. 87-91.

Mroz, E. J. and Zoller, W. H. (1975) Composition of atmospheric particulate matter from the eruption of Heimaey, Iceland, *Science*, vol. 190, p. 461-464.

Nemoto, T., Hayakawa, M., Takahashi, K., and Oana, S. (1957) Report on the geological, geophysical, and geochemical studies of Usu volcano (Showa-shinzan). *Rept. Geol. Surv. Japan*, no. 170, p. 1-149.

Olmez, I., Finnegan, D. L. and Zoller, W. H. (1986) Iridium emissions from Kilauea volcano. *Jour. Geophys. Res.*, vol. 91, p. 653-663.

Phelan, J. M., Finnegan, D. L., Ballantine, D. S., Zoller, W. H., Hart, M. A. and Moyers, J. L. (1982) Airborne aerosol measurements in the quiescent plume at Mount St. Helens: September, 1980. *Geophys. Res. Lett.*, vol. 9, p. 1093-1096

Quisefit, J. P., Toutain, J. P., Bergametti, G., Javoy, M., Cheynet, B. and Person, A. (1989) Evolution versus cooling of gaseous volcanic emissions from Momotombo Volcano, Nicaragua: Thermochemical model and observations. *Geochim. Cosmochim. Acta*, vol. 53, p. 2591-2608.

Symonds, R. B., Rose, W. I., Reed, M. H., Lichte, F. E. and Finnegan, D. L.

(1987) Volatilization, transport and sublimation of metallic and non-metallic elements in high temperature gases at Merapi Volcano, Indonesia. *Geochim. Cosmochim. Acta*, vol. 51, p. 2083-2101.

———, ———, Gerlach, T. M., Briggs, P. H., Harmon, R. S. (1990) Evaluation of gases, condensates, and SO_2 emissions from Augustine Volcano, Alaska: the degassing of a Cl-rich volcanic system. *Bull. Volcanol.*, vol. 52, p. 355-374.

———, Reed, M. H., and Rose, W. I. (1992) Origin, speciation, and fluxes of trace-element gases at Augustine volcano, Alaska: Insights into magma degassing and fumarolic processes. *Geochim. Cosmochim. Acta* vol. 56, p., 633-657

Toutain, J. P. (1987) Contribution a l'etude des sublimes volcaniques. Mineralogie, geochimie, thermodynamique. Exemples du Momotombo, du Piton del la Fournaise et due Poas. Ph. D. dissertation, Univ. of Paris, 190 p.

——— and Meyer, G. (1989) Iridium-bearing sublimates at a hot volcano (Piton de al Forunaise, Indian Ocean). *Geophys. Res. Lett.*, vol. 16, p. 1391-1394.

———, Aloupogiannis, P., Delorme, H., Person, A., Blanc, P., and Robaye G. (1990) Vapor deposition of trace elements from degassed basaltic lava, Piton de la Fournaise volcano, Reunion Island. *Jour. Volcanol. Geotherm. Res.*, vol. 40, p. 257-268.

Zeis, E. G. (1929) The Valley of 10,000 Smokes, the fumarolic incrustations and their bearing on ore deposition. *Nat. Geogr. Soc. Tech. Paper*, vol. 1, no. 4, p. 61-79.

Rept. Geol. Surv. Japan, No. 279, p. 176-178, 1992

Magmatic Contributions to the Hot Springs in the Hokusatsu Gold Metallogenic Province, Kyushu, Japan.

Sachihiro TAGUCHI[1], Hidemi INAMORI[2], Akito KOGA[3], Itsuro KITA[4] and Keisuke NAGAO[5]

[1] *Fukuoka University, Nanakuma Jonan-ku, Fukuoka 814-01, Japan*
[2] *Saibu Gas Co. Ltd., Higashihama, Higashi-ku, Fukuoka 812, Japan*
[3] *Emeritus Professor of Kyushu University, Tatomi, Shime-machi, Kasuya-gun, Fukuoka 811-22, Japan*
[4] *Akita University, Tegata-gakuen-machi, Akita 010, Japan*
[5] *Okayama University, Yamada, Misasa-cho, Tohaku-gun, Tottori 682-02, Japan*

Many epithermal gold vein deposits are located in the Hokusatsu gold metallogenic province of South Kyushu. All but one deposit formed in the Pleistocene (Kushikino gold deposit formed in the Pliocene). Izawa and Urashima (1987) pointed out that the site of gold mineralization migrated to the east, following the migration of volcanic activity.

Among the gold deposit, the Hishikari mine is famous for its anomalously high-grade ore and the large amount of estimated gold reserves (more than 250 metric tons of gold). The deposit was formed at 1 Ma, and 65°C hot spring water is still rising along the veins (Izawa *et al.*, 1990).

In and around the Hokusatsu gold metallogenic province, geothermal activity is common, ranging from high temperature geothermal systems (300°C on the flank of Kirishima volcano) to low temperature hot springs (20 to 40°C); these features are hosted by volcanic and sedimentary basement rocks (Shimanto Group). Besides the Hishikari gold mine, several gold deposits (Okuchi and Iriki) are also associated with hot springs. In this study, about 60 hot springs from the province were sampled and their composition analyzed.

The composition of the hot springs which discharge directly from sedimentary basement rocks are alkaline $NaHCO_3$ type (pH>9), with low concentrations of Cl and other total dissolved components. Furthermore, the dissolved sulfur species are dominantly reduced (i.e., low SO_4/H_2S).

On the other hand, hot springs issuing from the region of volcanic rock have relatively high Cl concentration and a near neutral pH, and oxidized sulfur species are dominant (i.e., high SO_4/H_2S).

This chemistry of sulfur species in hot spring waters suggests that the sedimentary basement rocks of the Shimanto Group play an important role during gold mineralization, preventing oxidation of the ore solution. If so, then we deduce that the boundary between volcanic rocks and the basement will be the best place for high grade ore mineralization. The Hishikari gold deposit is located in just such a geologic setting.

Hot springs associated with gold deposits of the Hokusatsu region (Hishikari and Iriki) are relatively high in Cl content and also high in free CO_2, and the dissolved sulfur species are dominantly oxidized. However, unfortunately, sampling of original hot spring water from the Okuchi mine is difficult at present, since the

Keywords: chemistry, hot spring, gold deposits, noble gas, magmatic contribution, Hishikari

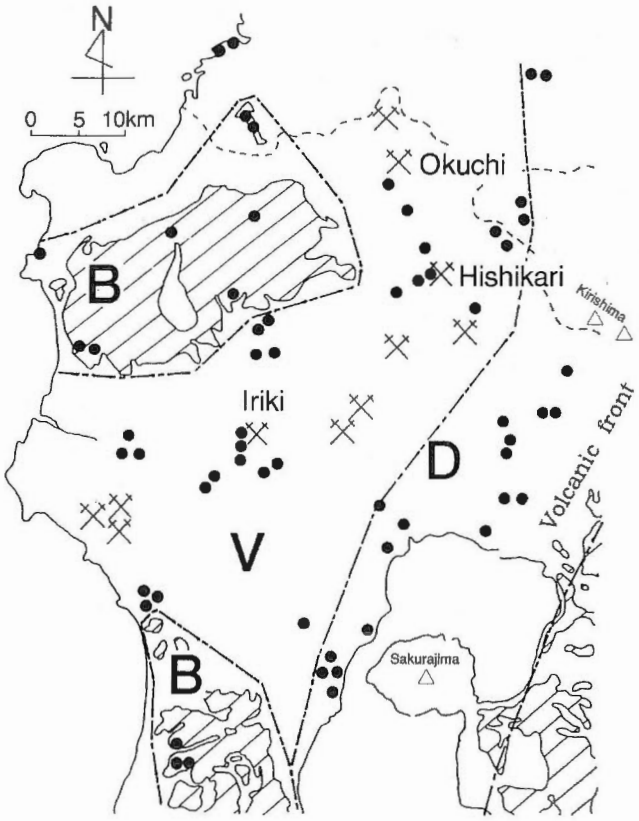

Fig. 1 Location of hot springs and gold deposits in the Hokusatsu metallogenic province, Kyushu, Japan.
Solid circle: hot springs, B: Basement zone (Shimanto group), V: Older volcanic zone (Late Miocene to middle Pleistocene), D: Depression zone where presently active volcanoes are distributed.

mine is filled by ground water.

The del 13 of carbon in CO_2 gas from the Hishikari gold deposits has a range of -5 to -6 per-mil, indicating a volcanic origin.

The isotopic composition of rare gases from the hot springs associated with the Iriki and Hishikari gold deposits indicate a magmatic origin; $^3He/^4He=9.18\text{-}5.34\times10^{-6}$, $^4He/^{20}Ne=37.5\text{-}212$. These values are similar to those of the volcanic gases from Kyushu ($^3He/^4He=10.2\text{-}10.6\times10^{-6}$, $^4He/^{20}Ne=16\text{-}64$; Nagao *et al.*, 1981). Why are Cl contents of hot springs from Hishikari and Iriki anomalouly high, as much as 450 and 1300 mg/l, respectively? Just below the Hishikari mine, Kawasaki *et al.* (1986) reported a low resistivity zone (less than 10 ohm-m) at more than 8km below the surface. Furthermore an anomalous low resistivity zone (less than 1 ohm-m) corresponds to a partially molten magma, deeper than 10km.

The geologic structure and the composition of hot springs and gases at Hishikari suggest that the fracture which formed gold vein systems extends to depths where the temperature is high, approaching magmatic conditions with CO_2 and rare gases of magmatic origin still ascending along the fracture. Therefore, the

high Cl content of hot springs at Hishikari and Iriki may have originated from HCl (now neutralized) from the deep heat source.

Refferences

Kawasaki, K., Okada, K. and Kubota, R. (1986) Geophysical surveys in the Hishikari mine area. *Mining Geol.*, vol. 36, p. 131-147 (in Japanese with English abstract).

Izawa, E. and Urashima, Y. (1987) Geologic and tectonic setting of the epithermal gold and geothermal areas in Kyushu. In Urashima, Y. ed., Gold Deposits and Geothermal Fields in Kyushu., *Soc. Min. Geol. Japan., Guidebook* 2, p. 1-12.

———, ——— , Ibaraki, K., Suzuki, R., Yokoyama, T., Kawasaki, K., Koga, A. and Taguchi, S. (1990) The Hishikari gold deposit: high grade epithermal veins in Quaternary volcanics of southern Kyushu, Japan. *Jour. Geochem. Explor.*, vol. 36, p. 1-56.

Nagao, K., Takaoka, N. and Matsubayashi, O. (1981) Rare gas isotopic compositions in natural gases of Japan. *Earth Planet. Sci. Lett.*, vol. 53, p. 175-188.

Rept. Geol. Surv. Japan, No. 279, p. 179-182, 1992

Geometrical Relationship Between Hydrothermal Convection Systems and Their Heat Source: Examples from the Hohi and Sengan Geothermal Areas in Japan

Shiro TAMANYU

Geological Survey of Japan
1-1-3 Higashi, Tsukuba, Ibaraki 305, Japan

Introduction

Deep geothermal drilling to 2 to 3 km in the Hohi and the Sengan geothermal systems identified the subsurface isotherms (MITI, 1987; NEDO, 1989a, b). These isotherms indicate that high temperature zones correlate with horst structures, where the top of pre-Tertiary basement is relatively shallow within Quaternary volcanic terrain. Based on these data, the geometrical relationship between the geothermal convection systems in the Tertiary and Quaternary formations, and high temperature conductive zones in the pre-Tertiary basement was determined.

Detailed volcano-stratigraphic study, including precise K-Ar dating of young volcanic rocks in these areas, clarified the stratigraphic subdivision, with special reference to geothermal activity (NEDO, 1990a, b). Based on these volcano-stratigraphic data, the geometrical relationship between the high temperature conductive zones in the pre-Tertiary basement and the magma chambers related to the young volcanism was determined.

Hohi geothermal area, northern Kyushu

Maps of subsurface isotherms indicate that high temperature zones at -500 m sea level are concordant with zones of high gravity anomaly which correlate with shallow pre-Tertiary basement (Fig. 1). This means that hydrothermal convection occurs mainly in porous Neogene formations, while conductive heat transfer occurs mainly in the pre-Tertiary basement. In other words, the deep subsurface temperature distribution pattern is primarily controlled by pre-Tertiary basement structure within young volcanic terrain. Also, volcano-stratigraphic data suggest that the magma chamber related to older volcanism of middle Pleistocene still plays an important role as a potential geothermal heat source, in addition to the magma chamber related to the youngest volcanism of late Pleistocene.

Sengan geothermal area, northern Honshu

Geothermal exploration drill holes proved that geothermal systems with potential for development are underlain by high temperature Neo granitic intrusive bodies (Fig. 2) (Nishi *et al.*, 1989; Doi *et al.*, 1990), and the high temperature zones are concordant with high gravity anomaly zones. These data may indicate that a

Keywords: hydrothermal convection, heat source, isotherms, Hohi geothermal area, Sengan geothermal area

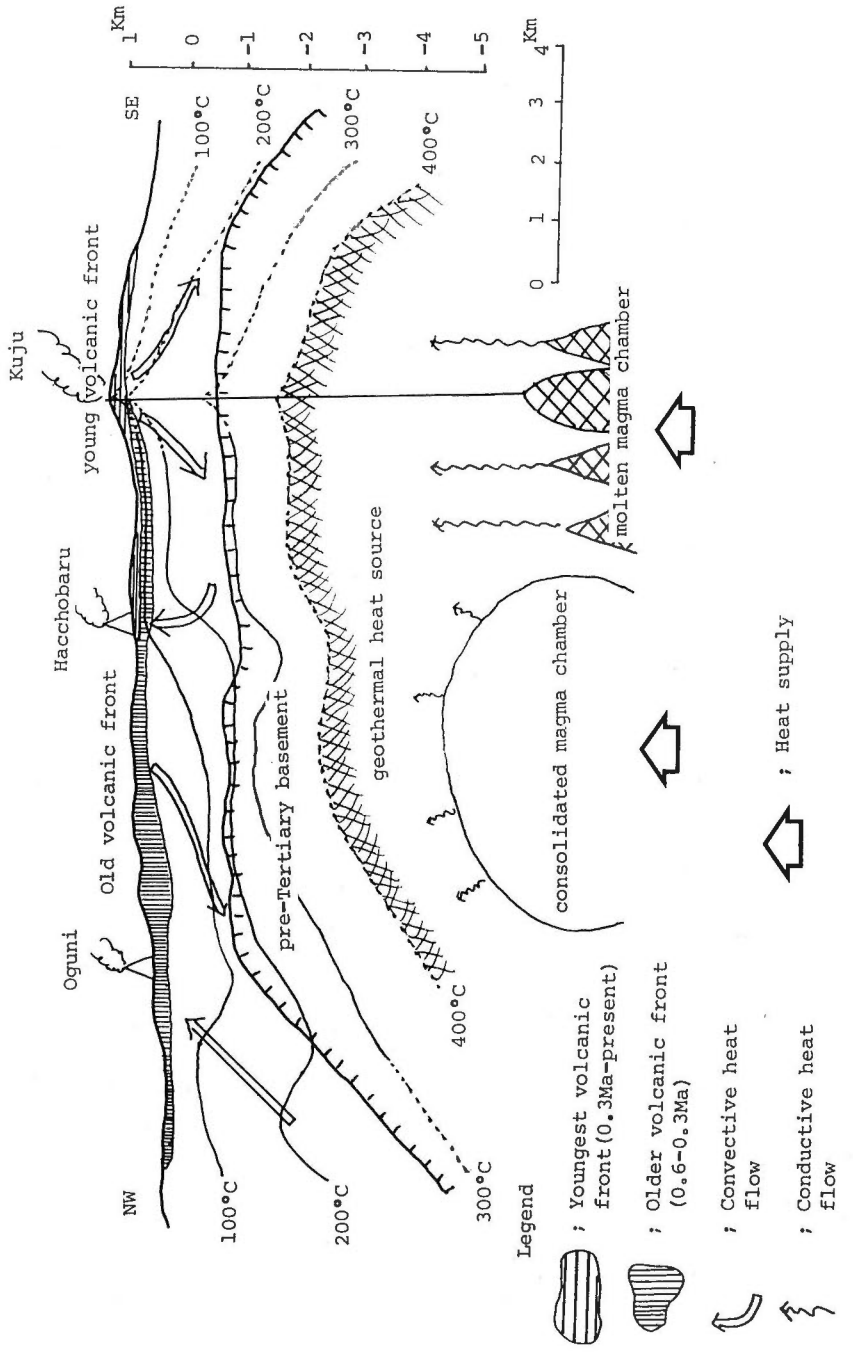

Fig. 1 Geothermal cross section in the Hohi area

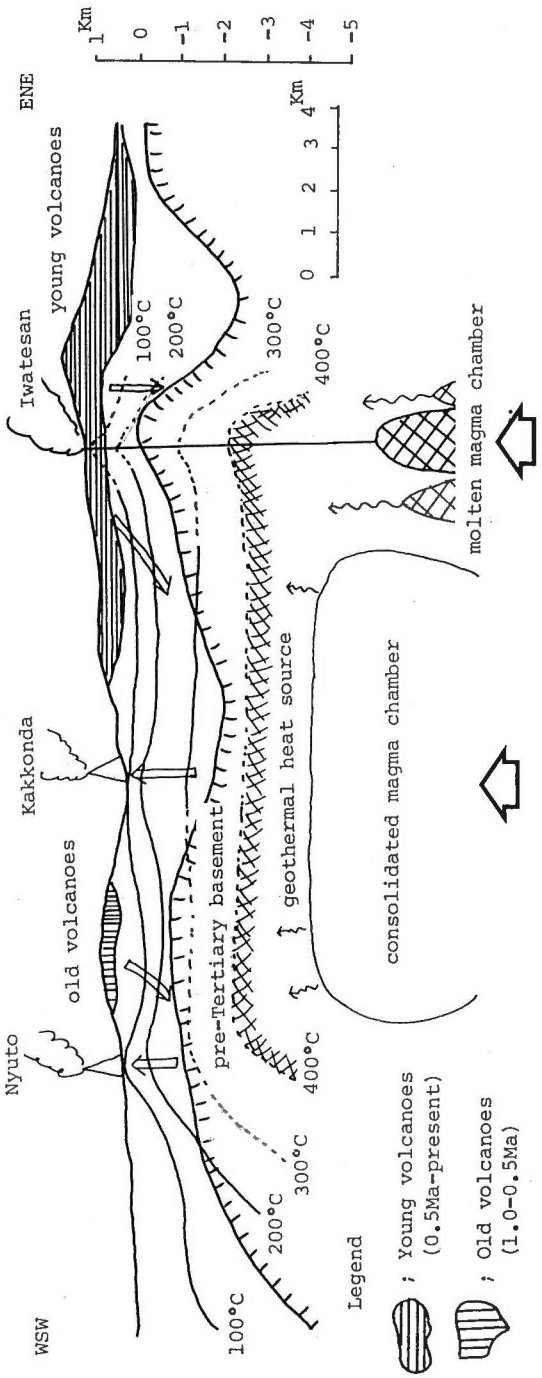

Fig. 2 Geothermal cross section in the Sengan area

granitic pluton, recently intruded, maintains a high residual heat potential, or has a very high thermal conductivity which allows a high heat flow from a deeper heat source to the overlying Neogene formations.

Future work

The heterogeneity of pre-Tertiary basement must be investigated from the view point of rock properties to help identify the potential for deep seated geothermal reservoirs.

Heat and mass balances of hydrothermal systems must be determined to evaluate the heat potential of the deeper geothermal heat sources.

Acknowledgement

The author would like to express his sincere thanks to Dr. J. Hedenquist for critical reading of the manuscript.

References

Doi, N., Kato, O. and Muramatsu, Y.(1990) On the neo-granite and geothermal reservoir in the pre-Tertiary rocks at the Kakkonda geothermal field, Iwate prefecture (abstract). *Geotherm. Res. Soc. Japan, 1990 Annual Meeting, Poster* 6.*

MITI (Ministry of International Trade and Industry)(1987) Synthetic evaluation report of the environmental assessment of large scale power generation using deep geothermal reservoir (Hohi area), 117 p.*

NEDO (New Energy Development Organization)(1989a) Final report of the survey to identify and promote geothermal development, no. 13 (Kuju area). 768 p.*

——— (1989b) Synthetic analytical report of the confirmation study of the effectiveness of prospecting techniques for deep geothermal resources, and its diagram collection. 438 p.*

——— (1990a) Final report and atlas of the nationwide geothermal resources exploration project (phase 3), regional exploration of geothermal fluid circulation system (Tsurumidake area). 86 p.*

——— (1990b) Summarized report of the 1990 fiscal year volcanic distribution and age determination survey for the nationwide geothermal resources exploration project (phase 3), regional exploration of geothermal fluid circulation system (Akitakomaarea). 98 p.*

Nishi, Y., Mimura, T., Abe, A., Takagi, S., Tamanyu, S. and Noda, T.(1989) N61-SN-7D well surveys of the confirmation study of the effectiveness of prospecting techniques for deep geothermal resources in Sengan geothermal area. *Geothermal Energy, Jour. Geotherm. Energy Development Center, N.E.F.*, vol. 14, p. 2-26.*

* written in Japanese

Rept. Geol. Surv. Japan, No. 279, p. 183-186, 1992

Chemical and Isotopic Composition of Fumarolic Gases from Kamchatka and the Kurile Islands

Yuri A. TARAN

Institute of Volcanic Geology and Geochemistry
Petropavlovsk-Kamchatsky 683006, Russia

During the last decade we succeeded in sampling many fumaroles of the Kamchatkan volcanoes and several volcanoes of the Kurile Islands. After 1981, gas samples were collected by the method of Giggenbach (1975) in alkaline solution. In addition to a large collection of high temperature gas analyses from Tolbachik volcano lava flows (Menyailov *et al.*, 1984), we managed also to collect a few high-temperature magmatic gas samples from the hornito of the 1988 eruption of Klyuchevskoy volcano at 4100m ASL (Taran *et al.*, 1991).

Our results and those of Menyailov are shown in Table 1; some have been published elsewhere (Flerov *et al.*, 1982; Taran, 1985; Menyailov *et al.*, 1988; Taran *et al.*, 1991, 1992). Here I outline several features of Kamchatka-Kurile volcanic gases:

1) All gas samples are water-rich and usually S >> Cl.

2) Volcanic vapor, even for basaltic volcanoes (Alaid, Mutnovsky, Klyuchevskoy, Kudryavy), is significantly enriched in deuterium relative to MORB or "Primary Magmatic" waters.

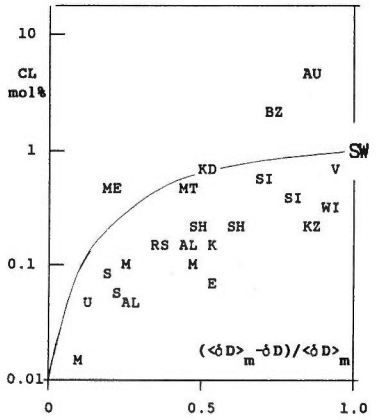

Fig. 1 Chlorine-deuterium correlation for fumarolic gases. Relationship between Cl-contents (log Cl, mol%) and relative deviation of fumarolic from the local meteoric water value - <δD>m. Volcanoes and references: AU - Augustine (Symonds *et al.*, 1990); BZ - Bezymyanny (Menyailov *et al.*, 1987); SI - Satsuma-Iwojima (Matsuo *et al.*, 1974), V - Volcano (Giggenbach and Matsuo, 1991); ME - Merapi (Allard, 1983); MT -Momotombo (Menyailov *et al.*, 1986); WI - White Island (Giggenbach and Matsuo, 1991); E - Ebeko (Menyailov *et al.*, 1985); AL - Alaid (Flerov *et al.*, 1982); U - Usu (Giggenbach and Matuso, 1991); S - Showashinzan (Mizutani and Sugiura, 1982); SH -Shiveluch; K - Koryak; KZ - Kizimen; M - Mutnovsky; RS - Rasshua; KD - Kudryavy (this study); SW - Seawater

Keywords: Kamchatka volcanoes, Kurile volcanoes, fumaroles, gas composition, isotopic composition

Table 1 Geochemical data on volcanic gases of the Kamchatka-Kurile Arc.

Volcano	Sampling date	t°C	H_2O mol %	H_2	CO_2 mol %	CO %	S_{tot} in dry gas	HCl	HF	N_2	Ar	He x10^4	δD	$\delta^{18}O$	$\delta^{13}C$	$\delta^{34}S_{tot}$	$^3He/^4He$ x10^6
							Fumarolic gases										
Shiveluch	11.09.79	216	98.2	0.09	94.33	0.00	1.9	3.67	0.01	-	-	-	-24	+3.7	-10.0	-	-
Shiveluch	12.09.79	152	99.3	0.42	95.64	0.00	1.06	2.86	0.01	-	-	-	-44	+1.4	-	-	-
Bezymyanny[1]	14.07.85	446	88.7	4.47	04.48	0.032	29.11	16.80	0.17	10.03	0.88	-	-28	+7.0		-	-
Kisimen	10.08.79	240	92.0	4.47	88.54	0.00	5.49	1.50	0.0	-	-	-	-16	+9.4	-14.4	-	-
Koryaksky	05.06.83	213	94.51	1.33	90.62	0.00	6.06	1.53	0.06	0.4	0.003	12	-58	+0.1	-11.5	-	6.8
Avacha	23.02.91	101	88.20	0.02	76.32	0.002	23.20	0.01	0.02	0.4	0.04	-	-	-	- 6.3	6.8	-
Mutnovsky	07.83	360	98.7	6.7	39.2	0.004	42.8	7.4	1.97	1.18	0.81	9	-90	-3.6	-11.8	7.0	-
Mutnovsky	07.83	272	98.8	2.9	83.1	0.001	11.08	1.32	0.08	1.5	0.06	5	-110	-11.4	-8.5	-	7.8
Mutnovsky	08.82	127	98.8	0.02	70.4	0.00	10.9	0.31	0.01	17.8	0.5	17	-65	-2.6	-	-	11.3
Mutnovsky	07.83	97	97.8	0.5	56.3	0.00	39.6	2.5	0.04	1.0	0.02	13	-74	-4.4	-	8.8	6.9
Alaid[2]	06.06.81	700	90.95	33.02	57.19	0.64	7.12	1.49	0.75	-	-	-	-44	+6.0	-	-	-
Alaid	07.81	160	91.26	6.5	86.62	0.03	6.15	0.71	0.08	-	-	11	-60	-2.3	-	-	4.4
Ebeko[3]	23.08.81	144	98.56	0.01	78.92	-	16.18	4.52	0.02	0.39	0.003	40	-36	-2.5	-10	5.3	6.6
Ebeko[3]	21.07.85	120	97.91	0.002	83.12	10^{-4}	16.47	0.28	0.04	-	0.087	-	-36	-3.3	-11.6	-	6.8
Ebeko[3]	30.06.84	101	94.81	0.01	96.6	-	3.35	0.05	0.02	0.01	-	-	-61	-8.5	-	-	-
Rasshua	06.86	100	98.21	2.97	63.04	0.00	28.14	0.69	0.002	5.12	0.04	-	-45	-3.3	- 8.6	-	-
Rasshua	06.86	151	96.21	0.9	50.35	0.00	43.41	3.05	0.001	2.24	0.02	16	-42	-2.0	- 6.4	-	5.4
Kuntamintar	07.86	155	93.5	0.4	70.1	0.00	26.4	1.5	0.02	1.3	0.02	-	-29	-0.9	-10.6	-	6.1
Kuntamintar	07.86	166	96.4	0.05	64.2	0.00	21.6	0.7	0.01	8.6	0.24	8	-44	-2.9	-	-	5.7
Kudryavy	08.90	770	96.0	8.98	63.78	0.19	20.11	6.52	0.4	-	-	-	-	-	- 4.7	2.0	-
Kudryavy	08.90	511	96.1	1.56	78.3	0.01	16.12	4.0	-	-	-	-	-38	+7.6	- 4.5	5.9	-
Kudryavy	08.90	430	96.7	8.52	40.55	0.035	37.02	13.09	0.69	-	-	-	-39	+2.7	- 5.2	-	-
Groxny	09.90	220	92.2	1.8	82.54	0.05	14.92	0.72	0.01	-	-	-	-39	-2.7	- 8.4	7.8	-
Groxny	09.90	160	96.6	18.75	49.9	0.0	24.25	7.02	0.11	-	-	-	-39	+2.5	- 7.1	-	-
							Magmatic gases										
Tolbachik[4]	1975	1000	78.56	33.3	52.7	4.32	2.1	6.3	1.2	-	-	-	-70	+4.0	- 3.5	-	1.8
Tolbachik[4]	1976	1100	97.77	35.2	4.4	0.05	13.2	40.6	6.5	-	-	-	-	-	-30.0	-	1.4
Klyuchevskoy	25.7.88	1050	90.84	18.86	49.58	1.72	1.66	24.96	3.21	-	-	-	-44	+8.4	-11.6	8.6	-

1-Menyailov *et al.*, 1987; 2-Flerov *et al.*, 1982; 3-Menyailov *et al.*, 1985; 4-Menyailov *et al.*, 1984.

3) Helium ratios are typical for island arc signatures, though the high values for the Mutnovsky volcano likely need additional checking.

4) Carbon of CO_2 is generally lighter in isotopic composition than "normal magmatic" carbon, even for the magmatic gases of Klyuchevskoy volcano. The values tend to be heavier in ^{13}C to the south. The $\delta^{13}C$ for the south Kuriles has typical island arc values (Allard, 1983). However, we need more data, since the observed trend is based on a few analyses only.

5) The total sulfur has a range typical of the isotopic composition for island arc volcanoes (Sakai and Matsubaya, 1977; Allard, 1983; Taylor, 1986).

The main problem is to explain the heavy hydrogen values. A simple plot shown in Figure 1 may shed some light on the problem. All the δD data and Cl contents in the available fumarolic gas samples are plotted on the coordinates: log[Cl] (mol%) versus (<δD>m - δD)/<δD>m, where <δD>m is the average local meteoric water value and δD is the observed value. The mixing line between meteoric water and seawater is shown for reference.

The data for low temperature fumaroles (<400°C) lie below the mixing line and appear to have an exponential (linear in semilogarithmic coordinates) dependence with respect to chlorine contents, relative to the deviation from average meteoric water values.

The majority of the data for high temperature fumaroles lie above the mixing

line, except for those strongly contaminated by meteoric water from Usu and Showashinzan volcanoes in Japan, as well as gas possibly contaminated by seawater from White Island, New Zealand.

Such a dependence may be related to the existence of a boiling acid solution (brine) inside the volcanic edifice. HCl distribution between steam (fumarolic gas) and solution will depend on various factors: pH (degree of neutralization, i.e., water-rock interaction); salinity (balance between magmatic and meteoric contributions, and the evaporation plus latent outflows), and depth (PT-conditions). This is not a new idea, but the question remains why most of the low temperature gases have Cl contents limited by the seawater value.

References

Allard, P. (1983) The origin of hydrogen, carbon, sulfur, nitrogen and rare gases in volcanic exhalations; evidence from isotope geochemistry. In Tazieff, H. and Sabroux, J-C., eds., Forecasting Volcanic Events, Elsevier, Amsterdam, p. 337-386.

Flerov, G. B., Ivanov, B. V., Andreyev, V. N. and Menayilov, I. A. (1982) Composition of the products of the 1981 eruption of Alaid volcano. *Volcanology and Seismology*, no. 6, p. 28-43 (in Russian).

Giggenbach, W. F. (1975) A simple method for the collection and analysis of volcanic gas samples. *Bull. Volcanol.*, vol. 39, p. 132-145.

——— and Matsuo, S. (1991) Evaluation of results from second and third IAVCEI field workshop on volcanic gases, Mt. Usu, Japan, and White Island, New Zealand. *Appl. Geochem.*, vol. 6, p. 125-141.

Matsuo, S., Suzuki, T., Kusakabe, M., Wada, H. and Suzuki, M. (1974) Isotopic and chemical compositions of volcanic gases from Satsuma-Iwojima, Japan. *Geochem. Jour.*, vol. 8, p. 165-173.

Menyailov, I. A., Nikitina, L. P. and Shapar, V. N. (1984) Geochemical features of volcanic gases. In Fedotov, S. and Markhinin, E., eds., The Large Tolbachik Fissures Eruption., Moscow, Nauka, p. 286-310 (in Russian).

———, ——— and ——— (1985) Results of geochemical monitoring of the activity of Ebeko volcano (Kurile Islands) used for eruption prediction. *Jour. Geodynamics*, vol. 3, p. 259-274.

———, ———, ——— and Pilipenko, V. P. (1986) Temperature increase and chemical changes of fumarolic gases at Momotombo volcano, Nicaragua, in 1982-1985: Are these indicators of a possible eruption? *Jour. Geoph. Res.*, vol. 91, p. 12199-12214.

———, ——— and ——— (1987) Chemical and isotopic composition of the gases from pyroclastic flows of 1985 eruption of Bezymyanny volcano. *Volcanology and Seismology*, no. 4, p. 40-49 (in Russian).

Mizutani, Y. and Sugiura, T. (1982) Variation in chemical and isotopic compositions of fumarolic gases from Showasinzan volcano, Hokkaido, Japan. *Geochem. Jour.*, vol. 16, p. 63-71.

Sakai, H. and Matsubaya, O. (1977) Stable isotope studies of Japanese geothermal systems. *Geothermics*, vol. 5, p. 97-124.

Symonds, R. B., Rose, W. I., Gerlach, T. M., Briggs, P. H., and Harmon, R. S. (1990) Evaluation of gases, condensates, and SO_2 emissions from Augustine volcano, Alaska: The degassing of a Cl-rich volcanic system.

Bull. Volcanol., vol. 52, p. 355-374

Taran, Y. A. (1985) The fumarolic activity of Koryak volcano in 1983. *Volcanology and Seismology*, no. 3, p. 53-56 (in Russian).

———— , Rozhkov, A. M., Serafimova, E. K. and Esikov, A. D. (1991) Chemical and isotopic composition of magmatic gases from the 1988 eruption of Klyuchevskoy volcano, Kamchatka. *Jour. Volcanol. Geoth. Res.*, vol. 46, p. 255-263.

———— , ———— , Pilipenko, V. P., and Vakin, E. A. (1992) A geochemical model for the fumaroles of Mutnovsky volcano, Kamchatka. *Jour. Volcanol. Geotherm. Res.*, vol. 49, p. 269-293.

Taylor, B. E. (1986) Magmatic volatiles: Isotopic variation of C, H and S. In Valley, J. W., Taylor, H. P., Jr., and O'Neil, J. R., eds., Stable Isotopes., *Reviews in Mineralogy*, vol. 16, p. 185-225.

Rept. Geol. Surv. Japan, No. 279, p. 187-189, 1992

Hydrogen Isotopes in Amphiboles and Micas from Quaternary Lavas of the Kamchatka-Kurile Arc System

Y. A. TARAN[1], B. G. POKROVSKY[2] and O. N. VOLYNTS[2]

[1] *Institute of Volcanic Geology and Geochemistry*
Petropavlovsk-Kamchatsky, 683006, Russia
[2] *Geochemical Institute*
7 Pyzhevsky P., Moscow, 109017, Russia

The hydrogen isotope composition and water content have been measured in amphiboles and micas (biotites) from lavas of Quaternary volcanoes of the Kamchatka-Kurile Arc. This is the first study of the δD variations in OH-bearing minerals of volcanic rocks along a whole arc system to determine if there is a systematic regional distribution of δD values in arc magmas. The D/H ratios in this suite of minerals display large variations, but their mean values reach a maximum (up to -25 per mil SMOW) in lavas of the Central Kuriles and decrease to the north and to the south (Fig. 1). Such behavior is similar to that reported for both $^{87}Sr/^{86}Sr$ ratios and ^{10}Be concentrations in volcanic arc lavas (Bailey *et al.*, 1987; Ikeda *et al.*, 1987; Tsvetkov and Volynets, 1990; Vinogradov *et al.*, 1986; Volynets *et al.*, 1988; Zhuravlev *et al.*, 1987).

Correlations between δD and halogens are observed for biotites only (Fig. 2 and 3). All biotites from the Kurile Islands are from submarine volcanoes and their D/H ratios decrease with increasing water and chlorine contents (Volynets *et al.*, 1989), whereas for biotites from Kamchatka lavas an increase in water contents is observed. These opposite trends overlap around δD values of -60 to -50 per mil, and such values may represent the isotopic composition of "subduction" water, i.e., water released from the subducted oceanic slab.

The observed maxima of δD and ^{10}Be contents and minimum of $^{87}Sr/^{86}Sr$ ratios in the Central Kuriles volcanoes correspond to the zone of thinner crust and probably to the least contamination of mantle wedge magmas by crustal material. The main processes responsible for the wide spectrum of δD values in OH-bearing minerals of magmatic rocking arc are as follows:

1. Mixing of mantle and oceanic crustal material (fluids) in the mantle wedge above the subduction zone.
2. Introduction of magmas into surrounding water-saturated rocks while residing in magma chambers and conduits.

As a result of the former process, aqueous fluids with δD of -60 per mil and with low Sr isotopic ratios and high ^{10}Be contents are generated. In the second case fluids with δD values from light meteoric ("continental") type to heavy marine ("submarine") type are in equilibrium with magmas which, in a "continental" environment, have high Sr isotope ratios and lower ^{10}Be contents.

References

Bailey J. C., Larsen, D. and Frolova, T. I. (1987) Strontium isotope variations in low

Keywords: hydrogen isotope, amphibole, biotite, Kamchatka-Kurile, volcanic arc

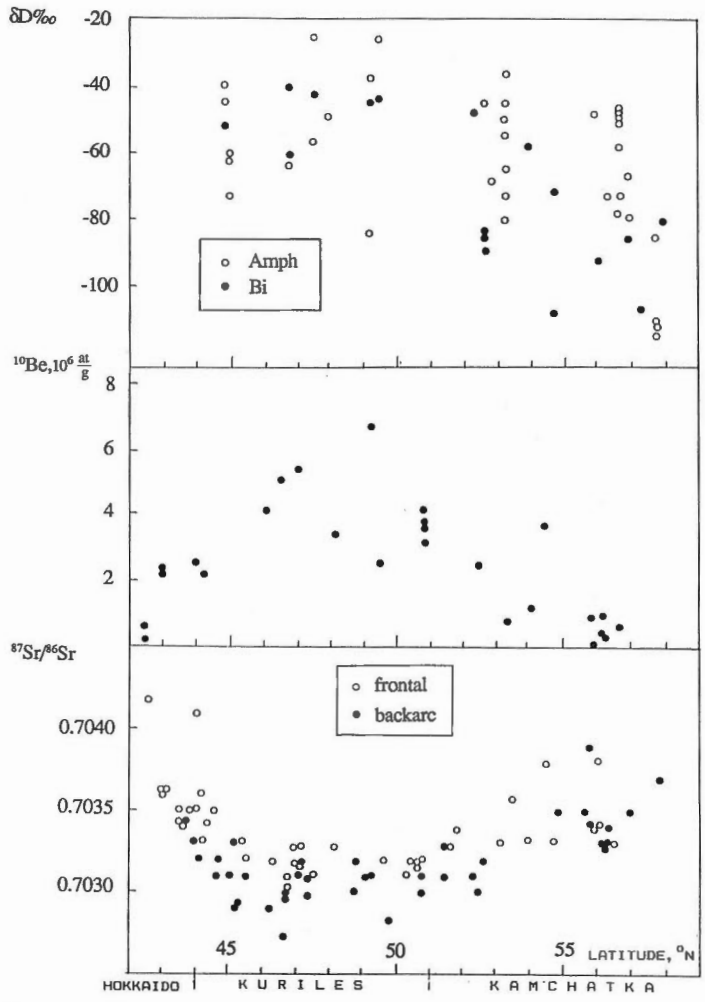

Fig. 1 Distribution of δD of OH-bearing minerals from recent lavas (this work), ^{10}Be contents and $^{87}Sr/^{86}Sr$ rations in recent lavas along the Kurile-Kamchatka Arc (see references).

Tertiary-Quaternary volcanic rocks from the Kurile Island Arc. *Mineral. Petrol.*, vol. 95, p. 155-165.

Ikeda, Y., Katsui, Y. and Kurasawa, H. (1987) Origin of lateral variations of $^{87}Sr/^{86}Sr$ ratios of Quaternary volcanic rocks from the Kurile Arc in Hokkaido, Japan. *Jour. Fac. Sci., Hokkaido Univ.*, ser. IV, vol. 22, p. 325-335.

Tsvetkov, A. A. and Volynets, O.N. (1990) First data on ^{10}Be in present volcanics of the Kurile-Kamchatka Arc in relation to sediment subduction. *Isotopenpraxis*, vol. 26, p. 803-807.

Vinogradov V. I., Grigoriev, V.S. and Pokrovsky, B.G. (1986) Isotopic composition of strontium and oxygen in the rocks of the Kurile-Kamchatka Arc: A key to some genetic suggestings. In Nauka, M. ed., Evolution of crust-mantle

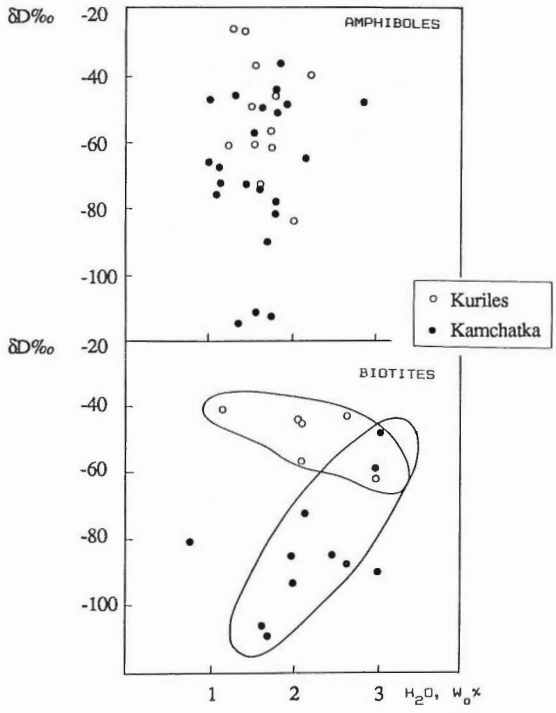

Fig. 2 Correlation between δD and water contents for amphiboles and biotites from Kurile-Kamchatka lavas.

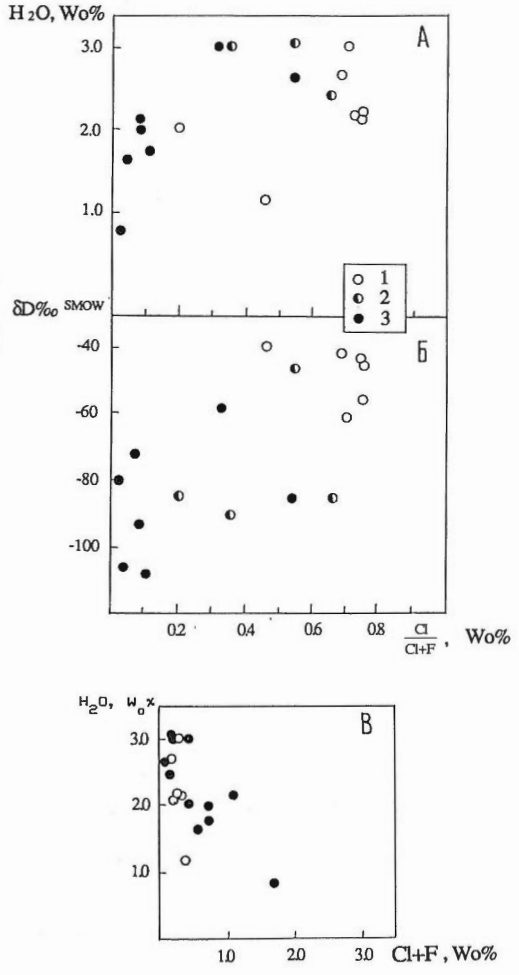

Fig. 3 Correlation between δD and Cl and also between H2O contents and Cl and F+Cl for biotites from Kurile-Kamchatka lavas. 1 - Kuriles; 2 - South Kamchatka; 3 - Central and North Kamchatka.

system. p. 78-103.

Volynets O. N., Avdeiko, G. P., Vinogradov, V. I. and Grigoryev, V. S. (1988) A Sr-isotope zonality in Quaternary lavas of the Kurile-Kamchatka Arc. *Thikhokeanskaya Geologia*, vol. 1, p. 19-27.

———, Bushlyakov, I. N. and Voronina, L. K. (1989) Halogens in micas from volcanic rocks of Kurile-Kamchatka Arc System. *Doklady Acad. Nauk SSSR*, vol. 309, p. 693-697.

Zhuravlev, D. Z., Tsvetkov, A.A., Zhuravlev, A.G., Gladkov, N.G. and Chernyshov, I.V. (1987) $^{143}Nd/^{144}Nd$ and $^{87}Sr/^{86}Sr$ ratios in recent magmatic rocks of the Kurile Island Arc. *Chem. Geol.*, vol. 86, p. 227-243.

Rept. Geol. Surv. Japan, No. 279, p. 190-194, 1992

Degassing of H_2O From Rhyolite Magma During Eruption and Shallow Intrusion, and the Isotopic Composition of Magmatic Water in Hydrothermal Systems

B. E. TAYLOR

Geological Survey of Canada
601 Booth Street, Ottawa, Ontario K1A 0E8, Canada

Introduction

The isotopic composition of magmatic water has long been a point of reference in isotopic studies of hydrothermal systems. The range of composition of the "magmatic water box" on a δD-$\delta^{18}O$ diagram was calculated from isotopic data on magmatic rocks. Hydrogen isotope studies of obsidian from tephra and related rhyolite flows of both small eruptions in western North America (Taylor *et al.*, 1983; Newman *et al.*, 1988) and very large eruptions in the Taupo Volcanic Zone, New Zealand (Taylor *et al.*, 1990) have revealed a common co-variation between δD and wt. % H_2O, now recognized as a fingerprint of H_2O degassing. The δD and water content of the magma decrease during depressurization, eruption, and shallow intrusion. "Second boiling" of magma at shallow levels has a more limited effect on δD because of the small amount (<10%) of the original water remaining. These studies suggest that the variation of δD in magmatic rocks is an indicator of a related magmatic process. If hydrous minerals in shallow-level magmatic rocks represent but a small fraction of the original water content of the melt at that level, then the δD of the rock is not necessarily representative of the accumulated magmatic water which may comprise a component of a hydrothermal system. The obsidian data permit an accurate estimate for the δD of the magma prior to degassing, i.e., of the total magmatic water, and is very similar for several different volcanic systems. The composition of the magmatic water which may accumulate in the hydrothermal system may be quite restricted, and not accurately represented by the "magmatic water box".

Isotopic systematics of obsidian

The δD and water contents of obsidian clasts co-vary in tephra from small (< 2 km^3), young deposits at Medicine Lake Highlands, Inyo Volcanic chain, and Mono Craters in California (USA). This variation is also stratigraphic: δD and wt. % H_2O both decrease upwards, from older to younger tephra layers. The general range of δD of the obsidian tephra clasts is -90 to -50 per mil, with a range of respective water contents from ca. 0.5 to as much as 3.1 wt. % H_2O. The young ages (<2000 yrs. old), narrow range of $\delta^{18}O$ (+7 to +8 per mil), and lack of petrographic evidence for hydration or alteration indicates that the δD-water content variation is a primary characteristic of these samples of quenched magma erupted with pumice to produce the layered tephra deposits. Subsequent obsidian flows contain glass with the lowest water contents (all <0.5 wt. % H_2O; to as low as 0.1) and lowest δD (as low as -130 per mil).

Keywords: magmatic water, degassing, hydrogen isotope, isotopic fractionation, rhyolite, obsidian, tephra

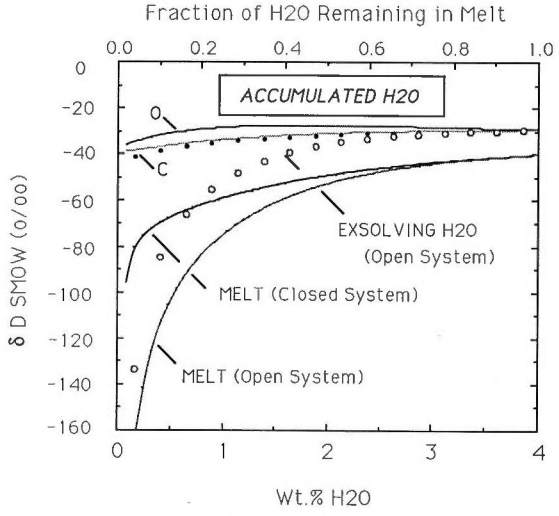

Fig. 1 Plot of δD versus wt. % H_2O and fraction of water remaining in a rhyolite melt similar to Obsidian Dome (δDinitial = -40 per mil; 4.1 wt. % H_2O). The δD of residual melt (and hydrous minerals) contrasts with the δD of exsolving H_2O (open and closed symbols) and with "accumulated magmatic water" contributed to a hydrothermal system after closed- or open-system degassing. These calculations incorporate the effects of changing H_2O/OH in the melt on the fractionation of hydrogen isotopes between melt and exsolved H_2O (see Taylor, 1992; Dobson *et al.*, 1989).

Obsidian clasts from very large tephra deposits (e.g., 23 km^3) in the Taupo Volcanic Zone, New Zealand exhibit a generally similar co-variation of δD and water content to that found for small deposits. The δD of obsidian varies from -90 to -58 per mil, and water contents from 0.4 to 1.33 wt. % H_2O. Obsidian flows cogenetic with the studied tephra deposits are not known. However, one distinct, but much older (100,000 yrs.) flow in the area had a similar composition (δD = -104 per mil; wt. % H_2O = 0.14) to obsidian from younger flows in California. Isotopic variations for both small and very large plinian tephra deposits are broadly similar, and suggest a common magmatic process. Moreover, the δD of local meteoric water is very different in both areas (California: ca. -95 to -125 per mil; New Zealand: ca. -40 per mil), suggesting insignificant isotopic exchange between magma and meteoric water.

H_2O Degassing and the isotopic fractionation of magmatic water

The fractionation of hydrogen isotopes between H_2O and a hydrous rhyolite magma varies primarily as a function of the hydrogen speciation (H_2O and OH) in the melt, which varies with water content (Newman *et al.*, 1988), and is therefore pressure dependent. The bulk fractionation between exsolved H_2O and vapor-saturated magma can vary from about 0 to 40 per mil as the relative abundance of OH increases (Dobson *et al.*, 1989), and is about 20 per mil for a magma with 3 wt. % H_2O (Taylor

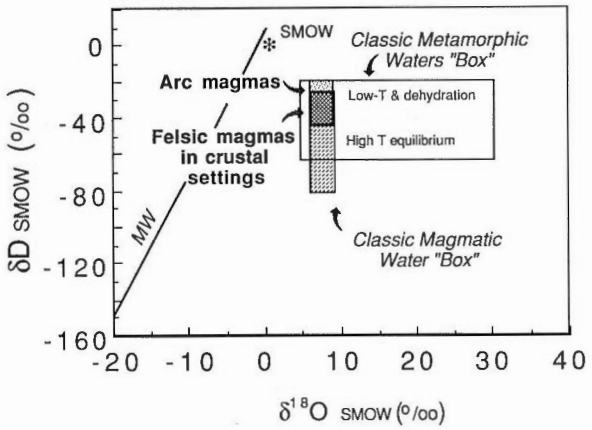

Fig. 2 Plot of δD versus $\delta^{18}O$ showing comparison of the isotopic compositions of magmatic waters from primarily andesitic arc volcanoes and from felsic magmas floored by continental crust with the range of compositions ("boxes") classically considered for metamorphic and magmatic waters. Initial dehydration of sediments yields waters with higher δD and $\delta^{18}O$ than derived by melting of or equilibration with high-grade metamorphic crust.

and Westrich, 1985). Thus, as water exsolves from the saturated melt, the residual melt is depleted in deuterium. The extent and rate of decrease in deuterium depend upon whether degassing is a open- or closed-system process, and on the ratio of the H_2O and OH species in the melt. Comparison of isotopic data for obsidian from individual small-volume eruptive centers to various models indicates that the degassing of magma columns prior to eruption of rhyolite flows proceeds in a step-wise open/closed system fashion. Periods of dominantly closed-system degassing, during which most of the exsolved water is retained in the magma as entrained bubbles, are terminated by eruption and water loss. In contrast, continuous eruption of large volumes of magma does not promote open-system isotopic fractionation; closed-system degassing is more closely approximated.

Degassing models based on water contents of obsidian tephra clasts and of ion-probe measured glass (melt) inclusions, plus experimentally-determined hydrogen isotope fractionation factors, permit calculation of the composition of magmatic water prior to the onset of degassing. For Obsidian Dome (Inyo volcanic chain, California), the initial δD of the magma was -40 per mil and the first-exsolved vapor was 3 to 11 per mil enriched in deuterium relative to the melt. The integrated δD value of exsolved vapor remaining entrained in the melt during could have varied from ca. -30 to -40 per mil as closed-system degassing proceeded. In contrast, the isotopic composition of biotite in such a magma would have a lower δD (e.g., -60 to -80 per mil).

Obsidian Dome magma degassed in a step-wise fashion. Periods of closed-system degassing were punctuated by eruption and open-system behavior. By analogy with step-wise closed-system degassing processes in other magma systems (e.g., CO_2 from Kilauea) magmatic water can be added to a hydrothermal system

upon pressure-equilibration of a magma after arrival in a high-level magma chamber.

The isotopic composition of magmatic water and the "magmatic signature"

From the above discussion, it is apparent that the large range and low δD of hydrous minerals and of the widely-quoted "magmatic water box" (δD = -80 to -40 per mil) generally may not correspond with the bulk of the first-exsolved, or accumulated magmatic water. The instantaneous δD of exsolving magmatic water changes continuously during degassing. Large deviations from the initial δD of the magma require open-system degassing. However, closed-system degassing most likely dominates in subvolcanic magmas (e.g., Dobson *et al.*, 1989) resulting in eventual release of water with a restricted range of δD, as is illustrated in Figure 1. The possible variation in δD of magmatic water in subvolcanic environments may be further limited by the amount of water lost. This varies with solubility as a function of initial water content of the magma and the depths to source and emplacement.

Magmatic water from Obsidian Dome magma, and from other rhyolites studied in the western U.S.A. and in New Zealand, has a δD (-40 ± 10 per mil). which is similar to, but slightly lower than that found for high-temperature fumaroles on dacite and andesite volcanoes (δD -30 to -20 per mil) e.g., references in Taylor, 1986; Matsuhisa, this volume; Figure 2). The first-released water during metamorphism and dewatering of sediments (e.g., along a subduction zone) has higher δD and $\delta^{18}O$ than water subsequently released during higher grade metamorphism (e.g., see Valley, 1986) or melting. Although intrinsic differences in the isotopic composition of source materials (e.g., variable mixtures of sediments and altered oceanic crust) are important, prograde metamorphism of similar rocks may itself cause a variation in the hydrogen isotope composition of magma sources which could explain the variation in δD of magmatic water in different tectonic settings.

Certainly, local meteoric waters comprise the principal fluid in continental geothermal systems, as does sea water in submarine hydrothermal systems. Early-formed vein minerals in deeper portions of a mineralized system may, however, record the passage of magmatic fluids which have a rather specific hydrogen isotope composition. Variations in δD of hydrous vein minerals may thus indicate mixing with non-magmatic fluids rather than variations in the δD of magmatic water. Reference to such a broad range of composition as represented by the classical "magmatic water box" may mask important early processes in the evolution of the hydrothermal system.

References

Dobson, P. F., Epstein, S. and Stolper, E. M. (1989) Hydrogen isotope fractionation between coexisting vapor and silcate glasses and melts at low pressure. *Geochim. Cosmochim. Acta*, vol. 53, p. 2723-2730.

Matsuhisa, M. (1992) Origin of magmatic waters in subduction zones: stable isotope constraints. In Hedenquist, J. W. ed., Extended Abstracts, Japan-U. S. Symposium on Magmatic Contributions to Hydrothermal Systems. *Rept. Geol. Surv. Japan*, no. 279, p. 104-109.

Newman, S., Epstein, S., and Stolper, E. (1988) Water, carbon dioxide, and

hydrogen isotopes in glasses from the ca. 1340 A.D. eruption of the Mono Craters, California: Constraints on degassing phenomena and initial volatile content. *Jour. Volcanol. Geotherm. Res.*, vol. 35, p. 75-96.

Taylor, B. E. (1986) Magmatic volatiles: isotopic variation of C, H, and S. In Valley, J. W., Taylor, H. P., Jr., and O'Neil, J. R., eds., Stable Isotopes. *Reviews in Mineralogy*, vol. 16, Mineral. Soc. America, Washington, D.C., p. 185-225.

——— (1992) Degassing of Obsidian Dome rhyolite, Inyo volcanic chain, California. In Taylor, H. P., Jr., O'Neil J. R., and Kaplan, I. R., eds., *Geochem. Soc.*, Spec. Pub. 3, p. 339-353.

———, Eichelberger, J. C., and Westrich, H. R. (1983) Hydrogen isotopic evidenced for rhyolitic magma degassing during shallow intrusion and eruption. *Nature*, vol. 306, p. 541-545.

——— and Westrich, H. R. (1985) Hydrogen isotope exchange and water solubility in experiments using natural rhyolite obsidian. *EOS, Trans. Amer. Geophys. Union*, vol. 66, p. 387.

———, Dunbar, N. W., and Kyle, P. (1990) Degassing of voluminous rhyolite magma, Taupo Volcanic Zone, New Zealand: Contrasts with smaller eruptions (abs.): *Geol. Soc. America Abs. with Programs*, vol. 22, no. 7, A54.

Valley, J. W. (1986) Stable isotope geochemistry of metamorphic rocks. In Valley, J. W., Taylor, H. P., Jr., and O'Neil, J. R., eds., Stable Isotopes. *Reviews in Mineralogy*, vol. 16, Mineral. Soc. America, Washington, D. C., p. 445-490.

Rept. Geol. Surv. Japan, No. 279, p. 195-196, 1992

Don't Work Hard at High Pressures, Ms. Magma!

Tetsuro URABE

Geological Survey of Japan
1-1-3, Higashi, Tsukuba, Ibaraki 305, Japan

Pressure has a significant influence on the partitioning of Pb and Zn between aqueous fluid and a granitic magma (Urabe, 1987). Shinohara *et al.* (1989) also pointed out the strong pressure dependence on the partition coefficients of HCl and NaCl between vapor and granitic melt. This result could be interpreted either by a pressure dependence on the nature of bonding in silicate melt or that in aqueous fluid. Since the partitioning coefficients are also a function of melt composition (Urabe, 1985), it seems that the melt structure may be sensitive to changes in pressure and composition.

However, Shinohara and Fujimoto (1989) observed a similar pressure dependence in a melt-free system; K-feldspar - quartz - muscovite - H_2O - NaCl - HCl. Therefore, it is evident that the pressure effect is not due to some unknown nature of the silicate melt, at least significantly, but rather is related to the nature of aqueous fluid under high temperature and relatively low pressure condition. The partial molar volume of chloride ions have a large negative partial molar volume under conditions where the density of H_2O is less than 0.5 g/cm^3 (Shinohara, 1991). Such low P- high T conditions are commonly achieved in magmatic hydrothermal systems.

Shinohara and Fujimoto's (1989) experiment suggests that circulating aqueous fluid becomes acidic when it ascends into a shallow portion of the earth's crust. The acidic fluid produced may react with rocks as it rises, and leach metals during hydrothermal alteration. Is this then the mechanism of ore-formation and associated wall-rock alteration?

If this is the case, there must exist alkali-enriched rocks beneath extinct hydrothermal systems, since the acidic solution exchanged hydrogen and alkalis with rocks at shallow depth. However, occurrences of such alkali-enriched rocks are not common except in porphyry environments where several lines of evidence indicate their magmatic origin. Therefore, high temperature magmatic fluid separated from high level magma reservoirs is ideal for the formation of mineral deposits and accompanied acidic alteration. So, see the title of this talk for the conclusion.

References

Shinohara, H. (1991) Geochemistry of magmatic hydrothermal systems. *Chikyukagaku*, vol. 25, p. 27-38 (in Japanese).

——— and Fujimoto, K. (1989) Pressure dependence of mineral-water reaction equilibrium in the low pressure range. *Proc. Intl. Symp. Water-Rock Interaction-6*, Malvern, p. 635-638.

———, Iiyama, T., and Matsuo, S. (1989) Partition of chlorine compounds between silicate melt and hydrothermal solutions: I. Partition of NaCl-KCl. *Geochim. Cosmochim. Acta*, vol. 53, p. 2617-2630.

Urabe, T. (1985) Aluminous granite as a source magma of hydrothermal ore depo-

Keywords: granitic magma, mineralization, pressure, partition, hydrothermal fluid

sits: an experimental study. *Econ. Geol.*, vol. 80, p. 148-157.
——— (1987) The effect of pressure on the partitioning ratios of lead and zinc between vapor and rhyolite melts. *Econ. Geol.*, vol. 82, p. 1049-1052.

Rept. Geol. Surv. Japan, No. 279, p. 197-199, 1992

Thermo-chronological Study of Hydrothermal Systems and Magma Intrusion: An Example from Goto-Fukue Island, Nagasaki, Japan

Koichiro WATANABE

Department of Mining, Kyushu University
Fukuoka 812, Japan

Introduction

In order to clarify the timing and potential of hydrothermal systems related to magma intrusion, thermo-chronological studies have been conducted in Goto-Fukue island, Nagasaki, in southwest Japan. Using techniques of fission track length analysis and K-Ar isotope analysis, it has been possible to elucidate the timing and interrelationships between magmatic intrusion, initiation and cessation of hydrothermal activity, and associated mineralization in the study area.

Technique

For the purpose of fission track length analysis, a technique to detect confined ^{238}U fission tracks using heavy ion irradiation has been investigated. Firstly, crystal samples were bombarded with heavy ions in an accelerator. Chemical etching of the sample causes the parallel heavy ion tracks to become visible. Confined fission tracks intersecting these etched heavy ion tracks also become visible (Fig. 1). As heavy ion tracks do not obstruct observation, the full length of the confined fission tracks can be measured precisely. In this study, zircon with spontaneous track densities lower than 10^6 cm^2 were irradiated with 90 MeV $^{58}Ni^{10+}$ ions perpendicular to the crystal surface using a tandem accelerator. Gold foil was used as a target in the scattering chamber. The fluence of the ion beam was controlled by varying the scattering angle between the sample and the incident beam. The fluence was measured using a semi-conductor detector, placed at the same scattering angle but on the opposite side of the incident beam. Confined fission tracks sub-perpendicular to the incident beam were measured under an optical microscope.

For fission track dating, prismatic crystal surfaces of zircon grains were polished, etched in a NaOH + KOH eutectic melt, and attached to a mica detector. Samples were then irradiated with thermal neutrons in a nuclear reactor. K-Ar isotopic analysis was performed at the Okayama University of Science using an isotope dilution method.

Thermal history analysis

The geothermal history of an altered granite porphyry in Goto-Fukue island was examined using the above mentioned fission track length analysis and K-Ar dating of hydrothermal minerals. Figure 2 shows a simplified geologic map of the study area and sample locations. In the area, three phases of igneous activity can be identified; 1) Middle Miocene granite porphyry, 2) Late Miocene rhyolite and basalt, 3) Pleistocene basalt. Intense hydrothermal alteration zones and active hot

Keywords: thermo-chronology, confined fission track, heavy ion irradiation, track length analysis

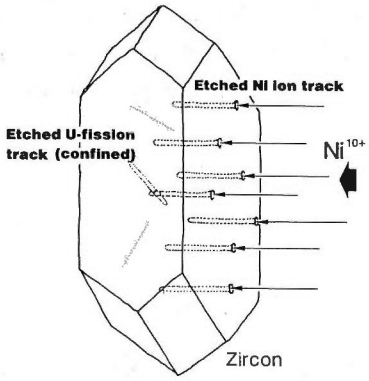

Fig. 1 Concept for detection of confined uranium fission tracks in minerals using heavy ion irradiation for thermal history analysis by track length pattern.

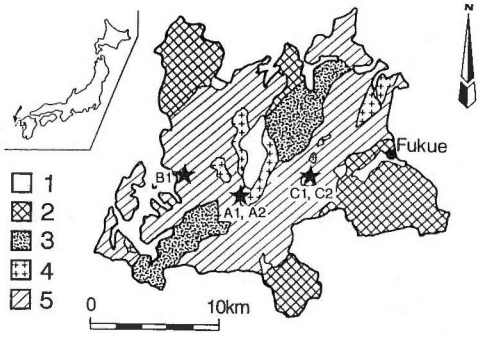

Fig. 2 Sample locations and geologic map of Goto-Fukue island simplified from Matsui and Kawada (1986). 1, Alluvium and diluvium; 2, basaltic rocks; 3, Fukue welded tuff; 4, Goto granite porphyry; 5, Goto group.

springs are also located in the western and eastern parts of the island. Sample A1 and A2 were collected from borehole FS-2 at a depth of 115 m and 945 m, respectively, and sample B1 from FS-3 (1481 m) in the western part of the island. Sample C1 and C2 were collected from the Goto pyrophyllite mine in the eastern part of the island (Fig. 2). These samples probably belong to the same granite porphyry. Sample A1 has not been hydrothermally altered, whereas sample B1 has been greatly altered to form chlorite. Sample A2 has been slightly altered. Sample C1 and C2 are altered rocks composed essentially of sericite.

Zircon separated from samples A1, A2 and B1 were employed for confined fission track length analysis. These same samples were also dated by conventional fission track dating techniques. Figure 3 shows the length distribution patterns of confined fission tracks and age data obtained. Neither sample A1 nor B1, with average lengths of 11 mm, indicate reduction patterns, even though their respective ages (11.3 Ma and 6.6 Ma) are different. Conversely the average length of sample A2 is

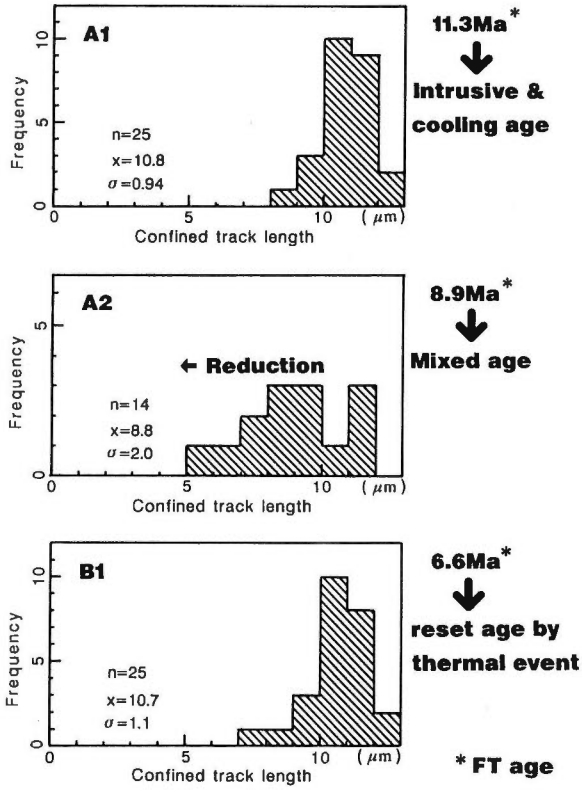

Fig. 3 Confined fission track length distribution for zircon crystals from boring core samples. Fission track ages indicated in the figure were obtained using the internal surface mica detector method. n, number of confined tracks measured; x, mean track length; s, standard deviation.

shorter (9 mm) and indicates 8.9 Ma, intermediate between the age of A1 and B1. The age of 11.3 Ma from sample A1 demonstrates the timing of cooling down to about 200°C in the western part of the island after the intrusion at about 15 Ma. On the other hand, B1 indicates that the sample age has been reset by a subsequent thermal event. The age obtained from A2 is likely to be due to mixed data. Thus, the confined fission track distribution patterns indicate that the peak of geothermal activity in the area occurred during the late Miocene, correlating with Late Miocene rhyolitic volcanism. Sericite from samples C1 and C2 indicates K-Ar ages of 14.4 and 14.5 Ma. These sericite minerals were formed at the almost same time as high temperature alteration minerals such as diaspore and corundum. Therefore in the eastern part of the island, the high level of alteration occurred just after the intrusion of the granite porphyry, but no subsequent thermal event can be detected.

Reference

Matsui, K. and Kawada, K. (1986) 1:200,000 geologic map "Fukue and Tomie". *Geol. Surv. Japan.*

PART II

THE BEHAVIOR OF VOLATILES IN MAGMA

Abstracts of the 4th Symposium on Deep-crustal Fluids
"The Behavior of Volatiles in Magma",
held at Tsukuba, November, 1991.

Rept. Geol. Surv. Japan, No. 279, p. 201, 1992

The Behavior of Volatiles in Magma: 4th Symposium on Deep-crustal Fluids

Tetsuro URABE and Akira TAKADA

Geological Survey of Japan
Higashi 1-1-3, Tsukuba, Ibaraki 305, Japan

On November 9, 1991, a symposium titled "The Behavior of Volatiles in Magma" was held at Geological Survey of Japan in Tsukuba, Ibaraki, Japan. This was the 4th Deep-crust Fluid-Rock Interaction Symposium organized by the "Deep-crust Fluid-Rock Interaction Study Group", which is an ad hoc group among geoscientists from several research institutes in Tsukuba. The symposium was attended by 71 people from six countries, with 13 presentations made (7 oral and 6 poster papers).

Volatile components in a magma exert a significant influence not only on the physical and chemical character of the magma but also on its evolution during solidification and crystallization. The behavior of the magmatic volatiles has been studied independently by petrologists and by magmatic fluid geochemists. Therefore, the main purpose of this symposium was to give researchers with different backgrounds and specialities the opportunity for discussion.

The morning session of the symposium was devoted to the behavior of CO_2, which usually has the second highest concentration after water in magma. The experimental determination of the solubility of CO_2 in silicate melt, accurate analytical methods to determine the concentration of CO_2 in volcanic glass, and degassing of CO_2 from active volcanoes were the main topics. These talks provided a comprehensive overview on the behavior of CO_2 gas in magma reservoirs.

Careful study of both the texture and isotopic composition of volcanic rocks revealed that we can find a trace of the now lost magmatic volatiles even after solidification. On the other hand, we can apply simulation methods to obtain the physical constraints on bubble separation from a magma. These were the main topics of afternoon talks and poster session. Bubble separation is a relatively new field of research which had received little attention before. However, these presentations clearly showed the importance of fluid mechanics to understanding the cause of rapid gas separation, which often leads to violent volcanic eruption.

In conclusion, we were exposed to a wide variety of approaches useful in understanding the behavior of volatiles in magma. In order to gain a more comprehensive and consistent view of these approaches, we must combine the models discussed during the symposium. The exchange of ideas was the most fruitful aspect of the symposium, as we all were exposed to different viewpoints on our mutual research target, volatiles in magma.

We appreciate the support from the Tsukuba EXPO '85 Memorial Foundation and the Geological Survey of Japan which made this symposium possible. We are also indebted to Ms. Toshiko Tomishima and Ms. Keiko Nagayoshi for their assistance in preparation of the symposium. Many oversea participants benefitted from the accomodation arrangements organized by Ms. Teiko Hiroyama.

Keywords: magma, crust, fluid, volatile

Rept. Geol. Surv. Japan, No. 279, p. 202, 1992

Experimental Studies Bearing on the Behavior of Volatiles in Magmas

Edward STOLPER

Division of Geological and Planetary Sciences
California Institute of Technology
Pasadena, California 91125, U.S.A.

Data on the speciation of water and carbon dioxide in silicate glasses and melts will be reviewed. In particular the proportions of water dissolved as water molecules and hydroxyl groups and of carbon dioxide dissolved as molecules of carbon dioxide and carbonate ion complexes in melts and their dependence on pressure, temperature, and melt composition will be discussed and evaluated in simple thermodynamic terms. Data on the solubility, diffusivity, and isotopic fractionations of these volatile components will also be presented and I will show how seeming complexities in these properties can be simply understood provided that the differing behaviors of the various dissolved species are considered. I will then present several case studies of natural, volcanic rocks and show how aspects of magmatic properties and behavior during eruption can be better understood by applying these data and principles. Examples will include the controls on the extent of degassing of submarine oceanic basalts from mid-ocean ridges, oceanic islands, and back-arc basins and the nature of degassing processes in rhyolitic volcanic systems.

Keywords: carbon dioxide, magma, solubility, volatile

Rept. Geol. Surv. Japan, No. 279, p. 203, 1992

Analysis of Water and Carbon Dioxide in Glass Inclusions Using a Laser Microprobe Technique

Genji SAITO*

Institute for Study of the Earth's Interior, Okayama University
Misasa, Tottori 682-01, Japan

The volatile composition of magmas can be obtained by micro-gas-analysis of glass inclusions in phenocrysts, which may be regarded as part of a "quenched magma" (Anderson, 1973). An analytical system was assembled to determine a minute amount of H_2O and CO_2 in glass inclusions. This system consists of a Nd-YAG laser with a beam diameter of 10 μm for selective heating of small areas of volcanic glasses and a gas chromatograph-mass spectrometer (GCMS) for determining an absolute amount of the gases extracted in vacuum from the glasses using a metal line which can be baked. A glass sample ground to less than 100 μm thick was pierced by the laser. The evolved gases were quickly transferred to the GCMS by helium carrier gas. Water and carbon dioxide concentrations of a glass sample were calculated from the measured amount of each gas and the mass of melted glass which was estimated from the volume of the laser pit and density of the glass. Analysis of CO_2 was carried out at a line temperature of 50°C after repeated baking of the line at 300°C to obtain a low CO_2 background with a good reproducibility, whereas H_2O analysis was carried out at a line temperature higher than 150°C to reduce the adsorption of H_2O onto the walls of the extraction line. The linear calibration curves were obtained for the range of 20-120 ng H_2O and 0.1-20 ng CO_2.

Homogenized basaltic glasses that had a bulk CO_2 concentration of 326 ppm was used to test this technique. The analysis of the glasses gave CO_2 concentrations of 270±70 ppm, in agreement with the bulk composition, when the extracted CO_2 exceeded 0.6 ng. Glass inclusions larger than 100 μm in diameter can be analyzed by the present method with an accuracy of ±70 ppm if the CO_2 concentration is 300 ppm. Details of H_2O analysis are in progress.

References

Anderson, A. T. (1973) The before-eruption water content of some high alumina magmas. *Bull. Volcanol.*, vol. 37, p. 530-552.

Keywords: carbon dioxide, inclusion, magma, laser microprobe

*Present address: Geological Survey of Japan,
Higashi 1-1-3, Tsukuba, Ibaraki 305, Japan

Rept. Geol. Surv. Japan, No. 279, p. 204, 1992

Importance of Volatiles on the Activity Model of Izu-Oshima Volcano

K. KAZAHAYA and H. SHINOHARA

Geological Survey of Japan
Higashi 1-1-3, Tsukuba, Ibaraki 305, Japan

The general pattern of basaltic activity of the central cone of Izu-Oshima volcano can be described as the following cycle: 1) Repose Period, 2) Fountaining Period, and 3) Degassing Period. We describe the activity cycle of Izu-Oshima volcano with an emphasis on the role of magmatic volatiles. We assume the magmatic parameters as follows; H_2O < 0.7 wt%, CO_2 > 0.05 wt%, density of gas-free basaltic magma = 2.7 g/cm^3, depth of magma reservoir = 4 km (1kb), and temperature = 1400 K.

Repose Period: The magma reservoir is thought to be at a depth where the density of the magma balances with that of the crust (neutral buoyancy). As the density of non-vesiculated magma is 10% larger than that of Izu-Oshima crust over the reservoir, some process which decreases the magma density is essential for the onset of magma ascent from reservoir. As CO_2 is already saturated under the magma reservoir condition (1kb), formation of CO_2-rich bubbles is an important process to decrease the density of magma. However, homogeneous vesiculation can only provide a density decrease of less than 1%. We conclude that accumulation of CO_2-rich bubbles to the upper part of the reservoir by bubble floatation is the most important process to decrease the magma density. Several to several tens times concentration of bubbles, which depends on the initial CO_2 content, is necessary to provide a density decrease sufficient to make magma ascend through the crust.

Fountaining Period: Excess magmatic pressure (ΔP) is believed to be the main driving force of the fountaining. The ΔP is given by an integration of the difference between the densities of the crust and magma column. As the ΔP is very sensitive to the volatile content, decrease in the volatile content reduces the ΔP, which will cause the termination of the fountainng. Since the ΔP, which is calculated with the initial volatile content, is almost zero, the fountain activity will terminate when the magma with accumulated volatiles is exhausted. Therefore, the amount of product of fountaining is controlled by the volume of magma reservoir and the initial volatile content.

Degassing Period: After the termination of the fountaining, the magma column will be balanced with its head below the surface. Ash, blocks and lapilli are ejected during the explosive degassing under the condition of high water/magma ratio, which is due to the entrainment of groundwater or the accumulation of magmatic water in the upper part of the column. Quiet degassing also occurs under conditions when the vertical gradient of water content inhibits the explosion. Magma convection in the column provides both the heat to keep the column molten and the amount of degassing volatiles.

Keywords: Izu-Oshima, volcano, volcanic gas, basalt, volatile

Rept. Geol. Surv. Japan, No. 279, p. 205-206, 1992

Degassing of CO_2 from Kilauea: Carbon Isotope Evidence and Implications for Magmatic Contributions to Sediment-Hosted Submarine Hydrothermal Systems

Bruce E. TAYLOR

Geological Survey of Canada
601 Booth Street, Ottawa, Ontario K1A 0E8, Canada

Carbon isotope data for CO_2 emitted from the summit of Kilauea Volcano and from the East Rift Zone (ERZ) on the flank of Kilauea comprise two populations which indicate a two-stage degassing process. Modelling of isotopic fractionation during degassing permits prediction of the $\delta^{13}C$ of undegassed (parental) magma. Comparison with the isotopic composition of CO_2 from sea-floor hydrothermal vents on sediment-covered ridges indicates the extent of present-day degassing from sub-sea floor magma chambers.

Kilauea summit CO_2 has a mean $\delta^{13}C$ of -3.19 per mil (n=159; std. err.=0.08), compared to the mean $\delta^{13}C$ of -7.82 per mil (n=9; std. err.=0.24) for CO_2 in high-temperature (>900°C) fumarole gases from the ERZ. Solubility constraints on the CO_2 content of basaltic magma suggest that these data can be modelled as a two-stage, closed-system degassing process. The first stage reprsents CO_2-bubble formation during ascent to the summit magma chamber 2-6 km below the Kilauea summit. Residence of the magma in this chamber allows the CO_2 to escape, and solubility constraints suggest that the parental magma releases >95% of its original CO_2 upon equilibration in the summit magma chamber. The second stage of degassing occurs when magma from the summit chamber escapes into the ERZ, and releases its CO_2 at or near the surface. The good fit of the isotopic data to a closed-system degassing model implies that magma ascent is sufficiently rapid that the exsolving CO_2 remains entrained in the magma until the magma is stored a sufficient time in the summit chamber to separate from the melt, or is transported with the magma and released during eruption. The variation of $\delta^{13}C$ of the CO_2 is a direct consequence of the nature of the degassing and the magma plumbing system. The carbon isotope composition of the mantle beneath Kilauea (-4.1 to -3.4 per mil, including uncertainties) is enriched in ^{13}C relative to that usually assumed for the mantle (5-7 per mil) on the basis of data for carbonatites and diamonds, or on mass balance estimates of crustal carbon.

The CO_2 was collected from sea-floor hydrothermal vents using the ALVIN submersible at two sediment-covered ridge sites: southern Escanaba Trough and Middle Valley on the southern and northern segments of the Juan de Fuca ridge system. Both sites are characterized by the lack of "black smokers"; sulfide plus sulfate chimneys do not appear to be presently undergoing active construction at the ocean floor. The maximum temperatures of vent fluids at Middle Valley and Escanaba Trough were, respectively, 276°C (in 1990) and 217°C (in 1989). Although the sediment cover in both sites is several hundred meters thick, the variation of $\delta^{13}C$ with CO_2 concentration indicates remarkably different CO_2 sources dominate the present carbon mixing in each hydrothermal system. In Middle Valley, pyrolysis of organic

Keywords: Kilauea, isotope, carbon dioxide, magma, hydrothermal

carbon in the sediments, and dissolution of biogenic carbonate, are principally responsible for the CO_2 ($\delta^{13}C$ = -38.9 to -10.6 per mil). In the southern Escanaba Trough, the increase of $\delta^{13}C$ with concentration of CO_2 from -12.2 to -3.9 per mil indicates dominance of magmatic (mantle) CO_2 in the system, inspite of the low hydrothermal temperatures and sediment cover. The $\delta^{13}C$ value of -3.9 per mil provides a more reliable estimate of mantle carbon composition sampled by MORB at this site than previous estimates based on fractionated, residual carbon. Because CO_2 may act as a carrier gas, transporting H_2O, S, rare gases and metals from the magma, carbon isotopic tracing of magmatic contributions is useful in submarine hydrothermal systems.

Rept. Geol. Surv. Japan, No. 279, p. 207, 1992

Interaction between Convection and Bubble Migration in Magmas

Takehiro KOYAGUCHI

Earthquake Research Institute, University of Tokyo
Yayoi, Tokyo 113, Japan

Laboratory experiments that model the behaviour of vesicles in two-layer magma chambers indicate that when a silicic magma is replenished by a mafic magma, vesicles formed in the lower mafic magma can strongly affect the fluid motion in the upper silicic magma layer. The vesicles formed in the lower layer cannot be held in suspension by the vigorous turbulent convection, but migrate upwards and accumulate beneath the silicic magma layer. The fluid motion changes as the accumulation rate changes with time. There are at least three stages of fluid motion in the upper layer. As bubbles accumulate, a gravitationally unstable vapour-rich layer is formed, which subsequently rises into the silicic magma layer as plumes (First Stage). The ascent velocity of each plume increases with increasing accumulation rate. After the plumes reach the top of magma chamber, steady convection follows, being driven by bubble migration (Second Stage). In these two stages vapour phases supplied from the underlying mafic magma can efficiently migrate as buoyant plumes through the viscous silicic magma, despite the small values of Stokes velocity for individual vesicles. On the other hand, if the supply of the bubbles ceases at the bottom of the upper layer, the concentration of bubble increases upward in the upper layer, which stabilizes bulk density stratification. If the stabilizing effect is greater than the density instability due to the thermal effect, convection in the upper layer in suppressed (Third Stage). In this stage the migration of bubbles in the upper layer is basically controlled by Stokes settling velocity of each bubble.

The accumulation rate varies as a function of pressure, degree of crystallization, the composition of volatile components and the geometry of chambers. For example, if the vapour phase is composed of pure water, vesiculation and hence accumulation occurs only after extensive crystallization in the mafic magma, whereas if the vapour phase is a mixture of water and carbon dioxide, the mixed gas can exsolve without extensive crystallization. The accumulation rate for a given volume of mafic magma increases as the aspect ratio of the chamber increases.

Keywords: convection, vesicle, magma, fluid dynamics

Rept. Geol. Surv. Japan, No. 279, p. 208, 1992

Possible Role of Pre-eruption Degassing History on the Groundmass Textures of Basaltic Lavas from Izu-Oshima Volcano, Japan: An Experimental Investigation on the Population Density of Plagioclase

Hiroaki SATO

Faculty of Integrated Arts and Sciences, Hiroshima University
Higashi-senda, Hiroshima 730, Japan

During a textural investigation on the eruption products of Izu-Oshima volcano, Japan, I found that population density of plagioclase differs by more than two orders of magnitude between pahoehoe and aa lavas. The pahoehoe lavas are coarser-grained and have a population density of $10^{7.0}cm^{-3}$, while the aa lavas are finer grained, and have a population density of plagioclase of $10^{9.3}cm^{-3}$. These lavas have virtually the same groundmass chemical compositions. I further conducted one atmosphere melting/crystallization experiments to evaluate quantitatively the effects of the cooling rate and initial melting temperatures on the population density of plagioclase. These are the major parameters that affect the textural development of basaltic magmas (Lofgren, 1980, 1983). The present experiment showed that 20°C difference of initial melting temperature near the liquidus temperature causes about five orders of magnitude difference in the population density of plagioclase after annealing at about 100°C below the liquidus temperature, whereas more than two orders of magnitude difference in the cooling rate brings about only less than one order of magnitude difference in the population density of plagioclase. The large effect of the initial melting temperature on the population density of plagioclase is interpreted to be the result of slow structural relaxation for nucleation during cooling. Nucleation in the experiment is mainly induced by the transformation of embryos into crystal nuclei by the reduction of the critical size of nuclei in the 100°C undercooled condition, where the initial size distribution of clusters in the melt largely affect the population density of plagioclase. In natural eruption processes, degassing of magmas produces strongly undercooled conditions, and it is conceivable that a slight difference in the degree of undercooling of magmas before final degassing and eruption may cause a large difference in the population density of plagioclase of pahoehoe and aa lavas.

References

Lofgren, G. E. (1980) Experimental studies on the dynamic crystallization of silicate melts. In Hargraves, R. B., ed., *Physics of Magmatic Processes*, Princeton Univ. Press, Princeton, p. 487-551.

——— (1983) Effect of heterogeneous nucleation on basaltic textures; a dynamic crystallization study. *Jour. Petrol.*, vol. 24, p. 229-255.

Keywords: degassing, texture, basalt, Izu-Oshima

Rept. Geol. Surv. Japan, No. 279, p. 209, 1992

Distribution and Evolution of H_2O and CO_2 in Some Rhyolitic Magmas

Alfred T. ANDERSON, Jr.

The University of Chicago
Chicago, Illinois 60637, U.S.A.

Studies of rhyolitic glass inclusions in phenocrysts by Newman, Hervig, Dunbar, Bacon, Skirius, Vogel, Chesner and others using spectroscopic or ion microprobe methods have revealed that rhyolitic magmas from Long Valley (Bishop), California, Valles (Bandelier), New Mexico, Crater Lake, Oregon, Timber Mountain, Nevada, Taupo, New Zealand, and Toba, Indonesia had about 4 to 6 wt. percent of H_2O dissolved in pre-eruptive melt. Early erupted plinian magmas generally had the most dissolved H_2O. However, there is some argument whether or not later erupted magmas, i.e., those producing ash flows, initially contained much less dissolved H_2O. Consideration of the effects of pre-eruptive reequilibration, post-eruptive cooling and sample bias suggest that the difference is more apparent than real. Detailed relations between uranium (incompatible in calc-alkaline rhyolitic magma) and dissolved CO_2 and H_2O support the interpretation that the Bishop plinian magma was gas saturated. It is uncertain whether the later-erupted parts of the Bishop magma were gas saturated. The amount of gas in the crystallizing Bishop plinian magma probably was at least 1-3 wt. percent. Interpretation of hour-glass inclusions to estimate the pressure at which pumice rigidified suggests that the amount of gas in pre-eruptive magma was, at least locally, as great as 10 wt. %. It is important to stress that melt that is gas saturated will contain less dissolved H_2O at shallower depths unless another gas species (such as CO_2) is present, because of the effect of pressure on solubility. Consequently a decrease in dissolved H_2O with successive eruption must imply either that part of the system is free of gas, or that the higher-pressure gas contains important proportions of another gas species. The late-erupted parts of the Bishop magma are characterized by generally high dissolved CO_2, consistent with saturation with a CO_2-rich gas. It is not certain whether other systems share this feature, especially because of the difficulty of obtaining well-preserved, rapidly quenched glassy inclusions in phenocrysts from hot, late-erupted ash-flow materials. Computations by Newman and Anderson show that there is a density maximum that occurs in crystallizing rhyolitic magma under closed-system, gas-saturated conditions. The maximum occurs at about 5 wt. % of H_2O in the melt: if there is less H_2O, crystallization produces little gas, and the magma becomes dense because of the crystals; if there is more H_2O, the larger amount of gas dominates over the dense crystals and cooling magma floats. This can lead to stable density stratification, magma ponding, roof sealing and flotation causing the accumulation of large amounts of magmatic foam. Probably this is the reason for the common observation of pre-eruptive concentrations of H_2O near 5 wt. % in many rhyolites. Many granitic magmas appear to contain less H_2O and may be largely complementary to rhyolitic magmas.

Keywords: rhyolite, glass inclusion, magma, gas, volcanic eruption

Rept. Geol. Surv. Japan, No. 279, p. 210, 1992

Explosive Volcanism Caused by Convective Instability in a Bubbling Magma Chamber

Naoyuki FUJII[1], T. NAKANO[2] and T. KIMURA[3]

[1] *Research Center Seismology & Volcanology, Nagoya University Chikusa, Nagoya, Aichi 464-01, Japan*
[2] *Geological Survey of Japan*
[3] *Research Institute, NTT Corporation*

Several triggering mechanisms of eruptive activities for polygenetic volcanoes have been proposed, such as the accumulation of bubbles in magma chambers, opening of cracks in the country rocks, and supply of new magmas below the magma chamber. The eruptive activities of polygenetic volcanoes generally indicate some intermittency, which suggests a nonlinear coupling in controlling mechanisms, instead of a monotonical magma cooling or a steady magma supply. Any set of governing dynamics should explain these intermittent activity variations during the whole evolution of polygenetic volcanoes.

The evolution of magmas in the cooling magma chamber is generally modelled by a double-diffusive convection system. By assuming a bubble concentration (or compositional) difference in the magma chamber, the stability conditions of the system is studied. The critical growth time of the double-diffusive convection system is of fundamental interests in this study, because it controls the characteristic time scales in the observed intermittency of volcanic activity.

For relatively low thermal Reynolds numbers (10^5 to 10^7), the characteristic time scales become 1 to 100 yrs by assuming a flattened magma chamber with 1 km height.

Keywords: volcanic eruption, bubble, magma chamber, double-diffusion

Rept. Geol. Surv. Japan, No. 279, p. 211, 1992

Vesiculation from the Bottom: A Mechanism for Large Scale Vesiculation in Magma Chambers

Kei KURITA, Miwa KURI and Yohji KOBAYASHI

Geoscience Insititute, University of Tsukuba
Tsukuba, Ibaraki 305, Japan

The generation of large volume ignimbrites associated with caldera formation involves a large scale vesiculation process within the magma chamber. Volcano-stratigraphic field observations show that once this type of vesiculation starts it evolves to affect a large volume in a very short time period. The factors which govern the triggering and development of this process are not well characterized and should be investigated in more detail since they are fundamental key points to understand the nature of caldera formation. The short time development requires an elemental process to form a positive feedback loop. Here we propose one possible mechanism for the intiation of vesiculation in the magma chamber which results in the positive feedback loop.

The factors which characterize the initiation of vesiculation in a magmatic body are classified into three categories depending on how the saturation curve is crossed : 1) vesiculation due to de-pressurization, 2) that due to crystallization and 3) that due to a temperature rise. De-pressurization, which has been commonly considered as the main process of caldera formation, starts from the upper-part of the magmatic body. "Vesiculation from the top" is considered to progress relatively slowly because of the density-stabilized nature of the magma. Particularly in a large magma reservoir which yields voluminous ignimbrites (up to $10^3 km^3$), the vesiculation front is expected to propagate downward at a slow speed. This is a difficult situation for the positive feedback to occur. Instead, if heat is supplied to a silicic magmatic body from below by, for example, intrusion of hot basic magma, vesiculation starts from the bottom due to the temperature increase. This vesiculated layer causes a strong Rayleigh-Taylor instability, assisted by both thermal expansion and vesiculation from the bottom thermal boundary layer, forming a buoyant plume. When the plume rises it gains more buoyancy due to further vesiculation because of the de-pressurization. This process works as a positive feedback, which easily evolves to large scale vesiculation. We demonstrate this by an analogue model experiment using viscous syrup containing sodium hydrogen carbonate ($NaHCO_3$) solution. The thermal decomposition of $NaHCO_3$ generates CO_2 gas in the thermal boundary layer at the bottom, heated from below. This fluid parcel forms a plume and begins to rise into the central part of the syrup. Successive formation and rise of the gas-rich plume transports heat upward and causes a violent fluid motion in the entire region of the syrup. Three characteristic periods of fluid movement are important to model in this series of processes; 1) the time necessary for the formation of the thermal boundary layer, 2) the time for growth of the plume from this thermal boundary layer and 3) the turn-around time of this vesiculation-assisted convection in the magma chamber. We will show a model of thermal consequence of the double-layered magma reservoir, taking into consideration these characteristic times.

Keywords: vesiculation, magma chamber, caldera, fluid motion

Rept. Geol. Surv. Japan, No. 279, p. 212, 1992

Hydrogen Isotope Ratios of Hydrous Minerals from Several Japanese Quaternary Volcanoes

Isoji MIYAGI and Osamu MATSUBAYA

Akita University Mining College
Tegata-gakuen, Akita 010, Japan

D/H values of water in high temperature volcanic gasses from basaltic volcanoes and in quenched glasses of MORB, as well as ocean island basalt, fall in a range between -70 and -100 per mil irrespective of their locations. In contrast, D/H values of high temperature steam from many andesitic and dacitic volcanoes in island arc regions, especially in Japan, fall in a narrow range of -15 to 35 per mil This higher D/H ratio is a characteristic of island arc magmas, reflecting magma genesis and the rising process. However, at present, we have little information about D/H value of water in island arc magmas, except for the D/H values of volcanic steam. In this study, we have measured the D/H values of hydrous minerals in lavas, tephras and essential lithic fragments (in pyroclastic deposits) from several Japanese Quaternary volcanoes. The main aim of this study is to know the D/H value of magmatic water.

The D/H value of hydrous minerals fall in a range between -130 to 0 per mil. Samples from lava flows, lava domes and pyroclastic flows showed significant hydrogen isotopic variation even within the identical flow unit, e. g., Myoko and Daisen volcanoes. On the contrary, samples from tephras or pumice flows gave a rather uniform D/H value among identical or different units, with most samples in a range from -50 to -30 per mil

We carried out experiments in order to elucidate the relationships of color change, water content and D/H value when amphibole was heated to magmatic temperatures in air. Accordingly, amphibole changes in a color from green to red when heated above 500°C, coinciding with a decrease in water content and a drastic increase in D/H value. Above 800°C, hydrogen isotope exchange between the mineral and the surrounding moisture is rapidly achieved.

The wide fluctuation of D/H value of hydrous minerals from identical lava flows and lava domes may be explained by some process such as the oxidation observed in this experiment, or hydrogen isotope fractionation through dehydration of the magma (Taylor *et al.*, 1983; Newman *et al.*, 1988). Hydrous minerals from tephra or pumice flows may not undergo this kind of alteration process, and may reflect the D/H value of magmatic water.

References

Taylor, B. E., Eichelberger, J. C. and Westrich, H. R. (1984) Hydrogen isotopic evidence of rhyolitic magma degassing during shallow intrusion and eruption. *Nature*, 306, p. 541-545.

Newman, S., Epstein, S. and Stolper, E. (1988) Water, carbon dioxide, and hydrogen isotopes in glasses from the CA. 1340 A. D. eruption of the Mono Craters, California: constraints on degassing phenomena and initial volatile content. *Jour. Volcanol. Geotherm. Res.*, vol. 35, p. 75-96.

Keywords: hydrogen isotopic ratio, hydrous mineral, volcano, magmatic water

Rept. Geol. Surv. Japan, No. 279, p. 213-214, 1992

Excess Pore Pressure of the 1991 Dacite Dome Lava of Unzen Volcano and the Generation of Pyroclastic Flows

Hiroaki SATO[1], Toshitsugu FUJII[2] and Setsuya NAKADA[3]

[1] *Faculty of Integrated Arts and Sciences, Hiroshima University Higashi-senda, Hiroshima 730, Japan*
[2] *Earthquake Research Institute, University of Tokyo*
[3] *Earth and Planetary Sciences, Kyushu University*

The 1991 eruption of Unzen volcano, southwest Japan, gave us good opportunities to observe various types of small scale pyroclastic flows (glowing avalanches) generating from lava domes. The extrusion of viscous lavas at the summit edge of the Fugendake dome of Unzen volcano began on May 20 and continued to grow at a rate of $3\times10^5 m^3$ per day. Among them, Peleean-type (lateral explosion) and Merapi-type (falling block) pyroclastic flows were recognized. Close examination of videotapes verified that almost instantaneous explosive fragmentation of a large block (several tens of meters high) took place just after detachment of the block from the lava front, which resulted in generation of a Merapi-type pyroclastic flow. This observation can easily be reconciled with an idea that excess pore pressure was near the limit of strength of lava. Upward compressional forces at the time of landing of the block generated lateral extensional force, which together with excess pore pressure induced greater expansive force than the strength of the lava (several tens of MPa). The presence of unaltered hornblende and biotite microlites in the groundmass of the Unzen dacite also supports the idea of high inner pressure of the dome lava.

Sparks (1978) already examined the conditions of formation of excess pore pressure by numerically simulating bubble formation, and pointed out that high viscosity, more than 10^8 poise, may cause an excess pore pressure more than several MPa for magma rise rate of 25 cm/sec. The viscosity of 1991 Unzen dacite (SiO_2=65 wt.%) has been calculated to be ca. 10^{11} poise based on the flow rate as well as lava thickness (50-100 meters thick) advancing on a slope with a dip of 20-25°. Low gas permeability for lavas with a porosity of 30-40% may have prevented the lowering of excess pore pressure over a short period after extrusion of the dome lava. Cooling of the lava near the surface may lower the excess pore pressure.

High water contents of early-stage pumices of explosive eruptions (Taylor *et al.*, 1983; Newman *et al.*, 1988) suggest the presence of high pore pressure (Sparks, 1978). These pumices contained ca. 3 wt.% water, corresponding to an equilibrium pressure of 50-70 MPa. It is likely that the pore pressures of the pumices were near the limit of strength of the lavas at the time of eruption.

Large excess pore pressure in the dome lava has implications for generation of pyroclastic flows. Macdonald (1972) classified glowing avalanche from dacite domes as Pelean (lateral explosion) and Merapi-type (falling blocks), both of which were clearly observed in the 1991 Unzen eruptions. When lava extrudes above the surface, lateral explosion may take place where the combination of tensile strength

Keywords: pyroclastic flow, Unzen volcano, dacite, pore pressure

and inner pore pressure is above the critical strength of lava, resulting in the generation of Pelean-type pyroclastic flows. In contrast, falling of a large block at the side of the lava dome may trigger the explosive fragmentation of the block, generating a Merapi-type flow. Lavas just extruded may have high pore pressure and tend to explode laterally. Pelean- and Merapi-type pyroclastic flows may generate from a continuous spectrum of extruded lavas in terms of excess pore pressure.

References

Macdonald, G. A. (1972) *Volcanoes*. Prentice-Hall, N.J., 510p.

Newman, S., Epstein, S. and Stopler, E. (1988) Water, carbon dioxide, and hydrogen isotopes in glasses from the ca. 1340 A.D. eruption of the Mono Craters, California: Constraints on degassing phenomena and initial volatile content. *Jour. Volcanol. Geotherm. Res.*, vol. 35, p. 75-96.

Sparks, R. S. J. (1978) The dynamics of bubble formation and grouth in magmas: a review and analysis. *Jour. Volcanol. Geotherm. Res.*, vol. 3, p. 1-37.

Taylor, B. E., Eichelberger, J. C. and Westrich, H. R. (1983) Hydrogen isotopic evidence of rhyolitic magma degassing during shallow intrusion and eruption. *Nature*, vol. 306, p. 541-545.

地 質 調 査 所 報 告

第273号
須田芳朗 ・ 矢野雄策： 日本の地熱調査における坑井データ その2 検層データおよび地質柱状図データ，1991
第274号
鹿野和彦 ・ 加藤碵一 ・ 柳沢幸夫 ・ 吉田史郎： 日本の新生界層序と地史，1991
第275号
玉生志郎編： 日本の地熱資源評価に関する研究，1991
第276号
村田泰章・須田芳朗・菊池恒夫： 日本の岩石物性値 －密度，磁性，P波速度，有効空間率－，1991
第277号
Matsuhisa, Y., Aoki, M. and Hedenquist, J. W. eds.： High-temperature Acid Fluids and Associated Alteration and Mineralization, 1991 (in English)
第278号
津 宏治編： 地質リモートセンシングに関する研究

REPORT, GEOLOGICAL SURVEY OF JAPAN

No. 273
Suda, Y. and Yano, Y. : Well data compiled from Japanese Nation-Wide geothermal surveys, Part 2 logging data geologic columnsdata, 1991 (in Japanese with English abstract)
No. 274
Kano, K., Kato, H., Yanagisawa, Y. and Yoshida, F. : Stratigraphy and geologic history of the Cenozoic of Japan, 1991 (in Japanese with English abstract)
No. 275
Tamanyu, S. ed. : Research on the geothermal resource assessment in Japan, 1991 (in Japanese with English abstract)
No. 276
Murata, Y., Suda, Y. and Kikuchi, T : Rock physical properties of Japan - Density, Magnetism, P-wave velocity, Porosity, Thermal conductivity - , 1991 (in Japanese with English abstract)
No. 277
Matsuhisa, Y., Aoki, M. and Hedenquist, J. W. eds. : High-temperature Acid Fluids and Associated Alteration and Mineralization, 1991 (in English)
No. 278
Tsu, H. ed. : Research on geologic remote sensing system, 1991 (in Japanese with English abstract)

平成4年8月25日　印　刷
平成4年8月31日　発　行

通商産業省工業技術院　地 質 調 査 所

〒305 茨城県つくば市東1丁目1－3

印 刷 所　創文印刷工業株式会社
〒116 東京都荒川区西尾久7-12-16

地　調　報　告
Rept. Geol. Surv. Japan
No. 279, 1992